ADVANCED MICROGEL-FUNCTIONALIZED POLYESTER TEXTILES ADAPTIVE TO AMBIENT CONDITIONS

Pelagia Glampedaki

ADVANCED MICROGEL-FUNCTIONALIZED POLYESTER TEXTILES ADAPTIVE TO AMBIENT CONDITIONS

Pelagia Glampedaki

Graduation committee:

Chairman	
Prof. Dr. F. (Rikus) Eising	University of Twente
Promoter	
Prof. Dr. Marijn M.C.G. Warmoeskerken	University of Twente
Internal members	
Prof. Dr. Remko Akkerman	University of Twente
Prof. Dr. Jacques W.M. Noordermeer	University of Twente
Assoc. Prof. Dr. Victoria Dutschk	University of Twente
External members	
Prof. Dr. Vincent Nierstrasz	University of Borås (SE)
Dr. Reinhard Miller	Max Planck Institute of Colloids and Interfaces (DE)
Dr. Jan Mahy	Colbond B.V. (NL)

The work presented in this dissertation was mainly financed by the project ADVANBIOTEX (MEXT-CT-2006-042641), a Marie Curie Excellence Grant (EXT) funded by the FP6 Programme of the European Union.

Advanced microgel-functionalized polyester textiles adaptive to ambient conditions

Pelagia Glampedaki

PhD Thesis with summary in English and Dutch

University of Twente, Enschede, The Netherlands

Cover design: Pelagia Glampedaki

Printing service: Gildeprint Drukkerijen, Enschede, The Netherlands

ISBN: 978-90-365-3301-0

DOI: 10.3990/1.9789036533010

ADVANCED MICROGEL-FUNCTIONALIZED POLYESTER TEXTILES
ADAPTIVE TO AMBIENT CONDITIONS

DISSERTATION

to obtain
the degree of doctor at the University of Twente,
on the authority of the rector magnificus,
Prof. Dr. H. Brinksma,
on account of the decision of the graduation committee,
to be publicly defended
on Friday, 16th of December 2011, at 12:45

by

Pelagia Glampedaki

born on the 24th of November 1977
in Kozani of Makedonia, Hellas

This dissertation was approved by the promoter:

Prof. Dr. Ir. Marijn M.C.G. Warmoeskerken

An egoist boasts about having learned a lot;

a wise man is saddened for not having learned more.

Aristotle (384–322 BC)

Real knowledge is to know the extent of one's ignorance.

Confucius (551–479 BC)

It is unwise to be too sure of one's own wisdom.

It is healthy to be reminded that

the strongest might weaken and the wisest might err.

Mahatma Gandhi (1869–1948 AD)

CONTENTS

INTRODUCTION

About functional-responsive-intelligent-smart materials

There is a plethora of terms in bibliography employed to describe materials which alter their properties according to changes in their environment. Some of the most common terms are functional, responsive, intelligent, smart (Shahinpoor *et al.* 2008; Urban 2011; Wang *et al.* 1998b; Woo *et al.* 2011), but there are other ones emerging, such as stimulus-active (Meng *et al.* 2010) or adaptive (Campolongo *et al.* 2011), in quest of appropriate terminology. All of them refer to systems engineered or developed to sense and consequently act on changes occurring around them due to external stimuli. Temperature, pH, light, pressure, ionic strength, electric and/or magnetic field are the main types of stimuli researchers apply to trigger changes in the properties of certain materials. These changes can be expressed as transitions in volume, shape, phase, viscosity, optical properties such as color and opacity, conductivity, and others. Few characteristic examples of such materials in advanced technology, as well as in daily life, are piezoelectric sensors of car airbags (Ashruf 2002), liquid crystal display screens (Den Boer 2005), photochromic sunglasses which darken when exposed to bright sunlight (Osterby *et al.* 1991), wound dressings and medicinal capsules which release drug substances at a controlled rate (Chang *et al.* 2011; Radhakumary *et al.* 2011). A simple search with general keywords in scientific databases yields more than 300,000 results referring to such materials (Library & Archive, University of Twente 2011 (http://www.utwente.nl/ub/)) whereas the results of common search engines exceed ten million. These figures illustrate the significance of multi-functional, stimuli-responsive materials in science and technology, and justify the continuously growing interest of researchers for developing novel types.

In search of appropriate terminology

Textiles described as functional/responsive/intelligent/smart form one of these novel types of materials which are flourishing during the last decade. According to Oxford Advanced Learner's Dictionary (1989), "functional" means having a special activity or purpose or operation, a term which could apply to any type of textile with a particular end-use. "Responsive" means reacting quickly or favorably, and/or being easily controlled; this term could, hence, refer mostly to a re-action rather than inter-action with the surroundings. "Intelligent", on the other hand, means having information – which could apply to e.g. embedded systems in textiles – or showing power of learning, understanding and reasoning, qualities far beyond any of engineered textiles. Last but not least, "smart" means clever, ingenious, having or showing intelligence – in which case, the above comments apply – or fashionable and chic, which are terms very suited for textiles but do not reflect responsiveness or interaction with the environment.

Research in this field was initiated mainly for the development of wearable electronics and information systems for biomedical and health-care applications (Carpi *et al.* 2005; Engin *et al.* 2005; Lymberis *et al.* 2003; Van Langenhove *et al.* 2004). Therefore, "smart" or "intelligent" textiles usually refer to integration of electronic chips and sensors into textiles and fibers (Cherenack *et al.* 2010) or – as it is eloquently described in Park *et al.* 2003 – to blending soft*ware* with soft*wear*. However, in recent years challenging perspectives have been explored for developing textiles with advanced properties and performance, tailored to interact with their environment through channels other than an electronic circuit. General terms used to describe such textiles are "multi-functional" or "responsive", although appropriate terminology for their description remains an issue. Functionalizing textiles or fibers with chemical modification, for example introducing amine groups or incorporating titanium dioxide particles on cotton (Kim *et al.* 2007; Lam *et al.* 2011), adds new functionalities to the preexisting properties of the textiles, i.e. it renders them multi-functional. However, these functionalities are permanent, not dynamic. On the other hand, if multi-functional textiles are developed using responsive materials, e.g. electrochemical sensors (Chuang *et al.* 2010), they become also responsive to changes in their environment by sending out a signal, for example. However, this response may occur only once and not reversibly. If multi-functional and responsive textiles are engineered to return to their initial state once the external stimulus ceases or if they are able to switch between two opposite states (e.g. hydrophilic to hydrophobic and *vice-versa*), then the term "switchable" is used to express their reversible behavior (Chhatre *et al.* 2009).

Regardless of their description, and based on increasing need to apply sophisticated technologies to eco- and user-friendly materials, multi-functional textiles rose rapidly to the surface as attractive solutions. A definitive boost for their development came with the booming industry of stimuli-responsive polymers (Cohen Stuart *et al.* 2010). Combining the two fields resulted in textile materials with biomimicking and self-cleaning/healing properties, conductive polyelectrolyte composite fibers, controlled transdermal drug-release capacity, and other (De Rossi *et al.* 2005; Nji *et al.* 2010; Shim *et al.* 2008; Simovic *et al.* 2010; Tiwary *et al.* 2007). The aim of this scientific match-making was either to upgrade existing functions and performances of textile materials or to develop novel textiles with unprecedented functions.

This thesis focuses on the latter aim providing proof of the concept that hydrogel-based surface-functionalization of commercial textiles can lead to novel multi-functional materials responsive to changes in their environment. In this sense, the functionalized textiles developed are considered *advanced* (as ready-to-use textiles are taken one step further) and *adaptive* to ambient conditions (as they change their properties to adjust to their environment). Therefore, the thesis title was formed using these terms to describe as suitably and accurately as possible the materials under study.

Hydrogel-functionalized textiles

Speaking of terminology, the acronym of Functional-Responsive-Intelligent-Smart is FRIS, a word which means "fresh" or "cool" in Dutch. During the process of searching for textile functionalization techniques, a fresh, indeed, idea was developed: to incorporate stimuli-responsive hydrogels into the surface layers of textiles (Jocic 2008; Jocic *et al.* 2009). Hydrogels are generally polymeric networks which can absorb large amounts of water without becoming soluble in it. If they consist of stimuli-responsive polymers, they can expel or re-absorb water depending on changes in pH, temperature, ionic strength etc.

Prior to the research presented here, extensive tests were performed with different hydrogel types and on different textile substrates, the results of which led to the final selection of an appropriate polymer and textile substrate combination. In all cases, the pH-responsive biopolymer chitosan (CS) and the thermo-responsive polymer poly(*N*-isopropylacrylamide) (poly-NIPAAm) were used for the hydrogel preparation. The tests included: (a) CS/poly-NIPAAm macro-hydrogels (continuous bulk) in the form of Interpenetrating Polymer Networks (IPNs) for the surface functionalization of cotton (Glampedaki *et al.* 2008a and 2008b); and (b) CS macro-hydrogels with embedded microparticles of the pH/thermo-responsive co-polymer poly(*N*-isopropylacrylamide-*co*-acrylic acid) (PNIAA) for the surface functionalization of polyamide 6,6 (Glampedaki *et al.* 2009; Glampedaki *et al.* 2011c). In the first case, crosslinking throughout the hydrogel polymer network was based on physical entanglements of the macromolecular chains of the two polymers, and hydrogel attachment on cotton was of physical nature, achieved using a pad-dry method (Glampedaki *et al.* 2008b). In the second case, crosslinking within a continuous hydrogel network was achieved through electrostatic interactions between positively charged CS and negatively charged PNIAA; attachment of the hydrogel on polyamide fabric was of chemical nature, achieved through the natural compound genipin which was used as a crosslinker between primary amine groups of CS and polyamide (Glampedaki *et al.* 2011c). In both cases, it was concluded that the stimuli-responsiveness of the functionalized textiles, expressed as water or moisture uptake/loss at different pH and temperature values, was not as pronounced as expected. In fact, substrate interference was so high that hydrogel contribution to the water

---

This paragraph contains information based on the following publications:

Glampedaki P, Jocic D, Warmoeskerken MMCG, Moisture absorption capacity of polyamide 6,6 fabrics surface functionalised by chitosan-based hydrogel finishes, *Progress in Organic Coatings* **72**(3), 562–571 (2011)

Glampedaki P, Tunable wettability of polyester fabrics functionalized by chitosan/poly(*N*-isopropylacrylamide-*co*-acrylic acid) microgels, in *Surface Modification Systems for Creating Stimul-responsiveness of Textiles* (D. Jocic Ed.), University of Twente, Enschede, The Netherlands, 61–76 (2010) (ISBN 978-90-365-3122-1)

Jocic D, Tourrette A, **Glampedaki P**, Warmoeskerken MMCG, Application of temperature and pH responsive microhydrogels for functional finishing of cotton fabric, *Materials Technology: Advanced Performance Materials* 24, 14–23 (2009)

uptake was not possible to be determined accurately. In other cases (especially in the case of cotton), functionalization gave an effect opposite to the expected, i.e. it turned the fabric more hydrophobic than hydrophilic (Glampedaki *et al.* 2008b). Similar effect has been reported also in literature for CS-coated textiles (Liu *et al.* 2008b). Moreover, it was observed that the initial macroscopic properties of the tested textiles deteriorated. For example, the bulk CS hydrogels formed a continuous relatively thick coating layer on the textile surface (e.g. about 5 % increase in fabric thickness for the polyamide fabric (Glampedaki *et al.* 2011c), which resulted in increased stiffness and harsher textile handle.

Therefore, it was decided to re-orient research from bulk hydrogels to microgels (i.e. hydrogels in the form of microparticulate suspension), using the same main components (CS and PNIAA). Microgels are known to have a faster response to external stimuli (Saunders *et al.* 1999) and their specific surface area is much larger compared with a bulk system (Hosokawa *et al.* 2007). Hence, more surface functionalizing material and consequently more functional groups become available per unit area of textile. Polyester was chosen as a more appropriate substrate because its higher hydrophobicity, compared with cotton and polyamide, was expected to allow the microgel effect to show. In this sense, higher values of water/moisture uptake were expected compared with the previous studies, and a more apparent responsiveness to pH and temperature changes. Poly(ethylene terephthalate) (PET) was the polyester type chosen for which higher homogeneity and less impurities on its surface are expected (e.g. compared with cotton), being a synthetic polymer. It was also decided to investigate the adaptive character of the microgel-functionalized polyester textiles to ambient conditions through water management properties rather than through other more common paths, such as substance controlled release under various stimuli.

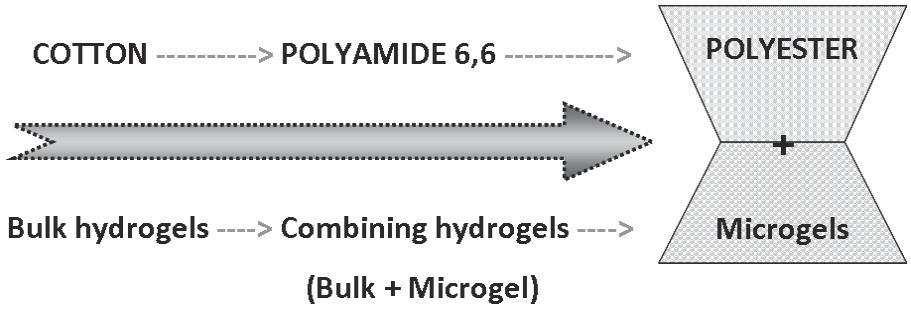

Graphical abstract 1: Route toward the objective of the thesis.

SCOPE & AIM OF THE THESIS

This thesis focuses on functionalization of polyester textiles through incorporation of stimuli-responsive polyelectrolyte microgels into their surface layers. Through this functionalization process, this thesis aims at proving an alternative concept for developing advanced textiles, the added functionalities of which render them adaptive to pH and temperature changes in their environment. As the main structural element of micro(hydro)gels is water, this thesis aims, additionally, at investigating the adaptivity of functionalized textiles in terms of water management properties under various ambient conditions of pH, temperature and relative humidity (RH).

Key points of this study are:

- The preparation of *pH/thermo-responsive polyelectrolyte microgels* with a novel combination of the biopolymer chitosan (CS) and the synthetic co-polymer poly(*N*-isopropylacrylamide-*co*-acrylic acid) (PNIAA) in the form of *polyelectrolyte complexes*.
- Functionalization of synthetic polyester using *biopolymers* and simple, *versatile methods*, without the need of organic solvents and complex or customized devices.
- *Direct and durable functionalization of commercial textiles*, not of single fibers intended for textile fabrication.
- Direct functionalization by *convergence of the opposites*: a hydrophilic functionalizing system (microgel) directly on a rather hydrophobic substrate (polyester) without *in situ* preparation of the microgel.
- *Water management properties* as a tool to investigate and confirm the microgel-imparted adaptivity of the functionalized textiles to ambient conditions.

CS and PNIAA polyelectrolyte microgels and complexes are thoroughly described and characterized in Chapter 1 in terms of their size, morphology, electrokinetic and rheological properties. The influence of the microgel composition, CS crosslinking and electrolytes (salts) on the physicochemical properties and stability of the microgels is also investigated.

The polyester functionalization methods used are described in Chapter 2. Two experimental paths are suggested; one involving UV irradiation and another one with low-temperature treatment. Characterization of the microgel-functionalized textiles by means of surface analysis is also provided in the same chapter. Surface morphology, chemical composition, charge and topography are the main aspects investigated. Some important physical parameters, such as crease recovery and whiteness index, are also determined.

Finally, the adaptivity of the functionalized textiles to ambient conditions is investigated in Chapter 3 in terms of dynamic wetting, capillarity, water vapor transmission, moisture sorption/desorption and regain, at various conditions of pH, temperature and RH values, depending on the technique applied.

Further challenges of each part of this thesis, that could not be explored during this research and that provide a platform for follow-up investigations, are briefly discussed at the end of each chapter.

Overall conclusions of these studies are compiled at the end of the main text of the thesis, after Chapter 3.

CHAPTER 1

POLYELECTROLYTE MICROGELS

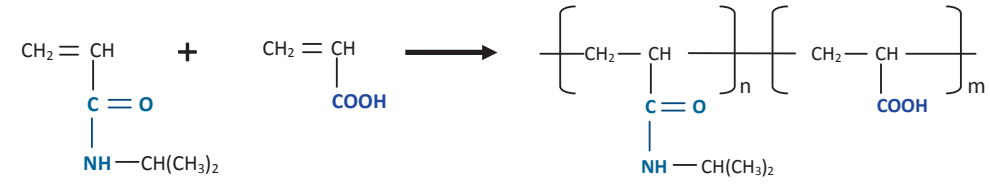

***N*-isopropylacrylamide** **Acrylic acid** **PNIAA**

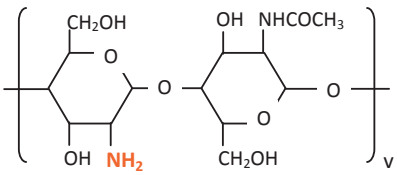

Chitosan

PNIAA
pH/thermo-responsive microparticles

Chitosan
pH responsive macromolecules

PNIAA/Chitosan
pH/thermo-responsive polyelectrolyte complexes

Graphical abstract 2: Formation of PNIAA/Chitosan polyelectrolyte complexes.

This chapter contains information included in:

Glampedaki P, Krägel J, Petzold G, Dutschk V, Miller R, Warmoeskerken MMCG, Polyester textile functionalization through incorporation of pH/thermo-responsive microgels. Part I: Microgel preparation and characterization (*submitted*)

Glampedaki P, Petzold G, Dutschk V, Miller R, Warmoeskerken MMCG, Physicochemical properties of biopolymer-based pH/thermo-responsive polyelectrolyte complexes (*submitted*)

1.1. THEORETICAL BACKGROUND

"Υδωρ (*hydor*, as in *hydro*, meaning *water*) *is the first principle of* (the existence of) *all"*
Cosmological thesis of Thales of Miletus (625–546 BC) [*]

1.1.1. Stimuli-responsive microgels

Microgels are hydrogels in the form of micro-particulate suspensions. According to the IUPAC Compendium of Chemical Terminology (Gold Book, http://goldbook.iupac.org/), a hydrogel is a polymer or colloidal network expanded throughout its volume by water. Common examples in every day life are contact lenses, baby diapers, body implants, and hydrogel beads as water resources in agriculture (Siemer *et al.* 1993; Xinming *et al.* 2008). Hydrogels are categorized based on size to macroscopic networks (continuous bulk hydrogels), and colloidal networks of micro/nano-particles (micro/nano-gels). According to the nature of crosslinks within the network, hydrogels are characterized either as physical, where crosslinking is achieved through physical entanglements or electrostatic interactions between the constituent polymers, or as chemical, where crosslinking is based on covalent bonds (Burchard et al. 1990; Djabourov 1991). The most common types of physically crosslinked hydrogels are full (or semi-) interpenetrating polymer networks (IPNs) and polyelectrolyte complexes (PECs). For this research study, PEC microgels were chosen as functionalizing systems, for reasons explained in the next paragraphs.

When microgels consist of stimuli-responsive polymers, their microparticles absorb or expel water depending on ambient conditions. As a consequence, at critical values of e.g. temperature and pH, they undergo volume/phase transitions from swollen to de-swollen (collapsed) and from hydrophilic to hydrophobic state, and *vice-versa* (Christodoulakis *et al.* 2010; Jones *et al.* 2000; Lapeyre *et al.* 2008; Pelton 2000). This switching behaviour has been the basis of multiple applications in the field of biomedicine and material science for the development of e.g. substance controlled-release systems and multi-functional materials (Berger *et al.* 2009; Helgeson *et al.* 2011; Karg *et al.* 2009; Kiser *et al.* 2000; Schmidt *et al.* 2010; Zhang *et al.* 2010a). For this research, pH- and thermo-responsive polymers were selected to create dually responsive microgel-based functionalizing systems.

[*] Thales of Miletus (625–546 B.C.) was a pre-Socratic Greek philosopher and one of the Seven Sages of Ancient Greece. The phrase is adapted after free translation based on the book of Dr. C. Vamvakas, *10 "current" dialogues with the pre-Socratics*, Savvalas (2008) (also found as *C.J. Vamvacas, The Founders of Western Thought – The Presocratics, Boston Studies in the Philosophy of Science* ***257****, Springer (2009)*).

1.1.2. Polyelectrolyte complexes (PECs)

Throughout the present study, the intention was to introduce functionalization solutions which would be as "green" as possible. Therefore, experimental procedures were planned to have a limited number of chemical reaction steps and to require few chemical reagents. To this end, it was decided to use micro(hydro)gels of the physical type. In general, physical gelation techniques include ionotropic, cold- or heat-setting mechanisms involving ionic complexation, hydrogen bonding and/or hydrophobic-hydrophobic interactions between the constituent polymers of the network (Burey *et al.* 2008; Singh *et al.* 2010). PEC microgels were chosen as functionalizing systems for various reasons: polyelectrolyte complexes form very strong networks with reversible electrostatic links, which could also be used for the polyester surface charge management; they are versatile in terms of composition, shape and stimuli-sensitivity; they are easy to prepare; each of their components maintains its individual characteristics (Shchipunov *et al.* 2009; Tsuchida 1994). In addition, PECs are generally well-studied systems, as they resemble physiological substrates, and they are extensively used in biomedicine as e.g. drug carriers (Hamman 2010; Thünemann *et al.* 2004). In Thünemann *et al.* 2004, PECs are described very eloquently as "living systems", as they are very sensitive to changes in their environment and they respond accordingly.

"Polyelectrolyte complexes" is a very broad term that generally describes polymer networks formed by the electrostatic attraction of oppositely charged polyions. There are many PEC types with the most common being formed between natural and/or synthetic (linear) polymeric polyelectrolytes (e.g. chitosan-sodium alginate or poly(*L*-lactide)), polymeric polyelectrolytes and salt polyelectrolytes (e.g. chitosan-pentasodium triphosphate), surfactants and polymeric polyelectrolytes (e.g. sodium dodecyl sulphate-poly(diallyldimethylammonium chloride) (PDADMAC)), or proteins and polyelectrolytes (e.g. collagen-chitosan) (Dakhara *et al.* 2010; Lee *et al.* 2004; Ostrowska-Czubenko *et al.* 2009; Zhang *et al.* 2010a). Apart from intermolecular ionic bonds, main PEC formation mechanisms include van der Waals interactions, hydrogen/coordination/covalent bonding, and/or steric matching (Krayukhina *et al.* 2008). Polyelectrolyte complexation usually follows three stages of primary complex, intra-complex and inter-complex formations (Dakhara *et al.* 2010). Important parameters that influence the complexation mechanisms are the ionization degree and the charge density of the oppositely charged polymers, their concentration and ratio in the reaction medium, as well as the temperature of the medium, and the duration of their interaction (Il'ina *et al.* 2005).

Considering that the scope of this research was ultimately the polyester textile functionalization rather than the organic synthesis of a completely new functionalizing microgel system, the polyelectrolytes used for the microgel preparation were searched for in literature. On the other hand, since textile functionalization was not to be achieved via novel processing techniques, e.g. weaving style or new fiber production, choosing a chemically appropriate functionalizing system was a key parameter. For this reason, a novel approach for using chitosan was engineered in order to avoid bulk hydrogel formation (undesired, as explained in the Introduction) and at the same time avoid the chemical modification (e.g. by copolymerization) of its macromolecules. Most of the PECs

reported in literature for chitosan refer to continuous bulk (macro)hydrogels, membranes, films, coacervation aggregates or flocculent precipitates, with the most common synthetic polyanion used for complexation being poly(acrylic acid) (Il'ina *et al.* 2005; Krayukhina *et al.* 2008; Mihai *et al.* 2009; Nge *et al.* 2002; Silva *et al.* 2008).

The novelty of the functionalizing system presented in this study regarded a different, less commonly encountered PEC type, formed between ionized microgel particles and oppositely charged macromolecular chains in solution. A study on a similar concept was reported in literature regarding complexation between negatively charged microgels of poly(*N*-isopropylacrylamide-*co*-methacrylic acid) and the positively charged standard polyelectrolyte PDADMAC (Kleinen *et al.* 2010). In the present thesis, the microgel particles used are of poly(*N*-isopropylacrylamide-*co*-acrylic acid) (PNIAA) and the oppositely charged polyelectrolyte is chitosan. Even though, chitosan hydrogels (macro, micro, nano) with either poly(*N*-isopropylacrylamide) alone or poly(acrylic acid) alone or coacervated with both have been prepared before, this particular combination of PEC type and components (i.e. a copolymer of *N*-isopropylacrylamide and acrylic acid in suspension, and free chitosan macromolecules in solution) is thoroughly studied here for the first time.

1.1.3. Chitosan, *N*-isopropylacrylamide, acrylic acid

Considering possible applications in the field of biomedical textiles and protective clothing for the functionalized polyester, it was essential that the microgels used would exhibit their stimuli-responsiveness within the range of physiological human body temperatures (average of 37°C) and the pH range of human skin (roughly, 4.5-7.5) (Schneider *et al.* 2007). Thus, the combination of components chosen for the PEC microgel preparation had triple purpose: a) to prepare a surface-functionalizing system pH-responsive between pH 4.5-7.5; b) to prepare a thermo-responsive system with a volume/phase transition temperature as close as possible to 37°C; and c) to maintain after preparation the desirable intrinsic properties of each constituent.

As already mentioned, three main components were chosen: chitosan (CS), *N*-isopropylacrylamide (NIPAAm) and acrylic acid. CS is a natural amine-rich polysaccharide with many beneficial properties. It is biocompatible, biodegradable and with good antimicrobial properties (Kong *et al.* 2010; Rinaudo 2006). It is derived by deacetylation from chitin, a structural compound of crustacean shells and fungi (Limam *et al.* 2011; Al Sagheer *et al.* 2009; Tajdini *et al.* 2010; Wang *et al.* 2008). Owing to its multiple deacetylated, therefore primary, amine groups, chitosan is a pH-responsive biopolymer with reported pK_a* values of 6.2-6.6 (Leane *et al.* 2004; Phillips *et al.* 2000; Prochazkova *et al.* 1999). It is widely used in dietary products, health care systems, waste processing, as well as in the textile industry for e.g. dye absorption (Lim *et al.* 2003; Zhang *et al.* 2010b). On the other hand, NIPAAm was chosen because in its polymeric form it is the most widely investigated thermo-responsive material (Geever *et al.* 2007; Makino *et al.*

* pK_a is the negative logarithm of the equilibrium dissociation constant of an acid (pK_a=-log K_a), thus, a measure of the strength of the acid in a solution.

2000; Schild 1992; Zhang *et al.* 2010c). The lower critical solution temperature (LCST)[*] of poly-NIPAAm in water is 32°C (Hirokawa *et al*. 1984). Owing to this property and to its biocompatibility and even though it is a synthetic polymer, poly-NIPAAm is very commonly used in biomedical applications (Cheng *et al.* 2008; Prabaharan *et al.* 2006; Zhang *et al.* 2010c). Finally, acrylic acid was chosen because when co-polymerized with NIPAAm, the polymer formed (poly(*N*-isopropylacrylamide-*co*-acrylic acid), denoted as PNIAA) is both thermo- as well as pH-responsive. This dual character is attributed to the fact that carboxylic groups of acrylic acid which can be ionized above pH 4 (Lee *et al.* 1999; Pradip *et al.* 1991) are attached to the poly-NIPAAm backbone. Moreover, acrylic acid in its polymer form is a well known superabsorbent material (Bahaj *et al.* 2010; Brannon-Peppas *et al.* 1990); hence, it is expected that microgels containing acrylic acid units will show high water/moisture absorption. Such a quality is important for functionalization of polyester textiles intended for apparel because it can promote moisture management and therefore improve wear comfort (Hu *et al.* 2005; Sampath *et al.* 2009). Finally, being a rather common reagent in the textile industry (Ferrero *et al.* 2004), as well as in pharmaceutical applications (Onuki *et al,* 2008), acrylic acid can be easily accepted as a functionalizing agent for clothing materials.

[*] The lower critical solution temperature, also known as cloud point, is a critical temperature below which a mixture is miscible.

1.2. EXPERIMENTAL PART

As explained in the previous paragraphs 1.1.2. and 1.1.3., the objective of this Chapter is the preparation and characterization of polyelectrolyte microgels consisting of PNIAA microparticles alone or complexed with CS. After their preparation, as described in paragraph 1.2.2., the microgels were analyzed using various techniques. More specifically, the morphology of PNIAA microparticles, as well as of their complexes with CS, was investigated by means of Scanning Electron Microscopy (SEM). The total charge and the zero-charge point of microparticles and polyelectrolyte complexes were determined through potentiometric titrations. These two parameters offer useful information about the complexation ratio of the oppositely charged polyelectrolytes, and about the pH-induced change of their charges to the point of neutralization or shift from positive to negative values. The thermo-responsiveness of the microgels was investigated using Differential Scanning Calorimetry (DSC), UV-Vis spectroscopy, and Dynamic Light Scattering (DLS), in order to determine the LCST, study the thermo-response rate, and express the temperature-induced volume/phase transition of microparticles and complexes through changes in their hydrodynamic size, respectively. Rheological measurements were also performed to investigate whether viscosity changes, that would influence the microgel thermo-responsiveness, occur. UV-Vis spectroscopy and DLS were also used to study the effect of pH changes on the thermo-responsive properties of the microgels. Their pH-responsiveness was further investigated through electrokinetic measurements, which provided data on the electrophoretic mobility and the ζ potential of microparticles and polyelectrolyte complexes. Finally, the physicochemical stability of the microgels with time, at various conditions of pH and temperature, was studied through an analytical centrifugation technique based on transmission profiling. The effect of the polyelectrolytes complexation ratio, of the crosslinking of CS and of the presence of salts on the microgel properties was also studied. The information obtained was considered useful for elucidating results related to the polyester microgel-functionalization described in the next Chapter (Chapter 2). The experimental procedures pertaining to the above-mentioned analyses are described in detail in paragraph 1.2.3.

1.2.1. Materials

N-isopropylacrylamide (NIPAAm, Acros Organics) and acrylic acid (Acros Organics) were used for the PNIAA microgel preparation. *N,N'*-methylenebisacrylamide (Sigma) was used as a crosslinker and ammonium persulfate (Sigma) as an initiator for the polymerization reaction. Chitosan (CS, Primex) with 95% deacetylation degree was used for the complexation reaction. Genipin (GP, Wako) was used as a crosslinker for primary amine groups. Poly(diallyldimethylammonium chloride) (PDADMAC, Sigma-Aldrich) was used as a standard cationic polyelectrolyte and sodium poly(ethylene sulfonate) (PSS, Sigma-Aldrich) as a standard anionic polyelectrolyte for the polyelectrolyte titrations. Sodium phosphate monobasic and dibasic dihydrate (Fluka and

Sigma) were used for the preparation of buffer solutions. All other reagents (acetic acid glacial, sodium chloride, sodium hydroxide, hydrochloric acid, potassium chloride, potassium hydroxide) were of analytical grade.

1.2.2. Microgel preparation

Microgel of poly(N-isopropylacrylamide-co-acrylic acid)(PNIAA)

The PNIAA microgel (denoted as **M**) was synthesized by a surfactant free emulsion polymerization method, based on a procedure described in Cai *et al.* 2002. The monomers (NIPAAm, 2.82 g, and acrylic acid, 0.18 g) were dissolved in 300 ml water and placed in a 1000-ml flask equipped with a reflux condenser and a mechanical stirrer. 0.06 g of the crosslinker *N,N'*-methylenebisacrylamide was added. The solution was purged with N_2 for 30 min. 0.3 g of the initiator ammonium persulfate was then added. The reaction was performed at 65 °C for 4 h. The mixture was left overnight at room temperature for the completion of the reaction. To purify the final product dialysis followed (4 spectra/Por, Fisher Scientific, cut-off 12.000-14.000) for 48-72 h against water.

Microgels of PNIAA polyelectrolyte complexes with chitosan

Suspensions with polyelectrolyte complexes between PNIAA negatively charged microparticles and positively charged chitosan macromolecules were prepared by mixing, under intense stirring, aliquots of dialyzed microgel **M** with a 0.2% (w/v) CS solution, prepared in 0.1 % (v/v) acetic acid. The pH of freshly prepared dialyzed microgel **M** was measured with an Alpha Titroline pH-meter (Schott 163 Instruments, Germany) and was found to be 4.6 ± 0.1 at 20°C, whereas the pH of the CS solution was 5.2 ± 0.1. The mixing ratio of microgel **M** to chitosan solution was 1/2.5 (v/v). Complexation occurred readily, as observed macroscopically by the increased turbidity, leading to the formation of microgel **CM** (measured pH at 20°C: 4.9 ± 0.1). For comparison reasons, another microgel was prepared with reverse mixing ratio, i.e. 2.5/1 (v/v) of microgel **M** to CS solution; it will be referred to as microgel **MC.**

Genipin (GP) was used for the polyester textile functionalization, as described in paragraphs 2.1.2.b and 2.2.2.b of Chapter 2, owing to its ability of crosslinking primary amine groups. Therefore, the effect of genipin on properties of CS-containing solutions and microgels was also investigated. For that purpose, GP was added to CS solutions and portions of microgel **CM** at CS/GP ratios ranging from 40/1 (w/w) to 2/1 (w/w). For the crosslinking reaction, the samples were placed in an oven for 1.5 h at 65°C. In all cases, a blue-green coloration developed, which is characteristic of the GP reaction with primary amine groups (Levinton-Shamuilov *et al.* 2005). The color intensity increased with increasing genipin concentration in the samples.

The codes and description of all samples under study are given in Table 1.1.

Table 1.1: Microgels and chitosan solutions under study

Sample codes	Description	CS/M ratio (v/v)	CS/GP ratio (w/w)
M	Microgel of PNIAA microparticles	-	-
CM	Microgel of polyelectrolyte complexes between PNIAA microparticles & CS	2.5/1	-
MC	Microgel of polyelectrolyte complexes between PNIAA microparticles & CS	1/2.5	-
GP0	0.2% CS solution or microgel **CM**, without GP		-
GP1-CS	0.2% CS solution with GP	-	40/1
GP2-CS	0.2% CS solution with GP	-	20/1
GP3-CS	0.2% CS solution with GP	-	4/1
GP4-CS	0.2% CS solution with GP	-	2/1
GP1-CM or **CM-GP**	microgel **CM** with GP	2.5/1	40/1
MC-GP	microgel **MC** with GP	1/2.5	40/1
GP2-CM	microgel **CM** with GP	2.5/1	20/1
GP3-CM	microgel **CM** with GP	2.5/1	4/1
GP4 -CM	microgel **CM** with GP	2.5/1	2/1

1.2.3. Microgel characterization

Scanning electron microscopy (SEM)

A High Resolution Scanning Electron Microscope LEO 1550 (Carl ZEISS, Germany) was used to observe the microgel surface morphology and size in dry state. Microgel samples were diluted 1:1000 and a drop of each of them was placed on silicon wafers. The samples were then air-dried either at room temperature or under conditioning for 24 h in a bench top test chamber SM-1.0-3800 (Thermotron, USA) at 20°C or 50°C and 65% RH.

Cryogenic scanning electron microscopy (cryo-SEM)

Samples of microgels **M** and **CM** were analysed with a cryogenic high resolution scanning electron microscope S-4800 (Hitachi, Germany) in order to estimate the microparticle or polyelectrolyte complex size in hydrated state. Microgel **M** was analyzed as is. In the case of microgel **CM**, for which the effect of salt and pH on its complexes size needed to be examined, sodium chloride was added at a concentration of 0.04 M and the pH was adjusted to pH 6 with sodium hydroxide 0.1N.

Aliquots of the above microgel samples diluted 1:10 were frozen by plunging into nitrogen slush at atmospheric pressure. Freeze-fracturing was carried out in a Gatan Alto 2500 cryo-preparation chamber at -150°C. After fracturing, the sample temperature was raised to -98 °C for freeze-etching (45 s) and then it was lowered again to -130 °C for sputtering with chromium. SEM micrographs were obtained at a stage temperature of -130 °C and an accelerating voltage of 2 kV.

Potentiometric titration

The zero-charge points of CS in aqueous solution and of PNIAA microparticles and **CM** complexes in aqueous suspensions were determined using a particle charge detector PCD-03 (Mütek, Germany). CS solution of 0.2% (w/v) concentration was prepared by dissolving chitosan in an aqueous solution of an equimolar amount of acetic acid. Samples of the CS solution and of microgels **M** and **CM** were diluted 1:10 and their initial pH was adjusted to the value of 3 with a solution of hydrochloric acid 0.1 N. Potentiometric titrations were performed in triplicate between pH 3-10 with sodium hydroxide 0.1 N as titrant.

Polyelectrolyte titration

A particle-charge detector PCD-04 with a PCD-T3 titrator unit (Mütek, Germany) was used to measure the total charge of microgel microparticles and polyelectrolyte complexes through polyelectrolyte titration. Microgel samples diluted 1:10 were placed in the measuring cell where also a pH probe was inserted. A polyelectrolyte of opposite

charge was added drop-wise to each sample from an automatic dispenser until the zero-charge point was reached. A solution of the standard cationic polyelectrolyte poly(diallyl-dimethyl-ammonium chloride) (PDADMAC) with a concentration of 0.001 M was used as a titrant for the negatively charged microgel **M**. For the positively charged samples – i.e. CS solutions and microgel **CM** samples, both uncrosslinked and genipin-crosslinked – a solution of the anionic polyelectrolyte sodium poly(ethylene sulfonate) (PSS) was used at a concentration of 0.001 M. Measurements were performed in triplicate for each sample.

Differential scanning calorimetry (DSC)

A DSC 822^e instrument (Mettler-Toledo, USA) was used to determine the lower critical solution temperature of microgels **M**, **CM** and **MC**. Weighed microgel aliquots were placed in an aluminium pan. The pan was sealed and placed in the sample holder next to an empty aluminium pan used as a reference. The temperature was raised from 25°C to 60°C at a rate of 5°C/min, held at 60°C for 2 min and decreased until 25°C at a rate of 8°C/min. Heating and cooling were performed under a N_2 gas flow of 30 ml/min.

Rheometry

Rheological measurements were performed using a Physica MCR 301 rheometer (Paar-Physica, Germany). Flow curves depicting viscosity η against shear rate were obtained at shear rates 1-100 1/s using a cone-plate system with a 50 mm diameter. The cone angle was 1°, the cone truncation 53 µm and the measuring gap 0.053 mm. Two to four measurements were performed for each sample at 20°C. Prior to the analysis, each sample was equilibrated for 10 min in the holder. The tested samples included microgel **M**, CS solutions of concentrations 0.02 to 2.0% (w/v) in acetic acid 0.1% (v/v), and microgels **CM** prepared as previously described but with CS solutions of varying concentrations ranging from 0.02 to 2.0% (w/v). In all samples sodium chloride was added at a concentration of 0.1 M.

Apart from the viscosity values, the above-described measurements were used to determine the CS critical concentration, C^*. This parameter reflects the concentration above which the chitosan macromolecular chains start to entangle (Shchipunov *et al.* 2009). The measuring procedure is described in Hwang *et al.* 2000. In brief, based on the viscosity values determined for the CS series of solutions, the shear specific viscosity (η_{sp}) was calculated for each CS solution, according to Equation (1.1):

$$\eta_{sp} = \frac{\eta}{\eta_0} - 1 \qquad (1.1)$$

where η is the solution viscosity and η_0 is the solvent (water) viscosity.

The obtained η_{sp} values were then plotted against shear rate. By extrapolation, the zero-shear-rate specific viscosity was determined for each CS solution. Finally, the obtained zero-shear-rate specific viscosity values were plotted against concentration. In the resulting graph, the point at which the zero-shear-rate specific viscosity increases

sharply corresponds to the CS critical concentration, above which entanglement of the CS polymer chains occurs.

Ultraviolet-Visible (UV-Vis) spectroscopy

A Cary 100 Bis (Varian, USA) spectrophotometer equipped with a temperature controller was used to investigate through light transmittance changes the temperature-response rate of the microgels and the reversibility of their thermo-responsiveness. Microgel samples were diluted 1:10 and placed in 10-mm disposable cuvettes. Then, they were analyzed as such or after pH adjustment at values between 2 and 12. Each sample was heated from 25°C to a selected temperature, up to 40°C. Transmittance values (%) were recorded at 480 nm wavelength over a period of 30 min at each temperature. Based on these values, the temperature-response curves were drawn for each sample. These curves were the combined result of both the heating up process of each sample, from room temperature to the selected tested temperature, as well as of the physicochemical changes that each sample undergoes at that temperature. It is assumed that the time needed to heat up each sample is small compared with the time needed for its temperature-induced volume-phase transition. Based on the same measurements, the transmittance values of each tested sample at steady state, i.e. at t = 30 min, were also determined.

Dynamic light scattering (DLS)

A ZetaSizer Nano ZS system (Malvern, UK) was used to determine the hydrodynamic diameter of **CM** complexes at 20°C (or 25°C) and 40°C. Microgel samples diluted 1:1000 were measured either as they were, without pH adjustment, or after adjusting pH with buffer solutions of pH 4, 6 and 8. Every analysis included three measurements of 20 runs each. The equilibration time before analysis was set to 4 min.

A separate set of measurements was performed, as described above, in order to test the effect of electrolytes (salts) on the size of **CM** polyelectrolyte complexes. For that purpose, microgel **CM** samples were prepared at different values of ionic strength using potassium and sodium chloride solutions. The salts were added individually at two different concentrations each (0.003 M and 0.006 M for potassium chloride (KCl); 0.02 M and 0.04 M for sodium chloride (NaCl)), as well as in combination. The salt concentrations were chosen to be within the concentration range found in human sweat (Buono *et al.* 2007; Patterson *et al.* 2000; Whitehouse 1935). All samples were analyzed at two temperatures (20°C and 40°C) and two pH values (pH 4 and 6). An overview of the salt combinations used (8 series in total) is given in Table 1.2.

Table 1.2: Electrolyte (salt) concentrations and ionic strength values used for preparation of microgel **CM** samples

Sample series	Salt concentrations for microgel CM	Ionic strength (mol dm^{-3})
1	KCl 0.003 M	0.003
2	KCl 0.006 M	0.006
3	NaCl 0.02 M	0.020
4	NaCl 0.04 M	0.040
5	KCl 0.003 M + NaCl 0.02 M	0.023
6	KCl 0.006 M + NaCl 0.02 M	0.026
7	KCl 0.003 M + NaCl 0.04 M	0.043
8	KCl 0.006 M + NaCl 0.04 M	0.046

The ionic strength of each solution was calculated according to Equation (1.2):

$$I = \frac{1}{2}\sum c_i z_i^2 \qquad (1.2)$$

where c_i is the concentration of each ion in the aqueous solution, and z_i is the charge number of each ion (IUPAC 1997).

Electrokinetic measurements based on electrophoresis

A ZetaSizer Nano ZS system (Malvern, UK) was used to determine the surface charge and electrophoretic mobility of microgel microparticles and polyelectrolyte complexes through electrophoresis. Measurements were performed at 20°C and 40°C, and at pH values from 4 to 7. Microgel samples were prepared with a concentration of 0.1 g/L in 0.001 M solution of sodium chloride. The obtained values were the average of three measurements, and every measurement included three runs of 10 s each.

Electrokinetic measurements based on streaming potential

An electrokinetic analyzer EKA (Anton Paar, Germany) was used to determine the *ζ* potential of microgel **CM** after it was dried as a uniform coating on silicon wafers. The obtained data were collected for comparison with *ζ*-potential data of microgel **CM** on polyester textiles (Chapter 2, paragraphs 2.2.3. and 2.3.3.). The measuring principle and experimental procedure of using EKA are described in Jacobasch 1989 and Jacobasch *et al.* 1996. Prior to the analysis, microgel **CM** was coated on rectangular-shaped silicon wafers using a spin-coater (S.P.S. Europe B.V., The Netherlands) in two steps of 20 s – 2000 rpm the first and 40 s – 2000 rpm the second, under vacuum. The electrode solution was 0.001 M potassium chloride. Titration was performed in the pH range 3-10 using 0.1 M hydrochloric acid and 0.1M potassium hydroxide.

Analytical centrifugation – Transmission profiling

A multi-sample analytical centrifuge LUMiSizer 610 (L.U.M., Germany) was used to characterize the microgel (storage) stability and demixing behavior based on the transmission profiles obtained at different temperatures, pH values and centrifugation speeds. The influence of CS and GP-crosslinking on the separation process of microgel particles was investigated under a variety of experimental conditions. The technique used employs the STEP™ technology (Space- and Time- resolved Extinction Profiles). This technology allows measurements of transmitted light intensity to be performed as a function of time and position, simultaneously, over the entire sample length. The evolution of the transmission profiles, i.e. of the position of the interface between the particle-free solution and the dispersion can yield information not only about the microgel stability, but also about particle–particle hydrodynamic interactions and deformability. The measuring principle and the analytical procedure are described in detail in Petzold *et al.* 2009 and in Detloff *et al.* 2007. Examples of transmission profiles obtained in this study are presented in Appendix I. The series of samples that were studied with this technique and the experimental conditions used are given in Table 1.3.

Table 1.3: Sample series and experimental conditions of measurements performed with analytical centrifugation

Experimental parameters	
Sample volume	1.8 ml
Range (cuvette length)	103-130 mm
Centrifugation speed	1000 – 2000 – 3000 rpm
Duration of each centrifugation step	500 s
Total duration of measurement	1500 s
Time interval of data collection	10 s
Temperatures	20°C; 36°C; 40°C
pH values	3-12
Sample series	0.2 % (w/v) CS; microgel **M**; microgel **CM**; GP1-CS; GP2-CS; GP1-CM; GP2-CM; GP3-CM; GP4-CM

1.3. RESULTS & DISCUSSION

1.3.1. Microgel M: microparticle morphology & response to stimuli

The basis of the functionalization method described in this study is PNIAA microparticles, whether alone or complexed with oppositely charged chitosan macromolecules. In the microgel suspension, these microparticles are in hydrated state but enter into dry state after their incorporation into the polyester surface layer. Therefore, it was considered useful to determine their size in both states, as an indication of how they would appear on the polyester surface.

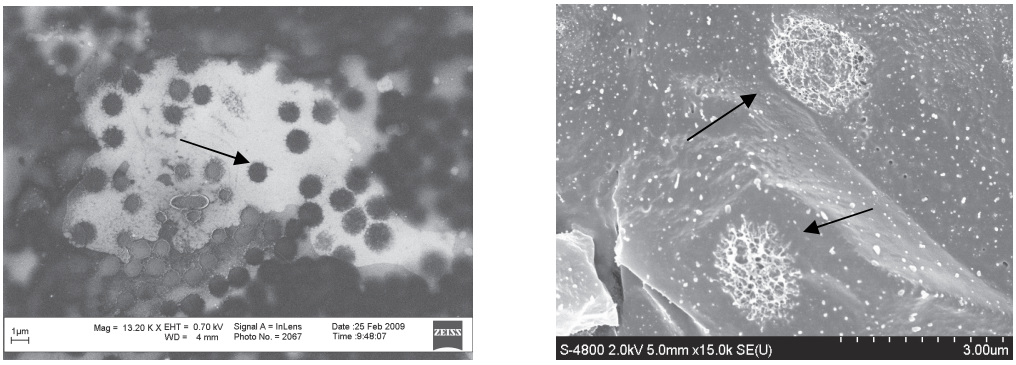

(a) **(b)**

Figure 1.1: (a) High resolution SEM images of PNIAA microparticles air-dried on silicon wafer; **b)** Cryo-SEM images of PNIAA microparticles in microgel **M**. The arrows point to the microparticles.

In Figure 1.1a, a high resolution SEM image of PNIAA microparticles in dry state (air-dried) is shown. Their spherical and rather uniform size is confirmed by this image. The estimated microparticle diameter is approximately 1 μm. In Figure 1.1b, an image of PNIAA microparticles hydrated natively in microgel **M** is shown (obtained by cryogenic SEM). In this case, the microparticle diameter is estimated to be approximately 1.5 μm. This difference in diameters between hydrated and dry states is expected because the microparticle structure collapses and shrinks when water is evaporated by air-drying (Saunders *et al.* 1996). Furthermore, the microparticles appear spherical and quite porous with an unsmooth "brush-like" periphery. It is generally known that high crosslinking density results into more rigid hydrogel structures and also hinders hydrogel swelling (Daly *et al.* 2000). Therefore, the amounts of crosslinker and of the two monomers used for the preparation of microgel **M** were thoughtfully chosen in order to achieve a low to medium crosslinking extent. The open structure of PNIAA microparticles shown in Figure 1.1b validates the initial choice.

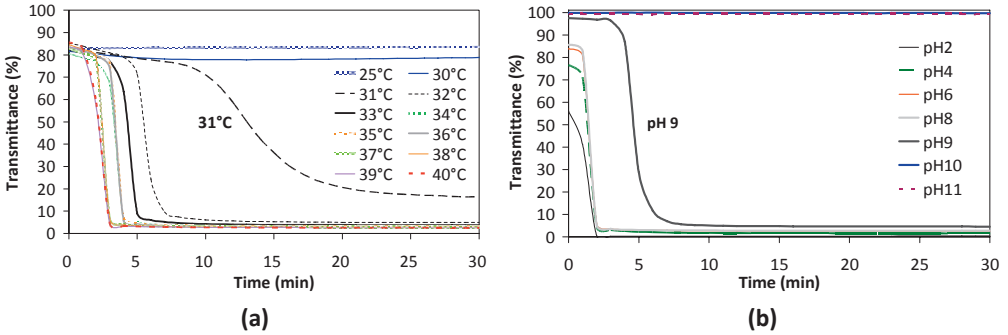

Figure 1.2: Temperature-response curves of microgel **M** based on light transmittance changes with time, at various temperatures **(a)** and at various pH values and 40°C **(b)**.

Light transmittance measurements were performed over time to assess the thermo-responsiveness of microgel **M**. In Figure 1.2a, the temperature-response curves are shown for temperatures ranging from 25°C to 40°C. From the curves it is evident that the higher the temperature is, the faster the transition of the microgel from translucent to opaque is. These light transmittance changes are the expression of the volume/phase transition that PNIAA microparticles undergo from swollen to collapsed and from hydrophilic to hydrophobic, owing to the poly-NIPAAm effect (Tanaka 1978). The transition starts to become obvious at 31°C, close to the pure poly-NIPAAm LCST, and as the temperature rises, the time needed for the transition to be completed shortens from approximately 17 min at 32°C to 3 min at 40°C. However, only above 34°C the final transmittance values coincide at almost zero, regardless of the time needed to reach that value. In Figure 1.2b, the effect of pH on this total transition at 40°C is depicted. At pH values 4-8, the temperature-response curves are very similar to the corresponding curve at 40°C in Figure 1.2a, although transmission is completed in even shorter time when pH is adjusted (i.e. in 2 min at pH 4-8, compared with 3 min at the native pH (4.9) of microgel **M**). At pH 2, the initial transmittance is 1.5 times lower than that at pH 6, and the final value is zero (i.e. even lower than at the intermediate pH values 4-8). These two features indicate higher hydrophobicity of the microgel at pH 2. At pH 9, the opposite effect is observed; the initial transmittance is almost 100%, the final value is higher, and the transition takes five times longer to be completed, than at pH 4-8. These facts indicate higher hydrophilicity of microgel **M** at pH 9. At even higher pH (10-12), the volume/phase transition does not occur (straight lines in Figure 2b), even though the temperature is 40°C. These results are not surprising as pure poly(acrylic acid) has a pK_a value close to pH 4 (Lee *et al.* 1999), above which its carboxyl groups become increasingly ionized. Extensive ionization causes strong electrostatic repulsion of the macromolecular chains, especially at high alkaline pH (Li *et al.* 2007; Yoo *et al.* 2000). Furthermore, as pH increases, the hydrogen-bonds between NIPAAm units (amide groups) and/or acrylic acid units (carboxyl groups) are destroyed (Ramirez-Fuentes *et al.* 2008). Therefore, the higher the pH is, the more hydrophilic the PNIAA microparticles are expected to be.

1.3.2. Microgel CM: complexes morphology & charge

Having determined the morphology and pH/thermo-responsiveness of the PNIAA microparticles, which are the basis for the **CM** complexes, the morphology and physicochemical properties of the latter were also investigated. In Figure 1.3b, a high-resolution SEM image of **CM** complexes is presented in comparison with PNIAA microparticles (Figure 1.3a), after both being air-dried at 20°C and 65% RH. These are the standard conditions for textile testing; hence, it was considered useful to observe the functionalizing microgels at the same conditions.

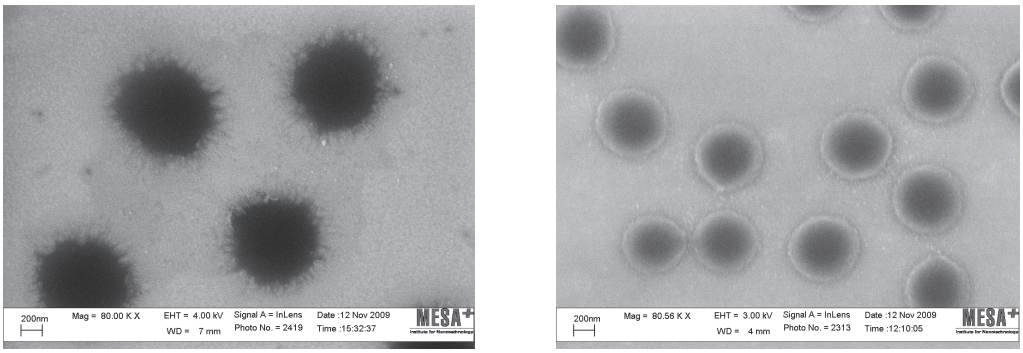

(a) **(b)**

Figure 1.3: High resolution SEM images of PNIAA microparticles **(a)** and **CM** complexes **(b)** air-dried on silicon wafers at 20 °C and 65 % RH for 24 h in a bench top test chamber.

Based on the edge-contrast and the differences in color effect of the depicted particles and complexes, the latter (i.e. **CM** complexes) appear more voluminous, yet smaller, and with a rounder periphery than PNIAA microparticles. The smaller size is expected owing to contraction of their structure caused by electrostatic attraction, known also as syneresis, (Mun *et al.* 2004) between protonated amine groups of CS and anionic carboxyl groups of PNIAA. In fact, the diameter of the air-dried **CM** complexes is estimated to be 600-650 nm, whereas that of PNIAA microparticles, under the same conditions, 700-800 nm. The fact that PNIAA microparticles exhibit a somewhat smaller diameter when air-dried conditioned (Figure 1.3a) compared with air-dried unconditioned (Figure 1.1a) underlines the effect of water/moisture in the structure of the microgel particles. In the first case, they retain some volume due to controlled drying at 65% RH, whereas in the second case, they are completely collapsed and flattened, therefore with a bigger diameter.

An important characteristic of polyelectrolytes is their zero-charge point, i.e. the pH value at which their total charge becomes zero. For ampholytic polymers, such as proteins, this value of zero net electric charge is better known as isoelectric point (pI) (IUPAC 1997). Based on Figure 1.4, the zero-charge points of CS macromolecules, PNIAA microparticles and **CM** complexes are determined to be 6.3, 3.4 and 6.0, respectively. The value for CS is similar to bibliographic values of CS pK_a (6.3-6.6) (Leane *et al.* 2004;

Rinaudo *et al.* 1999). Therefore, below pH 6.3 chitosan macromolecules exhibit a positive total charge.

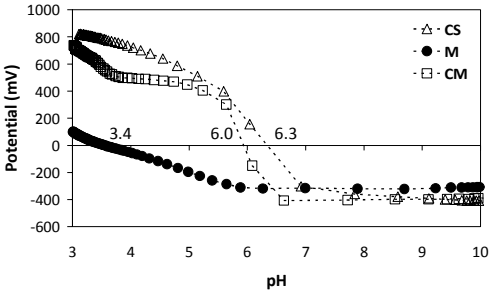

Figure 1.4: Potentiometric titration curves of 0.2% (w/v) CS solution, of microgel **M** and of microgel **CM** for the determination of their corresponding zero-charge points in 1:10 water-diluted samples.

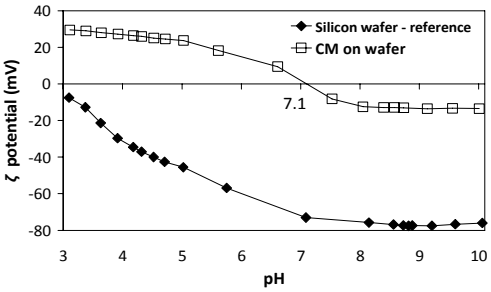

Figure 1.5: *ζ*-potential curve of microgel **CM** determined with streaming potential measurements after spin-coating on a silicon wafer (reference curve).

The value for PNIAA microparticles is lower than the reported pK_a values for pure poly(acrylic acid) (Ende *et al.* 1996; Lee *et al.* 1999), which is a weak acid. Above pH 3.4, PNIAA microparticles exhibit a negative total charge. The pH of freshly prepared microgel **CM** was measured to be 4.9 ± 0.1, at 20°C. At this pH, chitosan is positively charged and PNIAA negatively charged; thus, the formation of chitosan/PNIAA polyelectrolyte complexes occurs readily upon mixing due to electrostatic attraction (as it is schematically represented in Graphical abstract 2). Furthermore, CS was chosen to be in excess in microgel **CM** (i.e. not in stoichiometric analogy with PNIAA) in order to prevent aggregation of the complexes; by providing an excess of positive charges, CS stabilizes the **CM** complexes due to electrostatic repulsion. Additionally, owing to this CS excess, it was expected that the microgel **CM** total charge would shift from positive to negative values at a pH value close to the CS pK_a. Indeed, as shown in Figure 1.4, the zero-charge point for **CM** appears at pH 6.0, confirming that the pH-induced charge transition of **CM** complexes occurs within the physiological pH range, as initially planned. To have a reference point to compare with after polyester functionalization, this pH transition was also investigated with microgel **CM** being in dry state as a coating on a silicon wafer. In Figure 1.5, the *ζ*-potential curve for the **CM** coating is drawn from streaming potential measurements over a wide pH range. The shift from positive to negative values takes place close to neutral pH, even though at a higher value compared with microgel **CM** in suspension (i.e. at pH 7.1 instead of 6.0). This is expected as the charge density on the coating is higher than in the dilute sample. This curve is another manifestation of the PEC formation between CS and PNIAA; the maximum positive value of *ζ*-potential is higher than the negative one indicating excess of CS, like in microgel **CM**, and the negative values in the alkaline region are much smaller than those of the reference substrate suggesting that they derive from PNIAA after deprotonation of CS.

1.3.3. Rheological measurements

Despite the benefits of having CS in excess in microgel **CM**, it was imperative that this excess was kept to a low limit in order to avoid bulk gel formation or an increase in viscosity compared with microgel **M**. The former effect would lead to a continuous coating layer when applied on textile surfaces impairing the textile advantageous properties such as flexibility, crease recovery, water absorption; the latter effect would influence water diffusion inside the microgel and, therefore, the swelling/collapsing process of the microparticles would be affected (Routh *et al.* 2003; Tokita *et al.* 1991). To verify that the amount of CS used did not result in this effect, rheological measurements were performed in order to determine the viscosity of microgels **M** and **CM** and the CS critical concentration, C*, above which its macromolecular chains start to entangle. In order to explore which CS concentration does not cause an increase in the microgel viscosity, a series of microgels of the type **CM** were prepared with chitosan solutions of concentrations between 0.02 and 2% (w/v). The viscosities of these microgels, as well as of the corresponding CS-only solutions, in relation to advancing shear rate were measured. The results are given in Figure 1.6.

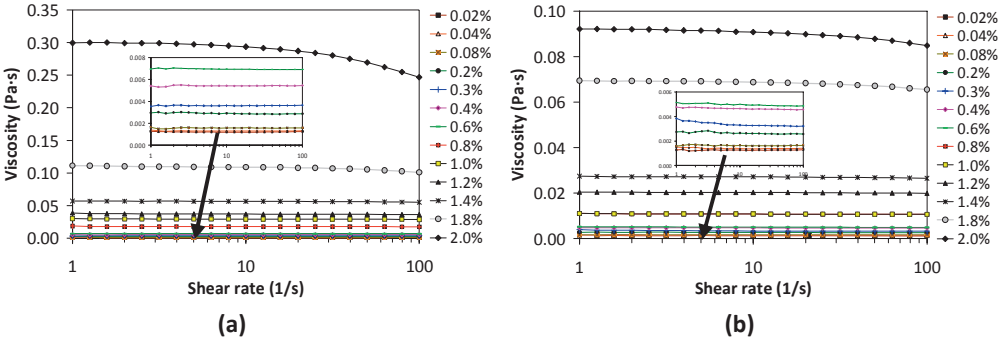

Figure 1.6: Viscosity flow-curves of CS solutions with concentrations from 0.02 to 2% (w/v) at 20°C **(a)** and of microgels **CM** at 20°C, prepared with CS concentrations ranging from 0.02 to 2% (w/v) **(b)**.

As expected, the microgel **CM** viscosity increases with increasing CS concentration (Figure 1.6b). Furthermore, for each microgel the viscosity remains practically constant throughout the studied shear rate range, until CS concentration reaches 1.4% (w/v). Microgels **CM** with CS concentrations higher than this value, i.e. with 1.8% and 2% (w/v), exhibit a decrease in their viscosity at higher shear rates (shear thinning), and so they behave as non-Newtonian fluids. Comparing with the corresponding CS solutions in Figure 1.6a, the shear thinning effect appears more noticeably at a higher CS concentration than for microgels **CM**, i.e. at 2% (w/v) compared with 1.8% (w/v), respectively. This difference could be attributed to the fact that in microgel **CM** the positive charges of CS are partly compensated by oppositely charged ions of the PNIAA microparticles. This charge compensation leads to compaction and higher flexibility of the macromolecular chains (Cho *et al.* 2006); therefore, shear

thinning appears more intense at CS-only solutions of higher concentration compared with their corresponding microgels **CM**. Another result derived from the rheological measurements of the CS-only solutions was the determination of the entanglement concentration of CS. Based on Figure 1.6a, Figure 1.7 was derived, as described in the experimental part. For the particular type of CS used in this study, the critical (entanglement) concentration was found to be approximately 0.6% (w/v).

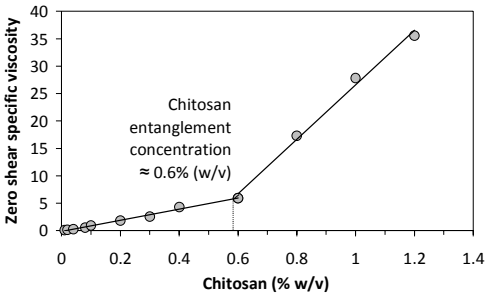

Figure 1.7: Rheological determination of the entanglement concentration of CS.

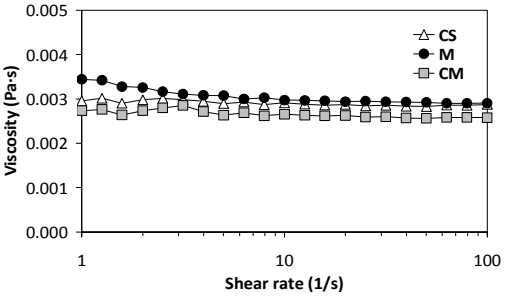

Figure 1.8: Comparison of viscosity flow-curves of 0.2% (w/v) CS solution, microgel **M** and microgel **CM**, at 20°C.

Above that value, the polysaccharide chains begin to overlap and entangle forming a continuous physical network. The 0.2% (w/v) CS concentration chosen for the microgel **CM** preparation is far below the critical concentration found and, therefore, the bulk gel formation is avoided, as it was desired. In any case, as shown in Figure 1.6b, microgel **CM** (with CS 0.2% (w/v)) is within the Newtonian flow region. More importantly, by comparing the viscosity values of 0.2% (w/v) CS solution and of microgels **M** and **CM** in a range of 1-100 s^{-1} shear rates at 20°C (Figure 1.8), it is evident that the microgel viscosity does not increase after addition of CS. Indeed, comparing all the samples studied, only CS solution of 0.2% (w/v) has very similar viscosity to that of microgel **M**; mixing the two lead to microgel **CM** with a slightly lower viscosity than that of the initial microgel **M**. After polyelectrolyte complexation, a decrease in viscosity is normal to occur (Mun *et al.* 2004).

1.3.4. Microgel CM: response to stimuli

In Figure 1.9, the temperature-response curves of microgel **CM** at different temperatures and pH values are presented. Owing to the PNIAA component, the **CM** complexes follow the same trend; the higher the temperature is, the faster their volume/phase transition occurs (Figure 1.9a). However, compared with PNIAA alone (Figure 1.2a), **CM** complexes undergo a much more gradual and slower transition, even at 40°C, which is completed in more than 15 min.

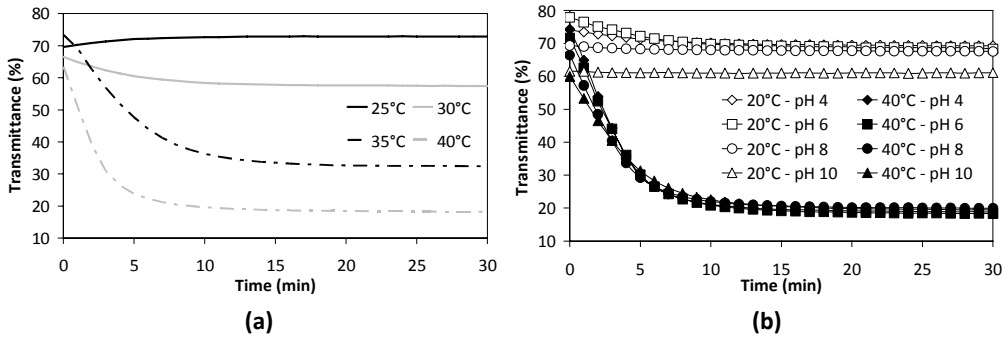

Figure 1.9: Temperature-response curves of microgel **CM** based on light transmittance changes with time, at various temperatures **(a)** and at various pH values at 20 °C and 40 °C **(b)**.

Two main factors that influence the phase transition of PNIAA microgels are the content of hydrophilic components within the microgels – related to the hydrophilic-lipophilic balance (HLB) used for the classification of surfactants (Griffin 1949) – and the concentration of thermoresponsive microparticles in the microgel samples under study (Wang *et al.* 2009). An increase in the former and a decrease in the latter factor, can lead to slower collapsing, but faster swelling, of the microparticle structure. This effect occurs due to greater affinity for, attraction, and adsorption of water molecules, the concentration of which affects the difference in osmotic pressure inside and outside the microparticles (Makino *et al.* 2000). In the case of PECs, there is a third parameter which influences the transition rate; the charge density and compensation. Through partial neutralization of the polyions, the polyelectrolyte complexes become more hydrophobic than the initially uncoupled microparticles (Shchipunov *et al.* 2009). Furthermore, depending on the nature of the oppositely charged polyelectrolyte, charge compensation results in either more flexible or stiffer structures (named “scrambled-eggs” and “ladder-like” structures (Shchipunov *et al.* 2009)). It can, thus, affect sterically the macromolecular reconfigurations during the volume/phase transition. Also, hydration of the counter-ions affects total pressure within the complexes; at equilibrium, the electrostatic osmotic pressure balances the one caused by excluded volume (Thünemann *et al.* 2004). Upon mixing CS solution with microgel **M**, polyelectrolyte complexation occurs, as well as dilution of microgel **M**. Complexation results in compensation of PNIAA charges by CS, whereas dilution results in a decrease of the content of PNIAA microparticles in the same volume of microgel **CM**. The effect of these two processes is reflected in the differences observed in Figure 1.9a compared with Figure 1.2a between the curves of microgels **CM** and **M**, respectively.

The same apply to Figure 1.9b compared with Figure 1.2b, with the added effect of pH changes. However, it is noteworthy that for microgel **CM** at 40°C – i.e. above the PNIAA LCST – changes in a wide pH range (from 4 to 10) do not seem to affect significantly the microgel thermoresponsiveness. This behavior is contrary to the behavior of microgel **M** under the same conditions. For microgel **CM**, the pH effect is more evident at 20°C, i.e. below the PNIAA LCST. At pH 6, where CS is close to its pK_a and PNIAA is almost fully ionized, according to Figure 1.4, microgel **CM** has the highest light

transmittance. This result indicates higher hydrophilicity compared with the other pH values, although the transmittance slightly decreases over time. As reported in literature, the structure of PECs is reconfigured with time; prolonged interaction of oppositely charged (weak) polyelectrolytes leads to a more compact and opaque structure of the formed complex (Mun *et al.* 2004). Therefore, light transmittance of microgel **CM** appears to decrease at pH 4 and 6 over time. At alkaline pH, CS becomes deprotonated and its macromolecular chains collapse increasing also turbidity; hence, at pH 10, the transmittance values are lower.

Having estimated the size of **CM** complexes in dry state (Figure 1.3b), size measurements were performed in hydrated state using dynamic light scattering at 20°C and 40°C and at various pH values. The data obtained are a measure of the amount of water that the complexes absorb or expel under certain pH/temperature conditions. The results are presented in Figure 1.10.

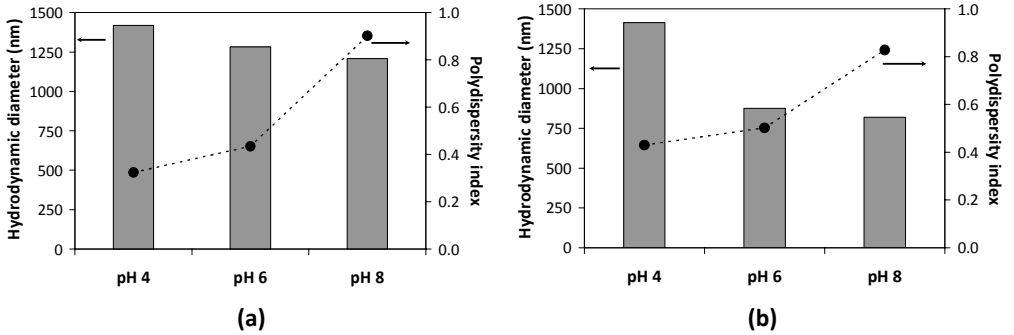

Figure 1.10: Hydrodynamic diameters and polydispersity indices of **CM** complexes determined with dynamic light scattering at various pH values and at 20 °C **(a)** and 40 °C **(b)**.

As shown, at pH 6 and 8 and at 40°C the hydrodynamic diameter* of the **CM** complexes decreases by approximately 36% compared with their diameter at the same pH and 20°C. At pH 4, however, the decrease in hydrodynamic diameter is practically undetectable. This is possibly attributed to the fact that at pH 4 chitosan macromolecules are highly protonated, whereas the PNIAA microparticles are very little ionized. Since the charge compensation is limited, chitosan macromolecular chains are extended due to mutual electrostatic repulsion, regardless of the temperature of the medium. Therefore the detected hydrodynamic diameter of the **CM** complexes depends significantly on the chitosan chain length extended from the microparticle periphery, even if the main body of the **CM** complexes, i.e. the microparticle itself, shrinks at 40°C. This suggestion is reinforced by the fact that at pH 8 the **CM** complexes have the smallest hydrodynamic diameter both at 20°C (Figure 1.10a) and at 40°C (Figure 1.10b). At that pH, chitosan

* Hydrodynamic diameter is the effective diameter of a particle in a liquid environment. The hydrodynamic diameter determined by DLS corresponds to the diameter of a sphere that has the same translational diffusion coefficient as the studied particle; it depends not only on the size of the particle "core", but also on the particle surface structure.

macromolecules are deprotonated causing chitosan chains to collapse; this effect allows PNIAA microparticles to be the main component that determines the detected hydrodynamic size of the **CM** complexes.

An important parameter supporting this assumption is the polydispersity index* (PDI) of the **CM** complexes at each pH. In both Figures 1.10a and 1.10b, the polydispersity index increases with increasing pH. In fact, it triples at 20°C between pH 4 and 8, and doubles at 40°C. From pH 4 to 6 the increase is comparatively small at both temperatures. These values reflect the reconfiguration that the **CM** complexes undergo as pH increases and as their components, chitosan and PNIAA, become consequently de-ionized or ionized. At pH 6, where the **CM** isoelectric point appears as shown in Figure 1.4, two opposite forces influence the **CM** complex size: one is PNIAA swelling owing to increased ionization of the carboxyl groups; the second is chitosan chain collapse owing to limited protonation of the primary amine groups. At higher pH, chitosan deprotonation occurs extensively leading eventually to precipitation. Since both chitosan and PNIAA are weak polyelectrolytes, these reconfigurations take place gradually and over a wide pH range. At 40°C a third parameter is also influencing the **CM** reconfigurations and that is the PNIAA volume/phase transition. All the aforementioned factors affect in combination the overall polydispersity index of the complexes, leading to the values obtained for microgel **CM**.

Size measurements in hydrated state were also performed on microgel **CM** without pH adjustment, at 25°C and 40°C, for reasons of comparison. The size distribution curves obtained are presented in Figure 1.11. At 25°C, **CM** complexes exhibit monomodal size distribution. As expected, their hydrodynamic diameter is approximately 55% bigger than their estimated one in dry state (Figure 1.3b) but also about 20% smaller than at adjusted pH 6 (Figure 1.10a). This discrepancy of sizes in hydrated states is attributed to two reasons. The native pH of microgel **CM** is 4.9 ± 0.1; when pH is adjusted to 6, the PNIAA component of the **CM** complexes swells even more because its carboxyl groups become extensively ionized. Moreover, pH was adjusted using buffer solutions, therefore, salts. It has been reported that addition of salts to PEC solutions results in weakened electrostatic interactions between the oppositely charged polyions; small mobile salt ions bond to counter-polyions with fixed charges rupturing the PEC structure (Gulyaeva *et al.* 1990; Thünemann *et al.* 2004). Depending on ionic strength, this effect leads to rearrangements within the PECs and consequent size increase (Thünemann *et al.* 2004). At 40°C, **CM** complexes exhibit bimodal distribution (Figure 1.11). A similar effect is reported in Wu et al. 1996 regarding poly-NIPAAm microgel particles in the presence of sodium dodecyl sulphate; it was explained by a possible release of the surfactant molecules as the microparticles collapse. Based on the maxima of the corresponding curves in Figure 1.11, **CM** complexes undergo almost 50% shrinkage compared with their size at 25°C. The smaller peak that appears on the curve of 40°C and corresponds to much higher sizes indicates that the polyelectrolytes

* The polydispersity index (PDI) in the DLS technique corresponds to the square of the normalized standard deviation of a Gaussian particle size distribution, and it is an estimate of the width of the distribution.

aggregate above the LCST, possibly due to increased hydrophobic interactions. It is reported in Kleinen *et al.* 2011 that thermoresponsive microgel-polyelectrolyte complexes of poly(*N*-isopropylacrylamide-co-methacrylic acid) and PDADMAC release partly the oppositely charged polyelectrolyte at temperatures above the microgel LCST; this release effect is attributed to increased charged density of the microparticles as their size decreases above their LCST (Daly *et al.* 2000). Therefore, less binding sites are available for the polyelectrolyte and it is possible that the ratio of microparticles to polyelectrolyte reaches almost 1. This can lead to precipitation or aggregation to larger complexes if polyelectrolyte macromolecules bridge or bind to two or more microparticles after the molecular reconfigurations that occur above the LCST.

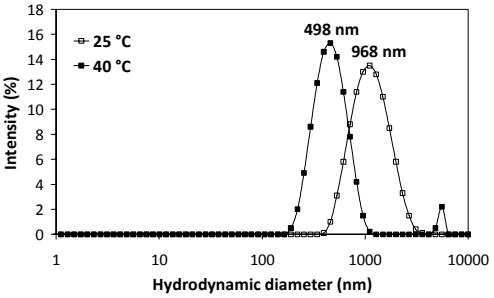

Figure 1.11: Hydrodynamic diameter distribution of **CM** complexes at 25°C and 40°C determined by dynamic light scattering.

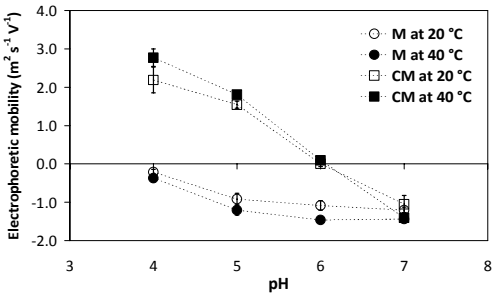

Figure 1.12: Electrophoretic mobility values for microgels **M** and **CM** at various pH values and at 20°C and 40°C.

Since charge and ion-mobility are important features of polyelectrolytes, the electrophoretic mobility of the **CM** complexes was determined at pH 4-7 and at temperatures 20°C and 40°C, as a more appropriate parameter than *ζ*-potential in the case of polyelectrolyte microgels (Hoare *et al.* 2008). The results are presented in Figure 1.12. For reasons of comparison, electrophoresis was performed under the same conditions for microgel **M,** as well. This comparison gives an insight into the combined pH/thermo-responsiveness of the microparticles both alone and when complexed with CS. As expected, the electrophoretic mobility for microgel **M** increases towards negative values with increasing pH, both at 20°C and 40°C. In the case of **CM**, as the pH increases the electrophoretic mobility decreases from positive values to almost zero at pH 6, i.e. as pH approaches the pK_a of CS. These data agree well with the graph in Figure 1.4 and they confirm that, in microgel **CM**, CS has enough protonated amine groups to complex negatively charged PNIAA microparticles and still maintain some functional groups free. With further pH increase, the electrophoretic mobility shifts to negative values for two reasons: the ionization degree of PNIAA microparticles increases, while at the same time CS macromolecules become gradually neutralized. Therefore, negative charges dominate in the microgel. The trend is the same at both 20°C and 40°C. However, at 40°C the electrophoretic mobility values are always somewhat higher than at 20°C, for both microgels. Above the LCST, the thermoresponsive microparticles collapse to smaller volumes but the amount of charges on each microparticle remains the same. Therefore,

the charge density of PNIAA microparticles is higher at 40°C than at 20°C. Consequently, the total electrophoretic mobility of microgels **M** and **CM** – which is inversely proportional to the microparticle size (Daly *et al.* 2000; Ha *et al.* 2010) – is higher at 40°C.

1.3.5. Physicochemical stability

To investigate more in depth the charge interactions between CS and PNIAA, polyelectrolyte titrations were performed. In Figure 1.13, the consumption of an oppositely charged standard polyelectrolyte is depicted for CS solution 0.2% (w/v), and microgels **M** and **CM**. PSS with a charge of -1 per monomer unit was used for titrating positively charged species, and PDADMAC with a charge of +1 per monomer unit, for negatively charged species. For this study, it was imperative to prepare a functionalizing system that would be colloidally stable; therefore, the formed PEC should not precipitate. For that purpose, a surplus of one of the two charges was required.

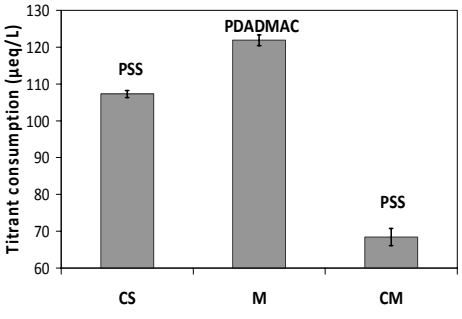

Figure 1.13: Titrant (PSS or PDADMAC) consumption after polyelectrolyte titration of 0.2% (w/v) CS solution, of microgel **M** and of microgel **CM**.

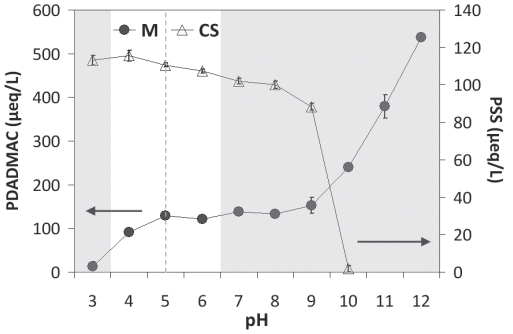

Figure 1.14: Titrant (PSS or PDADMAC) consumption after polyelectrolyte titration of 0.2% (w/v) CS solution and of microgel **M** at various pH values.

As shown in Figure 1.13, the CS solution has fewer positive charges than microgel **M** has negative charges, in their native state. After mixing them at the chosen ratio (2.5/1), the resulting microgel **CM** exhibits positive total charge (PSS consumption of 60-70 µeq/L). This result confirms that electrostatic repulsion among the complexes is present and keeps them in suspension. Furthermore, as concluded from Figure 1.14, pH 5 is the optimum pH for **CM** formation; at this pH, CS is very close to its highest ionization and PNIAA microparticles (microgel **M**) have the highest negative charge within the targeted pH range (4-8). In fact, pH 5 is exactly in the middle of the pH region that both components are ionized enough to be stable in the suspension. This pH region is from approximately 3.5 to 6.5. Below pH 3.5 (small grey area on the left of the graph), microgel **M** precipitates; above pH 6.5 (larger grey area on the right of the graph), CS starts gradually to precipitate, as well. These data not only validate the choices made for the microgel preparation, but also support the macroscopic observations that microgel **CM** is stable, at least in its native form when freshly prepared.

Its stability under various conditions was investigated further through analytical centrifugation tests. It is known that PECs undergo reconfiguration with time (syneresis) which can lead to compaction of their structure by expulsion of water and ultimately to phase separation (Kabanov *et al.* 1989; Mun *et al.* 2004). Apart form scientific reasons, providing information about the stability of the polyelectrolyte microgels in terms of sedimentation has a practical sense, too. One of the key parameters of this investigation was to provide a functionalizing system for textiles that can be prepared before and outside the textile functionalization procedure for reasons of versatility and facilitation of the textile industry. Once prepared, this functionalizing system needs to be stored and stay stable with time, at least until application on textiles. For these reasons, the sedimentation kinetics of microgels **M** and **CM**, as well as of the CS solution for comparison, were investigated through light transmission profiling under centrifugation. Indicative examples of the obtained transmission profiles for CS solution 0.2% (w/v) and microgels **M** and **CM** at 20°C, 36°C and 40°C, at pH 4, 6 and 8, and at 1000-3000 rpm centrifugation speeds, are given in Appendix I. Based on these profiles, the integral transmission for each sample was plotted against time. For CS, the corresponding graphs are presented in Figure 1.15.

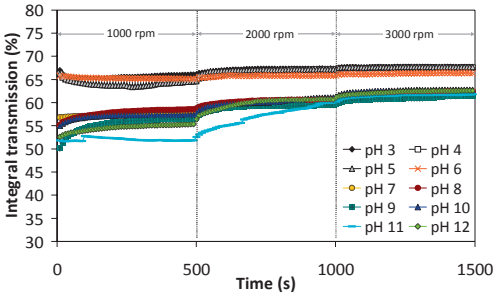

Figure 1.15: Integral transmission graphs of 0.2% (w/v) CS solutions drawn from transmission profiles (see Appendix I) obtained by analytical centrifugation at 1000, 2000 and 3000 rpm, at 20°C and various pH values.

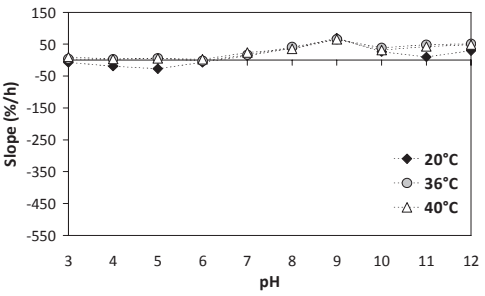

Figure 1.16: Slopes determined from the integral transmission graphs of 0.2% (w/v) CS solutions for the first 100 s they were centrifuged at 1000 rpm, and at 20, 36 and 40°C and various pH values.

From pH 3 to pH 6, and even at high acceleration, the CS solution appears very stable. As pH rises from 7 to 12, and at low speed of 1000 rpm, the integral transmission decreases because, with increasing pH, the CS macromolecules become deprotonated (confirmed also by Figure 1.14) and progressively unstable. At higher speeds, but still within the pH region of instability (7-12), transmission rises as the supernatant becomes clear from the precipitated CS. The slopes of the curves indicate the phase separation velocity and for the first 100 s of the measurement, i.e. at 1000 rpm and, thus, at low acceleration* (in order to approximate earth gravity), are given in Figure 1.16. This

* 1000 rpm correspond to 145 ×g force, for the particular rotor used.

specific time interval was chosen to enable comparison among all samples under all pH and temperature conditions tested, as it reflects the first stages of the separation process. Once more it is confirmed that above pH 7, where deprotonation becomes extensive, the slopes increase suggesting instability (Petzold *et al.* 2009). Temperature has apparently no obvious effect on the separation velocity of CS, as all slopes have similar values among the three temperatures studied.

Similarly, the integral transmission curves for microgels **M** and **CM** are given in Figure 1.17, and the corresponding slopes in Figure 1.18. As it can already be perceived from the transmission profiles of Appendix I, the combination of pH and temperature affect greatly the phase separation of PNIAA microparticles when they are either not at all or very little ionized. Comparing Figures 1.17a and 1.17b, it is evident that pH 3-4 is the instability region for microgel **M** (as expected from other measurements).

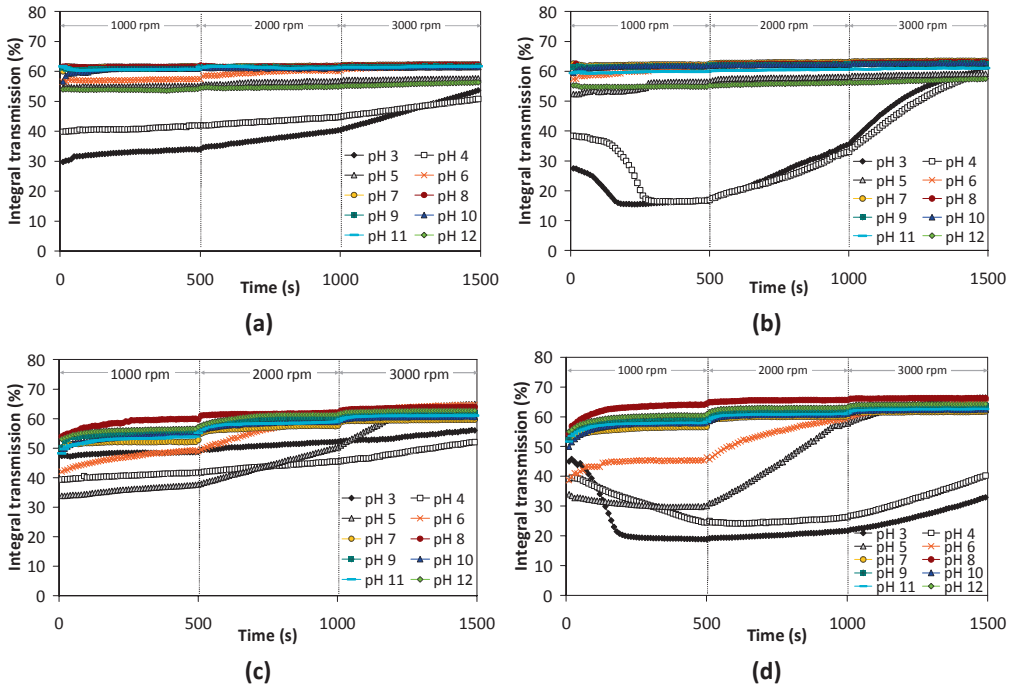

Figure 1.17: Integral transmission graphs drawn from transmission profiles (see Appendix I) obtained by analytical centrifugation at 1000, 2000 and 3000 rpm and various pH values of microgel **M** at 20°C **(a)** and 40°C **(b)** and of microgel **CM** at 20°C **(c)** and 40°C **(d)**.

However, at 40°C (i.e. above the LCST), the integral transmission graphs at those two pH values are very different from those at 20°C. For the first half of the first part of the measurements, i.e. for about 250-300 s at 1000 rpm, the curves have negative slopes. This interval coincides with the first 5 min of the volume/phase transition that PNIAA microparticles undergo above their LCST (note that the samples were not preconditioned at each temperature). It was shown in Figure 1.2 that this transition is completed within 5 min. Therefore, the integral transmission curves of Figure 1.17b

reflect also the particle-particle interactions that occur during the microparticle collapse and hydrophobization.

In Figures 1.17c and 1.17d it is shown that for microgel **CM** most reconfigurations occur in the pH region 3-6. In fact, this pH region is where the opposite progressions of CS and PNIAA ionization occur; CS becomes less charged moving from pH 3 to 6, whereas PNIAA microparticles become more charged in the same direction. When temperature also rises above the LCST (Figure 1.17d), apart from the pH-induced charge transition the temperature-induced volume/phase transition takes place, as well, resulting in curves similar to the ones of microgel **M**. However, the slopes of the **CM** curves for this particular pH region (3-6) suggest slower transition than in the case of microgel **M**. This result is supported by the graphs in Figure 1.9. During this triple reconfiguration (charge-volume-phase) of the **CM** complexes, the higher the pH is, the slower these reconfigurations occur, as the slopes of the curves show. After the transition is completed and acceleration increases (i.e. at 2000 rpm and 3000 rpm), microgel **CM** appears progressively unstable at pH 3-6. The results discussed above are summarized in Figure 1.18.

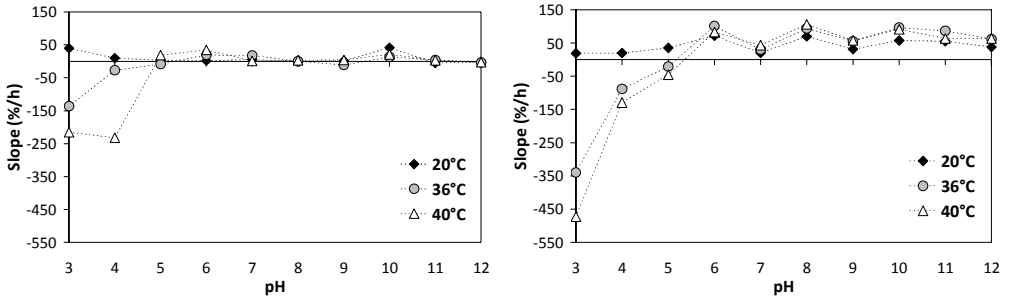

Figure 1.18: Slopes determined from the integral transmission graphs of microgel **M (a)** and microgel **CM (b)** for the first 100 s they were centrifuged at 1000 rpm, and at 20, 36 and 40°C and various pH values.

For both microgels **M** and **CM** it is evident that the combination of elevated temperature and low pH acts synergistically towards destabilization and phase separation. The negative values of the slopes at 36°C and 40°C reflect the temperature-induced volume/phase transition during which the microgels turn from translucent to opaque. However, the fact that at these temperatures the slopes increase with increasing pH, especially in the case of microgel **CM**, suggests destabilization with time. For microgel **M** (Figure 1.18a), the slopes have practically a constant value of almost zero above pH 5, suggesting high stability at all temperatures. For microgel **CM** (Figure 1.18b), until pH 5, temperature is the main factor affecting (de)stabilization. Above pH 5, the pH itself appears to be the main factor of destabilization; between pH 6-12, the slopes follow the same trend at all three temperatures but fluctuate under the pH influence. These data give useful information not only about the stability of the microgels with time but also about the optimum storage conditions for them. Moreover, they epitomize the

dually (pH- and thermo-) responsive nature of microgels **M** and **CM**, revealing the dynamics of these functionalizing systems.

1.3.6. Effect of polyelectrolyte ratio & genipin-crosslinking

The mixing ratio of polyelectrolytes is an important parameter that influences the properties of PECs (Thünemann *et al.* 2004). Thus, it was considered useful to study also the effect of the reverse CS/PNIAA mixing ratio on the properties of the functionalizing microgels. Moreover, as it will be explained in Chapter 2, one of the functionalization methods described in this research involved the use of a crosslinker between microgel **CM** and polyester. That crosslinker was genipin, a natural compound with the ability to react with primary amine groups (Butler *et al.* 2003); hence, the **CM** component that was linked to polyester was CS. In the process of binding CS macromolecules to polyester, genipin also cross-linked CS itself. Therefore, the effect of crosslinking through genipin on the properties of microgel **CM** was briefly investigated.

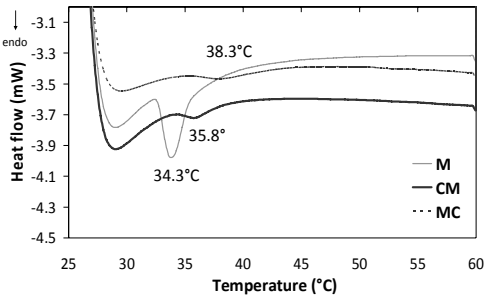

Figure 1.19: Differential scanning calorimetry (DSC) curves for the determination of the lower critical solution temperature (LCST) of microgels **M**, **CM** and **MC**.

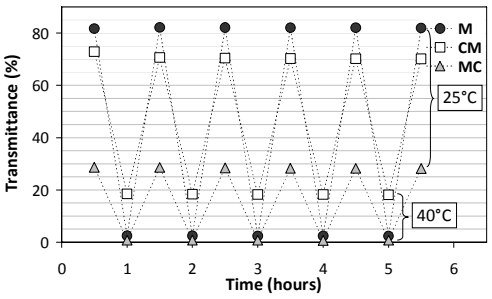

Figure 1.20: Light transmission values of microgels **M**, **CM** and **MC** at steady state after cycles of increasing and decreasing temperature between 25°C and 40°C.

In Figure 1.19, the DSC curves of microgels **M**, **CM** and **MC** are depicted (microgel **MC** is prepared with reverse polyelectrolyte ratio to that of microgel **CM**). From these graphs, the LCSTs of the microgels were determined to be 34.3°C, 35.8°C and 38.3°C, respectively. The LCST of microgel **M** is clearly identified by a strong and sharp endothermal peak on the graph, with its onset being around 32°C. This LCST value explains the differences in the temperature-response curves and the volume/phase transition rates of microgel **M** at different temperatures, presented previously in Figure 1.2a. It is noteworthy that the LCST of the microgels increases in the order $LCST_{M}$ < $LCST_{CM}$ < $LCST_{MC}$. The corresponding peaks become also broader in the same order. At elevated temperatures, the hydrogen bonds between water molecules and the amide and carboxyl groups of PNIAA break (Schild 1992). Owing to increased hydrophobic interactions, new hydrogen bonds are created between amide bonds and/or carboxyl groups of PNIAA itself. This effect results in reconfiguration of the polymer chains from extended to collapsed and coiled, causing the well-known temperature-induced

volume/phase transition. By complexing PNIAA with CS, an extra set of hydrogen bonds is created involving CS macromolecules. Thus, the energy needed to break them is higher than in the case of microgel **M**, and the LCST for microgel **CM** is shifted to a higher value. The broader difference between the onset (≈ 34°C) and offset (≈ 40°C) of the corresponding peak, compared with the one of microgel **M**, explains why the transition rate of microgel **CM** (Figure 1.9) was lower than that of microgel **M**. It is interesting, however, that even though microgel **MC** has higher content of PNIAA microparticles than microgel **CM**, its LCST is even higher than that of microgel **CM**, and the corresponding peak much weaker and broader. This result suggests that microgel **MC** has increased hydrophilicity or that its thermoresponsiveness is strongly buffered. Possible explanations for this effect are heterogeneities in the microgel network due to disruptions caused by CS macromolecules (Yoshinari *et al.* 2005) or extreme misfit of the polyelectrolytes regarding the distances between their charges, which may lead to higher degrees of swelling (Philipp *et al.* 1989; Thünemann *et al.* 2004).

In Figure 1.20, the reversibility of the thermo-responsiveness of microgels **M**, **CM** and **MC** is illustrated with cycles of increasing and decreasing temperature between 25°C and 40°C. All microgels exhibit reversible volume/phase transition, as expected for poly-NIPAAm–based hydrogels (Wang *et al.* 1998a; Zhang *et al.* 2008). However, microgel **MC** has approximately ¼ of the initial maximum transmittance values at 25°C compared with microgel **M**, indicating increased turbidity, but reaches similar minimum values (almost zero) at 40°C. Microgel **CM**, on the other hand, has both maximum and minimum values in between the ones of microgel **M**. The gridlines are drawn to help the eye trace the small decrease in the values at 25°C after each cycle. This decrease is less evident in the case of microgel **MC**, probably due to its higher content in PNIAA microparticles. However, it indicates in both cases that the PNIAA macromolecules lose their ability to fully reconfigure reversibly from coil to globule formations, just like a coil spring loses gradually its full elasticity after multiple uses. A similar effect is presented in Zhang *et al.* 2008 regarding the oscillatory shrinking-swelling kinetics of a PNIPAAm hydrogel. In the case of microgels **CM** and **MC**, CS appears to play a role in this gradually decreasing thermo-sensitivity, by buffering the volume/phase transition process, as concluded also from the temperature-response curves obtained using UV-Vis spectroscopy, and the DSC curves. Much of the research conducted with PNIPAAm-based hydrogels focuses on fast responding systems (Abd El-Mohdy et al. 2008; Zhang *et al.* 2001; Zhang *et al.* 2004; Zhang *et al.* 2008). The above conclusion regarding microgels **CM** and **MC** offers a new scope for developing systems with slow or gradual, controlled response.

Regarding the influence of crosslinking CS with genipin (GP), the first measurements involved determination of the total charge of crosslinked samples through polyelectrolyte titrations. Two series were studied; one of CS solutions only and another one of microgels **CM**. The results are given in Figure 1.21. As mentioned before, GP has the ability to react with primary amine groups. Studies reported for CS crosslinked with GP refer to optimum CS/GP ratios between 30/1 and 40/1 (w/w) (Khurma *et al.* 2005; Liu *et al.* 2008a), especially if limited but effective crosslinking is desirable. These analogies were used as a guideline in this study. The first CS/GP ratio used was 40/1 (sample GP1 of Figure 1.21).

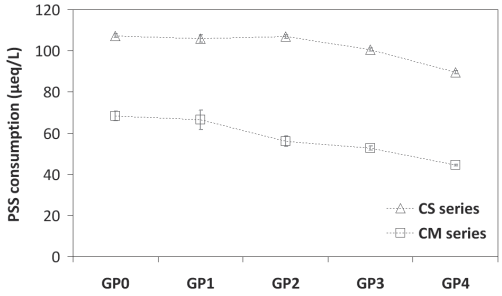

Figure 1.21: Titrant (PSS) consumption after polyelectrolyte titration of 0.2% (w/v) CS solutions and **CM** microgel samples crosslinked with various amounts of genipin.

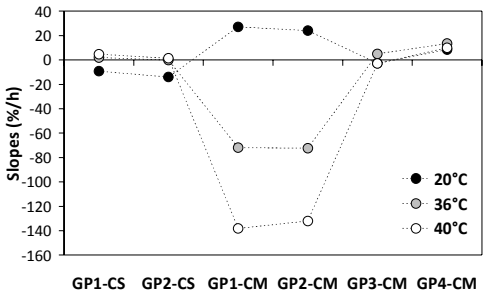

Figure 1.22: Slopes determined from the integral transmission graphs of 0.2% (w/v) CS solutions and of **CM** microgel samples crosslinked with various amounts of Genipin, for the first 100 s they were centrifuged at 1000 rpm, and at 20, 36 and 40°C and various pH values.

The rest of the samples were prepared with 2, 10, and 20 times more GP, for comparison reasons. Their description is given in Table 1.1 of the Experimental Part (paragraph 1.2.). As expected, the higher the GP content was, the lower the titrant consumption was, thus, the total positive charge of the samples. However, the decrease is more pronounced in the case of microgels **CM**. For CS, only when 10 times more GP was used (sample GP3), the crosslinking – i.e. the consumption of primary amine groups from GP – became obvious. This result can be explained by the influence that pH has on the crosslinking reaction but also by the higher availability of CS macromolecules for crosslinking. It has been reported that when the pH of the reaction medium increases, GP self-polymerizes forming long crosslink units (Mi *et al.* 2005). The pH of CS solutions is 5.2 ± 0.1 and of microgels **CM** 4.9 ± 0.1. Although the two values are seemingly the same, microgel **CM** contains an acidic component (PNIAA), even if it is a weak one. It is, hence, likely that GP in the CS solutions prefers self-polymerization, whereas in the case of microgels **CM** – the pH of which is somewhat lower – it prefers forming shorter crosslinks. In the former case, GP crosslinks only few CS amine groups, consequently leaving more positive charges available; in the latter case, it consumes more CS primary amine groups, and its effect on the total charge of the microgels is evident even at low GP contents. Furthermore, in microgels **CM**, the protonated primary amine groups of CS are ionically linked to oppositely charged PNIAA. According to Mi *et al.* 2003, GP does not compete with the ionic links. However, CS is in excess and the remaining primary amine groups are available for chemical crosslinking with GP. This dual crosslinking of CS decreases the microgel total charge much more than GP alone does in the corresponding CS solutions.

The stability of the GP-crosslinked samples was tested with analytical centrifugation at 20°C, 36°C and 40°C, and the slopes derived from the integration graphs, as described before, are given in Figure 1.22. For the CS samples with CS/GP ratios 40/1 (GP1-CS) and 20/1 (GP2-CS), there is no instability observed at any of the

three temperatures. The same applies for the microgel **CM** samples with high GP content, GP3-CM and GP4-CM. On the contrary, microgel **CM** samples with low GP content (GP1-CM and GP2-CM) have positive slopes at 20°C, and increasingly negative slopes as temperature increases to 36°C and 40°C.

As concluded also from Figure 1.23, these two latter samples exhibit higher instability below the microgel LCST (Figure 1.23a) than the more extensively crosslinked microgel samples. However, due to their limited extent of crosslinking, samples GP1-CM and GP2-CM have a more apparent volume/phase transition than that of GP2-CM and GP4-CM (Figure 1.23b, first part at 1000 rpm).

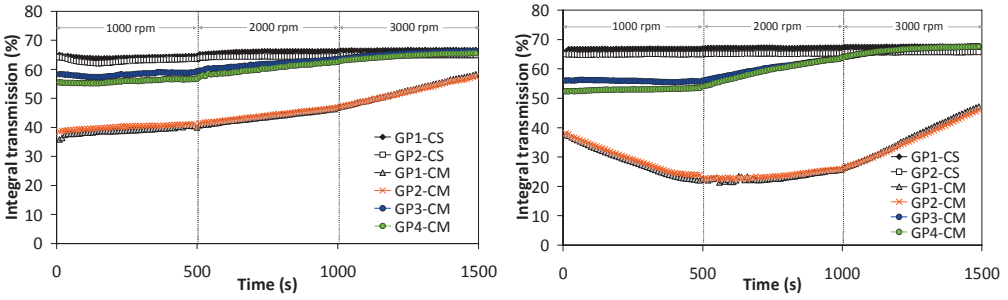

Figure 1.23: Integral transmission graphs drawn from transmission profiles (see Appendix I) of 0.2% (w/v) CS solutions and of **CM** microgel samples crosslinked with various amounts of GP, obtained by analytical centrifugation at 1000, 2000 and 3000 rpm and at 20°C **(a)** and 40°C **(b)**.

These results suggest that if microgels **CM** are crosslinked with low to moderate GP contents (i.e. CS/GP: 40/1 to 20/1 (w/w)), they will have the tendency to precipitate with time. This conclusion is useful for the incorporation of microgel **CM** via GP into polyester surface layers; it indicates an optimum extent of crosslinking, enough to increase the microgel hydrophobicity and, thus, its affinity to polyester.

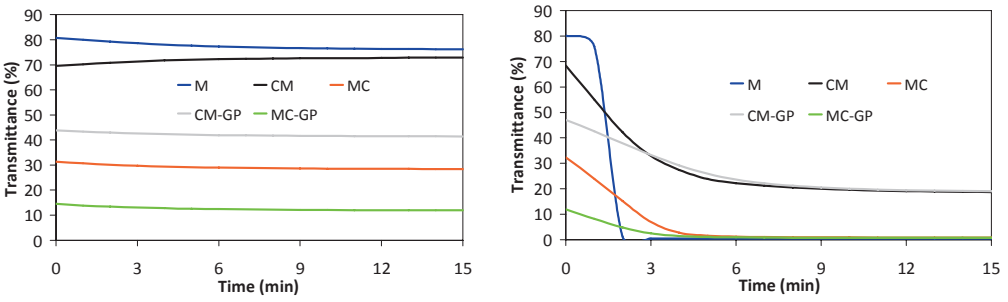

Figure 1.24: Temperature-response curves based on light transmittance changes of microgels **M**, **CM** and **MC**, with (**CM-GP**, **MC-GP**) and without GP-crosslinking, at 25°C **(a)** and 40°C **(b)**.

Having shown that low GP contents are preferable for microgel crosslinking, the temperature-response curves of microgels **CM** and **MC** with a CS/GP ratio of 40/1

(denoted in this case as **CM-GP** and **MC-GP**, for reasons of simplicity) were obtained based on light transmittance changes with time, at 25°C and 40°C. For comparison reasons, the corresponding curves of microgels **M** and **CM** are also presented in the same graphs (Figure 1.24). As expected, at 25°C, no volume/phase transition occurs for any of the microgels. It is confirmed, however, from the low transmittance values (Figure 1.24a), that crosslinking with GP at low content results in increased hydrophobicity of the microgels. At 40°C, the volume/phase transition occurs for all microgels but at different rates, as concluded from the slopes of the curves in Figure 1.24b. It is noteworthy that the PNIAA content of the microgels controls the final transmission values, i.e. the completion of the volume/phase transition, as shown in Figure 1.24b for the groups of samples **M**, **MC**, **MC-GP** (same final T%: zero) and **C**M, **CM-GP** (same T%: ≈ 20). On the other hand, the CS content of the microgels controls the initial transmission values, i.e. the increased/decreased hydrophobicity, and the rate of volume/phase transition. In fact, regardless of the PNIAA content and as long as the CS/GP ratio is the same, the temperature-induced transition rate of the crosslinked microgels is also the same, as concluded from the slopes of **CM-GP** and **MC-GP** (Figure 1.24b).

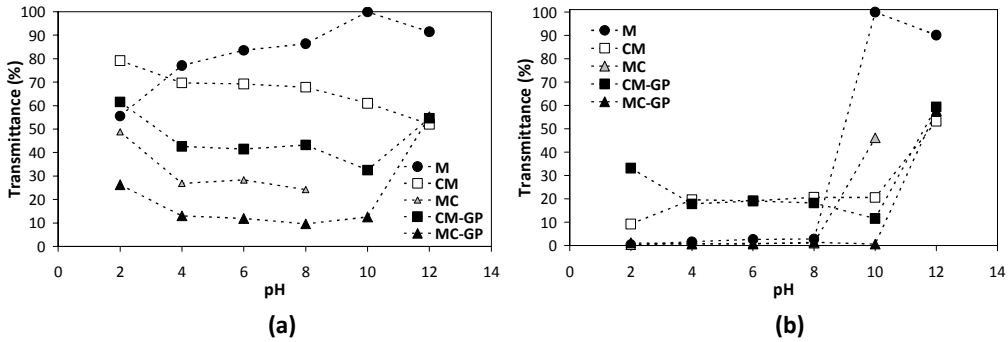

Figure 1.25: Light transmission values at steady state of microgel **M** and of microgels **CM** and **MC**, with (**CM-GP**, **MC-GP**) and without genipin crosslinking, at various pH values and at 25°C **(a)** and 40°C **(b)**.

To test whether the above behaviors are pH-dependent, the transmission values at steady state were plotted against pH, as shown in Figure 1.25. At 25°C, the light transmittance of microgel **M** increases with increasing pH, owing to the increasing ionization of PNIAA microparticles. For microgel **CM**, the opposite effect is observed of decreasing light transmittance with increasing pH, as CS chains collapse at alkaline pH, increasing turbidity. Its GP-crosslinked equivalent, microgel **CM-GP**, follows the same trend but with lower transmittance values for reasons explained before. It is noteworthy that microgel **MC** precipitates above pH 8; therefore, no values are shown in the graph for pH 10 and 12. Strangely enough, its GP-crosslinked equivalent (**MC-GP**) does not exhibit the same behavior and despite its very low transmittance values, it appears stable throughout the pH range. Moreover, the GP-crosslinked microgels have the same transmittance value as microgel **CM** does, at pH 12 (Figure 1.25a). This result is explained based on Figure 1.14 which shows that CS has remaining positive charges until pH 10, at which they completely disappear. Apparently, when that occurs, CS collapses within the

PNIAA network clearing the bulk, while PNIAA microparticles are extensively swollen. These two factors explain the increase in light transmittance at pH 12 for the GP-crosslinked microgels. This effect is even more evident at 40°C (Figure 1.25b), where the pH influence is expressed mainly in the highly alkaline region with increased transmittance values.

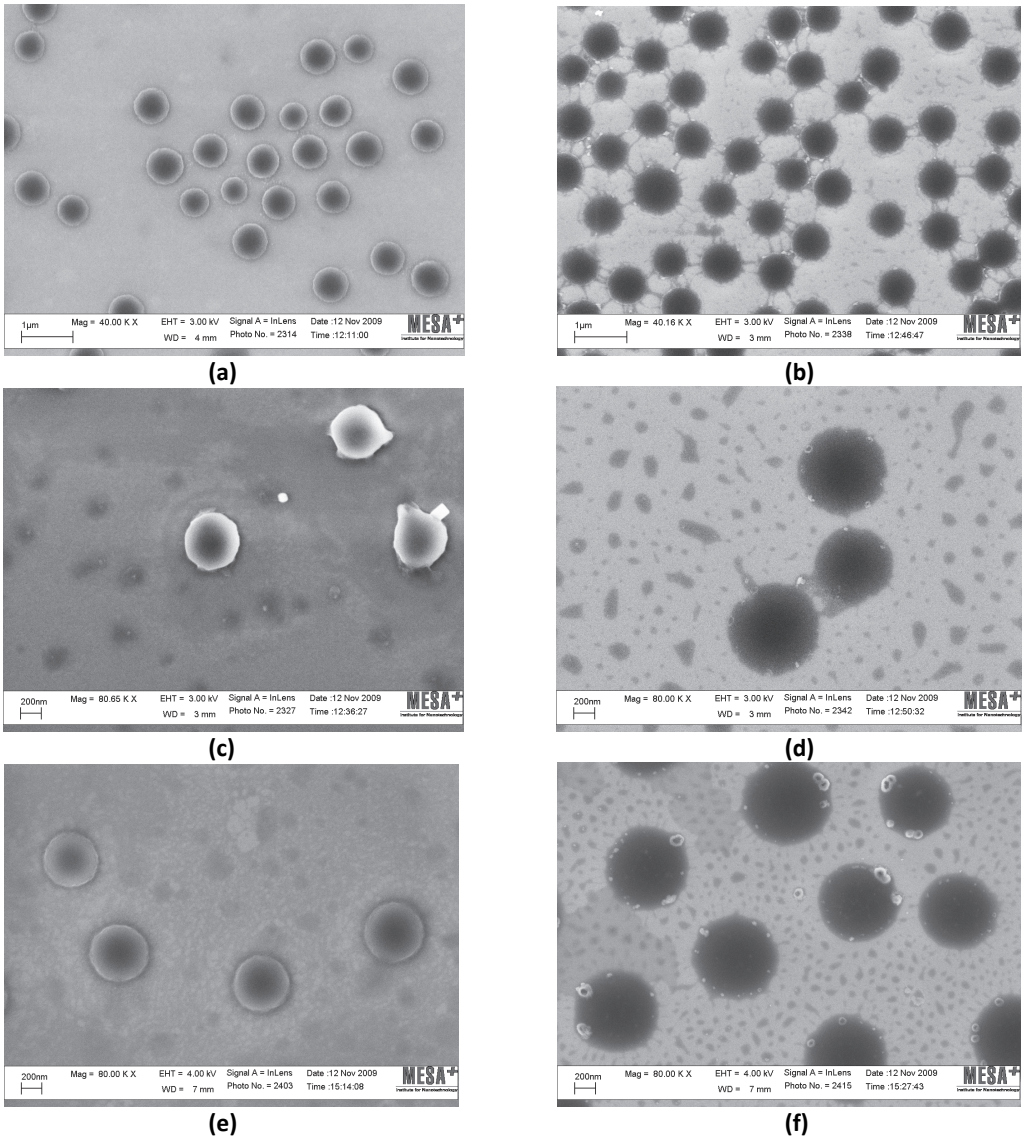

Figure 1.26: High resolution SEM images of microgel **CM** air-dried at 20°C-65% RH **(a)** and at 50°C-65% RH **(c)**, of microgel **MC** air-dried at 20°C-65% RH **(b)** and at 50°C-65% RH **(d)**, of microgel **CM** crosslinked with GP (**CM-GP**) air-dried at 50°C-65% RH **(e)**, and of microgel **MC** crosslinked with GP (**MC-GP**) air-dried at 50°C-65% RH **(f)**.

Finally, besides the influence of pH in hydrated state, the influence of temperature on the size of crosslinked and uncrosslinked **CM** (or **MC**) complexes in dry state was also investigated through SEM. Figure 1.26 depicts high-resolution SEM images of all studied polyelectrolyte complexes when air-dried at 20°C (below the LCST) or 50°C (above the LCST) and 65% RH. The major influence that CS has on the physicochemical properties of the microgels, as confirmed by all previous measurements, is reflected also on the morphology of the polyelectrolyte complexes. The general impression derived from these images is that when CS is in excess (**CM** complexes: Figures 1.26a, 1.26c, 1.26e), the complexes are more voluminous, smooth-shaped and smaller in size compared with their reverse complexes with PNIAA in excess (**MC** complexes: Figures 1.26b, 1.26d, 1.26f). In fact, **MC** complexes resemble more to the pure PNIAA microparticles (Figure 1.3a), as they appear dark, flattened, and with a rough periphery.

Based on SEM images such as those in Figures 1.3 and 1.26, the size of the PNIAA microparticles and of their complexes with CS was estimated in dry state, after they collapsed only from water evaporation (20°C-65% RH), as well as from temperature-induced volume/phase transition (50°C-65% RH). In Figure 1.27, the difference in sizes for each microgel between the two temperatures is presented, along with the corresponding percentage of shrinkage. As expected, microgel **M** shows the highest shrinkage of 29%, followed by microgel **CM** with 27% shrinkage in dry state, and its reverse microgel **MC** with 19% shrinkage. Apparently, both GP-crosslinked microgels (**CM-GP** and **MC-GP**) shrink 1/3 and 1/5 less than their uncrosslinked equivalents, respectively. In the case of **MC** complexes, their size is very similar to the size of pure PNIAA microparticles (microgel **M**) but the influence of CS is shown in their limited shrinkage.

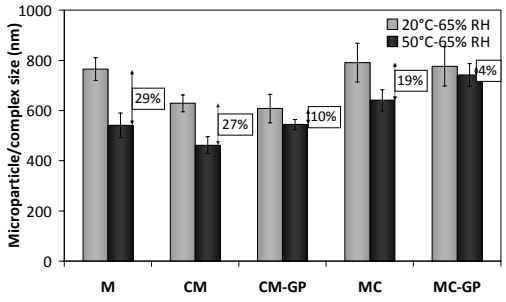

Figure 1.27: Microparticle size of microgel **M** and polyelectrolyte complex size of microgels **CM** and **MC** – with (**CM-GP**, **MC-GP**) and without genipin crosslinking – in dry state after being air-dried at 20°C or 50°C and 65% RH. The percentage of size decrease between 20 and 50°C is also depicted in the graph for each sample.

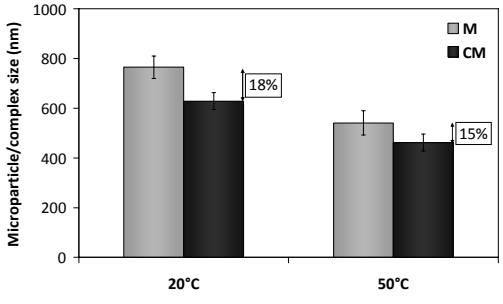

Figure 1.28: Size comparison between microgels **M** and **CM** after being air-dried at 20°C or 50°C and 65% RH. The size difference between the two microgels is also depicted in the graph for each temperature.

Finally, in Figure 1.28, the sizes of PNIAA microparticles and **CM** complexes in dry state are compared at each set of conditions used for drying. As it appears, complexation of PNIAA with CS results in 18% size reduction at 20°C and 65% RH, due to the electrostatic attraction forces that cause compaction of the particles. Furthermore, the presence of CS in the complexes limits by 15% the extent of collapse that occurs above the microgel LCST. This information will be helpful in elucidating the morphology and the properties of microgels **M** and **CM** on polyester.

1.3.7. Effect of salts

The presence of salts is another important parameter that influences the properties of PECs (Thünemann *et al.* 2004). Moreover, salts are basic constituents of human sweat. In order to assess the behavior of microgel-functionalized textiles under perspiration conditions, it was considered useful to investigate first the salt effect on microgels alone. Sodium and potassium chloride were used to prepare samples at various ionic strengths. A list of the samples is given in the Experimental Part (Table 1.2).

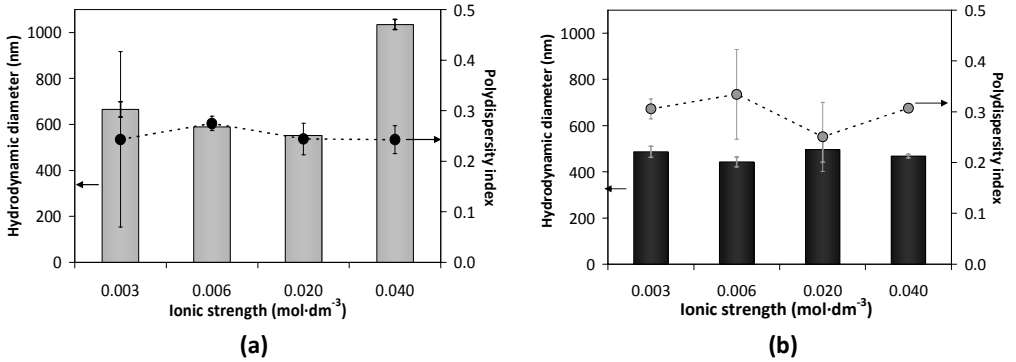

Figure 1.29: Hydrodynamic diameters and polydispersity indices of **CM** complexes determined with dynamic light scattering at various values of ionic strength – adjusted by addition of either KCl or NaCl – and at 20°C **(a)** and 40°C **(b)**.

Figure 1.29 shows the changes in the hydrodynamic diameters of **CM** complexes at 20°C and 40°C in the presence of either sodium chloride (NaCl) or potassium chloride (KCL). Below the microgel LCST, the higher the ionic strength is, the smaller the complex size becomes, until moderate values of ionic strength. This result is not surprising because small and mobile counter-ions can infiltrate the PEC network, compete with polyions of the same charge and cap the fixed charges of oppositely charged polyions. Therefore, salts can disrupt the PEC structure (Gulyaeva *et al.* 1990), and depending on the strength of their charges, they can cause high compaction of the microparticles (Lopez-Leon *et al.* 2006). Higher ionic strength (corresponding to 40 mM of NaCl, in this case) results in almost double hydrodynamic diameter at 20°C (Figure 1.29a). It is reported in Thünemann *et al.* 2004 that PECs of polyanions with carboxylic groups swell extensively in the presence of salts, until a critical salt concentration is reached, at which

PECs even dissolve. At 40°C (Figure 1.29b), the temperature-induced volume/phase transition dominates over the salt effect, as the size of **CM** complexes is similar at all ionic strengths. The average PDI, however, is higher in this case than at 20°C, indicating on-going reconfigurations of the complexes.

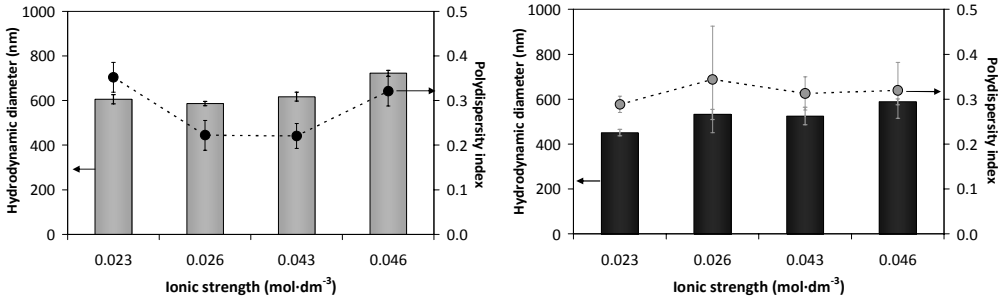

Figure 1.30: Hydrodynamic diameters and polydispersity indices of **CM** complexes determined with dynamic light scattering at various values of ionic strength – adjusted by addition of both KCl and NaCl – and at 20°C **(a)** and 40°C **(b)**.

Combining the two salts using the same concentrations, results in the graphs presented in Figure 1.30. Even though the differences in ionic strength are not as big as before, the resulting graphs are much different. The reason is that there are two types of small electrolytes in the same solution, sharing a common anion (Cl^-) but with a different cation in size and strength (polarizability), affecting greatly but also distinctly the PEC compaction and hydration (Klitzing 2006). Both below and above the microgel LCST (Figures 1.30a and 1.30b, respectively), the higher the ionic strength is, the larger the **CM** complexes become. Even after the volume/phase transition, the complex sizes decrease only by approximately 1/6 of their initial corresponding sizes.

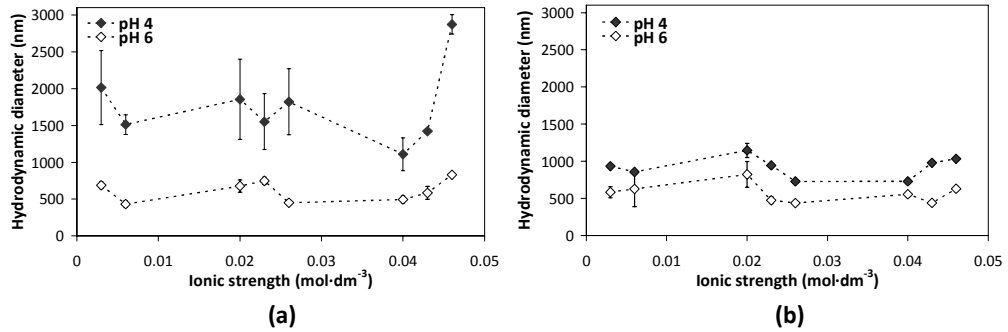

Figure 1.31: Hydrodynamic diameters of **CM** complexes determined at pH 4 and 6 with dynamic light scattering at various values of ionic strength – adjusted by addition of either one (KCl *or* NaCl) or two (KCl *and* NaCl) salts – and at 20°C **(a)** and 40°C **(b)**.

The same **CM** microgel samples were tested for changes in their hydrodynamic diameter under the same range of ionic strengths, with or without combining the two salts, and at two different pH values (within a physiological pH range). The results are presented in Figure 1.31. Below the microgel LCST, only at pH 4 and at the highest ionic strength studied (0.046 mol dm^{-3}), the hydrodynamic diameter of the **CM** complexes becomes significantly larger. Above the microgel LCST (Figure 1.31b), neither the different ionic strengths nor the presence of one or two salts affect the temperature-induced collapse of the complexes, as their mean diameter remains within the same range. It is noteworthy, however, that both at 20°C and 40°C, the complex sizes are larger at pH 4 rather than at pH 6. Moreover, throughout the tested range of ionic strengths, only at pH 4 the temperature-induced volume/phase transition is pronounced. Apparently, at pH 6 and in the presence of salts, no noticable changes in size occur between 20°C and 40°C. These results can be attributed to the fact that at pH 4, only CS is highly ionized; therefore, the volume/phase transition of the PNIAA component, which is more hydrophobic at this pH, is far more obvious than at pH 6. At the latter pH, PNIAA microparticles are extensively ionized and swollen. Thus, small electrolytes under certain concentrations and pH conditions can balance through hydration and/or by provoking aggregation (Kabanov *et al.* 1984) the water-expulsion and volume-exclusion effect of the temperature-induced volume/phase transition.

As shown in Figure 1.32, at pH 6 and in the presence of NaCl, **CM** complexes appear to have a diameter of about 500 nm, as determined also by DLS and shown in Figure 1.31a. This diameter is almost half of that of PNIAA microparticles in Figure 1.1b, due to compaction caused by electrostatic attraction forces of CS and Na^+. On the other hand, the **CM** structure appears much denser than the PNIAA structure illustrated in Figure 1.1b, owing to the pH-induced swelling and to the presence of CS macromolecular chains within the PNIAA network.

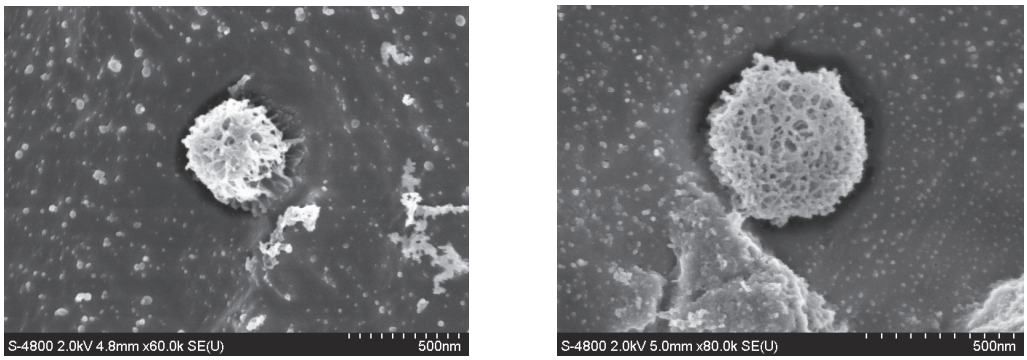

(a) **(b)**

Figure 1.32: Cryo-SEM images of CM polyelectrolyte complexes at pH 6 and in the presence of salt (0.04 M NaCl) at lower magnification **(a)** and in cross-section and higher magnification **(b)**.

These cryo-SEM images correlate well with the SEM images in Figures 1.3 and 1.26 of **CM** complexes in dry state. They also help explain the morphological differences observed between PNIAA microparticles and **CM** complexes. Finally, they confirm that

the **CM** complexes remain porous. Thus, their structure is expected to be permeable, as well, allowing water, gases, small organic molecules, salts etc. to pass through. Good permeability is one of the important characteristics of PECs, as described also in Dakhara *et al.* 2010.

1.4. FURTHER CHALLENGES & RECOMMENDATIONS

As mentioned previously in this chapter, PECs are truly unique systems, sensitive and responsive to multiple external stimuli. Their applications are multifold and in numerous fields of science and technology (Cametti 2008; Hartig *et al.* 2007; Lichter *et al.* 2009). Complexation of stimuli-responsive microgels with polyelectrolytes offers great opportunities to develop novel materials. The PECs of this investigation formed between the cationic natural polysaccharide CS and anionic PNIAA microparticles were studied at different mixing ratios and crosslinking extents in terms of their basic physicochemical properties, morphology and stability, under various conditions of pH, temperature, and ionic strength. One aspect of the CS/PNIAA PEC microgels that was not investigated is a possible application of the particular systems. A few suggestions are briefly presented below, regarding possibilities for follow-up research steps:

- Scale down the proposed PEC microgels to nano-sized systems for e.g. encapsulation of active components, fragrance, drugs etc.
- Combine or interpose a third compound in the CS/PNIAA PECs, such as a protein, which is an amphiphilic polymer, to develop new dynamic structures, prone to interact with ambient conditions.
- Develop advanced PEC microgels using advanced polymers, (e.g. molecularly imprinted, known as MIPs) based on CS and PNIAA, as highly selective functionalizing (biomedical) systems.
- Test the performance of the PEC microgels in terms of substance controlled release.

CHAPTER 2

POLYESTER TEXTILE FUNCTIONALIZATION

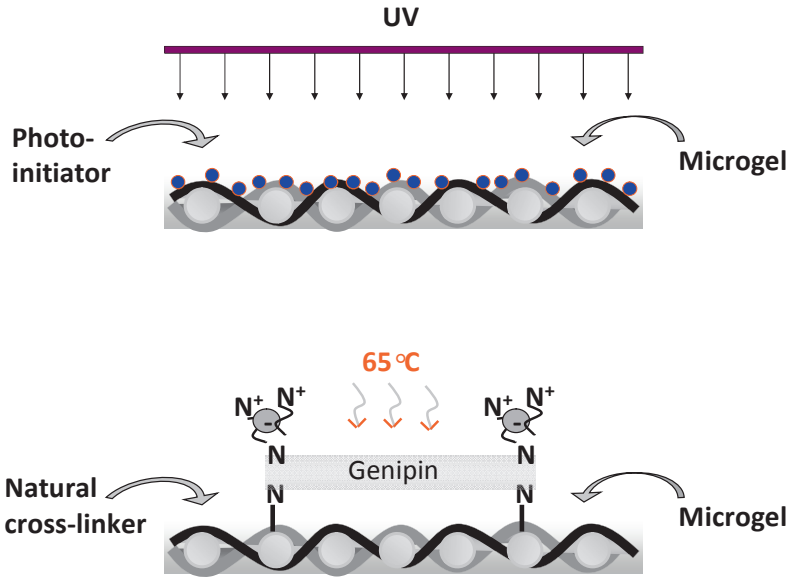

Graphical abstract 3: Microgel incorporation into polyester surface layers.

This chapter contains information included in:

Glampedaki P, Calvimontes A, Dutschk V, Warmoeskerken MMCG, Polyester textile functionalization through incorporation of pH/thermo-responsive microgels. Part II: Polyester functionalization and characterization, *Journal of Materials Science* (2011) (DOI: 10.1007/s10853-011-6006-6) (*in press*)

Glampedaki P, Dutschk V, Jocic D, Warmoeskerken MMCG, Functional finishing of aminated polyester using biopolymer-based polyelectrolyte microgels, *Biotechnology Journal* **6**(10), 1219–1229 (2011)

2.1. THEORETICAL BACKGROUND: FROM PASSIVE TO ACTIVE

"Harmony is unification of the multiplicity of the whole and concurrence of divergences"
Thesis on the "harmony of cosmos" & "music of the spheres",
Pythagoras of Samos (570–496 B.C.)[*]

2.1.1. An overview of polyester functionalization techniques

As explained in the Introduction, this research focuses on a novel approach for developing advanced textile materials with biopolymer-based functionalities: the incorporation of hydrophilic stimuli-responsive systems based on polyelectrolyte microgels into rather hydrophobic polyester surface layers. The philosophy behind this approach was dual; convergence of opposites (hydrophilic with hydrophobic, active with passive) and activation of the inert (making a rather passive material, multi-responsive).

A plethora of polyester functionalization techniques is reported in bibliography. They include single fiber or textile batch treatments, surface-only modifications, activation methods through irradiation (e.g. UV light, magnetron and plasma), thermal curing, chemical finishes for continuous coating or specific grafting of functional groups (Alem *et al.* 2008; Bessada *et al.* 2011; Geismann *et al.* 2007; Gupta *et al.* 2009; Huang *et al.* 2009; Jiang *et al.* 2010; Lopez-Santos *et al.* 2010; Mihailovic *et al.* 2010; Parvinzadeh *et al.* 2011; Sawada *et al.* 2003; Xing *et al.* 2011; Yoo *et al.* 2010). The classical pad-dry-cure method is still widely applied (Liu *et al.* 2008b; Ploymalee *et al.* 2010) especially for batch treatments. However, in search of "greener" technologies, plasma techniques in all variations of gas type, power etc. (Gouveia *et al.* 2011; Lei *et al.* 2011; Lopez-Santos *et al.* 2010; Parvinzadeh *et al.* 2011) seem to be preferred, while enzymatic treatments (Akkaya *et al.* 2011; Donelli *et al.* 2009; Kardas *et al.* 2011) are gaining interest. Furthermore, the attention for functionalization has shifted in the recent years towards localized modifications, such as photo-grafting or immobilization of functional groups and polymers on specific reactive sites of the substrate (Ito *et al.* 2007; Vladkova 2010). Another approach reported for polyester fiber functionalization involves electro-spinning in the presence of nano-particles and carbon nano-tubes (Chen *et al.* 2009; Mazinani *et al.* 2010; Xing *et al.* 2011).

Main objectives of the above forms of polyester functionalization include enhancement of its hydrophilicity (Gouveia *et al.* 2011; Sawada *et al.* 2003), wettability (Bessada *et al.* 2011; Huang *et al.* 2009), dyeability (Hossain *et al.* 2009; Kamel *et al.* 2011), electrical conductivity (Jin *et al.* 2006; Mazinani *et al.* 2010), biodegradability (Xing *et al.* 2011), and addition of new functionalities for e.g. substance entrapment and/or controlled release (Boyd *et al.* 1993; Drobota *et al.* 2010; Kaetsu *et al.* 1999). Achieving these objectives, results in new perspectives for polyester applications in the field of

[*] Pythagoras of Samos (570–496 B.C.) was a Greek pre-Socratic philosopher and mathematician, best known for his Pythagorean Theorem. The phrase is adapted after free translation based on the book of Dr. C. Vamvakas *10 "current" dialogues with the pre-Socratics*, Savvalas (2008), with reference to D. Bohm's "Wholeness and the implicate order", London: Routledge (1983).

biomedicine, technical and protective clothing, even customized apparel (Deo *et al.* 2008; Grafahrend *et al.* 2011; Xing *et al.* 2011; You *et al.* 2010).

However, none of the above-mentioned technologies is panacea for polyester functionalization and the development of novel textile-based advanced materials, as they exhibit also disadvantages and limitations. For example, chemical modifications may require multiple reaction steps (You *et al.* 2010) and large consumption of reagents. If the functionalizing system needs to be prepared *in situ* (Huang *et al.* 2009), purification and washing of the final material can become a laborious and time-consuming process. In other cases, a customized set-up is required increasing production costs. Furthermore, the final effect may be short termed; in the case of plasma treatments, for instance, the radicals produced have a short life before their deactivation (Buyle 2009). On the other hand, some techniques offer a permanent effect of e.g. increased hydrophilicity (Ploymalee *et al.* 2010) or hydrophobicity (Liu *et al.* 2008b), with no option for dynamic on-demand changes in the textile properties. Last but not least, it is often difficult to maintain a balance between the benefits of added functionalities and the drawbacks of deterioration of the starting material due to the applied functionalization (e.g. loss of elasticity or color imperfections).

2.1.2. Polyester functionalization in this study

Two techniques are proposed in this study for polyester textile functionalization with incorporation of polyelectrolyte microgels. One involves UV irradiation of polyester and the other one a low-temperature treatment. Even though both techniques are based on common practices (photo- and thermo-crosslinking), their novelty lies in the microgel-based functionalizing systems used, as well as in the use of the natural crosslinker genipin in the second case. More specifically, the first technique involves incorporation of pH/thermo-responsive microgels of CS and PNIAA (microgels **M** and **CM**, investigated in Chapter 1) in the surface layers of poly(ethylene terephthalate) (PET) textiles through UV irradiation at low wavelength (254 nm) in the presence of the photo-initiator benzophenone. PET was chosen as it is the most widely used type of synthetic polyester in the textile industry. The second technique requires first amination of polyester so that primary amine groups are introduced onto its surface; then, the aminated polyester is impregnated consecutively with a genipin solution and microgel **CM**. Microgel incorporation is expected to be achieved by the thermally induced crosslinking between polyester and chitosan primary amine groups through genipin. Evidently, the second technique is more specific as chitosan should be present in the microgel to provide the reaction groups, and polyester should be also aminated, for the same reason. In the first case of UV irradiation, any type of polyester (aminated or not) can be used, as well as all microgel types studied in Chapter 1, regardless of whether or not they contain chitosan. The reason is that, upon UV irradiation, excited photo-initiator molecules generate free radicals by abstracting hydrogen atoms from any macromolecule they interact with (Deng *et al.* 2009), whether it is of PET, PNIAA or CS origin. These radicals are capable of initiating surface graft (anchoring) reactions between PET, aminated or not, and any microgel component if it can provide hydrogen atoms.

a) UV irradiation (photo-crosslinking)

In general, benzophenone is a widely used photo-initiator of the Norrish II type* (He *et al.* 2009); upon UV irradiation its molecules shift from an excited singlet to a triplet state by intersystem crossing (ISC) (Deng *et al.* 2009). Being in that state, they initiate hydrogen-abstraction reactions from substrates, consequently providing surface radicals (Ranby 1998). On the other hand, PET is highly photo-reactive (Yang *et al.* 1996a) but it has a strong screening effect for the far UV light (200-300 nm) (Yang *et al.* 2003; Yang *et al.* 1996b). The combination of a photoinitiator highly efficient in producing surface radicals with a substrate which filters far UV light is expected to restrain the photo-crosslinking between polyester and microgels only to the irradiated surface, thus, leaving the polyester bulk practically unaffected (Yang *et al.* 2003). It is expected that in this way main intrinsic physical properties of PET would not deteriorate significantly due to photo-degradation. Usually the use of benzophenone is reported for photo-grafting reactions where a monomer is polymerized and at the same time grafted on the surface of a substrate. In this study, the material which is to be tethered on PET surfaces is already a polymeric system containing either PNIAA (microgel **M**) or PNIAA and CS (microgel **CM**). The concept is to photo-crosslink, therefore anchor, the microgels on polyester in order to covalently – thus, durably – bind the functionalizing system with the textile. Generally, photo-crosslinking of polymers (i.e. irradiation subsequent to polymerization) is used in many variations to create interpolymer networks (e.g. to produce hydrogels directly from polymer solutions (Lopergolo *et al.* 2003)) and control the morphology and properties of polymer blends, membranes etc. (He *et al.* 2009; Tran-Cong *et al.* 1991). The main requirement is the use of polymers with hydrogen-donor moieties. Photo-induced reactions of hydrogen abstraction have been reported for poly(acrylic acid) (Ranby 1998), which is one of the PNIAA components, as well as for cellulose acetate, which resembles CS structurally, in the presence of acrylic acid (Yang *et al.* 1996a). In the former case, hydrogen atoms were abstracted from the tertiary hydrogen atoms of poly(acrylic acid) chains (Ranby 1998). In the latter case, competing hydrogen-abstraction reactions were observed between cellulose acetated and acrylic acid which led to slower, thus controlled, photo-grafting (Yang *et al.* 1996a). Studies on CS wavelength–dependent photosensitivity showed that at 260 nm, CS possibly undergoes deacetylation, as well as chain scission at the glucosidic linkage, forming heterocyclic ketamines (i.e. primary amine and carbonyl groups increase) (Andrady *et al.* 1996). Amide groups, in which PNIAA is rich, are generally susceptible to photo-cleavage under certain conditions, as thorough studies on proteins and peptides have shown (Hawkins *et al.* 2001; Turecek *et al.* 2003). Also PET undergoes chain scission under UV irradiation which leads to formation of carboxylic acid groups (Fechine *et al.* 2004). The formation of radicals from

* Norrish type I photo-initiators undergo photo-cleavage, when irradiated, forming two radicals; Norrish type II photo-initiators shift to excited states and by colliding with other molecules they abstract hydrogen atoms from them creating radicals. The former type is more efficient for high polymerization yields and rates, the latter for surface grafting (Deng *et al.* 2009; He *et al.* 2009; Yang *et al.* 1996b).

any moiety depends on bond energies which need to be overcome to achieve hydrogen abstraction. Benzophenone reaches its highest energy level when irradiated at far UV (110 Kcal/mole at 258 nm) (Ranby 1998), therefore it can abstract hydrogen atoms from bonds with lower energies than that (Yang *et al.* 1996b). C–H bonds adjacent to carbonyl groups have much lower energies, thus they are prone to undergo hydrogen abstraction; C–H bonds involving tertiary hydrogen atoms have higher energy than the carbonyl-adjacent ones but lower energy than those of secondary hydrogens; bonds of primary hydrogens have the highest energy among all types mentioned, therefore, it is harder to abstract hydrogen atoms from them (Ranby 1998; Yang *et al.* 1996b). Evidently, there are many possibilities for radical formation when complex systems, such as the microgels used in this research, are irradiated. Competition among molecules with various bond types can affect the course of photo-crosslinking, as mentioned earlier; in order to favor microgel anchoring on the PET substrate rather than crosslinking microgel components with each other, PET was first impregnated with benzophenone solution and was left to dry prior to microgel impregnation and subsequent irradiation. It has been reported that allowing benzophenone to adsorb on the substrate surface as a coating, before applying acrylic acid solutions and UV irradiation, leads to higher surface-graft selectivity (Ulbricht 1996; Ulbricht *et al.* 1996). Since benzophenone is only slightly soluble in water, radical formation on the microgel components is expected to be assisted by water radiolysis. It has been reported that in aqueous solutions UV irradiation generates hydrogen atoms and hydroxyl radicals from water molecules (Janata 2002; Lopergolo *et al.* 2003). These water hydroxyl radicals can react with polymers bearing photo–reactive species, and thus generate macroradicals (Lopergolo *et al.* 2003). One of the resulting reactions of these macroradicals is recombination, leading to crosslinking.

A schematic representation of the possible photo-reaction sites of CS, PNIAA and PET is given in Figure 2.1.

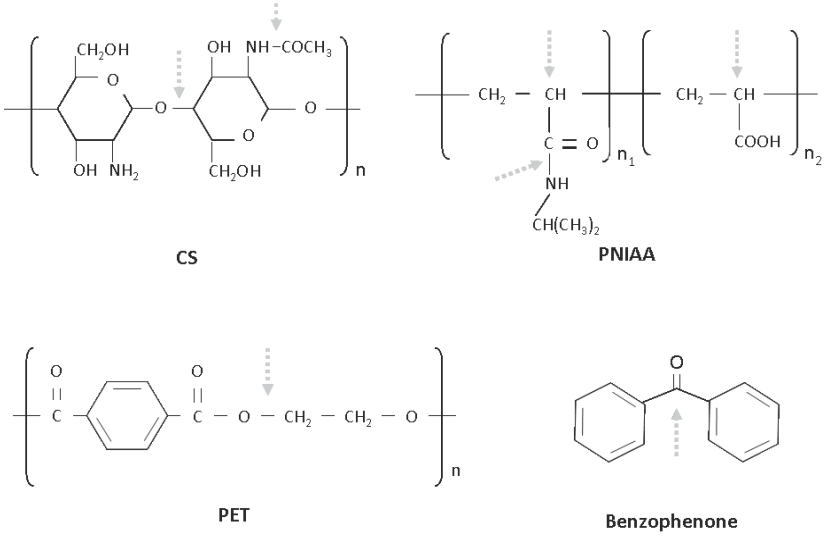

Figure 2.1: Photoreactive sites of CS, PNIAA, PET, and benzophenone.

b) Low temperature treatment (thermo-crosslinking)

As previously mentioned, the low temperature treatment suggested here is based on the use of the natural crosslinker genipin (GP), in order to covalently – thus durably – bind microgel **CM** through CS amine groups to polyester. GP is increasingly used as crosslinker for primary amine groups instead of conventional toxic crosslinkers such as glutaraldehyde and formaldehyde. To enable its use, it was necessary to introduce primary amine groups on the polyester surface.

Amination is a common polyester treatment and is carried out using various reagents (Bendak *et al.* 1991; Holmes 1996; Mazrouei-Sebdani *et al.* 2011; Nissen *et al.* 2008; Ohe *et al.* 2007). In this research, ethylenediamine was used. During amination, polyester undergoes chain scission which results in formation of amide bonds with one of the terminal primary amines of ethylenediamine (Noel *et al.* 2011; Ohe *et al.* 2007). This aminolysis effect often translates to polyester degradation with loss of weight and appearance of cracks on the polyester surface (Holmes 1996) but it provides polyester with functional surface groups. Even though, polyester was aminated in this study in order to undergo, at a second stage, thermo-crosslinking through genipin, samples of aminated polyester were used in some cases for the photo-crosslinking technique, as well, for reasons of comparison.

After amination, polyester is treated with GP for the crosslinking reaction. The reaction mechanism is not completely elucidated yet but plausible explanations of possible paths are reported in Butler *et al.* 2003, Chen *et al.* 2004, and Mi *et al.* 2005. Depending on the pH of the reaction medium, genipin forms either short dimer bridges between the crosslinked amine groups (at acidic or neutral pH) or long crosslink chains of polymerized genipin (at alkaline pH) (Butler *et al.* 2003, Chen *et al.* 2004). In brief, genipin undergoes ring opening at acidic or neutral pH due to nucleophilic attack by the nitrogen atom of primary amines (of CS or aminated PET, in this study). Thereafter, a heterocyclic amine is formed linked to the glucosamine unit of CS or to PET. A secondary reaction also takes place through nucleophilic substitution of the genipin ester group by the nitrogen atom of a primary amine group, which leads to formation of an amide bond (Chen *et al.* 2004; Mi *et al.* 2005). At basic pH, the ring-opening reaction of genipin occurs via nucleophilic attack by hydroxyl groups of the aqueous solution. Consequently, aldehyde groups are formed which undergo polycondensation, resulting in genipin oligomers or polymers. A Schiff-base* reaction possibly takes place between the terminal aldehyde groups of the polymerized genipin and primary amine groups of e.g. chitosan, which leads to formation of a crosslinked network.

In this study, the crosslinking reaction between primary amine groups of CS and PET takes place at slightly acidic pH, considering that in Chapter 1 the pH of microgel **CM** was determined to be approximately 5. Therefore, it is expected that genipin will react forming preferably heterocyclic amines and, as crosslinks, short dimer bridges rather

* Imines of the type $R_2C=NR'$, where R' is not a hydrogen atom. *IUPAC. Compendium of Chemical Terminology, 2nd ed. (the "Gold Book"), compiled by A. D. McNaught and A. Wilkinson, Blackwell Scientific Publications, Oxford (1997).*

than long polymer chains. It should be noted that in parallel with the reaction of crosslinking microgel **CM** to polyester, partial inter/intra-molecular crosslinking of CS amine groups is also expected to occur within microgel **CM** because genipin reacts with primary amine groups regardless their origin. Hence, it is possible that a network among **CM** complexes is created on the polyester fibers with genipin crosslinks in between.

A schematic representation of the polyester amination and the thermo-crosslinking reaction between microgel **CM** and aminated polyester is given in Figure 2.2.

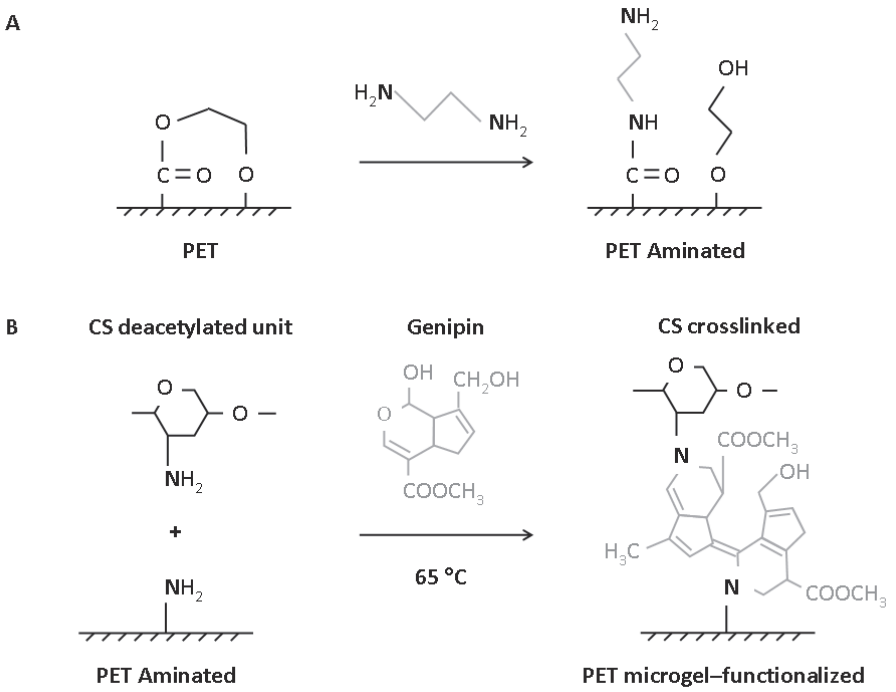

Figure 2.2: Schematic representation of the possible reaction paths involved in the low temperature functionalization technique.

Advantages and points of concern for both techniques

Main advantages of both techniques are: the few and facile reaction steps; the simple equipment and accessories required; the fact that preparation of the functionalizing system takes place outside the textile functionalization procedure, offering versatility in the microgel composition and easiness at the final cleaning step. Also, the application of a ready-to-use hydrophilic system directly on polyester textile, as opposed to single fibers, offers the advantage that ready-made commercial textiles can be functionalized, without adjusting the actual textile production line. Furthermore, using stimuli-responsive microgels for polyester textile functionalization offers a unique

advantage: tailored and regulated water management properties. Microgels contain by definition large amounts of water. Therefore, microgel-functionalized polyesters are expected to exhibit increased wettability under certain conditions. Moreover, as explained in paragraph 1.1.1 of Chapter 1, pH/thermo-responsive microgels attract or expel water according to the ambient conditions of pH and temperature. Hence, polyester textiles functionalized with stimuli-responsive microgels are expected to exhibit not only improved but, more importantly, controlled and tunable water management properties, according to the demands of their environment. Additionally, both functionalization techniques are expected to have a long-lasting effect owing to the covalent bonds created during the cross-linking reactions. Last but not least, the use of biomaterials, the absence of toxic organic solvents from the reactions involved, and the low energy requirements due to the use of UV light and low temperatures constitute an eco/user-friendly alternative to conventional textile finishes.

Despite the many advantages, the proposed functionalization techniques present also drawbacks. For instance, in the case of UV irradiation, it is possible that polyester degradation occurs with consequent deterioration of the textile physical, mechanical, even tactile intrinsic properties (Fechine *et al.* 2004). Furthermore, uniformity of the incorporated microgel on the polyester fibers can be a concern, as it depends strongly on the uniform creation of reactive sites on the fibers. The same points of concern apply also to the low-temperature treatment, with the addition of the development of a green-blue coloration due to the genipin reactions (Butler *et al.* 2003). Whether or not these effects appear and to what extent will be discussed in the following pages.

2.2. EXPERIMENTAL PART

2.2.1. Materials

Two types of woven PET textiles (Verosol, The Netherlands) were used as starting materials for functionalization. They were chosen on the basis of availability, weight difference (one is light-weight, the other one is of almost double weight), and density of structure (one has an openness factor of 0.5%, the other one of 0%). The basic characteristics of both PET types are given in Table 2.1, and their different surface morphology is depicted in Figure 2.3. Both polyesters were thermo-fixed by the production company; the first type (PET 1) at 210°C and the second one (PET 2) at 170°C.

Table 2.1: Types and features of polyester textiles used for functionalization

Textile features	**PET 1**		**PET 2**	
Type	Woven (crêpe)		Woven (plain)	
Weight (g/m^2)	73 ± 3		142 ± 3	
Openness factor (%)	0.5		0.0	
Yarn features	**Warp**	**Weft**	**Warp**	**Weft**
Type	Flat	Textured	Flat	Flat
Fineness (dTex)	72	167	167	167
Density (threads/cm)	38.5 ± 1.5	22.0 ± 1.5	34.5 ± 1.5	22.0 ± 1.5

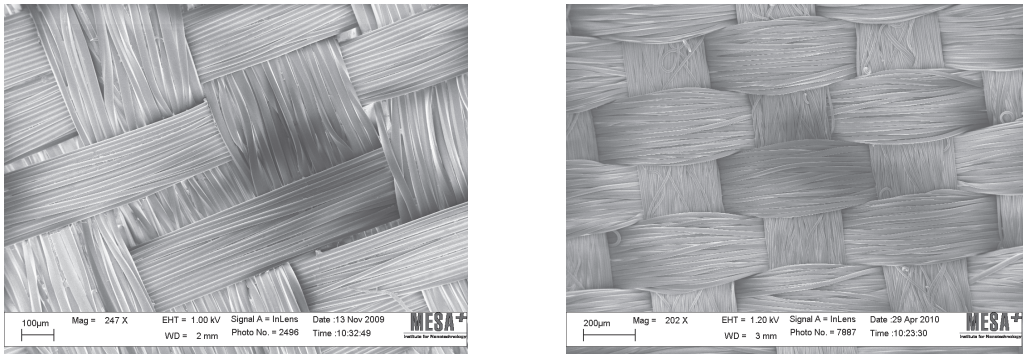

(a) **(b)**

Figure 2.3: High-resolution SEM images of the reference polyester textiles PET R 1 **(a)** and PET R 2 **(b)** used as starting materials for functionalization.

Microgel **CM** was the main functionalizing system used (*see* Chapter 1); however, microgels **M** and **MC** were also applied in some cases for reasons of comparison. Ethylenediamine (Sigma-Aldrich) was used for the polyester amination. Benzophenone (Acros Organics) was used as a photo-initiator for microgel incorporation in polyester surface layers using UV irradiation. According to Geismann *et al.* 2005, a photoinitiator of

opposite charge than that of the treated surface leads to higher grafting efficiencies. Thus, for the UV irradiation of aminated polyesters the anionic photoinitiator 4-benzoyl-benzoic acid (Acros Organics) was used. For the low-temperature treatment of aminated polyesters and the incorporation of microgel **CM**, genipin (Wako, Japan) was used as a crosslinker of primary amine groups.

The non-ionic detergent Tanaterge EP5071 (Tanatex, The Netherlands) was used for textile washing. Acid Orange 7 (C.I. 15510, Aldrich) was used for the colorimetric determination of the total amine contents, and Methylene Blue hydrate (C.I. 52015, Acros Organics) for the total carboxyl contents of polyester samples. Tris(hydroxymethyl)aminomethane (Tris, Aldrich), sodium phosphate monobasic (Fluka) and dibasic dihydrate (Sigma) were used for buffer solutions. All other reagents were of analytical grade.

2.2.2. Microgel incorporation into polyester surface layers

a) UV irradiation (photo-crosslinking)

PET 1 and PET 2 pieces of dimensions 4 cm x 12 cm were first impregnated with a benzophenone solution of 0.05 M in 90% ethanol. In the case of aminated polyester (*for its preparation, see below in paragraph 2.2.2b*), pieces of the same dimensions were impregnated with a 4-benzoyl-benzoic acid solution of the same concentration. The chosen sample dimensions were dictated by the size of the ultra-violet (UV) lamp used. After impregnation with the photo-initiator solutions, the samples were air-dried and subsequently immersed into 20 ml of microgel **M**, **CM** or **MC** for 1 h. Then, they were placed on clean Teflon substrates 3 cm below an ENF-260C dual-wavelength UV lamp (Spectroline, U.S.A.) with tubes of 6-Watt power each. The samples were irradiated at 254 nm wavelength for 30 min. After being dried, they were thoroughly rinsed for 24 h under mild shaking with a 50% (v/v) ethanol solution periodically refreshed, to remove benzophenone and any unreacted, thus physically adsorbed, microgel. After air-drying at room temperature and in order to test the durability of the functionalization, polyester samples were also washed with a detergent solution of 5 g/L Tanaterge EP 5071 and 2 g/L Na_2CO_3 at 50:1 liquor-to-cloth ratio. Washing was performed with a Linitest (SDL Atlas, United Kingdom) apparatus under mild rotation for 30 min at 60°C. Finally, the samples were air-dried at room temperature and kept in a desiccator until further use.

b) Low-temperature crosslinking (thermo-crosslinking)

Polyester amination

For the low-temperature treatment, amination is a prerequisite in order to introduce primary amine groups on the polyester surface with which the crosslinker genipin can react. The amination procedure followed was based on a protocol described in Bhat *et al.* 2008. PET 1 and PET 2 pieces were immersed into a 50% (v/v)

ethylenediamine solution with a liquor-to-cloth ratio of 50:1. Amination proceeded in a 60°C water bath for 1 h under shaking. The samples (denoted as PET A 1 and PET A 2) were then thoroughly rinsed with periodically refreshed water for 24 h. Finally, they were air-dried and kept in a desiccator until further use.

Thermo-crosslinking using genipin

PET A 1 and PET A 2 samples of dimensions 5 cm × 5 cm were first immersed into a 1.8 g/L genipin solution* in 90% (v/v) ethanol and were passed through a laboratory padder with 100% add-on. After drying for 30 min at room temperature, the samples were impregnated with microgel **CM** and were passed again through the padder. The cross-linking reaction of genipin with chitosan and polyester primary amine groups took place at 65°C for 1.5 h. Finally, the functionalized polyesters (denoted as PET ACM 1 or PET ACM 2) were washed with a non-ionic detergent solution as described above for the UV-irradiated samples. Air-drying and storage were also conducted in the same way.

Table 2.2: Combinations of polyester and microgel types under study

Polyester – Microgel sample combinations	**Microgel types**		
Polyester types (& techniques)	**M**	**CM**	**MC**
PET R 1 (UV)	X	X	X
PET R 2 (UV)	X	X	
PET A 1 (UV)	X	X	X
PET A 1 (T-GP)		X	
PET A 2 (T-GP)		X	

The combinations of polyester and microgel types used for the two functionalization techniques are given in Table 2.2. The general sample code PET R corresponds to reference non-functionalized polyesters (either of the PET 1 or PET 2 type), and PET A to aminated polyesters. The specific sample codes of the polyesters prepared, their description and their microgel dry add-ons are presented in Table 2.3.

* Ideally, it would be preferable that half of the amount of genipin used would react with the polyester amine groups and the other half with CS amine groups, forming dimer bridges between them. Other reactions may occur, such as intermolecular CS crosslinking or genipin polymerization. These reactions are more likely to occur when genipin is in excess, in which case an intense blue-green coloration is developed, which is undesired for polyester. Furthermore, in paragraph 1.3.6 of Chapter 1 it was shown that low genipin amounts (CS/GP 40/1 or 20/1 (w/w)) that partly crosslink CS chains increase hydrophobicity of microgel **CM**, and they are, thus, expected to favor the microgel affinity with polyester. For these reasons, low genipin concentrations were chosen for the polyester thermo-crosslinking with microgel **CM**. The genipin solution was prepared with the minimum quantity of genipin required to crosslink the primary amine groups of polyester, which were determined colormetrically, as described further in this chapter.

Table 2.3: Polyester textile samples under study

Polyester textile sample codes	Type	Description	Dry microgel add-on (%)
PET R 1 or 2	Reference	PET 1 or PET 2 textile type	_
PET RM 1 or 2	Microgel-functionalized	PET R 1 or 2 with microgel **M** UV-irradiated	PET RM 1: 0.4 ± 0.2 PET RM 2: 0.6 ± 0.2
PET RCM 1 or 2	Microgel-functionalized	PET R 1 or 2 with microgel **CM** UV-irradiated	PET RCM 1: 0.6 ± 0.2 PET RCM 2: 1.1 ± 0.3
PET RMC 1	Microgel-functionalized	PET R 1 with microgel **MC** UV-irradiated	0.9 ± 0.2
PET A 1 or 2	Aminated	PET 1 or PET 2 treated with ethylenediamine	_
PET AM 1	Microgel-functionalized	PET A 1 with microgel **M** UV-irradiated	0.7 ± 0.2
PET ACM 1	Microgel-functionalized	PET A 1 with microgel **CM** UV-irradiated	0.5 ± 0.1
PET AMC 1	Microgel-functionalized	PET A 1 with microgel **MC** UV-irradiated	0.9 ± 0.3
PET ACM-T 1 or 2	Microgel-functionalized	PET A 1 or 2 with microgel **CM** genipin-treated at low temperature	PET ACM-T 1: 1.0 ± 0.2 PET ACM-T 2: 1.4 ± 0.1

2.2.3. Textile surface analysis and characterization

Scanning electron microscopy (SEM)

The polyester surface morphology was observed using a high-resolution scanning electron microscope LEO 1550 (Carl ZEISS, Germany) with a field emission gun operating at 0.5-2.0 kV, depending on the sample. PET textile specimens of approximately 0.5 cm × 0.5 cm were glued with double-face tape on the sample holder and, if necessary, they

were gold-sputtered prior to analysis. Otherwise, they were observed without further pretreatment.

Fourier-transform infra-red spectroscopy with attenuated total reflectance (FTIR-ATR)

A Spectrum 100 series (Perkin Elmer, USA) FTIR spectrophotometer with an ATR accessory was used to collect the polyester infrared spectra and detect any changes in the polyester chemical groups before and after functionalization. For each sample, 32 scans were performed between 650 and 4000 cm^{-1} with a resolution of 2 cm^{-1}. To facilitate the data evaluation and explain the results of the functionalized polyester analysis, the spectra of CS and PNIAA were also collected. Samples of CS solution 0.2% (w/v) and of microgel **M** (containing PNIAA microparticles) were cast in petri-dishes and were left to dry at room temperature. The films that were formed were then analyzed using the above-mentioned spectrophotometer with the same parameters as those used in the case of the polyester samples.

X-ray photoelectron spectroscopy (XPS)

The polyester surface chemical composition was determined by X-ray photoelectron spectroscopy using a Quantera scanning microprobe spectrometer (Physical Electronics, USA). Samples were irradiated with monochromatic Al Kα X-rays (1486.6 eV) at 25 W. The standard beam and detector input angle was 45°. Survey spectra were recorded from -5 eV to 1345 eV with pass energy of 224 eV and a step of 0.8 eV. Spectra fitting were done with respect to the reference binding energy of the aliphatic carbon 1s orbital at 284.8 eV.

Colorimetric determination of functional groups (staining)

a) Methylene Blue assay for carboxyl groups

For the determination of the total carboxyl content of PET samples, staining with methylene blue was performed as described in Bide *et al.* 2006b. Samples of 1 cm x 1 cm were immersed for 1 h in 5 ml of working solution of methylene blue (16 µM methylene blue in buffer solution of 0.1 M Tris of pH 8). The samples were then removed and the absorbance of the solutions at 611 nm was read (A_1). The stained PET samples were afterwards immersed for 1 h in 5 ml of 0.1 M Tris (wash solution, pH 8). The samples were then removed and the absorbance of the wash solutions was read at 611 nm (A_2). In order to determine the dye concentrations corresponding to the recorded absorbances, a calibration curve was drawn with six standard solutions of methylene blue in 0.1 M Tris with known concentrations between 0.5 and 16 µM. Since all PET samples were immersed in the 16 µM working solution of methylene blue, the maximum dye uptake of the samples would correspond to the absorbance of the 16 µM working

solution (A_0). Therefore the maximum amount of dye μmoles found in the 5 ml of the working solution is known (D_0). From the A1 value and the calibration curve, the amount of dye μmoles remaining in the working solution after the staining can be calculated (D_1). Subtracting D_1 from D_0 gives the amount of dye μmoles found on each PET sample. However, this value needs to be corrected by subtracting the amount of dye μmoles that leached out in the wash solutions. This amount (D_2) is determined based on A_2 and the calibration curve. Since methylene blue has only one positive charge in its molecule, 1 mole of dye corresponds to 1 mole of carboxyl groups and therefore the carboxyl content of the samples per gram of textile can be calculated. All measurements were done in triplicate.

b) Acid Orange 7 assay for amine groups

For the determination of the total amine content of PET samples, staining with Acid Orange 7 was performed based on a procedure described in Geismann *et al.* 2005. Briefly, a working solution was prepared with a dye concentration of 0.5 M and with a pH value adjusted to 3 with hydrochloric acid. PET samples of 1 cm x 1 cm were immersed for 1 h in 5 ml of the working solution. Afterwards, the stained samples were rinsed three times with a hydrochloric solution of pH 3 to remove any excess of dye adsorbed on the samples that was not electrostatically bound. Then, the samples were immersed for 1 h in 5 ml of a sodium hydroxide solution with pH 12 to release the dye. The absorbance of this last solution at 479 nm was recorded for all samples and the corresponding dye concentrations were calculated from a calibration curve drawn in advance with standard dye solutions. Since Acid Orange 7 is a dye with only one sulphate group, 1 mole of dye corresponds to 1 mole of sulphate groups which corresponds to 1 mole of amine groups on the PET samples. All measurements were done in triplicate.

Electrokinetic analysis (streaming potential measurements)

The ζ potential of polyester textiles was determined with streaming potential measurements using an electrokinetic analyzer (EKA, Anton Paar) according to the procedure described in Stawski *et al.* 2009. The measuring cell was cylindric with a diameter of 26 mm. The electrode solution was of potassium chloride 0.001 M and titration was performed in the pH range 3-10 using 0.1 M hydrochloric acid and 0.1 M potassium hydroxide.

Surface topography with optical scanning and confocal microscopy

The surface topography of the polyester samples was characterized using an optical non-contact 3D scanner, MicroGlider (FRT, Germany). The measuring principle which is based on chromatic aberration of light and any related calculations are described in detail elsewhere (Calvimontes 2009; Calvimontes *et al.* 2010a; Hasan *et al.* 2008). Parameters such as the textile dimensional changes (relaxation, shrinkage), macro-roughness (waviness), surface macro-porosity and micro-porosity were

determined based on images of dimensions 2 mm × 2 mm. Indicative and characteristic examples of such images are presented in Appendix II. The sequence of these images helps to explain how certain topographic parameters are derived.

The fiber mean arithmetic roughness (R_a) was determined for a measuring length of 50 μm along the fiber length, using a confocal microscope Nanofocus μsurf explorer (Nanofocus AG, Germany) and appropriate software. For this analysis, a textile specimen of 2 mm x 2 mm was first glued with double-faced tape on a microscope objective plate; then the plate itself was also glued on the microscope base. This was done to avoid misplacement of the sample between measurements and therefore keep the same x-, y-co-ordinates for all analyses. Light intensity and z- values were adjusted according to the required focus. Each sample was analyzed first dry. Then, it was impregnated with a drop of a pH 4 buffer solution; it was characterized through imaging, and finally, it was again dried. The same steps were followed for the analysis with buffer solutions of pH values 6 and 8.

Reflectance spectroscopy

A SpectroEye (X-Rite, USA) reflectance spectrophotometer was used to determine the CIE whiteness index (WI) and the ASTM 313 yellowness index (YI) of polyester samples. The values were automatically derived at the end of each measurement, after calculations based on the colorimetric coordinates measured. The CIE L*a*b* values and the reflectance spectra were also obtained from the same measurements. Each sample was folded twice (four layers) to avoid background interference and it was measured five times at different spots of the textile with a D65 illuminant and a CIE 1964 supplemental standard 10-degree observer.

Crease recovery angle[*]

A crease recovery tester (Mesdan, Italy) was used to measure the polyester crease recovery angles. PET samples with dimensions 1.5 cm x 4.0 cm were cut along the weft or the warp direction of the textiles and were conditioned for 24 h at 20°C and 65% RH prior to the measurements. Each cut specimen was evenly folded face-to-face and a load of 10 N was placed onto it for 5 min. A small piece of paper was inserted beforehand between the two folded sides to avoid that they stick together after the load was lifted. After 5 min under load, the sample was rapidly removed and placed with one side on the holder with an adjacent goniometer. As one side of the sample was freely unfolding on the holder, caution was taken so that this unfolding part was kept always aligned with the axis of the goniometer. The angle that the sample reached after 5 min of monitoring and aligning was recorded as its crease recovery angle. All measurements were done in triplicate.

[*] It is a measure of crease resistance expressing the ability of a creased or wrinkled fabric to recover its original shape over time (http://www.textileglossary.com).

Mechanical strength

The strip method, according to the standard ISO 13934-1 (Bilisik *et al.* 2010; Rukuiziene *et al.* 2006), is one of the most common techniques for mechanical testing of textiles. However, in the case of the UV-irradiated polyester samples it was not possible to follow the specifications of that standard which required samples 20 cm long, because the maximum sample length was 12 cm due to the size of the available UV lamp. Moreover, it was wished for to measure at least a triplicate from each specimen, preferably prepared from the same batch in order to avoid any discrepancy in results attributed to differences during preparation. Therefore, a general standard for thermoplastics, the DIN EN ISO 527-2/S2/ 50, was followed. The instrument used for the measurements was a pneumatically operated Zwick 8195.05 tensile tester employed in the traverse mode. The load applied on samples with 20 mm width was 1 kN with 0.5 N preload and with elongation rate of 50 mm/min. The specimens were cut along the weft direction to enable comparison between the PET 1 and PET 2 sample types, as in that direction both types have the same yarn density and fineness values. Moreover, it is known that the tensile strength depends on the textile structure, as well as on the yarn density and fineness (Bilisik *et al.* 2010; Rukuiziene *et al.* 2006). Since both PET types have lower weft densities compared with their warp ones and, furthermore, the PET 1 weft yarns are textured, any effect on the tensile strength was expected to be more noticeable in the weft direction of the textiles. All samples were conditioned and measured at 23°C and 50% RH.

2.3. RESULTS & DISCUSSION

Microgel-functionalized polyester samples were characterized in terms of surface morphology, chemical composition, charge, topography, physical and mechanical properties. Various samples were compared to investigate the effect of different microgel types (e.g. comparison of PET RM 1, PET RCM 1 and PET RMC 1), polyester types (comparison of PET 1 with PET 2, and their aminated equivalents), and functionalization techniques (e.g. comparison of PET ACM 1 with PET ACM-T 1). The results are presented in the following paragraphs.

2.3.1. Surface morphology

In Figures 2.4 and 2.5, the surface morphology of PET 1 polyester samples is presented, as observed through SEM.

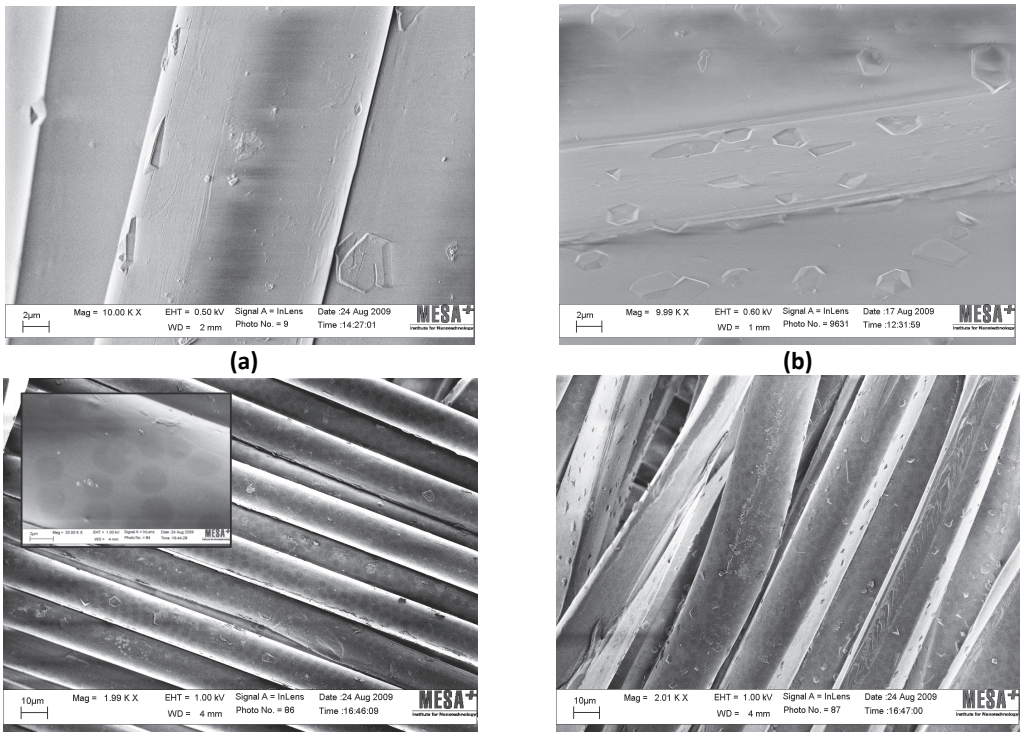

Figure 2.4: High-resolution SEM images of PET R 1 warp **(a)** and weft **(b)** yarns, and of PET RCM 1 warp **(c)** and weft **(d)** yarns. The inset in image **(c)** depicts a warp filament in 10-times higher magnification.

Compared with reference polyester PET R 1 (Figures 2.4a and 2.4b), the functionalized polyester PET RCM 1 (Figures 2.4c and 2.4d) appears to have dark circular formations uniformly distributed on its warp and weft fibers. The angular protrusions

found present on the surface of both warp (Figures 2.4a) and weft (Figures 2.4b) fibers of the reference polyester are oligomers resulting from the fiber production process and they unavoidably leach out from the fiber bulk, even after thorough washing.

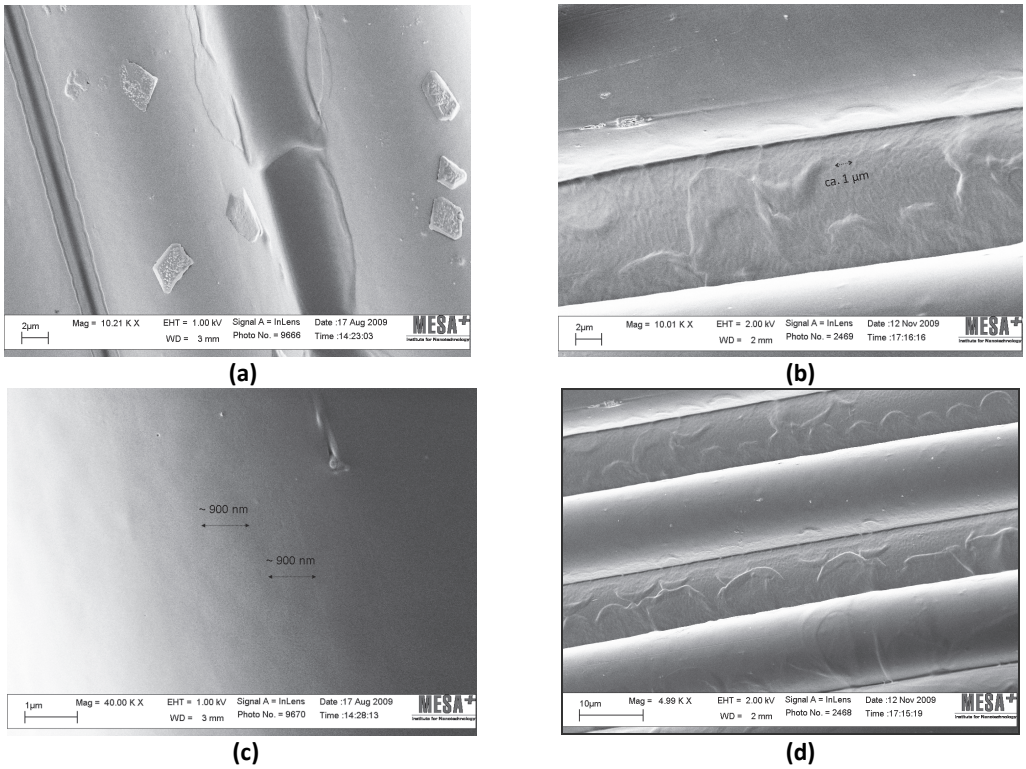

Figure 2.5: High-resolution SEM images of PET RM 1 **(a)** and PET RMC 1 **(b)** functionalized textiles. Image **(c)** depicts an area of image **(a)** at higher magnification for better observation of the microparticle presence. Image **(d)** depicts an area of PET RMC 1 at lower magnification than image **(b)**, for better observation of the microgel layer on adjacent fibers.

In Figure 2.5, high-resolution images of PET RM 1 and PET RMC 1 are given for comparison. Their fiber surface morphology is quite different than that of PET RCM 1. In the latter case, **CM** complexes appear as non-voluminous dark imprints completely integrated and more sparsely distributed on the fiber surface, with an estimated diameter of about 2 µm. In the cases of PET RM 1 and PET RMC 1, continuous microgel layers are formed on the polyester fibers. The morphology of these layers also varies. For PET RM 1 (Figure 2.5a), the coating appears homogeneous and comprised of uniform closely packed spheroid formations with an estimated diameter of approximately 900 nm (Figure 2.5c). This value approximates the estimated diameter of air-dried PNIAA microparticles on a silicon wafer (Figure 1.1a, Chapter 1), and it is almost half of the approximate diameter of the **CM** complexes on PET RCM 1. This size difference can be attributed to the fact that upon complexation of PNIAA with CS, which actually results in contraction of the microparticles due to electrostatic attraction as explained in Chapter

1, dilution of microgel **M** takes place, as well. This means that for the same volume of microgels **M** and **CM**, fewer microparticles are present in microgel **CM** than in **M**. Polyesters PET RM 1 and RCM 1 were treated with the same liquor-to-cloth ratio and were not padded but rather transferred under the UV lamp for irradiation; therefore, microgel was not pushed out of the sample structure and away of the surface. Since microgel **M** is denser than microgel **CM** in terms of PNIAA microparticle content, more microparticles are expected to be found on the PET RM 1 fibers compared with PET RCM 1. Since these microparticles are densely accumulated one next to another, there is not enough space for them to completely collapse and flatten. On the other hand, **CM** complexes, the circular shape of which is based on the PNIAA microparticles, are more sparsely scattered on the fibers and have more space to stretch out completely their collapsed (because of drying) structure.

In the case of PET RMC 1, functionalized with microgel **MC** (hence, with higher PNIAA microparticle content than **CM**), a continuous layer is also formed. However, this layer has a lacy appearance (Figure 2.5d) composed of ribbon-like formations and collapsed pancake-like particles of 900-1000 nm (Figure 2.5b). Although this size range correlates well with PNIAA microparticle diameters in dry state, the morphology of the layer can be attributed possibly to the actual preparation of microgel **MC**. It is known that the order of component addition for the preparation of polyelectrolyte complexes influences the properties of the complexes (Philipp *et al.* 1989). For microgel **MC**, CS solution was added to microgel **M** at a ratio of 1/2.5 (v/v) (whereas for microgel **CM** the mixing ratio and order were reverse). As CS macromolecules enter microgel **M**, they interact electrostatically with oppositely charged microparticles in a random way and under intense stirring. It is possible that during addition under agitation, CS macromolecular chains form strings along which multiple PNIAA microparticles are anchored, as shown schematically in Figure 2.6, forming ribbon-like structures on fibers.

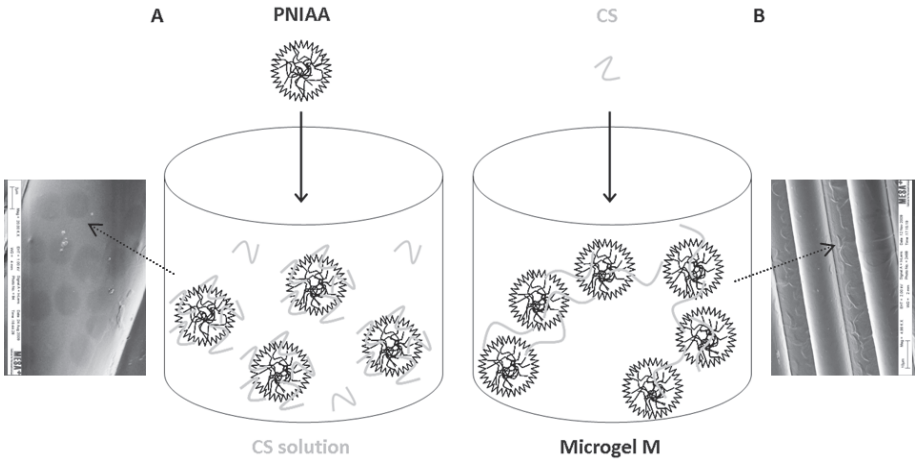

Figure 2.6: Schematic representation of the possible effect of the PNIAA and CS mixing order on the formation of microgel **CM** (A) and microgel **MC** (B). The SEM images of functionalized PET RCM 1 (left) and PET RMC 1 (right) are placed beside each complexation vessel to help correlate each microgel morphology in the vessels and on the fibers.

In Figure 2.7, the surface morphology of aminated PET 1 samples is presented. Even after amination, the irregular oligomeric protrusions remain on the polyester surface, as shown for PET A 1 (Figure 2.7a). Like on PET RCM 1, **CM** complexes appear also on the UV irradiated PET ACM 1 (Figure 2.7b) as dark circular formations. However, their distribution on the fibers does not seem uniform, neither does their size (*see inset of image 2.7b*). In the case of the genipin/thermo-treated PET ACM-T 1 (Figure 2.7c), non-voluminous dark circular formations are again present. Their size and shape appears quite uniform but their distribution on the fibers is also in this case heterogeneous and rather scattered.

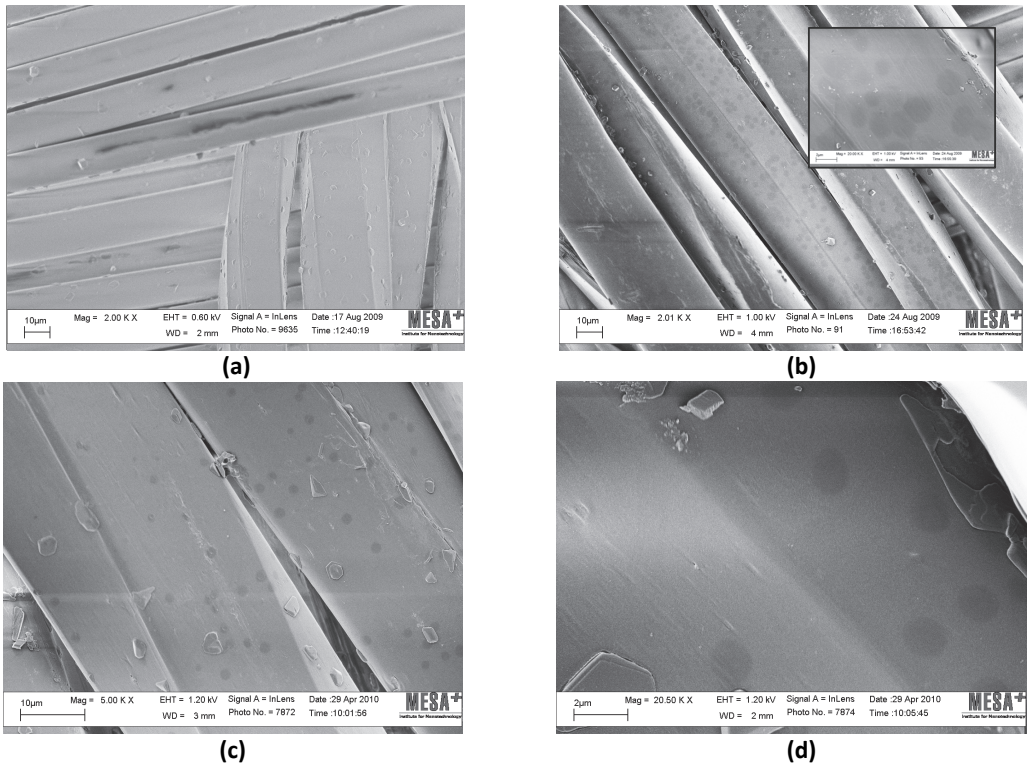

Figure 2.7: High-resolution SEM images of aminated polyester PET A 1 **(a)**, of UV-irradiated PET ACM 1 **(b)**, and of genipin-treated PET ACM-T 1 **(c)**. Image **(d)** provides a 4-times higher magnification of PET ACM-T 1 for better observation. The inset in image **(b)** provides a 10-times higher magnification of functionalized PET ACM 1.

The diameter of **CM** complexes on PET ACM-T 1 estimated based on Figure 2.7d is approximately 1.5 µm. It is ca. 25% smaller than that on PET RCM 1 because for the preparation of PET ACM-T 1, the microgel-impregnated polyester is treated at 65°C for 1.5 h. Therefore, the PNIAA microparticles and hence the **CM** complexes, which are found above their LCST, collapse. As they crosslink with genipin at the same time, it is possible that they are pinned down on the fiber surface in their shrunk dimensions. The small fiber coverage and the irregular **CM** complex distribution suggest inhomogeneous

amination of polyester. In other words, the reactive sites on the aminated fibers (i.e. the introduced primary amine groups) appear to be scarce and poorly distributed. The scarcity can be explained by the fact that relatively mild conditions were chosen for the amination reaction (short reaction time, medium temperature, medium concentration of ethylenediamine) compared with other studies (e.g. Nissen *et al.* 2008) in order to avoid extended polyester degradation (Holmes 1996). Apparently, this choice affected also the uniformity of the result. The same reasoning applies to the UV irradiated PET ACM 1. However, the fiber coverage appears bigger than in the case of PET ACM-T 1, possibly because the photoinitiator used was of opposite charge compared with the substrate and based on the study of Geismann *et al.* 2005 it is expected to facilitate the photo-crosslinking. Moreover, in this case, reaction is initiated by free radicals provided not only by the primary amine groups of polyester but also by other sites of the fiber (polyester chain scission).

It is noteworthy that all the microgel sizes (of microparticles alone or polyelectrolyte complexes) estimated on dry polyester fibers are larger than the corresponding estimated dry sizes on silicon wafers given in Chapter 1 (paragraph 1.3). This is a possible indication that microgels are not merely adsorbed on the polyester surface but rather pinned down as crosslinking also occurs during drying. Therefore, microparticles and complexes do not shrink on the polyester fibers as much as they would if they were not bound to the substrate and were free to move their structure. Furthermore, in Chapter 1, **CM** and **MC** complexes were found to be more hydrophobic than PNIAA microparticles of microgel **M**. Therefore, the affinity of microgels **CM** and **MC** with polyester is expected to be higher than that of microgel **M**. This effect combined with the fact that **CM** and **MC** complexes are less densely distributed on the polyester fibers – therefore, they have more unoccupied space around them – than microgel **M** microparticles, can cause the complexes to spread on the fibers and produce bigger diameters than on silicon wafers.

Similar surface morphologies are expected for the corresponding PET 2 samples, as all procedures were performed in the same way.

2.3.2. Surface chemical composition

FTIR-ATR analysis

In order to evaluate the effect of the functionalization process on the chemistry of the polyester surface, FTIR-ATR analysis was performed. There were certain hindrances regarding this analysis. One of them was the fact that the main chemical groups characteristic of PNIAA and CS absorb in the same wavelength range, as shown in Figure 2.8. The bands of amide groups (-NHCO-), specific to PNIAA owing to the repeating units of NIPAAm, appear at 1632 cm^{-1} (amide I, C=O stretching) and 1530 cm^{-1} (amide II, N-H bending) (Bulmus *et al.* 2003). The bands of carboxylic acid (-COOH), specific to PNIAA owing to the repeating units of acrylic acid, appear at 1256 cm^{-1} (C-O stretching), 1733 cm^{-1} (C=O stretching) and 3300 cm^{-1} (O-H stretching), even though they are weak.

The bands of the isopropyl groups (-CH(CH_3)$_2$), attributed to NIPAAm units, appear at 1366 cm^{-1} and 1385 cm^{-1} (C-H bending). Finally, the bands that appear at 2870 cm^{-1} and 2920 cm^{-1} (C-H stretching) are attributed to the propyl (-CH-) and ethyl groups (-CH_2-) (Bulmus *et al.* 2003). On the other hand, CS also absorbs at 1632 cm^{-1} (C=O stretching, N-H bending) and 1550 cm^{-1} (N-H bending). These absorptions correlated with the broad peak that appears centered at 3300 cm^{-1} (O-H and N-H stretching) are attributed to its primary amine groups (-NH_2), residual acetylated units (-$NHCOCH_3$), and alcohol groups (Brugnerotto *et al.* 2001; Zhou *et al.* 2008). The bands at 1378 cm^{-1} and 1403 cm^{-1} (C-H bending) are assigned to the –CH_2– groups. Furthermore, the characteristic saccharide units of CS absorb at 1031 cm^{-1} and 1072 cm^{-1} (-C-O-C- bridge stretching), and at 1148 cm^{-1} (-C-O-C- bridge anti-symmetric stretching) (Zhou *et al.* 2008; Kumirska *et al.* 2010).

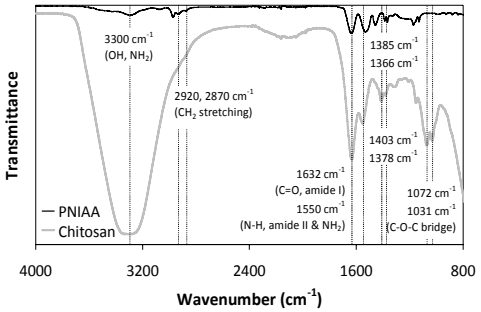

Figure 2.8: FTIR-ATR spectra of the microgel components chitosan and PNIAA analyzed in the form of films.

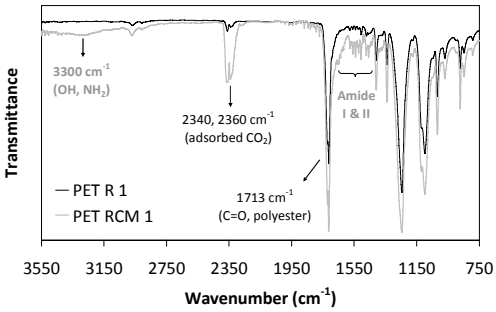

Figure 2.9: FTIR-ATR spectra of the reference polyester PET R 1 and of the functionalized polyester PET RCM 1.

With many of the FTIR-ATR bands of PNIAA and CS overlapping, it was difficult to distinguish the differences among the various microgel-treated polyesters. Another hindrance was that, due to the strong absorbance of the polyester substrate itself, any microgel bands that would appear close to the polyester bands (e.g. of carbonyl groups) are weak or even undetected. The small dry microgel add-on of the samples also accounts for that. As reported in literature, the spectral differences among chitosan-treated and untreated polyesters are quite small, even when polymer blends and films are investigated (Manyukova *et al.* 2009; Wu 2011), where the amount of chitosan is much higher than that on the functionalized polyesters investigated here. However, by increasing the dry add-on of microgel **CM** to 5%, it was possible to detect few but important spectral differences between reference polyester PET R 1 and PET RCM 1. As seen in Figure 2.9, PET RCM 1 exhibits a broad band centered at 3300 cm^{-1} which is attributed to hydroxyl and primary amine groups, as discussed previously for Figure 2.8. It is reported in Manyukova *et al.* 2009 that the basic spectral region of interest for chitosan-treated polyester is 3000–3500 cm^{-1}, as it is characteristic of vibrations of hydroxyl groups involved in hydrogen bond formation; the broad bands in that spectral region allow differentiation between treated and untreated samples. Additionally, it is shown in Figure 2.9 that a strong double band appears at 2340 and 2360 cm^{-1} for PET RCM 1. These are characteristic vibration bands of adsorbed CO_2 molecules (Brugnerotto

et al. 2001), and indicate the presence of amine groups tethered on the surface (Danon *et al.* 2011). Similar but much smaller bands appear also in the PET R 1 spectrum. In this case, the adsorption is attributed to the affinity of the non-polar CO_2 with the hydrophobic polyester. Also, in the region 1400–1700 cm^{-1} bands of increased absorbance are observed for PET RCM 1, compared with reference PET R 1. In this spectral region, polyester absorbs due to its benzene rings (ring C-H bending, and stretching of the C-C bond between the benzene ring and the carbonyl group) (Liang *et al.* 1959; Donelli *et al.* 2009). However, the stronger bands of PET RCM 1 indicate the presence of amide groups on the polyester surface, which are, therefore, assigned to microgel **CM** based on Figure 2.8.

Similar difficulties in spectral evaluation were encountered also in the case of the aminated genipin/thermo-treated polyester samples. However, characteristic bands of hydroxyl and amine groups (3100–3500 cm^{-1}), aliphatic C-H groups (2867 cm^{-1}, 2908 cm^{-1}), and amide I (C=O) groups (1691 cm^{-1}) were observed for PET ACM-T 1, even though they were of small absorbance (the spectra are not shown here but they are reported in Glampedaki *et al.* 2011a). These results were in agreement with findings of Ohe *et al.* 2007 for glucosamine-treated polyester.

XPS data of surface elemental composition

Surface analysis was performed on thoroughly rinsed and washed samples, therefore the differences observed so far through SEM and FTIR-ATR should not be a result of species merely adsorbed on the polyester surface. However, more insight was needed to understand if the chemical nature of the reference polyester changed after functionalization. XPS data in Table 2.4 show that PET R 1 has atomic concentrations close to the theoretical values of PET presented in Table 2.5.

Table 2.4: Elemental composition (%) of the polyester surfaces determined by XPS

Polyester samples	Atomic concentration (%)			Atomic ratios	
	C 1s	**O 1s**	**N 1s**	**O/C**	**N/C**
PET R 1	73.2	26.8	-	0.37	-
PET RM 1	74.8	18.4	6.8	0.26	0.09
PET RCM 1	74.0	21.9	4.1	0.30	0.06
PET A 1	73.8	24.3	2.0	0.33	0.03
PET ACM-T 1	72.4	24.2	3.4	0.33	0.05

PET RM 1 and PET RCM 1 have increased nitrogen surface concentrations compared with PET R 1, which has no nitrogen detected on its surface. Furthermore, the N/C ratio of PET RM 1 is 30% higher than that of PET RCM 1; this difference is attributed to the smaller coverage of the PET RCM 1 fiber surface with **CM** complexes compared with the continuous layer that microgel **M** formed on PET RM 1, based on SEM images of Figures 2.4 and 2.5. Owing to the simultaneous increase in total carbon atoms attributed

to the polymeric backbones of PNIAA and CS, the O/C atomic ratios between PET RM 1 and PET RCM 1 do not differ significantly.

Table 2.5: Theoretical values of atomic concentrations (%) and ratios of PET, CS and PNIAA, based on their individual repeating units

Component	Atomic concentration (%)			Atomic ratios	
	C 1s	O 1s	N 1s	O/C	N/C
PET	71.4	28.6	-	0.4	-
CS (5% acetylated)	54.7	36.3	9.0	0.66	0.16
NIPAAm (repeating unit of PNIAA copolymer)	75.0	12.5	12.5	0.17	0.17
Acrylic acid (repeating unit of PNIAA copolymer)	60.0	40.0	-	0.67	-

Based on Table 2.5 of the theoretical values of atomic concentrations of the individual components, it is evident that both CS and acrylic acid, hence PNIAA, have high and similar O/C ratios. Thus, whether only PNIAA is present on polyester or CS *and* PNIAA, with CS at a higher percent than PNIAA based on the composition of microgel **CM**, the final O/C ratios on the two polyesters should be indeed comparable. In the case of aminated polyester, the introduction of amine groups on the polyester surface is confirmed by the 2% of nitrogen concentration on PET A 1. This relatively low percentage, along with the fact that the O/C ratio of PET A 1 is practically the same as that of PET R 1, suggests that amination was not extensive. However, incorporation of microgel **CM** increased nitrogen surface concentration of aminated polyester by more than 40%, despite the low fiber coverage observed by SEM for PET ACM-T 1.

In order to assess changes in chemical bonds, XPS deconvolution data were obtained and are presented in Table 2.6. With respect to the differently bound carbon atoms, the deconvolution spectra (not shown) depicted five bands designated to equal carbon atom types (C1-C5). The corresponding binding energies for each atom on each polyester sample are given in Table 2.6. As expected, C2 with a binding energy of 284.8 eV has the highest atomic concentration on all polyester samples; it corresponds to **C**-**C** and **C**-H bonds, attributed mainly to the carbon atoms of the PET aromatic ring (Lang *et al.* 1997). C3 corresponds to aliphatic carbon atoms single-bonded with oxygen (-**C**-O), and C5 to carbonyl carbon atoms, i.e. double-bonded with oxygen (-**C=**O), attributed to ester, carboxyl or amide groups depending on the sample (Curti *et al.* 2005; Lang *et al.* 1997; Yang *et al.* 1990). There are two more types of carbon atoms, designated as C1 and C4, derived from the deconvolution spectra of all polyester samples which are not usually encountered in PET XPS spectra. C4 with a binding energy of ca. 287 eV was reported also elsewhere (Lang *et al.* 1997) where it was attributed to another type of oxidized carbon atom with no further specification. In other studies, C4 is assigned to **C**-N bonds (Neoh *et al.* 1998; Yang *et al.* 2005). C1, on the other hand, with no obvious origin is possibly a product of impurities or an artifact of the measurement.

Table 2.6: XPS deconvolution data for the differently bound carbon and oxygen atoms of the surface of polyester samples of the PET 1 series

Polyester samples	Carbon & oxygen atoms							
	C1	**C2**	**C3**	**C4**	**C5**	**O1**	**O2**	**O3**
	Binding energy (eV)							
	283.6	284.8	286.0	287.3	288.7	531.7	533.2	534.6
	Atomic concentration (%)							
PET R 1	2.3	51.1	16.8	13.8	16.0	46.7	46.5	6.8
PET RM 1	1.7	56.2	9.4	9.3	23.4	64.0	36.0	-
PET RCM 1	4.9	60.3	18.2	6.2	10.4	64.3	35.7	-
PET A 1	2.1	51.5	17.8	13.9	14.7	51.1	43.1	5.8
PET ACM-T 1	2.4	49.6	25.0	7.8	15.2	51.0	43.3	5.7

PET RM 1 shows a significant increase in C5 and O1 and a decrease in C3 and O2 atomic concentrations compared with PET R 1. This result is possibly attributed to the presence of PNIAA multiple amide and carboxyl groups and to the fact that microgel **M** forms a continuous layer on PET (according to SEM images); thus PNIAA atomic ratios influence more the surface composition data rather than PET atomic ratios. For PET RCM 1, the results for C3 (%) and C5 (%) are opposite of those for PET RM 1, with an increase and a decrease observed, respectively. This result can be explained by the plethora of CS C–O bonds belonging to its –C–O–C– glucosidic linkages and alcohol groups (C–OH), with exceed the PNIAA contribution of carbonyl bonds based on the composition of microgel **CM**. The –C–O–C– bonds are considered single for C atoms but double for O atoms; therefore, the O1 (%) and O2 (%) do not follow the trend of C5 (%) and C3 (%), respectively, and they remain at the same levels as those of PET RM 1. In the case of the aminated samples, PET A 1 shows a slight increase in C3 (%) and a slight decrease in C5 (%) compared with PET R 1, owing to the amination reaction which leads to chain scission and formation of hydroxyl groups on PET surface. On the other hand, PET ACM-T 1 has significantly increased C3 (%) compared with PET A 1, possibly owing to the –C–O–C– glucosidic linkages and alcohol groups of CS.

Regarding bound oxygen atoms, PET R 1 has three types; O1, corresponding to double bonded oxygen (carbonyl group), O2, to single-bonded oxygen of an ester group, and O3, to single-bonded oxygen of an alcohol end group. The corresponding bands of the deconvolution spectrum for oxygen (not shown) were attributed to binding energies shifted with respect to the aliphatic carbon binding energy (284.8 eV). O1 and O2 have similar atomic concentrations, as they both belong to the ester (**O**=C–**O**) or carboxyl (**O**=C–**O**H) groups of PET with a ratio 1:1. The third type of oxygen atom belongs to the alcohol end groups of PET (C–**O**H) and the fact that it is absent from the surface of PET RM 1 and PET RCM 1 indicates that all hydroxyl end groups have reacted. The increased O1 atomic concentration determined for PET RM 1 (64.0% compared with 46.7% of PET R 1) and PET RCM 1 (64.3% compared with 46.7% of PET R 1) can be attributed to the multiple carbonyl groups of the PNIAA amide bonds (Curti *et al.* 2005). The carboxyl groups of acrylic acid in the PNIAA structure contribute also to the above-mentioned

increase. However, their amount is not comparable to that of the amide groups in the PNIAA backbone (based on monomer feeds and FTIR-ATR data); consequently, the O2 atomic concentration does not show the same increase as that of O1. In the case of PET A 1, an increase in the O1/O2 ratio is observed (1.2) compared with PET R 1 (O1/O2 = 1.0), as well as a small decrease in O3, which suggests a decrease in single-bonded oxygen atoms. This result is expected, as amination is known to lead to partial loss of small ethyleneglygol molecules (Bide *et al.* 2006a). The fact that PET ACM-T 1 has similar levels of oxygen atomic concentrations but much higher C3 (%) compared with PET A 1, is attributed to the same reasons described above for PET RCM 1 compared with PET RM 1.

Colorimetric determination of functional groups

Colorimetric determination of carboxyl and amine groups present on PET fibers was performed in order to assess the effect of the microgel type, polyester type and functionalization technique on the functional groups of polyesters. As shown in Figure 2.10a, PET functionalization through UV irradiation leads to reduced carboxyl content. In the case of microgel **M**-functionalized polyesters (PET RM 1 and PET RM 2), the decrease is attributed to the formation of a continuous layer on polyester, in which the amide groups exceed the amount of carboxy groups, as expected based on the XPS data and the initial monomer concentrations during preparation of microgel **M**. Therefore, as it appears, the concentration of carboxyl groups on PET is higher than that in microgel **M**. In the case of microgel **CM**-functionalized polyesters (PET RCM 1 and PET RCM 2), the carboxyl content is slightly higher than for the corresponding PET RM 1 and PET RM 2 because **CM** complexes do not cover completely the polyester fibers; thus, microgel-free spots on the polyester fibers contribute as well to the carboxy content.

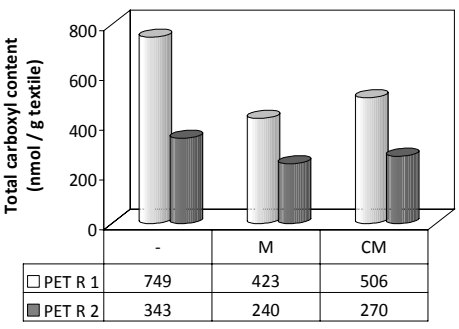

(a)

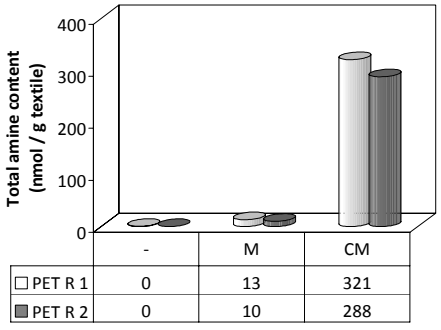

(b)

Figure 2.10: Total carboxyl **(a)** and amine **(b)** contents of polyesters PET R 1 and 2, PET RM 1 and 2, and PET RCM 1 and 2, determined by colorimetry.

Regarding the polyester amine contents, it is shown in Figure 2.10b that functionalized polyesters containing CS (PET RCM 1 and PET CM 2) have a significant increase in amine groups. Though XPS data showed that the nitrogen atomic concentration of PET RM 1 is higher than that of PET RCM 1, the much higher total amine

group content determined for PET RCM 1 can be attributed to three factors: XPS analyzes only the top ca. 5 nm of the surfaces; surface roughness was reported to affect conclusions drawn from XPS results regarding functional group quantification, whereas colorimetric determination with Acid Orange 7 (known also as Orange II) does not (Noel *et al.* 2011); XPS analysis was performed on dry samples, the colorimetric measurements in liquid medium where microgels can swell and functional groups become more accessible to the dye molecules.

In the case of aminated polyesters microgel-functionalized through UV irradiation, Figure 2.11 shows that PET ACM 1 has much higher amine content than PET AM 1, like PET RCM 1 compared with PET RM 1, but much lower carboxyl content, unlike PET RCM 1 compared with PET RM 1. The latter result is attributed to the fact that **CM** complexes cover only partly the aminated polyester fibers. The uncovered parts also contribute to the carboxyl content but to a smaller extent than in the case of PET R 1 samples, because during amination carboxy groups become amide groups.

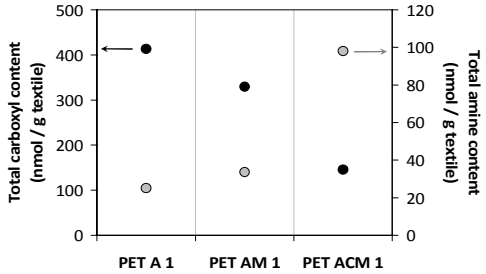

Figure 2.11: Total carboxyl and amine contents of aminated polyesters PET A 1, PET AM 1 and PET ACM 1, determined by colorimetry.

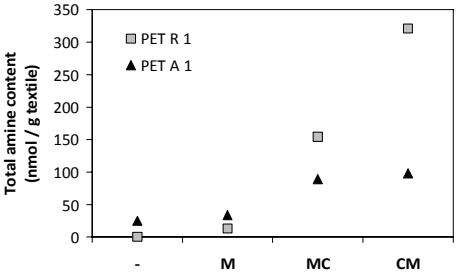

Figure 2.12: Comparison of the total amine contents of polyesters PET R 1, PET RM 1, PET RMC 1 and PET RCM 1 with those of PET A 1, PET AM 1, PET AMC 1 and PET ACM 1.

In Figure 2.12, the total amine contents of samples of the PET R 1 series are compared with their corresponding ones of the PET A 1 series, in order to assess the effect of the microgel type on samples similarly functionalized with UV irradiation but of modified substrate. It is evident that the presence of CS causes significant increase in the amine content of UV irradiated polyesters, even when microgel **MC** is used which has reverse concentrations of CS and PNIAA compared with microgel **CM**. On the other hand, it is also evident that microgel-functionalized aminated polyesters have either similar (PET AM 1) or much lower (PET AMC 1 and PET ACM 1) amine contents than the corresponding PET R 1 samples. This result was unexpected, as aminated PET is expected to be more photo-reactive than the non-aminated PET, based on studies comparing nylon to PET which report that $–C(H_2)–N$ bonds are more reactive than $–C(H_2)–O$ bonds (Yang *et al.* 1996a). Moreover, for the UV irradiation of aminated polyester an anionic photoinitiator was used because, according to Geismann *et al.* 2005, a photoinitiator of opposite charge than that of the treated surface leads to higher reaction efficiencies. A possible explanation for the opposite effect shown by the obtained results is the fact that the anionic photo-initiator is more hydrophilic and water-soluble than benzophenone.

Thus, during the microgel-impregnation step of the UV irradiation procedure, it is likely that a quantity of the anionic photoinitiator migrates from the aminated polyester surface to the liquor, leaving less photoinitiator available for reaction when polyester is transferred under the UV lamp.

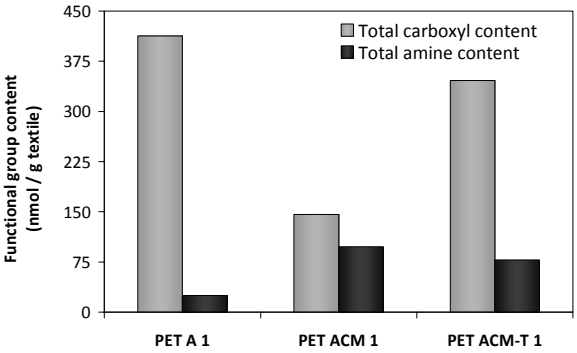

Figure 2.13: Comparison of the total carboxyl and amine contents of aminated polyesters PET A 1, PET ACM 1 and PET ACM-T 1.

Finally, comparison between photo- and thermo-crosslinked aminated polyesters showed that the low-temperature treatment results in much more limited decrease of the polyester carboxyl content compared with UV irradiation (Figure 2.13). This effect can be attributed to the limited coverage of the PET ACM-T 1 fibers by **CM** complexes compared with PET ACM 1, as observed by SEM. However, the total amine content of PET ACM-T 1 is similar to that of PET ACM 1 and three times higher than the amine content of PET A 1. Considering that only few primary amine groups are needed for the crosslinking reaction with genipin, and that the levels of amine content between the two microgel-functionalized aminated polyesters are similar, it is suggested that the proposed thermo-crosslinking technique can be as efficient as the UV irradiation technique, with the minimum amount of reagents.

2.3.3. Surface charge

Figure 2.14 depicts the ζ potential curves of PET 1 and PET 2 polyester samples. Both reference polyesters PET R 1 and PET R 2 have mainly negative ζ potential values, as expected, owing to their carboxylic end groups. The low positive values shown below ca. pH 3.5 are probably an artifact of the analysis attributed to cation adsorption from the solution or even protonation of the carboxylic end groups at such low pH (Zhu *et al.* 2006). It is clearly seen that both polyesters PET RM 1 and PET RM 2 have lower negative values than the corresponding reference polyesters PET R 1 and PET R 2 at pH 4–10. Hence, functionalization with microgel **M** reduces the surface charge of polyester. Moreover, in both cases of PET RM 1 and PET RM 2, the ζ potential appears to reach a plateau above pH 5, a result in accordance with the electrophoretic mobility data of PNIAA microparticles in microgel **M** (Figure 1.12, Chapter 1).

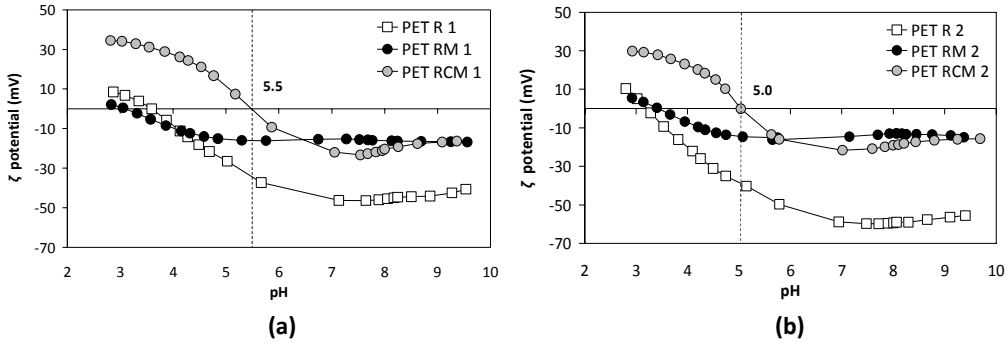

Figure 2.14: *ζ*-potential curves of PET R 1, PET RM 1 and PET RCM 1 **(a)**, and of PET R 2, PET RM 2 and PET RCM 2 **(b)**, obtained by streaming potential measurements.

The *ζ* potential curve of microgel **CM**-functionalized polyester PET RCM 1 follows the same trend as that of PET RCM 2. Above ca. pH 7, the curves approximate those of the corresponding microgel **M**-functionalized polyesters, and above pH 8.5 they coincide. These results are in good agreement with the electrophoretic mobility data of microgel **CM** (Chapter 1, Figure 1.12), as well as with the CS polyelectrolyte titration data which revealed that above pH 9, CS has no ionized groups (Chapter 1, Figure 1.14). Therefore, above pH 9 only PNIAA is expected to contribute to the *ζ* potential of microgel **CM**-functionalized polyesters; hence, above pH 8.5 the *ζ* potential curves of microgel **M**- and microgel **CM**-functionalized polyesters coincide. The similarity of the curves between corresponding PET 1 and PET 2 functionalized samples, and the coincidence of curves above certain pH between microgel **M**- and microgel **CM**-functionalized samples of the same polyester type, suggests that microgel properties are indeed imparted to polyester textiles, regardless the polyester type. However, the zero-charge points of the polyesters differ. In the case of both PET RM 1 and PET RM 2, their zero-charge points appear close to pH 3.4 which is the zero-charge point of microgel **M** (Chapter 1, Figure 1.4). As microgel **M** was found to form a continuous layer on polyester surface, the determined zero-charge points are not surprising because PNIAA ionization controls the ionization of the functionalized polyester surface. If complete coverage was achieved also by microgel **CM** on polyester surfaces, then the polyester zero-charge points would be expected to appear at pH 7 (Chapter 1, Figure 1.5). However, PET RCM 1 exhibits it at pH 5.5 and PET RCM 2 at pH 5.0. These shifted zero-charge points reflect variable surface charge density and suggest that the polyester surfaces are not completely covered by **CM** complexes (Goddard *et al.* 2007; Luxbacher 2010), as observed also by SEM.

On the other hand, aminated polyesters PET A 1 and PET A 2 show clear transitions from positive to negative *ζ*-potential values at pH 4.9 and 6.1, respectively (Figure 2.15). Apparently, amination affected PET R 2 much more than PET R 1, as the pH-transition point of the former polyester is shifted to a higher pH compared with the one of the latter polyester. Also, the sigmoidal curve of PET A 2 covers a larger *ζ* potential range than PET A 1 does. A possible explanation for this effect is the dense structure of PET R 2. Even though the same amination procedure was used for both polyesters, PET R 2 has an openness factor of zero.

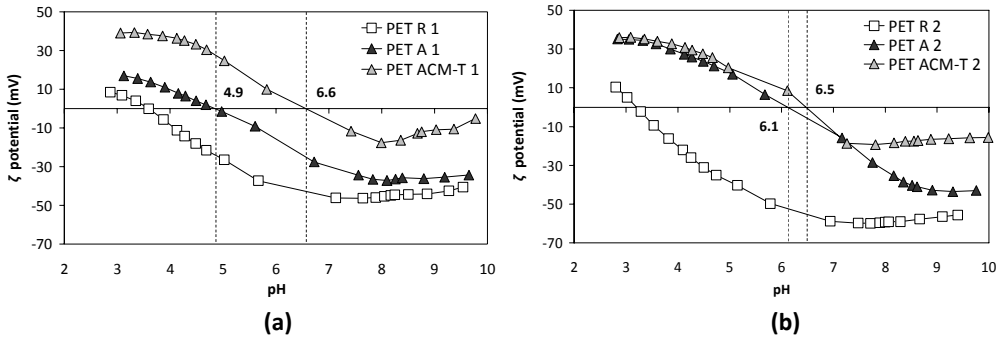

Figure 2.15: *ζ*-potential curves of PET R 1, PET A 1 and PET ACM-T 1 **(a)**, and of PET R 2, PET A 2 and PET ACM 2 **(b)**, obtained by streaming potential measurements.

Therefore, it is possible that ethylenediamine molecules were not drained in the yarns interior structure but they were rather consumed mainly on the surface of PET R 2. In the case of thermo-crosslinked microgel-functionalized aminated polyesters, PET ACM-T 1 exhibits a curve similar to the one of PET RCM 1, but the zero-charge point is shifted to pH 6.5. This value, even though it is closer to the zero-charge point of microgel **CM**, it does not suggest higher coverage because the initial zero-charge point of PET A 1 before functionalization is already much higher than that of PET R 1. Therefore, ionized groups of the polyester substrate contribute also to the total *ζ* potential values. In the case of PET ACM-T 2, microgel **CM** seems to affect little the polyester zero-charge point by shifting it slightly to the right, at pH 6.5. Although the first half of the curve coincides with the corresponding part of the PET A 2 curve, the second half with the negative values resembles the curves of microgel **M**-functionalized polyesters. This result suggests that **CM** complexes are present on PET ACM-T 2, and therefore the *ζ*-potential changes are not attributed only to polyester itself. It is also possible that polyester carboxylic end groups might have reacted with CS macromolecules that are in excess in microgel **CM** and not bound electrostatically to PNIAA microparticles, e.g. through esterification due to elevated temperature (Hu *et al.* 2002). In that case, the reacted polyester carboxylic groups would not contribute to the total negative charges, and the PNIAA effect would be more visible.

In conclusion, the *ζ*-potential data showed that the pH-induced transitions of functionalized polyesters are dependent on microgel type and coverage. Microgel **CM** imparted to all corresponding polyesters pH sensitivity within the physiological pH range of human skin (Schneider *et al.* 2007). Apparently, the applied functionalization techniques are suitable for fixing microgels on polyester surfaces, while leaving enough functional groups free (e.g. primary amine groups) for the expression of pH-related properties. This effect was noticed even in the case of GP-treated aminated polyesters, where GP consumed primary amine groups of CS. The presence of remaining free functional groups after reaction with GP is also supported by the polyelectrolyte titration results of microgel **CM** crosslinked with GP, which showed decrease but not complete disappearance of the total charge of the **CM** complexes (Chapter 1, Figure 1.21).

2.3.4. Surface topography

Topographical measurements produced data regarding overall dimensional changes of the textiles (relaxation, shrinkage) after functionalization, macro- and micro-roughness, as well as surface macro- and micro-porosity. Macro-roughness is expressed as the overall waviness of the textiles and micro-roughness as the average arithmetic roughness (R_a) of the filament surface in the warp and weft direction of the textiles. Macro-porosity refers to the inter-yarn average pore size (throughout the whole textile surface) and micro-porosity to the intra-yarn average pore size (within the yarns in the warp and weft direction of the textiles).

Textile (macro-) topography

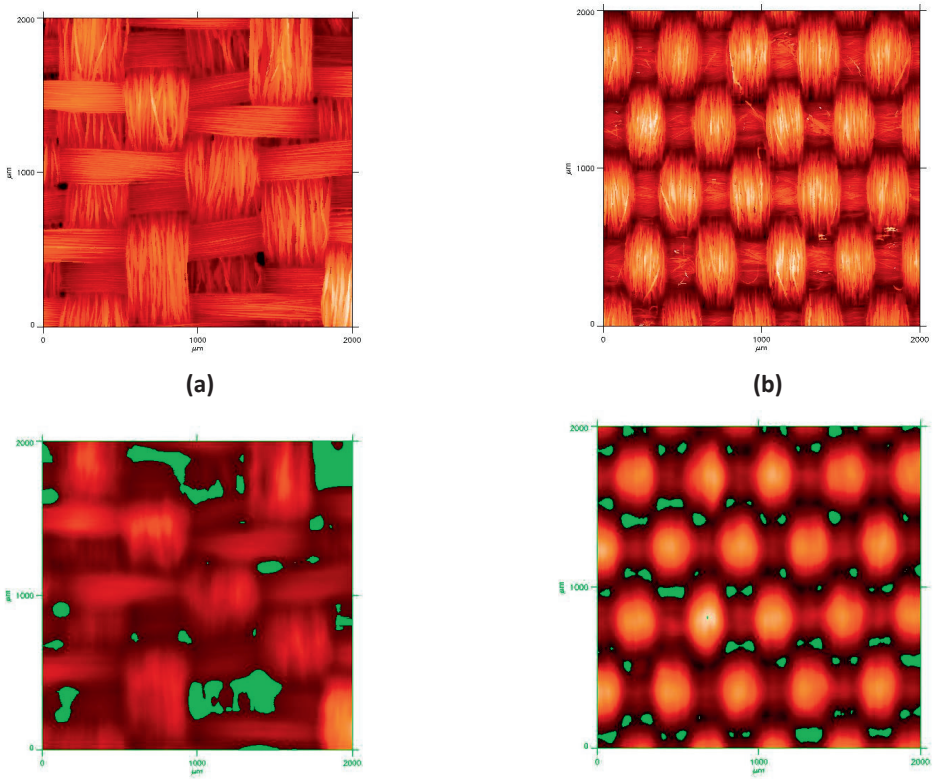

Figure 2.16: 2D images of PET R 1 **(a)** and PET R 2 **(b)** obtained with an optical scanner, and corresponding images of PET R 1 **(c)** and PET R 2 **(d)** with chromatic aberrations, based on which the textile macro-porosity was determined.

Figure 2.16 depicts an example of how different textile macro-porosities can be measured based on chromatic aberrations from 2D projections of filtrate images (Figures

2.16c and 2.16d) of corresponding scanned images (Figures 2.16a and 2.16b). The sequence of the created measuring images is given in Appendix II. Evidently, the weaving structure influences greatly the results, as concluded by comparing PET R 1 and PET R 2, which have different warp yarn densities and openness factors.

As shown in Table 2.7, the woven structure of PET RM 1 and PET RCM 1 underwent relaxation compared with the reference PET R 1. This means that the overall distance among yarns increases, even though no mechanical force was used during the microgel incorporation. In addition, the textile waviness decreases by approximately 11% for PET RM 1 and by 30% for PET RCM 1. In practice, this means that the polyester surface becomes more even after the microgel incorporation. The macro-porosity at the same time increases considerably for PET RM 1 but remains almost unchanged for PET RCM 1.

Table 2.7: Topographical parameters of the textile surface of polyesters of the PET 1 and PET 2 series

Sample	Textile surface topography				
	Dimensional changes (%)			Macro-roughness (waviness)	Macro-porosity
	Warp	Weft	Overall	(μm)	($\mu m^3/\mu m^2$)
PET R 1	0	0	-	115	0.709
PET RM 1	-2.1	8.8	6.7 (relaxation)	102	0.927
PET RCM 1	-1.5	11.4	9.9 (relaxation)	81	0.702
PET R 2	0	0	-	74	0.091
PET RM 2	1.5	-2.7	-1.2 (shrinkage)	77	0.131
PET RCM 2	0.5	-1.8	-1.3 (shrinkage)	79	0.068
PET A 1	0	0	-	109	0.955
PET ACM-T 1	4.5	1.4	5.9 (relaxation)	91	0.662
PET A 2	0	0	-	72	0.102
PET ACM-T 2	-0.6	-0.6	-1.2 (shrinkage)	83	0.083

When comparing the macro-topography of the samples, it is necessary to consider these three parameters together and not individually. In the case of PET RM 1, the dimensional increase along the *x*-axis (reflected in the relaxation observed) is followed or caused by a decrease in the *y*-axis (reflected in waviness), which is normal if no compaction of the material occurs. The fact that also the inter-yarn pores appear bigger for PET RM 1 than for PET R 1 suggests that the expansion of the polyester textile structure was indeed caused by the microgel **M** incorporation. The reason is possibly that the dense PNIAA microparticle layer formed on the polyester fibers (as shown by SEM, Figure 2.4b), pushed the yarns apart from one another during functionalization (i.e. when

PNIAA microparticles were wet and swollen). Upon drying, the layer collapsed leaving larger voids between the yarns than the initial ones. Considering that this polyester textile type is thermo-fixed and thermo-stable, it is assumed that the dimensional changes observed are a result of the microgel effect only. In the case of PET RCM 1, the fabric structure is more expanded and its surface more even than for PET RM 1, but the macro-porosity is unaffected compared with PET R. This is supported by SEM images which show **CM** complexes completely flattened on the fiber surface and in a less dense distribution than in the case of PET RM 1, neither blocking the inter-yarn pores nor expanding them.

Contrary to the above effects, PET RM 2 and PET RCM 2 show shrinkage and increased macro-roughness compared with PET R 2. Macro-porosity follows similar trends as in the case of the corresponding PET R 1 samples, with the exception that in the case of PET RCM 2 it appears to decrease rather than remain unaffected. This result can be attributed to the initial structure of PET R 2. Being severely dense, it can retain most of microgel **CM** on the surface during functionalization rather than letting it drain within and/or out of the textile structure. This effect is reflected also on the dry microgel add-on values, which for PET R 2 functionalized samples are bigger than for the corresponding PET R 1 ones (Table 2.3). In fact, PET RCM 2 has almost double add-on than PET RCM 1. Thus, it is expected that inter-yarn pores will be partly blocked and the textile macro-porosity decreased. The observed textile shrinkage can also be a result of this effect. As the microgel layers formed on the PET R 2 surface are possibly denser compared with PET R 1 samples (in terms of more microgel being present on the same surface area), more crosslinking sites are available; thus, bridging between yarns becomes possibly more extensive and it pulls fibers closer together resulting in shrinkage.

Similar trends are observed among the aminated polyesters. Even though padding pressure was applied on both thermo-crosslinked aminated polyesters during their preparation, PET ACM-T 1 exhibits relaxation compared with PET A 1, whereas PET ACM-T 2 shrinkage compared with PET A 2. Macro-roughness decreases for the former microgel-functionalized sample, whereas it increases for the latter one. Finally, macro-porosity decreases for both PET ACM-T 1 and PET ACM-T 2 compared with their corresponding reference samples PET A 1 and PET A 2, although by a higher percentage in the former case (ca. 30%) than in the latter one (ca. 20%). These results indicate that although microgel functionalization affects the textile topography in many aspects, the influence of the initial structure of the polyester substrates plays a key role in the final topographical characteristics.

Yarn/fiber (micro-) topography

Regarding the micro-topography of the textile samples, Figures 2.17, 2.18 and 2.19 present data related to surface micro-porosity and micro-roughness. More specifically, it is shown in Figure 2.17a that the micro-porosities of PET RM 1 and PET RCM 1 warp and weft yarns remain in the same range as those of PET R 1, with a slight tendency for increase.

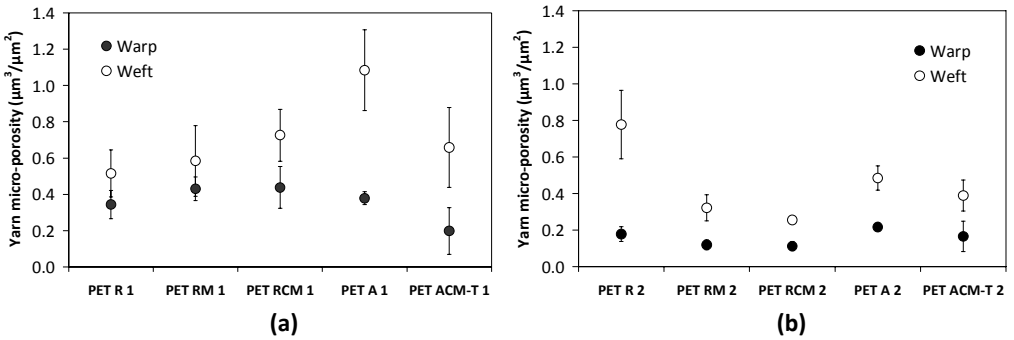

Figure 2.17: Micro-porosity values of warp and weft yarns of polyesters of the PET 1 **(a)** and PET 2 **(b)** series.

In the case of the corresponding PET R 2 samples, warp micro-porosities remain practically the same, whereas weft ones decrease significantly, almost by 50%. The effect is more obvious in the weft yarns of both series of samples because weft yarns have by production smaller density in the textile structure. These results support the previously made assumption that due to the dense textile structure of PET R 2 microgel does not drain as much as in the case of PET R 1. Based on Figure 2.17a, the intra-yarn pores of PET R 1 are smaller (ca. 0.3–0.6 μm) than the size of PNIAA microparticles (≈ 1.5 μm) and **CM** complexes (≈ 1.0 μm) in hydrated state (Chapter 1, Figures 1.1b and 1.11, respectively). These data, combined with the fact that PET R 1 has a more open structure than PET R 2, lead to the suggestion that as microgels tend to drain form the PET R 1 surface, they push fibers further apart resulting in overall relaxation of the textile structure. In the case of PET R 2 and even though weft intra-yarn pores are almost equal in size to the microparticle size, the dense polyester structure retains them leading to shrinkage after functionalization.

The effect of the initial textile structure is more pronounced in the case of aminated polyesters. As shown in Figure 2.17a, amination of PET R 1 results in expansion of the weft intra-yarn pores, as observed also macroscopically by the loosened structure of PET A 1. After microgel-functionalization with genipin crosslinks, intra-yarn pores are partly covered with microgel **CM** (decreased surface micro-porosity for PET ACM-T 1 compared with PET A 1) pushing yarns apart (relaxation of PET ACM-T 1 compared with PET A 1). Regarding PET A 2 in Figure 2.17b, a decrease in weft micro-porosity is observed, whereas warp micro-porosity remains unaffected, compared with PET R 2. Possibly for that reason, PET ACM-T 2 shows shrinkage compared with PET ACM-T 1 which exhibits relaxation. Once again, the structure of the reference textiles appears to have a predominant influence on the micro-topographical changes, as it did on the macro-topographical, too.

In Figure 2.18, examples of fiber micro-roughness profiles are presented. As shown in Chapter 1 (paragraph 1.3.4), pH influences significantly the polyelectrolyte microgel properties, including their swelling. Evidently, this pH effect is reflected also on the micro-roughness of microgel-functionalized polyester fibers.

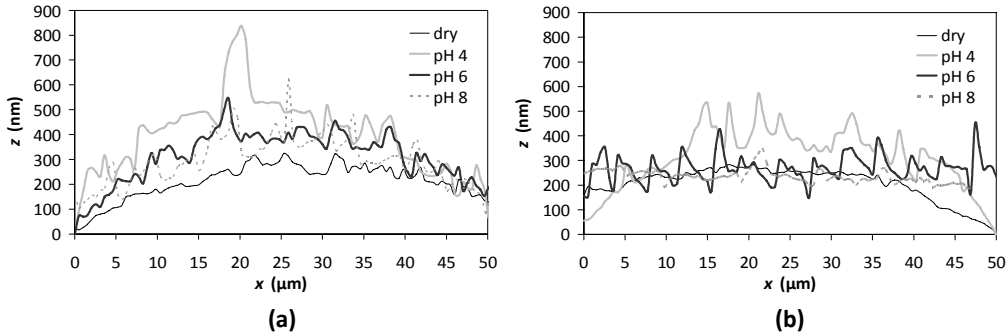

Figure 2.18: Micro-roughness profiles of warp fibers of PET RCM 1 **(a)** and PET ACM-T 1 **(b)**, when samples were dry and then impregnated with buffer solutions of pH 4, 6 and 8.

In Figure 2.18a, the PET RCM 1 profiles reveal that functionalized fibers impregnated with buffers of pH 4–8 have increased surface roughness, compared with dry state. The same conclusion is derived for the thermo-crosslinked PET ACM-T 1 (Figure 2.18b), for which the micro-roughness profile at dry state is almost flat. For both microgel **CM**-functionalized samples, the highest *z* values are observed at pH 4 where CS is expected to have its macromolecular chains extended owing to high degree of protonation.

Based on profiles like those of Figure 2.18, the average arithmetic roughness (R_a) was determined for microgel-functionalized polyester fibers, in an attempt to quantify their pH-sensitivity. The average arithmetic roughness is generally derived from the absolute values of roughness profile ordinates (*x, z*). It refers to the area between the profile height (*z*-values) and its mean line (mean height) over a specific measuring length (*x*-value). Indicative R_a data are given in Figure 2.19 for microgel **CM**-functionalized polyester fibers in the warp direction.

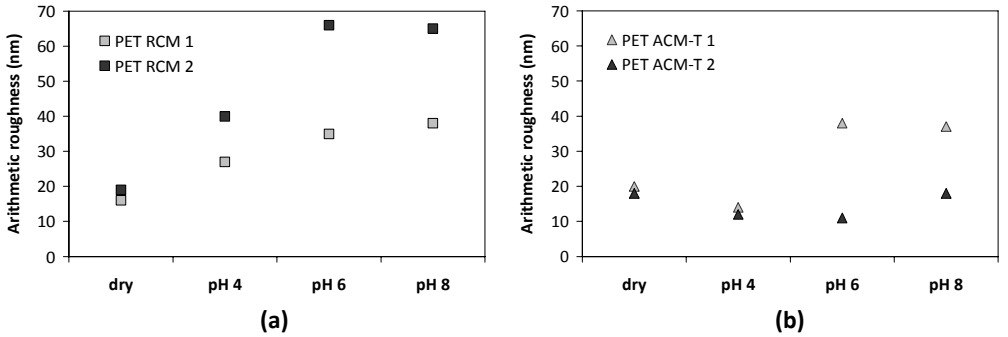

Figure 2.19: Average arithmetic roughness (R_a) of warp fibers of polyesters PET RCM 1 and PET RCM 2 **(a)**, and PET ACM-T 1 and PET ACM-T 2 **(b)**, determined using confocal microscopy.

Warp fibers were chosen instead of weft ones in order to facilitate comparison among samples; one of the two polyester types (PET 1) has textured weft fibers and the pre-existing irregularity of their geometry might interfere with the results. In Figure

2.19a, both PET RCM 1 and PET RCM 2 show an increase in R_a with increasing pH. This result is not surprizing as **CM** complexes become increasingly swollen when pH shifts from acidic to alkaline values owing to extensive ionization of PNIAA, whereas CS chains collapse. On the other hand, PET ACM-T 1 and PET ACM-T 2 (Figure 2.19b) also show an increase in R_a as pH shifts from 4 to 8. However, even though their initial R_a at dry state is almost the same as the R_a of the corresponding PET RCM 1 and PET RCM 2 samples, the changes in R_a at different pH values are much smaller for the aminated thermo-crosslinked samples than for the non-aminated photo-crosslinked ones. This result can be attributed to the scarcity and heterogeneous distribution of **CM** complexes on the aminated samples. Both effects of scarcity and heterogeneity result in irregularly deeper or shallower valleys among the complexes. Thus, they can influence the value of the mean height, as well as the average distance of each point of the measuring length of the fiber from that height; therefore they can influence the R_a values.

2.3.5. Physical & mechanical properties

Among the much valued properties of polyester are high degree of whiteness, resistance to wrinkling and tensile strength. The effect of functionalization on those properties is investigated in the following paragraphs.

Reflectance spectroscopy results

A surface is considered white when it reflects strongly (usually more than 70%) throughout the visible spectrum. A theoretically "perfect white" surface is assigned the whiteness index (WI) value 100. On the other hand, yellowness index (YI) measurements are usually performed to assess degradation of the white color due to processing or exposure to light.

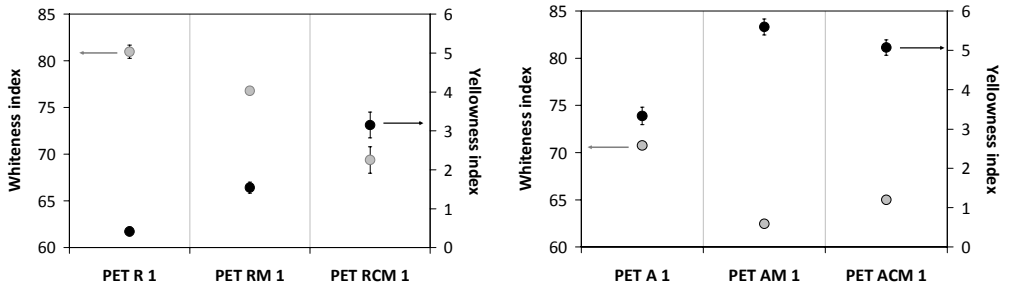

Figure 2.20: Whiteness and yellowness indices of PET R 1, PET RM 1 and PET RCM 1 samples **(a)**, and of the corresponding aminated samples PET A 1, PET AM 1 and PET ACM 1 **(b)**, determined with reflectance spectroscopy.

In Figure 2.20, the WI and YI of photo-crosslinked polyesters are given, as determined by reflectance spectroscopy. It is evident from Figure 2.20a that PET RCM 1

has the lowest WI and highest YI among the three polyesters analyzed. More specifically, compared with PET R 1, the WI of PET RCM 1 decreases by 10 units, whereas its YI increases by 3 units. Two parameters can account for these effects: the UV irradiation, even though of low wavelength (254 nm), which may cause degradation of polyester (Fechine *et al.* 2004); and the presence of CS, the solutions and gels of which are by nature colored yellowish. Even though CS is used in a solution of a rather low concentration, and although visual inspection of the polyester samples does not show severe differences, spectrophotometrically it was proven otherwise.

In the case of aminated photo-crosslinked polyesters (Figure 2.20b), a third factor affects whiteness, the amination procedure itself. This effect is suggested by the much lower value of the PET A 1 WI compared with those of PET R 1 in Figure 2.20a. PET AM 1 and PET ACM 1 have even lower values than PET A 1. However, the WI and YI of PET ACM 1 are at the same levels as those of PET AM 1, unlike in the case of the corresponding non-aminated samples. This effect occurs possibly due to the lower microgel add-on of PET ACM 1 (0.5%) compared with that of PET AM 1 (0.7%) (PET RCM 1 has 0.6% add-on and PET RM 1 0.4% (Table 2.3). Therefore, the CS yellowness effect is limited.

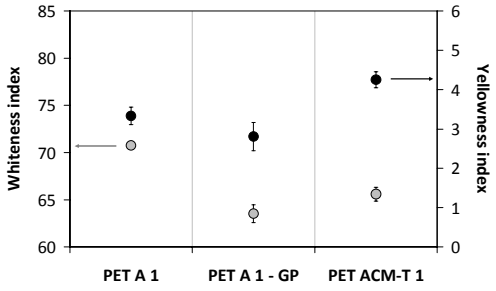

Figure 2.21: Whiteness and yellowness indices of the aminated samples PET A 1, PET A 1 – GP and PET ACM-T 1, determined with reflectance spectroscopy.

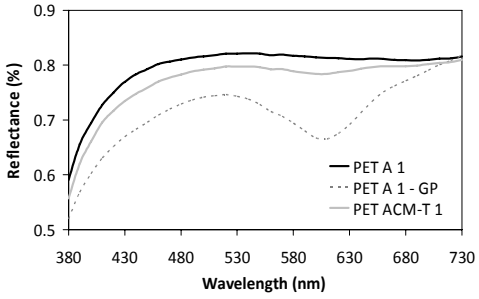

Figure 2.22: Reflectance spectra of polyesters PET A 1, PET A 1 – GP and PET ACM-T 1.

The WI and YI values of aminated thermo-crosslinked polyesters are given in Figure 2.21. A blank sample was prepared as control with only genipin on aminated polyester (coded PET A 1 – GP), which underwent the same procedure as PET ACM-T 1, only without microgel **CM** present. It is shown that the thermo-crosslinked PET ACM-T 1 has almost the same WI as the photo-crosslinked PET ACM 1, but approximately 20% lower YI. Two possible factors can account for this effect: the smaller coverage of PET ACM-T 1 fibers by **CM** complexes compared with PET ACM 1, as observed by SEM; the genipin coloration effect, known as gardenia blue (Lee *et al.* 2003), that masks partly the developed yellowness. Indeed, the reflectance spectrum of PET A 1 – GP (Figure 2.22) revealed a strong band at 610 nm, characteristic of the blue-green coloration that genipin develops when it reacts with primary amine groups. This band appears also in the PET ACM-T 1 spectrum but much weaker.

The CIE L*a*b* values obtained for PET A 1, PET A 1 – GP and PET ACM-T 1 helped elucidate this effect. As shown in Table 2.8, the control sample PET A 1 – GP has increased negative a* value compared with its positive b* value, indicating green color over yellow. For PET ACM-T 1, the positive b* value (yellow) is increased compared with PET A 1, but so is the a* value (green). These results support the explanation proposed for the limited yellowness effect observed for PET ACM-T 1.

Table 2.8: CIE L*a*b* values of polyesters PET A 1, PET A 1 – GP and PET ACM-T 1

CIE values	L*	a*	b*
PET A 1	92	-1.2	2.1
PET A 1 – GP	87	-4.2	1.7
PET ACM-T 1	91	-1.6	2.7

Crease recovery angle

In Figure 2.23, the crease recovery angles of samples of the PET 1 and PET 2 series are compared. From the graph of Figure 2.23a it is concluded that functionalization with UV irradiation results in decreased recovery angles both in the warp and weft direction of microgel **M**-functionalized polyester, PET RM 1. CS-containing polyesters have warp recovery angles in the same range as reference PET R 1, whereas their weft angles are slightly decreased. However, all samples show large recovery angles, thus good resistance to crease.

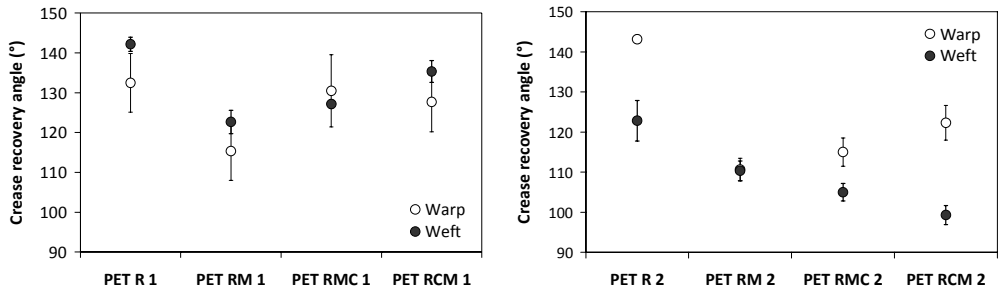

Figure 2.23: Crease recovery angles in the warp and weft direction of polyesters PET R 1, PET RM 1, PET RMC 1 and PET RCM 1 **(a)**, and of the corresponding ones of the PET 2 series **(b)**.

In Figure 2.23b it is shown that the crease recovery angles of all microgel-functionalized polyesters of the PET 2 series appear much more affected than their corresponding ones of the PET 1 series. The biggest angle decrease in the warp direction (ca. 24%) is observed again for the microgel **M**-functionalized polyester, PET RM 2. However, in the weft direction, PET RCM 2 has the smallest recovery angle among all samples, decreased by almost 20% compared with PET R 2.

For the majority of the PET 1 samples of Figure 2.23a, weft yarns show larger angles, except for PET RMC 1 for which warp and weft angles are very similar. For the PET 2 samples of Figure 2.23b, warp angles are larger then weft ones, except for PET RM 2 for which warp and weft angles coincide. A possible explanation for this difference between PET 1 and PET 2 samples is the different fiber structure. When the yarn density in one direction is higher than in the other, the crease load applied in the denser direction is divided among more yarns; hence, its crease recovery angle is expected to be larger than that of the less dense direction (Omeroglu *et al.* 2010). In the case of PET 2, the warp yarn density is bigger than the weft yarn density; therefore, the warp yarns of the PET 2 samples show better crease recovery than the weft ones. For PET 1 samples, the warp yarn density is also bigger than the weft one. However, the fineness of the warp fibers is less than half of the fineness of the weft fibers. Therefore, the crease recovery in the weft direction is expected to be better, as illustrated in Figure 2.23a.

To test whether amination affected this property, photo-crosslinked polyesters of the PET R 1 series were compared with corresponding aminated polyesters of the PET A 1 series. Their crease recovery angles in the weft direction are given in Figure 2.24.

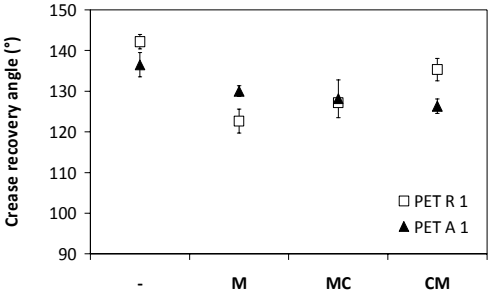

Figure 2.24: Crease recovery angles in the weft direction of reference and UV-irradiated polyesters of the PET R 1 series, compared with corresponding reference and UV-irradiated aminated polyesters of the PET A 1 series.

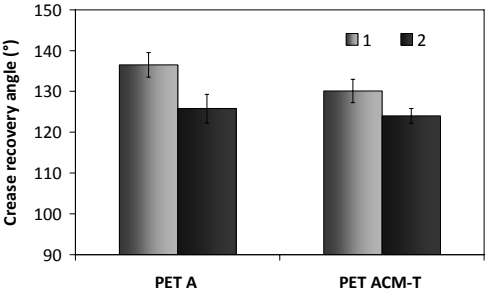

Figure 2.25: Crease recovery angles in the weft direction of thermo-crosslinked aminated polyesters PET ACM-T 1 and PET ACM-T 2, compared with their corresponding reference polyesters PET A 1 and PET A 2.

It appears that amination did not alter significantly the crease recovery of the polyester samples (in weft), and despite the angle decrease observed for PET A 1 and PET ACM 1 compared with PET R 1 and PET RCM 1, respectively, the recovery angles of the aminated polyesters remain still large. In fact, in the case of PET AM 1, the recovery angle increased compared with PET RM 1, whereas in the case of PET AMC 1 it remained practically the same compared with PET RMC 1. A possible explanation is that the amination procedure results in a less dense, looser structure; such a structure allows fibers and yarns to move more freely, hence with less friction in their relative movement. The looser structure combined with the presence of a continuous soft layer of microgel **M** on the fibers results in improved crease recovery (Omeroglu *et al.* 2010; Saville 2000).

In the case of genipin-treated thermo-crosslinked aminated polyesters, Figure 2.25 reveals that PET A 2 and PET ACM-T 2 have smaller crease recovery angles (in weft)

than the respective PET 1 samples, possibly due to their denser woven structure. However, PET ACM-T 2 shows better crease recovery compared with the UV irradiated PET RCM 2 in Figure 2.23b, possibly because the aminated textile structure is less tight. Also, **CM** complexes are scarcer on PET ACM-T 2 than on PET RCM 2; therefore, PET ACM-T 2 is expected to have a smoother fiber surface and, consequently, develop less friction during fiber or yarn movements, affecting crease recovery positively.

Tensile strength tests

Testing of polyester textile tensile strength resulted in strain-stress curves like those of Figure 2.26. It appears that microgel-functionalization with UV-irradiation deteriorates the polyester tensile strength (Figure 2.26a). Even greater is the negative impact of the amination procedure on polyester tensile strength (Figure 2.26b); however, microgel incorporation after amination does not deteriorate it further.

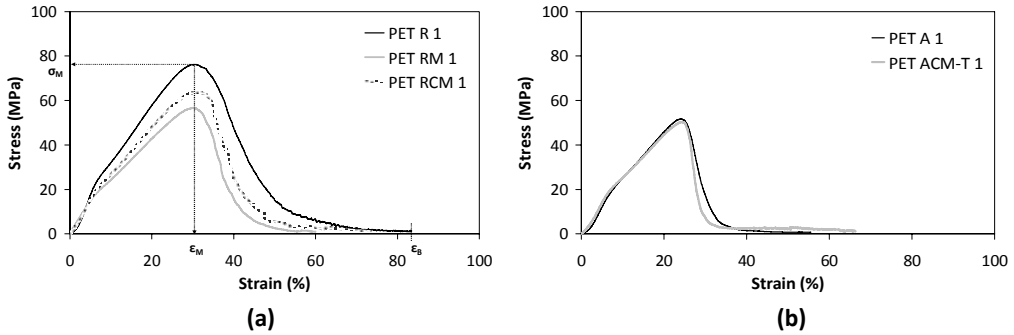

Figure 2.26: Strain-stress curves of polyesters PET R 1, PET RM 1 and PET RCM 1 **(a)**, and of the aminated polyesters PET A 1 and PET ACM-T 1 **(b)**, for samples prepared in the weft direction.

Based on curves such as the above, basic mechanical properties were determined for the polyester samples. The symbols σ_M, ε_M and ε_B in Figure 2.26a refer to maximum force, elongation at maximum force and elongation at break, respectively. The results of polyester tensile strength and elongation at break are given in Table 2.9. It is shown that both microgel **M**- and **CM**-functionalized polyesters of the PET 1 and PET 2 types have decreased tensile strengths compared with their respective reference samples PET R 1 and PET R 2. The deterioration is much more pronounced for the PET RM 2 and PET RCM 2 samples that show almost 50% decrease in tensile strength compared with PET R 2. Amination also degrades both types of polyester in terms of tensile strength; its effect is more severe in the case of PET A 2 that exhibits almost 75% loss of strength compared with PET R 2. Unlike for the UV irradiated microgel **CM**-functionalized polyesters, incorporation of microgel **CM** into aminated polyester surfaces via thermo-crosslinking does not influence tensile strength. On the contrary, it increases elongation at break for almost all samples and particularly for PET RCM 2.

Table 2.9: Mechanical properties of polyesters PET R 1, PET RM 1, PET RCM 1, PET A 1, and PET ACM-T 1, and of the corresponding PET 2 polyesters

Sample	**Thickness (mm)**	**Tensile strength (MPa)**	**Elongation at break (%)**
PET R 1	0.17 ± 0.01	77 ± 3	83 ± 5
PET RM 1	0.21 ± 0.01	57 ± 3	60 ± 7
PET RCM 1	0.19 ± 0.01	65 ± 4	74 ± 13
PET R 2	0.21 ± 0.00	93 ± 6	69 ± 5
PET RM 2	0.22 ± 0.01	47 ± 1	59 ± 12
PET RCM 2	0.23 ± 0.01	47 ± 1	85 ± 14
PET A 1	0.18 ± 0.01	52 ± 4	55 ± 6
PET ACM-T 1	0.20 ± 0.01	51 ± 2	66 ± 17
PET A 2	0.22 ± 0.01	22 ± 3	28 ± 11
PET ACM-T 2	0.23 ± 0.00	25 ± 4	33 ± 16

The decrease in tensile strength observed for all functionalized samples can be ascribed to the UV irradiation and amination procedures, which are known to lead to polyester degradation via chain scission and subsequent loss of molar mass and embrittlement (Fayolle et al. 2008; Mazrouei-Sebdani *et al.* 2011). The microgel presence on the polyester surfaces can also be an important factor, as finishes are reported to affect mechanical properties of textiles (Abdel-Halim *et al.* 2010). However, the results of Table 2.9 show practically no differences in tensile strength between PET RM 2 and PET RCM 2, PET A 1 and PET ACM-T 1, and PET A 2 and PET ACM-T 2, whereas the difference between PET RM 1 and PET RCM 1 is not dramatic. Therefore, it is concluded that the actual activation procedures of polyester through UV irradiation and amination influence the textile tensile strength, rather than the microgels used. It is possible that the latter, being soft matter, reduce the rigidity of the polyester fibers, thus leading to higher elongation values.

2.4. FURTHER CHALLENGES & RECOMMENDATIONS

UV irradiation effect

Photo-crosslinking with UV irradiation is a powerful technique for polyester functionalization. Due to the complexity of the microgel functionalizing systems used in this research, the components of which share common types of chemical groups and have various photo-reactive sites available, it was not made possible to elucidate the course of the photo-crosslinking reactions. Therefore, a challenge beyond the present research is to clarify through which chemical bonds the microgels are tethered on polyester and to what extent.

Furthermore, as already mentioned in this chapter, PET screens far UV light. Consequently, functionalization of PET at low wavelength is expected to affect mostly the top irradiated side of the samples rather than the bottom side. Studies on the photo-grafting of acrylic acid in the interlayer of two films, where PET was either one of the films or it was used as a filter on top of the films, revealed pronounced differences between the top and the bottom films in terms of photograting efficiency (Yang *et al.* 1996a; Yang *et al.* 1996b). For PET RCM 1 samples studied in this research, it was also found that their top irradiated side had different surface morphology than the bottom one. In Figure 2.27a, it is shown that complexes **CM** appear like imprints completely integrated with the polyester surface on the top side; on fibers of the bottom side (Figure 2.27b), the complexes appear more voluminous with a “pancake” structure.

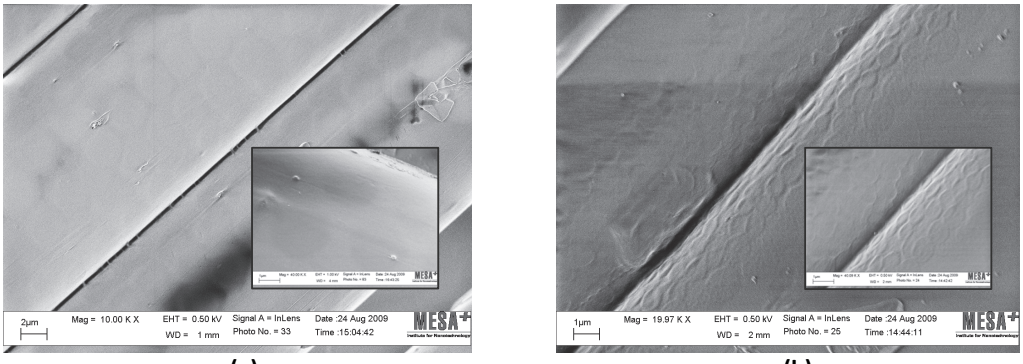

(a) **(b)**

Figure 2.27: High-resolution SEM images of the top (irradiated) **(a)** and bottom **(b)** side of polyester PET RCM 1. The insets depict microgel-functionalized areas at higher magnification.

In addition, the reflectance spectrum of the bottom side of PET RCM 1 shows less changes compared with the reference PET R 1, than the top irradiated side (Figure 2.28). PET RM 1 which contains no CS shows practically no difference between the reflectance spectra of its two sides.

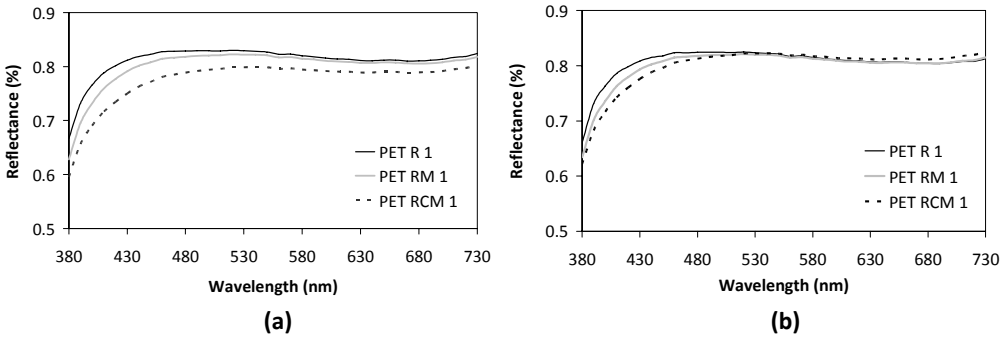

Figure 2.28: Reflectance spectra of the top (irradiated) **(a)** and bottom **(b)** side of polyesters PET R 1, PET RM 1 and PET RCM 1.

Such observations of differences between top and bottom sides of UV irradiated polyesters offer a scope for single-side functionalization, if the parameters of e.g. duration of irradiation, amount of photoinitiator, microgel content, etc. are tuned appropriately. In any case, optimization of the UV irradiation technique is recommended in order to balance sufficient microgel incorporation for functionalization and limited polyester photodegradation.

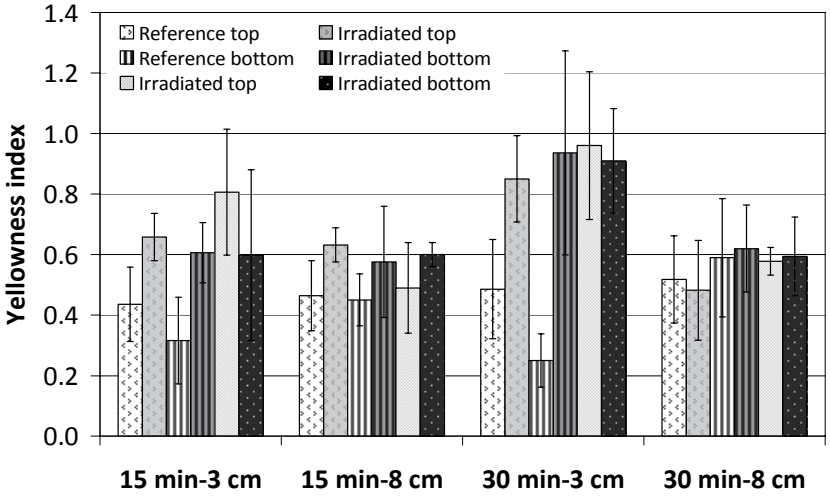

Figure 2.29: Yellowness indices of the top and bottom side of PET R 1 polyester samples before and after UV irradiation at different distances and durations.

In Figure 2.29, it is shown that both time of irradiation and sample distance from the UV lamp affect the yellowness index of reference polyester, even in the absence of photoinitiator and microgel. For the first pair of sides (reference top-irradiated top), the top side of a non-irradiated sample PET R 1 was used as a reference for the measurement of the top side of an irradiated sample. For the second pair (reference bottom-irradiated bottom), the bottom side of a non-irradiated sample PET R 1 was used

as a reference for the measurement of the bottom side of an irradiated sample. For the third pair (irradiated top-irradiated bottom), the top side of an irradiated sample PET R 1 was used as a reference for the measurement of the bottom side of an irradiated sample. Apparently, the conditions chosen for the research presented in this chapter (30 min irradiation–3 cm distance from the lamp) are the most severe, as they result in the biggest differences between non-irradiated and irradiated polyester and in the highest yellowness indices of the irradiated samples. This could be the reason for the complete integration of **CM** complexes on polyester fibers observed by SEM for the top side of PET RCM 1. However, a deeper and thorough analysis is necessary to draw sound conclusions that could lead to optimization of the method.

Substance adsorption/release

A colorimetric method of staining with Acid Orange 7 was used in this chapter to determine the amine content of microgel-functionalized polyesters. The same method was employed to test the reversibility and durability of the pH-responsiveness imparted from microgel **CM** to polyester. In Figure 2.30, the reflectance spectra of PET RCM 1 are presented, after 3 staining-decolorization cycles.

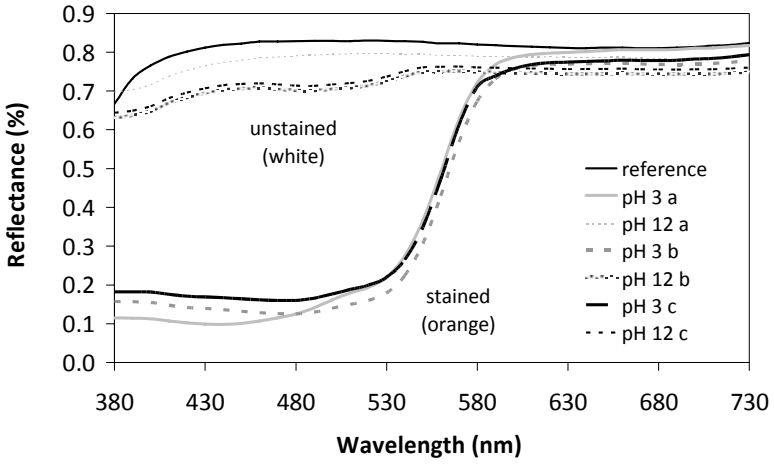

Figure 2.30: Reflectance spectra of PET RCM 1 after cycles of being stained with Acid Orange 7 at pH 3 and of releasing the dye at pH 12 (decolorization).

Evidently, the microgel-functionalized polyester maintains its ability to retain and release the dye when it shifts from acidic to alkaline pH and *vice versa*. This result, combined with the finding that polyesters functionalized with microgel **CM** have zero surface charge at slightly acidic to neutral pH values, can be explored further also for narrower pH shifts within the physiological range of human body. Such investigations could be useful for testing the controlled adsorption and release of substances such as proteins, medicinal drugs for transdermal use and so on.

Durability

An important parameter of functionalization is the durability of the microgel functionalizing system on polyester. Washing fastness is a common method of testing durability. The functionalized polyesters studied in this research were all thoroughly rinsed and washed prior to each analytical technique; therefore, some degree of durability was confirmed. SEM images of PET RCM 1 samples taken after consecutive wash-dry cycles, performed according to the washing protocol described in this chapter, show that microgel complexes are present on polyester fibers, even after 10 (Figure 2.31a) or 30 (Figure 2.31b) washes. However, a deeper investigation is recommended, including wettability tests, to explore how long-lasting the functionalizing effect is for all types of polyester used.

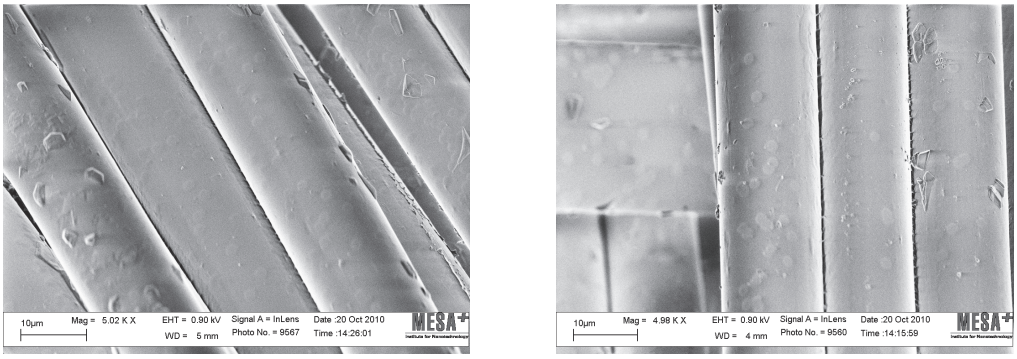

(a) **(b)**

Figure 2.31: High-resolution SEM images of PET RCM 1 washed 10 times **(a)** and 30 times **(b)** with a non-ionic detergent at 60 °C and for 15 min each time.

Thermo-crosslinking optimization

All the above recommendations apply also to the GP-treated aminated polyesters. Optimization of the thermo-crosslinking method should be explored first in terms of amination conditions, for the introduction of more amine groups on polyester without enhancing degradation of good intrinsic properties. Second, tests on different combinations of heating temperatures and times could lead to a shorter functionalization procedure and energy savings. Finally, the durability of the thermo-crosslinked microgel **CM** on aminated polyesters is important to be investigated not only in terms of the microgel physical presence on polyester after certain washes, but also in terms of maintaining the reversibility of its pH/thermo-responsive properties.

CHAPTER 3

POLYESTER ADAPTATION TO AMBIENT CONDITIONS THROUGH WATER MANAGEMENT PROPERTIES

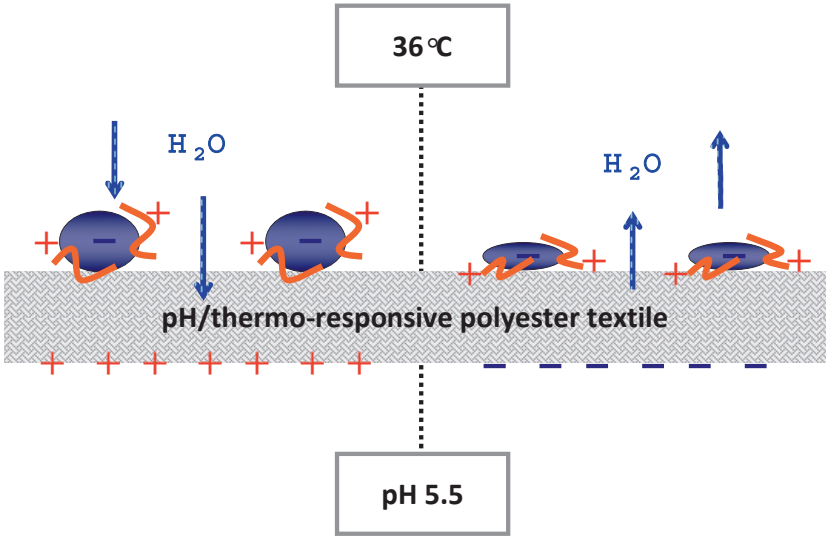

Graphical abstract 4: Microgel-functionalized polyester textiles with pH/thermo-responsive properties.

This chapter contains information included in:

Glampedaki P, Calvimontes A, Dutschk V, Warmoeskerken MMCG, Polyester textile functionalization through incorporation of pH/thermo-responsive microgels. Part II: Polyester functionalization and characterization, *Journal of Materials Science* (2011) (DOI: 10.1007/s10853-011-6006-6) (*in press*)

Glampedaki P, Dutschk V, Jocic D, Warmoeskerken MMCG, Functional finishing of aminated polyester using biopolymer-based polyelectrolyte microgels, *Biotechnology Journal* **6**(10), 1219–1229 (2011)

3.1. INTRODUCTION: FROM ACTIVE TO INTERACTIVE

"In the struggle for survival, the fittest win out at the expense of their rivals because they succeed in adapting themselves best to their environment"
Charles R. Darwin (1809—1882)[*]

The stimuli-responsiveness of hydrogels, thus also of hydrogel-functionalized substrates, is usually investigated in two ways: either through substance release/adsorption, color/shape changes etc. or through water uptake/loss gravimetric measurements, under the effect of stimuli (pH, temperature, light etc.) to which the particular hydrogels are sensitive (Abdel-Halim *et al.* 2010; Chen *et al.* 2002; Hu *et al.* 2006; Liu *et al.* 2005; Noel *et al.* 2011). In studies reported in literature for hydrogel-functionalized polyester substrates, the hydrogel applied is often of the continuous bulk type, which consequently forms a continuous, and relatively thick, film coating on the polyester surface (Chen *et al.* 2002; Hu *et al.* 2006; Huang *et al.* 2009; Liu *et al.* 2005; Ploymalee *et al.* 2010). In such cases, weight measurements for the determination of water uptake, after immersion of the samples in solutions of various e.g. pH and temperature values, are used as a generic method to show the interaction of the functionalized material with its surroundings.

Consequently, there is little information available in literature on polyester functionalized with microgels (rather than bulk hydrogels) where the substrate is textile (rather than a polyester film or membrane). Also, the effect of incorporated microgels on textile water management properties, even when no particular stimulus is applied, is poorly explored in literature. Possible reasons for this lack of information are the complexity of the response mechanisms of microgels to different stimuli (molecular reconfigurations, (de)ionization of functional groups, creation and breaking of hydrogen bonds within the hydrogel or between the hydrogel and the liquid medium, and others), as well as the plethora of factors influencing water management properties of textiles (weaving structure, porosity, surface roughness, presence of hydrophilic groups, and others). Therefore, distinguishing the role of each parameter in the behavior of microgel-functionalized textiles becomes a complex task.

This chapter attempts to elucidate certain aspects of the interaction of polyester textiles functionalized with pH/thermo-responsive polyelectrolyte microgels with their surrounding environment. The expression of this interaction is studied through water management properties at various ambient conditions. Water is the basis of the structure and of the responsive nature of microgels, as well as the driving force for the expression of their stimuli-responsiveness. Therefore, the adaptivity of microgel-functionalized polyester textiles to ambient conditions is investigated here in the presence of water in liquid or vapor state, both with and without pH/temperature

[*] A famous quote of the English naturalist and author of the Origin of Species, Charles Darwin; the quote is often abbreviated as "the survival of the fittest" which is actually attributed to Herbert Spencer, according to Darwin himself (http://www.darwin-literature.com).

changes applied. To this end, dynamic wetting, capillarity, water vapor transmission, moisture sorption/desorption, and moisture regain measurements were performed.

Dynamic wetting measurements provided information about the contact angle changes with time of water droplets in contact with the textile surfaces. From the same set of measurements the total absorption times of these droplets by the textile substrates were determined (absorption in lateral direction). The droplets were of purified water, with and without added salt, or of buffer solutions of pH values 4, 6 and 8. The data derived from dynamic wetting measurements were correlated with textile roughness and surface porosity data (Chapter 2, paragraph 2.3.4.), and with microgel pH-responsiveness data such as charge and size changes, with/without pH adjustment and salt addition (Chapter 1, paragraphs 1.3.4. and 1.3.7.). Capillarity measurements provided useful information about the amount of water absorbed in the capillaries of the textile structure (absorption in vertical direction). These data were expected to be particularly insightful for the swelling of the microparticles and polyelectrolyte complexes on the polyester fibers. The microparticle/complex swelling was expected to block partly the capillaries without diminishing their capacity for water absorption, as water would be distributed within the microparticle/complex structure. Capillarity data were, thus, correlated with fiber micro-roughness data (Chapter 2, paragraph 2.3.4.) and microparticle/complex size data (Chapter 1, paragraph 1.3.4.).

Water vapor transmission (WVT) measurements were performed to investigate how the increased hydrophilicity (below LCST) or hydrophobicity (above LCST) of microgels affects the moisture permeability of polyester textiles, in relation to their structure and surface porosity (Chapter 2, paragraphs 2.3.1. and 2.3.4.). For that purpose, tests were conducted at 20°C and 40°C, and at various RH values, on polyester samples of two different types of openness factors and macro/micro-porosities (PET 1 and PET 2, Chapter 2). Generally, 20°C and 65% RH are the standard testing conditions for textiles, so these values were chosen as starting conditions; the rest of the measurements were performed at increasing RH from 65% to 95% in order to simulate highly moist environments in an attempt to correlate the WVT data with data of microparticles/complexes in hydrated state. Furthermore, moisture sorption curves were drawn after continuous conditioning of the polyester textiles in the same range of temperatures and RH values, in order to estimate the contribution of microgels to the increased hydrophilicity or hydrophobicity of the functionalized polyester textiles. To elucidate in particular the influence of the thermo-responsive nature of the microgels on the polyester ability for moisture absorption, moisture regain measurements were performed. Such measurements require that the samples are first dried above 100°C and then placed in a conditioned environment of certain temperature and RH to determine how much moisture is regained. Since microgels act as hydrophobic above 36°C, it was expected that drying the functionalized polyesters at temperatures >100°C would have a marked impact on the ultimate moisture regains of the textiles.

3.2. EXPERIMENTAL PART

3.2.1. Materials

The materials used for studies in this Chapter are polyester textile samples of the types described and discussed in Chapter 2. The sample codes that appear in this Chapter are the same as the ones presented in Table 2.3 of Chapter 2.

Any buffer or salt solutions used were prepared with the same reagents as the ones mentioned in paragraph 1.2.1. of Chapter 1.

3.2.2. Dynamic wetting

Dynamic wetting measurements based on the sessile drop method were performed using a FibroDAT 1122HS dynamic contact angle tester (Fibro System, Sweden), equipped with a high speed video camera, in an environment of controlled temperature and humidity of 23°C and 50%, respectively. Water drops with a volume of 13 μl were applied on polyester textile surfaces by a short stroke from an electromagnet. After deposition of a drop, data were collected for 40–250 s, depending on the sample, based on which a dynamic contact angle curve was obtained. The time needed for the drop to disappear from the sample surface, as determined by the imaging system for a contact angle of 0°, equals to the total (water) absorption time of the textile sample. The values presented here for each sample are the average of five to ten measurements. The same procedure was applied using drops of buffer solutions of pH 4, 6 and 8, as well as of an aqueous solution of 0.04 M NaCl. From the same set of measurements, graphs of the drop volume, base radius, and height evolution with time were also drawn.

3.2.3. Water uptake & capillarity

Capillarity (%) of polyester samples was determined according to Leroux *et al.* 2006 using a 3S Balance (GBX Instruments, France), and it referred to the amount of water absorbed in the capillaries of the textile after a certain period of time in contact with water. Specimens of dimensions 3 cm × 5 cm were suspended vertically from a hook attached to the balance and their weight was recorded (W_{dry}). For every measurement, samples were carefully moved vertically towards the surface of water contained in a holder below the suspended textile samples. The moment at which each sample came in contact with water, without being immersed in it, was noted as t=0. The duration of each measurement was 3 min during which the textile samples were continuously taking up water. At the end of the measurement, the samples were withdrawn from the water surface with an automatic upward motion and as soon as they were detached from it their weight was recorded (W_{final}). The weight of the water that was absorbed through the capillaries (W_{cap}) was determined for each sample by subtracting W_{dry} from W_{final}. The capillarity (%) of each sample was then calculated from Equation (3.1):

$$Capillarity = \frac{W_{cap}}{W_{dry}} \times 100 \quad (3.1)$$

with W_{cap} being the weight of water absorbed by capillaries after t=3 min of contact, and W_{dry} the initial weight of each textile sample. The values presented here are the average of four measurements.

From the same set of measurements, water uptake curves were also obtained for a fixed period of time determined by the duration of the measurements (3 min), i.e. not until steady state. The water uptake (%) of each polyester sample at each time point was determined by Equation (3.2):

$$Water\ uptake = \frac{W_t - W_{dry}}{W_t} \times 100 \quad (3.2)$$

in which W_t is the weight of the sample in *g* at each point of time that the sample is in contact with water.

Note that at the beginning as well as at the end of each measurement, the surface tension of the water that was in contact with the sample was measured with a T.D. 2000 Prolabo tensiometer to check if microgel had leached out from the samples. In all cases, no significant decrease of surface tension was observed, thus W_{cap} does not include in its calculation microgel losses.

3.2.4. Water vapor transmission

Water vapor transmission (WVT) measurements were performed according to the standard UNI 4818-26 using aluminium containers filled with 25 ml water each. The container lids had a round opening of 1000 mm^2 to allow vapor exhaust during testing. Polyester textile samples of 4 cm × 4 cm were placed under the lid openings; rubber sealing gaskets were placed on top of them to prevent leakage, and the containers were then weighed. A bench top test chamber SM-1.0-3800 (Thermotron, USA) was used for conditioning the samples for 24 h at 20°C or 40°C, and 65–95% RH. After each conditioning run, the containers were weighed again and the difference in weight before and after 24 h was used to calculate the water vapor transmission rate (WVTR), according to Equation (3.3):

$$WVT\ Rate = \frac{\Delta m \times 24}{S \times t} \quad (3.3)$$

with Δ*m* being the weight difference in *g* before and after conditioning, *S* the testing surface area in m^2, and *t* the conditioning time in *h*. The values presented in this study were the average of six measurements.

3.2.5. Moisture sorption/desorption

Moisture sorption-desorption measurements were performed at different temperatures and RH values. Polyester samples were placed in a bench top test chamber SM-1.0-3800 (Thermotron, USA) and were conditioned using two different

temperature/RH programs. First, samples were conditioned for 4 h at constant temperature and RH of 20°C and 65% (standard textile testing conditions), respectively, to test whether steady state of moisture sorption/desorption is reached within this time interval. The same test was performed at 40°C. Then, samples were subjected to a cycle of increasing and decreasing RH between 65% and 95% at a constant temperature of 20°C. Each RH step of the cycle was of 10%, i.e. 65%, 75%, 85% and 95%, for both sorption and desorption. Samples were kept at each set of conditions for 4 h. From these measurements, the values of moisture uptake or loss at steady state were obtained at each set of conditions for each sample.

The second temperature/RH program involved two separate cycles of increasing and decreasing temperature and RH between 20°C and 40°C, and 65% and 95%, respectively, in a continuous mode. First, samples were conditioned at 20°C and 65% RH for 4 h. Then, RH was increased from 65% to 95% over a period of 4 h, and decreased from 95% to 65% during another 4 h. After the end of this cycle, samples were kept at 20°C and 65% RH for 4 h to equilibrate their moisture content. Then, temperature was raised almost instantly to 40°C and a second cycle began of increasing and decreasing RH between 65% and 95%, as in the first cycle. The two temperature/RH programs applied are shown schematically in Figure 3.1.

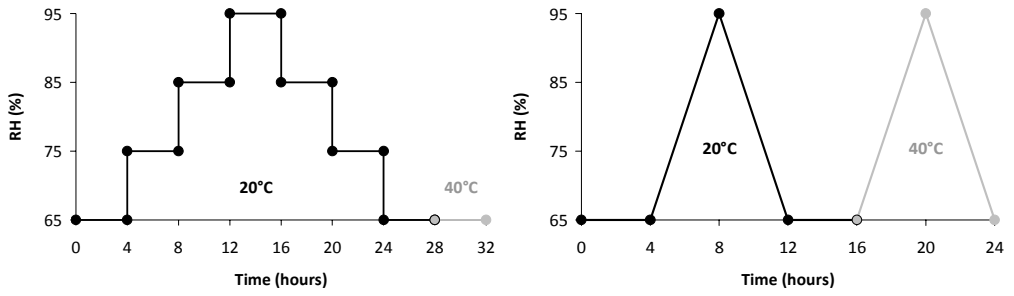

Figure 3.1: Temperature/RH programs applied for the moisture sorption-desorption cycles of polyester textiles. Two programs were set with: **(a)** 10% RH steps between 65% and 95% of 4 h each; **(b)** RH gradually changing between 65% and 95% over a period of 4 h. Black lines regard measurements at 20°C, and grey lines at 40°C.

The weight of each sample was recorded online, throughout all cycles of both temperature/RH programs, using a Mettler-Toledo WXS high-precision analytical balance. From the obtained data, moisture sorption-desorption curves were drawn for each polyester sample. The moisture uptake or loss (%) at each point of the cycles was determined using Equation (3.4):

$$Moisture\ uptake/loss = \frac{W_t - W_{20°C-65\%}}{W_t} \times 100 \quad (3.4)$$

in which W_t is the weight of each sample in *g* at each time point of the cycle, and $W_{20°C-65\%}$ is the reference weight of each sample after being conditioned for 4 h at 20°C and 65% RH. The obtained values are the average of three measurements.

3.2.6. Moisture regain

Moisture regain (M_R, %) was determined by weight measurements. Polyester textile samples were first dried at 105°C for 1 h and were left to cool down in a dessicator before weighing (W_d) with a high precision WXS analytical balance (Mettler-Toledo, The Netherlands). Then, they were conditioned for 24 h at certain temperature (20°C or 40°C) and RH (65, 75, 85 or 95%) and were weighed again ($W_{T\text{-}RH}$). The M_R was calculated using Equation (3.5):

$$M_R = \frac{W_{T-RH} - W_d}{W_d} \times 100 \qquad (3.5)$$

The values presented here are the average of three measurements.

3.3. RESULTS & DISCUSSION

3.3.1. Dynamic wetting

In order to explore the effect of microgels on the polyester wettability, dynamic wetting measurements were performed using the sessile drop method. The evolution with time of the volume and the base radius of the applied drop on the polyester surface provides useful information about the hydrophilicity of the surface, as well as of the influence of the surface structure (roughness, porosity) on the textile wettability (Calvimontes *et al.* 2010b).

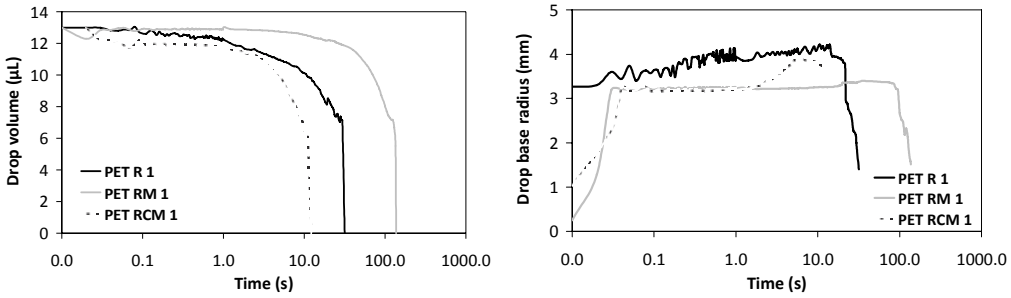

Figure 3.2: Evolution with time of the volume **(a)** and the radius of the base **(b)** of a water drop applied on the surface of polyester textile samples PET R 1, PET RM 1 and PET RCM 1.

In Figure 3.2a it is shown that the volume of a water drop on the surface of reference PET R 1 gradually and continuously decreases with time and the drop disappears after approximately 30 s. In the case of PET RM 1, the water drop volume decreases only slightly during the first milliseconds, then it increases again and remains stable for almost 10 s, after which it gradually decreases over a period of more than 100 s, until the drop disappears ca. 35 s later. For PET RCM 1, the volume decrease starts much earlier than for PET R 1 and PET RM 1; however, like for PET RM 1 and unlike for PET R 1, the drop volume remains shortly stable before its gradual decrease begins and it reaches a value of zero after ca. 12 s from the beginning of the measurement.

In Figure 3.2b, the changes of the radius of the drop base are shown with time for the same polyester samples. According to Calvimontes *et al.* 2010b, there are three wetting regimes for a water drop on a textile surface: a) dynamic wetting (spreading), during which the drop base increases gradually; b) quasi-static wetting, during which the drop base remains unchanged; and c) penetration, during which an abrupt decrease in the drop base occurs signifying absorption of the water drop within the textile structure. Water drops seem to follow these patterns on all three surfaces of PET R 1, PET RM 1 and PET RCM 1. However, for PET RM 1 and PET RCM 1, the initial drop base increase is much larger and sharper than for PET R 1. In the case of PET RCM 1, a sudden increase of the drop base radius is observed right before the penetration stage at ca. t=1.5 s, whereas its

volume starts to decrease at that same time, according to Figure 3.2a. This result indicates that for PET RCM 1, apart from the initial spreading that occurs as soon as the drop comes in contact with the textile surface, a second spreading phase occurs suddenly after an "incubation" period during which the drop's volume and base remain constant. This effect is possibly attributed to the swelling of **CM** complexes as they come in contact with water. The observed incubation period can be explained by the fact that microgel **CM** forms a "skin" on the polyester surface, as it dries out after functionalization; this air-dried skin needs to be wetted first before it swells. This effect is known for air-dried hydrogels compared with freeze-dried hydrogels; the latter ones maintain almost intact their original porous structure upon drying, therefore they swell much more and faster than their collapsed air-dried equivalents (Kumari *et al.* 2009). As soon as this wetting of the microgel layer is achieved, **CM** complexes swell fast enough to cause a sharp increase in the water drop base and decrease in its volume. A similar effect is observed in the case of PET RM 1, only the drop base increase which is observed at t=20 s (Figure 3.2b) is much smaller than in the case of PET RCM 1, and the incubation period much longer. This difference may be ascribed to the fact that microgel **M** forms a continuous layer with closely packed PNIAA microparticles on polyester fibers, as shown in Chapter 2. Therefore, it is assumed that more time is needed to wet all collapsed PNIAA microparticles rather than **CM** complexes which are fewer on the fibers. Another possibility is that the microgel **M** layer swells evenly on the spot where the water drop is, rather than letting the drop wet adjacent microparticles. This suggestion assumes that the time needed for the microparticles to swell after they have been wetted is much shorter than the time needed for them to become wetted. This phenomenon could account for the fact that both the drop volume and base remain constant during the "incubation" period of PET RM 1, after which the swelling of adjacent microparticles instigates a secondary spreading of the drop, thus an increase in its base and a decrease in its volume.

From the same set of dynamic wetting measurements, the total (water) absorption times were determined for the polyester samples, with and without adjustment of the pH of the water used (purified with innate pH 6.4). From Figure 3.2a, it was concluded that PET RM 1 has the longest total absorption time and PET RCM 1 the shortest one among the three samples and compared with reference PET R 1. In the case of reference PET R 1, the water drop is in direct contact with the substrate and can diffuse faster into the pores; in the case of PET RM 1, the swelling of the microparticles hinders and delays the penetration of water into the textile structure; and in the case of PET RCM 1, where the **CM** complexes do not cover the fibers completely, water can be absorbed both by the **CM** complexes and the textile structure, leading to shorter total absorption times.

As shown in Figure 3.3, the same trend is observed also at pH 4, 6 and 8. However, PET R 1 has similar absorption times at all studied pH, whereas PET RM 1 exhibits approximately 30–50% shorter absorption times at pH 6 and 8 compared with pH 4. Similar data were reported in Glampedaki *et al.* 2011b using another technique. This result can be attributed to the PNIAA gradual ionization above pH 4 (Chapter 1, Figures 1.12 and 1.14).

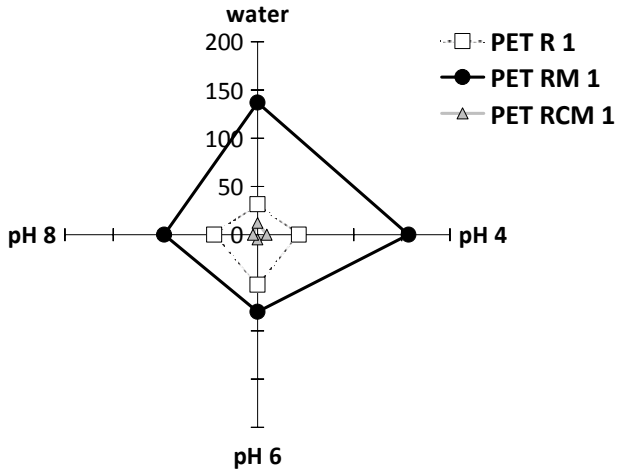

Figure 3.3: Total absorption times (in *s*) of samples PET R 1, PET RM 1 and PET RCM 1 determined by the sessile-drop method using water and buffer solutions of pH 4, 6 and 8.

As a consequence, the surface of polyester PET RM 1 becomes increasingly negatively charged, reaching plateau in the alkaline region (Chapter 2, Figure 2.14a). The fact that PET R 1 does not behave similarly, even though its surface is also increasingly negatively charged with increasing pH, could be attributed to the different nature of its carboxyl end groups compared with that of the PET RM 1 ones. Although acrylic acid (component of PNIAA and therefore **M**) is a weak acid, in its polymeric form it uses its multiple carboxyl groups to attract large amounts of water (Brannon-Peppas *et al.* 1990), especially when fully ionized. Therefore, the difference in absorption times among different pH values is more evident for PET RM 1 than for PET R 1. The shorter absorption times of PET RCM 1 at all pH, compared with those of both PET R 1 and PET RM 1, can be attributed to the simultaneous ionization of both CS and PNIAA on the surface of PET RCM 1, even though this ionization occurs at different degrees for each component. At pH 4, CS amine groups are highly protonated whereas PNIAA carboxylic groups are just starting to be ionized. At pH 8, on the other hand, CS amine groups are almost completely deprotonated whereas PNIAA carboxylic groups are fully ionized. This synergistic interaction appears to favor water absorption by PET RCM 1 in both the acidic and alkaline region.

These conclusions correlate well with data derived from the dynamic contact angle curves of PET R 1 and RCM 1, as shown in Figure 3.4. PET R 1 exhibits similar wetting behavior at all pH studied, having initial values of water contact angles of approximately 75°, 70°, and 70°, respectively (Figure 3.4a). On the other hand, PET RCM 1 shows a different wetting pattern. Although, its total absorption times are at all pH much shorter than those of PET R 1, its initial contact angles are higher than 120° (therefore, higher than those of PET R 1) at all three pH values (Figure 3.4b).

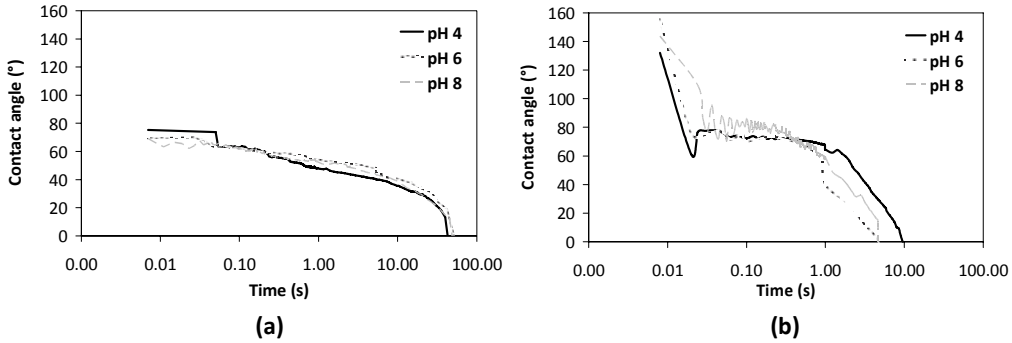

Figure 3.4: Dynamic contact angle measurements for PET R 1 (a) and PET RCM 1 (b) using the sessile-drop method and buffer solutions of pH 4, 6 and 8.

It was reported in Liu *et al.* 2008b that, in the presence of CS, polyester exhibits a higher water contact angle than without CS on its surface. Also, the fact that the initial base radius of a drop of plain water on PET RCM 1 is much smaller than that on PET R 1 (Figure 3.2b) supports the suggestion that microgel **CM** forms a rather hydrophobic "skin" on the polyester surface; thus, relatively high water contact angles should not be surprising. Once the barrier of the dryness of this "skin" is overcome by the primary spreading of the drop (first milliseconds) and the initiation of the subsequent wetting process (start of the "incubation" period described above), the contact angles are expected to decrease rapidly, as shown in Figure 3.4b for water drops of different pH. During "incubation" and much earlier than the final (equilibrium) swelling of the **CM** complexes, it is assumed that the first water molecules are adsorbed on the microgel "skin" and their gradual diffusion begins inside the structure of **CM** complexes. At this stage, the contact angle of the drop on the substrate is expected to remain almost constant, until extensive wetting of the microgel layer is achieved and the contact angle drops abruptly due to swelling of the complexes (or microparticles). However, this assumption cannot be used as an absolute criterion for the surface hydrophilicity of the material (Holly 1992); it has been reported that even fully hydrated hydrogels with an equilibrium water content of approximately 40% can exhibit a water contact angle of the same magnitude as hydrogels with only 1.5% water content at equilibrium (Holly *et al.* 1975).

Nonetheless, at pH 4 PET RCM 1 has the smallest initial contact angle (132°), but the longest total absorption time (9.5 s), compared with corresponding values at pH 6 (155° and 4.8 s, respectively) and pH 8 (144° and 4.7 s, respectively). This effect can be ascribed to the higher degree of swelling of **CM** complexes at pH 4, as reported in Chapter 1 (Figure 1.10). These results are also supported by the increased micro-roughness observed for PET RCM 1 at pH 4 in Chapter 2 (Figures 2.18 and 2.19).

In Figure 3.5, the total absorption times of water (without pH adjustment) are compared for samples of the PET 1 and PET 2 series which are functionalized with microgel **CM**, using UV-crosslinking or thermo-crosslinking after amination. It is generally known that the textile structure influences significantly the absorption process (Calvimontes *et al.* 2010a; Hasan *et al.* 2008).

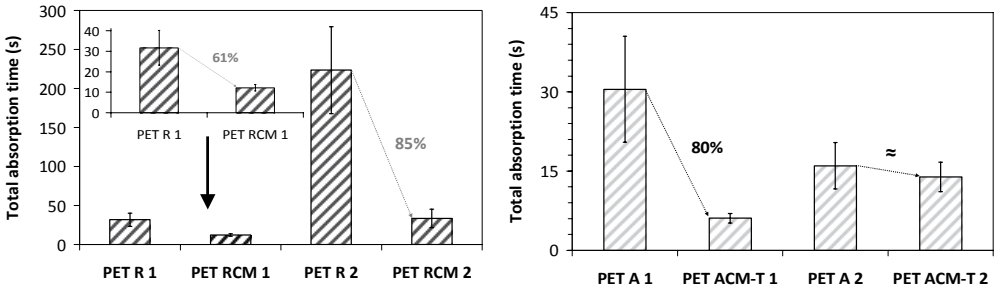

Figure 3.5: Total water absorption times of PET R 1 and 2, and PET RCM 1 and 2 **(a)**, and of aminated polyesters PET A 1 and 2, and PET ACM-T 1 and 2 **(b)**, determined by the sessile-drop method.

As expected, PET R 2 exhibits a much longer absorption time than PET R 1 (Figure 3.5a) owing to the much denser structure of the former polyester with zero openness factor and smaller surface porosity than the latter polyester. Moreover, PET R 1 is of crêpe weave, which resembles twill weave (Gokarneshan 2004), whereas PET R 2 is of plain weave. Also, PET R 1 has a higher waviness value compared with PET R 2 (Chapter 2, Table 2.7). According to Calvimontes *et al.* 2010b, the spreading rate of a water drop on twill woven textiles is increased with waviness, and decreased for plain woven textiles. For these reasons, it is not surprising that PET R 2 has almost a 10 times longer total absorption time than PET R 1.

PET RCM 2 shows also longer absorption times than PET RCM 1, influenced by the textile structure. PET RCM 2 exhibits similar macro-roughness (waviness) with PET RCM 1. However, PET RCM 2 exhibits shrinkage and smaller macro-porosity, compared with PET R 2, whereas PET RCM 1 exhibits relaxation and no significant changes in surface macro-porosity, compared with PET R 1 (Chapter 2, Table 2.7). Therefore, it can be assumed that, in the case of PET RCM 2, water is principally absorbed by the microgel layer of **CM** complexes, whereas in the case of PET RCM 1, both microgel complexes and textile structure contribute to the water absorption. Thus, in the latter case, the absorption times are expected to be shorter, as it is indeed observed in Figure 3.5a. However, the difference between them is approximately five times smaller than that between PET R 1 and PET R 2.

On the other hand and as expected, both PET RCM 1 and PET RCM 2 show much shorter absorption times compared with their references PET R 1 and PET R 2, respectively. However, for PET RCM 2 the observed decrease in the water absorption time is 85% compared with PET R 2, whereas for PET RCM 1 the decrease is 61% compared with PET R 1, based on the mean values as shown in Figure 3.5a. This result can be attributed to the different structure of each polyester type. PET R 2 is rather hydrophobic and has a quite dense plain woven structure with an openness factor of zero. Incorporating a hydrophilic component (microgel **CM**) in its surface layers is expected to enhance significantly its wettability, as it would possibly do in the case of a non-porous PET film. This effect is reflected in the pronounced decrease of 85% in the

total water absorption time observed for PET RCM 2. In the case of PET RCM 1, the rather hydrophobic initial substrate PET R 1 has a crêpe woven structure of 0.5% openness factor (Chapter 2, Table 2.1), and a macro-porosity almost seven times larger than that of PET R 2 (Chapter 2, Table 2.7). Therefore, any enhancement of the PET R 1 wettability caused by incorporation of microgel **CM** is expected to be less evident than in the case of PET R 2.

The reverse effect is observed in the case of aminated polyesters, as shown in Figure 3.5b. PET A 2 has a shorter average absorption time compared with PET A 1, unlike PET R 2 compared with PET R 1. On the other hand, PET ACM-T 2 exhibits slower water absorption than PET ACM-T 1, like PET RCM 2 compared with PET RCM 1. However, PET ACM-T 1 exhibits an 80% decrease in the average absorption time compared with PET A 1, whereas PET ACM-T 2 exhibits similar absorption times to those of PET A 2. This result is opposite compared with the corresponding samples of Figure 3.5a. These differences are ascribed less to the structural differences between the samples and more to their hydrophilization. Based on Table 2.7 of Chapter 2, PET ACM-T 2 does not exhibit severe topographic changes compared with PET A 2 and PET R 2. However, amination yielded more primary amine groups on PET A 2 than on PET A 1 (Chapter 2, Figure 2.15). On the other hand, functionalization with microgel **CM** was not as extensive on PET ACM-T 2 as on PET ACM-T 1. Therefore, it is expected that the amination process influenced more the wettability of the PET 2 type rather than the microgel functionalization through thermo-crosslinking. Thus, the total water absorption times of PET A 2 and PET ACM-T 2 appear similar but both much shorter than that of PET R 2. In the case of PET A 1, its average absorption time approximates the one of PET R 1; despite the increased, by ca. 25%, surface macro-porosity of the aminated polyester (Chapter 2, Table 2.7), its hydrophilization through amination was not extensive (Chapter 2, Figures 2.12 and 2.15). On the other hand, PET ACM-T 1 exhibited relaxation and had higher amine content, compared with PET A 1 (Chapter 2, Table 2.7 and Figure 2.13). These two factors possibly account for its shorter, by 80%, water absorption time.

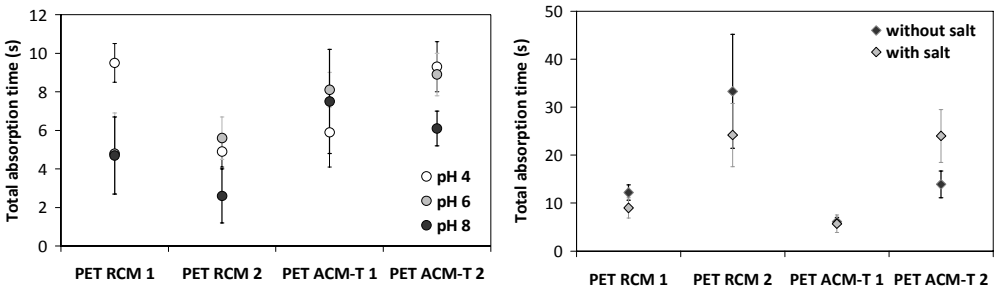

Figure 3.6: Total absorption times of microgel **CM**-functionalized polyesters PET RCM 1 and 2, and PET ACM-T 1 and 2, determined by the sessile-drop method using buffer solutions of pH 4, 6 and 8 **(a)**, and water with/without 0.04M NaCl **(b)**.

In Figure 3.6, the effect of different pH values and salt on the total absorption times of microgel **CM**-functionalized polyesters is shown. Since **CM** complexes are pH-responsive, it is expected that in contact with buffer solutions or in the presence of an electrolyte they swell/deswell on the fibers to different extents. This variable extent of swelling, which is a result of water attraction by ionic, ionizable or generally polar groups on the polyester surface, influences total absorption times in two ways; by regulating hydrophilicity, as previously described, as well as surface roughness. Depending on the extent of the surface roughness produced, wettability may be enhanced or hindered according to the Wenzel and Cassie-Baxter theories, even though intermediate regimes may occur (Cassie *et al.* 1944; Chow 1998; Ishino *et al.* 2008; Wenzel 1936).

In Figure 3.6a, total absorption times at pH 4, 6 and 8 are compared. Even though the differences among samples are in the magnitude of few seconds and standard errors are not negligible, it can be roughly concluded that PET RCM 1 and PET ACM-T 1 exhibit more differentiated absorption times at pH 4, whereas PET RCM 2 and PET ACM-T 2 at pH 8. Apparently, PET RCM 1 absorbs water more slowly at pH 4 than at pH 6 and 8, possibly owing to the poor ionization of PNIAA at pH 4. On the contrary, PET ACM-T 1 absorbs water faster at pH 4, possibly because any remaining primary amines of polyester that were not crosslinked with **CM** complexes become also protonated. However, for PET ACM-T 1 the absorption times at all three pH values are very similar to one another. These results correlate well with micro-roughness data presented in Figure 2.19b (Chapter 2), where the average arithmetic roughness (R_a) values for PET ACM-T 1 were found to be in the same range at all three pH studied. In the case of PET RCM 1, R_a was smaller at pH 4 compared with pH 6 and 8 (Chapter 2, Figure 2.19a); these data are in agreement with the corresponding absorption times observed, as they suggest that the PNIAA microparticles are not as swollen at pH 4, as they are at pH 6 and 8. Thus, **CM** complexes are also not as swollen and the total absorption time is increased. In a similar mode, PET RCM 2 and PET ACM-T 2 appear to absorb water faster at pH 8 rather than at pH 4 or 6, as their corresponding R_a values also reveal. The smaller differences observed for PET RCM 2, compared with PET RCM 1, at the three pH values can be possibly attributed to the fact that PET RCM 2 has a ratio of total amine groups to total carboxyl groups of approximately 1, whereas PET RCM 1 of 0.6 (Chapter 2, Figure 2.10). Therefore, hydrophilic groups ionizable in acidic and alkaline medium are expected to contribute to water absorption by PET RCM 2 to a similar extent.

A low molecular weight electrolyte like NaCl at a concentration of 0.04M does not seem to affect the total water absorption times of microgel **CM**-functionalized polyesters of the PET 1 series, as shown in Figure 3.6b. However, in the case of the PET 2 series, the average absorption time of PET RCM 2 appears to decrease by 10 s in the presence of salt, compared with the average time of water absorption without salt. For PET ACM-T 2 the opposite effect is observed, even though in both cases the standard errors are not marginal. For PET RCM 1 the standard errors are much smaller but so is the difference between the water absorption times with and without salt. In Figure 1.29a of Chapter 1 it was shown that an aqueous solution of NaCl 0.04M added to microgel **CM** at 20°C caused an increase in the hydrodynamic diameter of **CM** complexes. Therefore, it was expected that the wettability of microgel **CM**-functionalized polyesters would be

enhanced in the presence of salt due to higher water absorption by the **CM** complexes. To investigate whether "unusual" swelling occurred, the evolution with time of the height and the base radius of a water drop with 0.04M NaCl was recorded on the surface of PET RCM 1. The curves (average of eight measurements) are presented in Figure 3.7 with the time axis (*x*-) being partly in logarithmic scale and partly in normal scale to make the differences between the curves more visible.

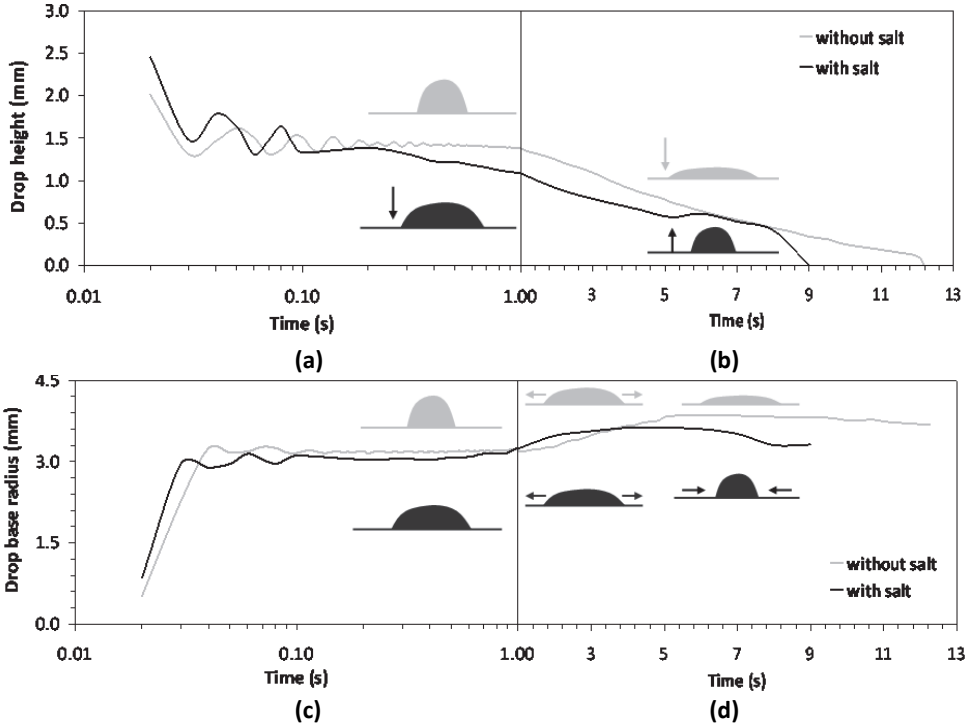

Figure 3.7: Evolution with time of the height **(a, b)** and the radius of the base **(c, d)** of a drop of a 0.04M NaCl solution or plain water in contact with the surface of PET RCM 1. The time axis in graphs **(a)** and **(c)** is in logarithmic scale, whereas in **(b)** and **(d)** in linear scale, to underline in each case the differences between the curves.

By comparing Figures 3.7a and 3.7c, it appears that while the bases of both water drops evolve similarly, the height of the drop with salt starts to decrease earlier, indicating that wetting begins earlier in the presence of salt. Reported studies on the wetting transitions of ionic solutions (including of NaCl) near charged solid substrates have shown that even very low salt concentrations are sufficient to induce changes in the wetting behavior of solvents (Denesyuk *et al.* 2004). In Figure 3.7b it is shown that the height of the water drop without salt decreases gradually until total absorption by the substrate, while the corresponding drop base in Figure 3.7d appears to stabilize to a constant value almost halfway of the measurement. For the water drop with salt, the respective curves in Figures 3.7b and 3.7d reveal a sudden increase in the drop's height at t=5.4 s, while at the same time the drop's base starts to decrease before it stabilizes

again just before total absorption. These results suggest that, in the presence of salt, wetting of the microgel complexes is achieved faster; after **CM** complexes are wetted, the remaining volume of the water drop is consumed for swelling the complexes before being eventually absorbed by the textile structure. However, more detailed experiments are necessary to verify the above suggestion.

3.3.2. Water uptake & capillarity

Textiles are complex substrates and their special structural characteristics influence greatly their physicochemical properties, including wettability. As already discussed, water can travel, spread and absorb through different paths on the textile surface depending on particularities of the surface topography. However, it is also distributed within the textile structure through capillaries. To elucidate how water progresses via the capillaries of functionalized polyesters, capillarity measurements were performed via water uptake measurements (in vertical position), as mentioned also in Glampedaki *et al.* 2010. The results are presented in Figures 3.8 and 3.9.

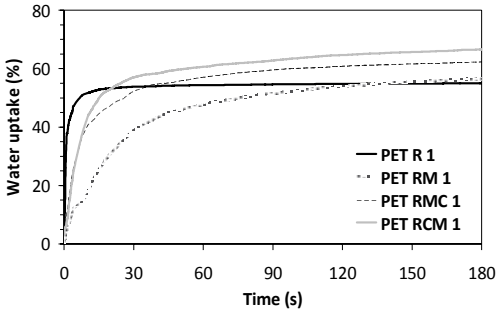

Figure 3.8: Water uptake measurements for PET R 1, PET RM 1, PET RMC 1 and PET RCM 1 performed with a tensiometer for a period of 3 min.

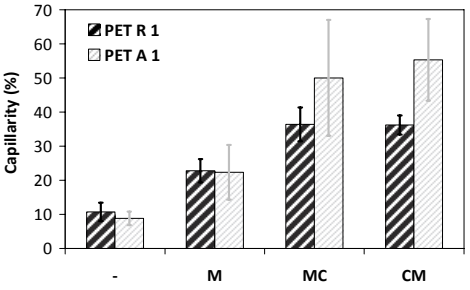

Figure 3.9: Capillarity of reference and UV irradiated polyester samples PET R 1, PET RM 1, PET RMC 1 and PET RCM 1, and of their aminated equivalents, determined through weight measurements using a tensiometer.

Based on Figure 3.8, it is clear that water uptake of polyesters is enhanced after functionalization with microgels. Reference polyester PET R 1 exhibits a sharp increase in water uptake as soon as it comes in contact with water, and reaches equilibrium within the first few seconds. The functionalized polyesters appear to take up water at slower rates, based on the slopes of the curves up until approximately 30 s, with PET RM 1 exhibiting the slowest rate. The latter result can be attributed to two factors: the "incubation" period needed for the microgel **M** layer to be wetted (Figure 3.2a), and the subsequent swelling of PNIAA microparticles which is likely to block partly the capillaries and hinder water rise. Based on Figures 1.1b and 1.11 in Chapter 1, PNIAA microparticles are bigger in size than **CM** complexes, in hydrated state. Furthermore, it was shown in Figures 2.4 and 2.5 in Chapter 2 that microgel **M** forms a rather continuous layer on

polyester fibers, whereas **CM** complexes have discrete and more sparsely distributed positions on the fiber surface. For these reasons, it is expected that PNIAA microparticles demand more time to fully swell on PET RM 1 fibers, compared with **CM** complexes on PET RCM 1 fibers. Therefore, PET RM 1 exhibits the slowest water uptake rate, and PET RCM 1 the fastest, among the three functionalized polyesters. The rate for PET RMC 1 lies between those of PET RM 1 and PET RCM 1, though it approximates more the one of PET RCM 1. This result is not surprising; it was shown in Chapter 1 (paragraph 1.3.6.) that although microgel **MC** has a PNIAA content closer to the one of microgel **M** than that of microgel **CM**, its properties in hydrated state do not resemble the properties of microgel **M**. Even though the water uptake decelerates after approximately 2 min for all functionalized polyesters, equilibrium is not reached within the measurement time frame. This result indicates that microparticles and complexes swell gradually on the polyester fibers as they come in contact with water. These data also reveal that the water capacity of functionalized polyesters remains unsaturated for a period more than 60 times longer compared with reference polyester. These observations are significant, as they underline that polyesters functionalized with microgels can have regulated water uptakes in terms of uptake rate, as well as water content.

From the same set of measurements, the capillarity of polyesters was determined, as described in paragraph 3.2.3. The results are shown in Figure 3.9. It is evident that all microgel-functionalized polyesters have higher capillarity values than the reference polyester. More specifically, compared with PET R 1, PET RM 1 has approximately 100% higher capillarity, whereas PET RMC 1 and PET RCM 1 have almost 300% higher values than PET R 1. To explore whether these results can be attributed to the microgel effect only, the corresponding aminated polyesters (i.e. microgel-functionalized through UV irradiation, not thermo-crosslinking) were also tested. As shown in Figure 3.9, similar trends are observed for the samples of the PET A 1 series. However, the CS-containing aminated polyesters exhibit higher capillarity values but also higher standard errors. A possible explanation is that, after amination, the polyester structure became less tight and its fiber surface more hydrophilic. Moreover, the subsequent microgel functionalization did not yield homogeneous coverage of the fibers (Chapter 2, Figure 2.7); thus, the standard errors might be reflecting these irregularities, as microparticles and complexes swell along the fibers.

The lower capillarity values found for both PET RM 1 and PET AM 1, compared with the CS-containing samples of both series PET R 1 and PET A 1, support the previously made suggestion that microparticle swelling blocks partly the capillaries and hinders further water rise. Apart from the volume exclusion caused by microparticle (or complex) swelling, the assumed increase in fiber surface roughness due to swelling is also expected to influence the capillary rise by affecting liquid-solid contact angles (Morrow *et al.* 1978; Nakae *et al.* 2005). It was shown in Figure 2.18 in Chapter 2 that PET RCM 1 fibers exhibit increased values of arithmetic roughness when they are impregnated with buffer solutions, compared with their fiber roughness when they are dry. The extent of this influence on capillarity needs to be further investigated with appropriate techniques.

3.3.3. Water vapor transmission

Water vapor transmission, transfer, transport, flux or permeability are terms used to describe the breathability of textiles. Better breathability is often translated as improved wear comfort. The above parameters are usually expressed as the rate at which water vapor is transmitted through a material of certain thickness. The rate values depend as much on ambient conditions during testing, such as temperature, relative humidity and air flow (Gibson 2000), as they do on the nature and the properties of the tested material, such as hydrophilicity, hygroscopicity, porosity, thickness, coatings etc. (McCullough *et al.* 2003; Schmidt *et al.* 2005). Water vapor transfer involves two processes: a) diffusion from the air to the textile (or from the textile to the air); and b) diffusion within the textile structure (Li et al. 2000; Stroeks 2001).

In Figures 3.10 and 3.11, the water vapor transmission rates (WVTRs) at 20°C and 40°C and at 65% and 95% RH are given for UV-crosslinked and aminated thermo-crosslinked functionalized polyesters of the PET 1 series, respectively, in relation to corresponding reference polyesters. In Figure 3.12, the effect of intermediate RH values on WVTR is investigated by performing the measurements, additionally, at 75% and 85% RH.

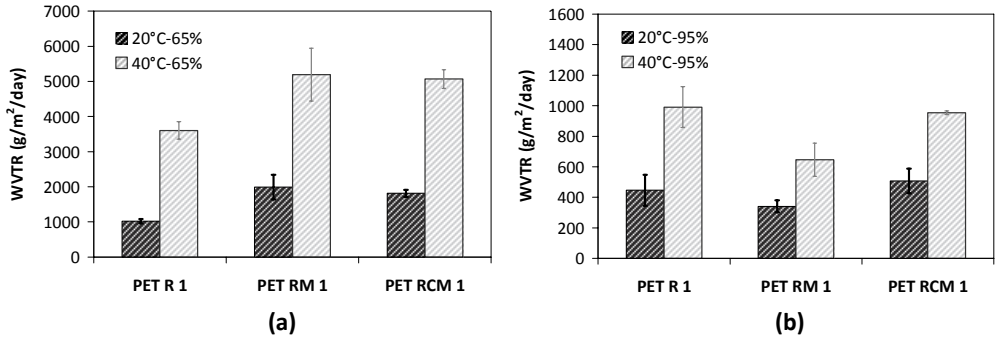

Figure 3.10: Water vapor transmission rates of polyesters PET R 1, PET RM 1 and PET RCM 1 at 20°C and 40°C, and 65% RH **(a)** or 95% RH **(b)**.

At 65% RH, the functionalized polyesters PET RM 1 and PET RCM 1 have higher transmission rates than reference polyester PET R 1, both at 20°C and 40°C (Figure 3.10a). In the case of PET RM 1, this result is attributed to two factors; the increased textile macro-porosity after functionalization (Chapter 2, Table 2.7), and the microgel presence on the polyester fibers which helps attract more moisture. For PET RCM 1, the second factor seems to play the main role, as the macro-porosity remained practically unaffected after functionalization. When RH rises to 95% (Figure 3.10b), all polyester samples have much lower WVTR compared with their corresponding rates at 65% RH. This result is not surprizing because the higher the humidity is, the more limited becomes the driving force for vapor transmission (Huang *et al.* 2010). This driving force is, in fact, the difference between the amounts of moisture in the spaces below and above the textile sample. At 40°C and 95% RH, PET RM 1 has the lowest WVTR among the three

samples, owing to the thermo-responsive nature of PNIAA microparticles which become rather hydrophobic above 36°C. Also at 20°C and 95% RH PET RM 1 has the lowest WVTR, even though its macro-porosity – which affects permeability (Ogulata *et al.* 2010) – was found to be bigger than that of PET R 1 and PET RCM 1. This peculiarity can be attributed to the fact that microgel **M** forms a continuous layer on the fibers. As PNIAA microparticles become increasingly swollen due to high RH, they possibly block the polyester pores hindering vapor transmission. Similar effects were observed in the previous paragraph (3.3.2.) regarding water uptake and capillarity of PET RM 1.

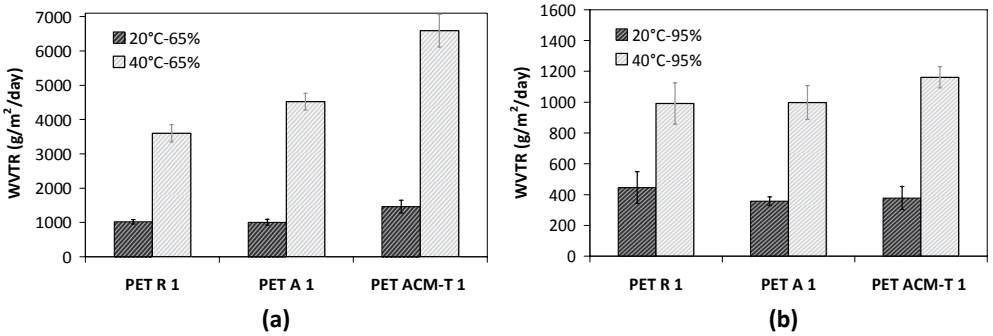

Figure 3.11: Water vapor transmission rates of reference and aminated thermo-crosslinked polyesters PET R 1, PET A 1 and PET ACM-T 1, at 20°C and 40°C, and 65% RH **(a)** and 95% RH **(b)**.

In the case of aminated polyesters, Figure 3.11a reveals that, at 20°C and 65% RH, PET R 1 and PET A 1 exhibit similar WVTRs, whereas PET ACM-T 1 has an average rate approximately 40% higher. At 40°C and 65% RH, PET A 1 has an increase of 26% in WVTR and PET ACM-T 1 of 83%, compared with PET R 1. Two reasons can account for these results: the looser structure of polyester after amination (Chapter 2, Table 2.7), which facilitates water evaporation at elevated temperature; and the ability of **CM** complexes to attract water. At 20°C, **CM** complexes are below their LCST; thus, they are prone to retain a large amount of the water molecules they attract. At 40°C, **CM** complexes are above their LCST; thus, any adsorbed water molecules are released rather than retained. Consequently, water vapor transmission of PET ACM-T 1 becomes more pronounced at 40°C and 65% than at 20°C and 65%.

At 20°C and 95% RH (Figure 3.11b), owing to the almost saturated humid atmosphere around the samples, moisture transfer between the bottom and top surface of the textiles is expected to reach equilibrium quickly. Thus, the transmission rates of all three samples (PET R 1, PET A 1, and PET ACM-T 1) are more than 50% lower than at 20°C and 65% RH (Figure 3.11a). It is also possible that swelling of **CM** complexes on the polyester fibers, induced by the high humidity levels, partly blocks the intra- and inter-yarn pores of PET ACM-T 1. For these reasons, PET ACM-T 1 does not exhibit a higher WVTR at 20°C-95% RH, neither compared with PET R 1 and PET A 1 under the same conditions, nor with its own WVTR at 20°C-65% RH. At 40°C and 95% RH (Figure 3.11b), the hydrophobic effect of **CM** complexes on water vapor transmission is expressed through the small but noticeable increase in the WVTR of PET ACM-T 1, compared with

the values of PET R 1 and PET A 1 at the same conditions. Nevertheless, this slightly increased rate is five times lower than the WVTR of PET ACM-T 1 at 40°C and 65% RH (Figure 3.11a), for reasons described above.

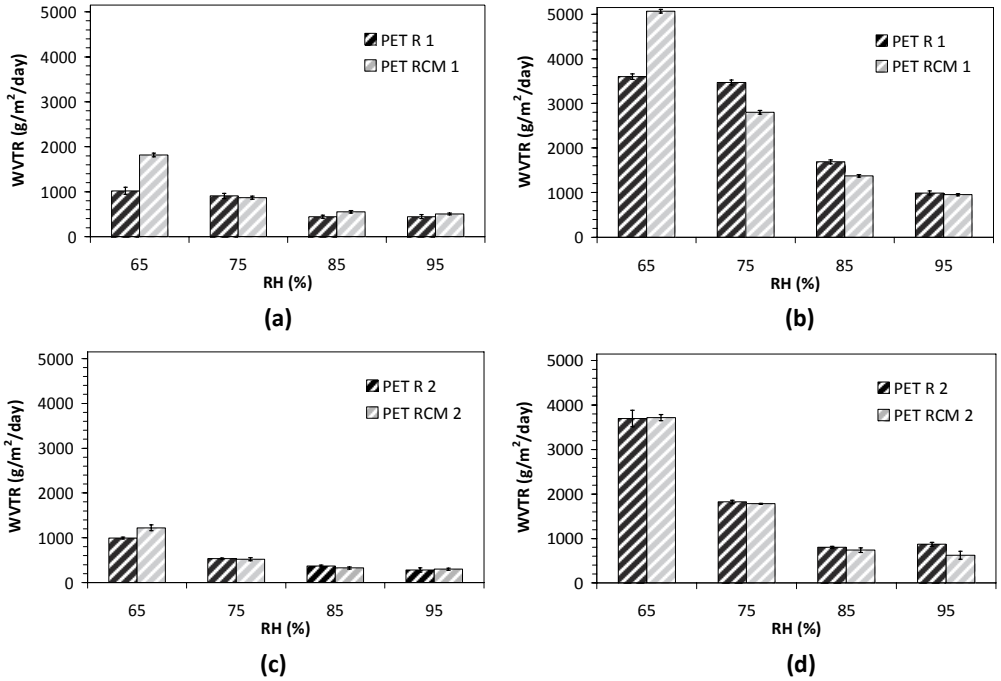

Figure 3.12: Water-vapor transmission rates of reference polyesters PET R 1 and 2, and of functionalized polyesters PET RCM 1 and 2, at RH values 65%, 75%, 85% and 95%, and at 20°C **(a, c)** and 40°C **(b, d)**. The results for the PET 1 series of samples are presented in graphs **(a)** and **(b)**, and for the PET 2 series in graphs **(c)** and **(d)**.

The combined impact of the ambient relative humidity and temperature and of the textile enhanced hydrophilicity or hydrophobicity, structure and porosity on moisture transfer is better understood from Figure 3.12. At both 20°C and 40°C, the higher the RH is, the lower are the WVTRs of PET R 1 and PET RCM 1 (Figures 3.12a and 3.12b), as expected due to concentration-dependent diffusion. Also, the higher the temperature is, the higher are the WVTRs, due to the added effect of drying. At both 20°C and 40°C, the biggest difference in WVTR between PET R 1 and PET RCM 1 is observed at lower RH (65%), owing to the partial swelling of **CM** complexes. It is assumed that the lower the RH is, the longer is the time needed for them to reach equilibrium swelling. Until then, part of the moisture that is adsorbed on the textile surface and subsequently diffuses within the textile structure is considered to be consumed for the complexes swelling rather than being transmitted to the other side of the textile. This suggestion is supported by findings reported in literature for complexes of poly(acrylic acid) compared with non-complexed polymers (Chang *et al.* 1997). These findings showed that complexes had a high degree of swelling but a low water diffusion coefficient; this effect was attributed to

formation of hydrogen bonds within the complexes, among polar groups such as carboxyl (COOH) and carbonyl (C=O) (Chang *et al.* 1997). As RH rises, moisture absorption by the **CM** complexes is enhanced. At the same time, the surrounding air becomes more saturated and the driving force for water vapor transmission weakens, while the textiles pores are closing off. As a consequence of this enhanced hydrophilicity induced by the **CM** complexes, at 20°C, the difference between each WVTR of PET RCM 1 at 75%, 85% and 95% RH, and its value at 65% RH is bigger than the corresponding differences of the WVTRs of PET R 1. This effect of bigger WVTRs steps for PET RCM 1 compared with PET R 1 as RH rises is observed also at 40°C. However at 20°C, as RH rises, the WVTRs of PET RCM 1 remain either higher or become equal to those of PET R 1, whereas at 40°C, they become gradually lower owing to the increased hydrophobicity of **CM** complexes. The latter result underlines how the thermo-responsive nature of the **CM** complexes can regulate the water vapor transmission through the functionalized polyesters.

The effect of the textile structure on the above mechanisms is evident in Figures 3.12c and 3.12d. PET R 2 has an openness factor of zero (Chapter 2, Table 2.1) and is approximately 14% thicker than PET R 1 (Chapter 2, Table 2.9). Therefore, moisture transfer is significantly impeded, and for intermediate RH values there is no difference in WVTRs between PET R 2 and PET RCM 2. Nonetheless, at lower RH (65%) and 20°C, PET RCM 2 exhibits higher WVTR than PET R 2, and at higher RH (95%) and 40°C, it exhibits a lower rate than PET R 2. These results verify the contribution of the **CM** complexes to the water vapor transmission process, as they are derived from measurements were the role of the textile porosity is minimized.

3.3.4. Moisture sorption/desorption

To investigate whether the above suggestions about moisture absorption by the **CM** complexes during water vapor transmission are valid, moisture sorption-desorption measurements were performed at various RH values and temperatures. The first set of measurements was used to determine how much time is needed for equilibrium moisture absorption at 20°C-65% RH (standard textile testing conditions) and 40°C-65% RH. The obtained curves of moisture uptake (or loss) vs. time at these conditions are presented for PET R 1 and PET RCM 1 in Figure 3.13. It is shown that, at 20°C-65% RH, both polyesters gradually absorb moisture until a maximum value is reached. PET R 1 reaches its maximum (ca. 0.5%) in approximately 15 min, while PET RCM 1 reaches its own (ca. 7%) in 30 min. This delayed moisture absorption of PET RCM 1 compared with PET R 1 can be attributed to a similar suggestion made previously about an “incubation” period needed until **CM** complexes start to absorb water. A similar concept was reported in Thijs *et al.* 2007; there, the formation of a “first hydration shell” on dried hydrophilic polymers, conditioned under various RH values, was conjured to explain sharp increases in the moisture uptakes of these polymers. In the same study it was concluded that there was a certain difficulty in the formation of a first hydration shell, after which additional hydration shells could form more easily. After PET R 1 and PET RCM 1 reach their maximum values, a slight decrease is observed for both samples and equilibrium is

reached after approximately 2 h. The moisture uptake of PET RCM 1 at equilibrium was found to be 11 times higher than that of PET R 1 (Figure 3.13).

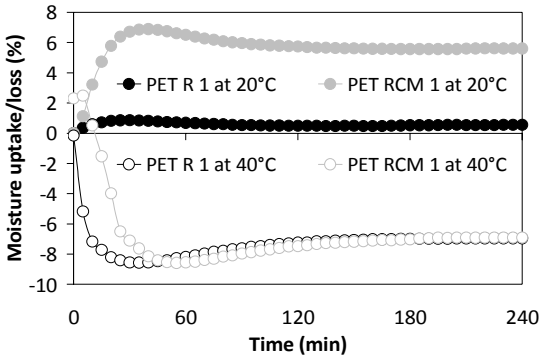

Figure 3.13: Curves of moisture sorption (at 20°C) and desorption (at 40°C) for PET R 1 and PET RCM 1, at 65% RH and over a period of 4 h.

At 40°C-65% RH, the curves are of similar shape. However, PET R 1 appears to lose rapidly more than 8% of its moisture content within the first 10 min, while PET RCM 1 appears to gain moisture, instead of losing, during the first few minutes. This peculiar behavior of PET RCM 1 is possibly attributed to the molecular reconfigurations that **CM** complexes undergo during their volume-phase transition above LCST and before they reach steady state. While they create intra-polymer hydrogen bonds turning hydrophobic, more ionic groups are exposed towards their outer surface, as discussed in Chapter 1. Hence, it is possible that **CM** complexes absorb moisture through their "exposed" hydrophilic sites, until reconfigurations are completed. For both PET R 1 and PET RCM 1, it takes longer to reach equilibrium at 40°C-65% RH (after ca. 3 h) than it does at 20°C-65% RH, possibly due to the added effect of drying through evaporation occurring simultaneously with moisture adsorption on their surfaces. However at the end, PET RCM 1 loses overall less moisture (roughly +2.5% (at t=0) - 7% (at t =4 h) =4.5%) than PET R 1 (ca. 7%). This result verifies the previously made suggestion (paragraph 3.3.3.) that, at 40°C-65% RH, the WVTR difference of PET RCM 1 with PET R 1 is smaller than their difference at 20°C-65% RH because PET RCM 1 retains some moisture at 40°C-65% RH.

Having shown that 4 h are enough for both polyesters to reach equilibrium at 65% RH, samples of PET R 1 and PET RCM 1 were further conditioned for 4 h at RH values higher than 65%. The decision to test at RH values higher than 65%, rather than lower, was based on the expectation that changes in moisture contents would be more pronounced. In fact, it was reported in Thijs *et al.* 2007 that even dried superabsorbent polymers like poly(acrylic acid)-sodium salt and poly(ethylene glycol) exhibit a steep moisture uptake between 60% and 90% RH, but not at lower RH. The equilibrium moisture uptakes (sorption) or losses (desorption) of PET R 1 and PET RCM 1 were plotted against RH at 20°C, and the corresponding curves are shown in Figure 3.14a.

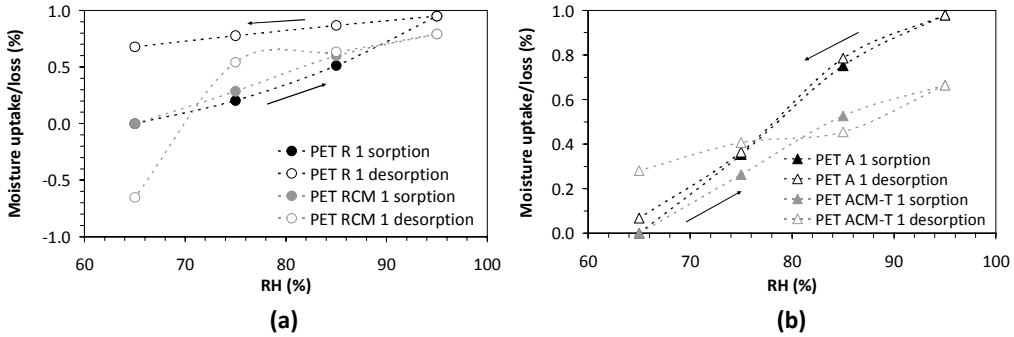

Figure 3.14: Moisture uptake or loss of PET R 1 and PET RCM 1 **(a)** and of PET A 1 and PET ACM-T 1 **(b)**, at 20°C and increasing (sorption)/decreasing (desorption) RH. The values at each RH point represent moisture uptake/loss at steady state, after 4 h conditioning at each set of conditions (first temperature/RH program (Figure 3.1a) of paragraph 3.2.5.).

Evidently, PET R 1 and PET RCM 1 follow the same trend during moisture sorption at increasing RH from 65% to 95%. However, PET RCM 1 appears to reach a slightly lower maximum at 95% than PET R 1 does, possibly due to the previously discussed swelling of the **CM** complexes at high RH. During desorption at decreasing RH, PET R 1 exhibits a clear hysteresis with a final value of 0.65% moisture uptake at the end of the cycle, whereas PET RCM 1 follows a much different trend. It appears that when RH decreases from 95% to 75%, the moisture loss of PET RCM 1 is not as significant as when the RH drops from 75% to 65%. This effect could be explained by the formation of water molecule clusters around the hydrophilic sites of **CM** complexes during sorption. The degree of clustering depends on the type of polar groups in the polymers, as well as on their complexation (Change *et al.* 1997). As RH decreases while being maintained at relatively high levels (until 75%), it is possible that these clusters undergo only a small reduction in the molecules that comprise them. When RH decreases even more reaching 65%, the clusters cannot be further sustained and moisture loss becomes sharp and more evident.

Similar measurements of sorption-desorption at 20°C were performed also on aminated polyesters PET A 1 and PET ACM-T 1. The resulting curves are shown in Figure 3.14b. PET A 1 shows no hysteresis compared with PET R 1 in Figure 3.14a. The ca. 30% increase in surface porosity after amination (Chapter 2, Table 2.7) seems to be responsible for this effect, as it does not favor moisture retention. Nonetheless, PET ACM-T 1 exhibits a sorption curve very similar to the one of PET RCM 1 in Figure 3.14a, underlining the contribution of **CM** complexes to the ability of functionalized polyester for moisture absorption. However, the desorption curve of PET ACM-T 1 shows a more gradual and step-wise reduction in moisture, with the biggest steps being from 95% to 85% RH, and from 75% to 65% RH. At the end of the cycle, PET ACM-T 1 appears to retain some moisture. More specifically, it exhibits almost 0.3% of moisture uptake, compared with the almost 0% of PET A 1 or the -0.7% of PET RCM 1 (the negative sign signifies loss beyond the initial moisture content of the sample). It is possible that formation of water

molecule clusters between primary amine groups of polyester and amine, carboxyl or amide groups of **CM** complexes is responsible for this effect.

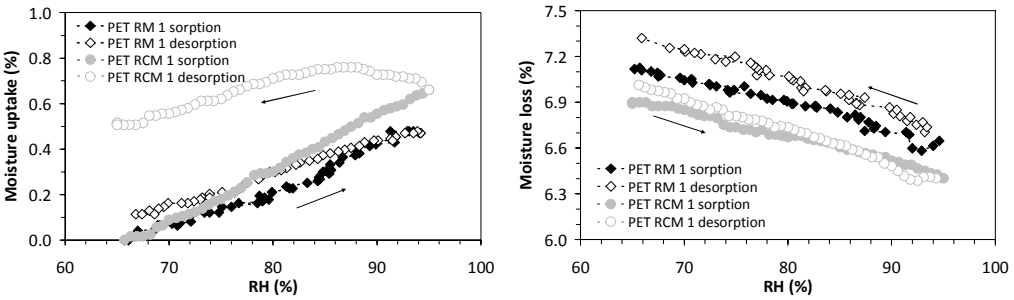

(a) **(b)**

Figure 3.15: Moisture sorption-desorption curves of PET RM 1 and PET RCM 1 at 20°C **(a)** and 40°C **(b)**, during continuous cycles of increasing and decreasing RH between 65% and 95% (second temperature/RH program (Figure 3.1b) of paragraph 3.2.5.).

In order to investigate the effect of thermo-responsiveness in the moisture sorption-desorption of functionalized polyesters, measurements were performed on PET RM 1 and PET RCM 1, at both 20°C and 40°C, during cycles of continuously increasing and decreasing RH (second temperature/RH program, paragraph 3.2.5.). The curves obtained are shown in Figure 3.15. Two observations are striking in Figure 3.15a, which depicts the sorption-desorption curves at 20°C: a) the desorption curve of PET RCM 1 is much different than its desorption curve of equilibrium values in Figure 3.14a; and b) PET RM 1 exhibits a very limited hysteresis during desorption, in contrast with PET RCM 1 which exhibits a rather significant one. The first observation emphasizes the previously made assumption about water clusters and formation of hydrogen bonds within the **CM** complexes. Since RH is continuously decreasing before samples reach equilibrium at each set of conditions, **CM** complexes do not dehydrate readily. Thus, moisture loss is hindered and possibly replaced by re-distribution, rather than release, of water molecules on the polyester surface and within the complexes. This effect is possibly responsible for the PET RCM 1 marked hysteresis, as well, as there is not enough time for the complexes' de-swelling to be completed. These results suggest that **CM** complexes, thus also PET RCM 1, respond slowly to RH changes at 20°C. Therefore, they could retain moisture for longer periods of time, and could possibly be used in slow release systems. On the other hand, the limited hysteresis of PET RM 1 is not surprising; isothermic curves of similar shape have been reported for pure PNIPAAm (Thijs *et al.* 2007). The lower moisture uptake values of PET RM 1, compared with PET RCM 1, can be attributed to the almost continuous layer that microgel **M** forms on polyester. Consequently, the microgel layer needs to be hydrated first before moisture is distributed within the polyester structure. As mentioned above, the "first hydration shell" of dry hydrophilic polymers needs time to be formed, and since RH changes rather fast during the studied cycles, equilibrium swelling of PNIAA cannot be reached.

At 40°C (Figure 3.15b), the sorption-desorption curves for both PET RM 1 and PET RCM 1 are similar. Note that the initial moisture content of the samples at the beginning of the cycle is the one obtained after 4 h at 20°C and 65% RH. Thus, when they are placed in an environment of 40°C they are expected to lose moisture even though RH is rising. The higher moisture loss observed for PET RM 1 at the very beginning of the cycle, i.e. at 40°C-65% RH of the "sorption" curves, can be attributed to the faster volume-phase transition of PNIAA microparticles compared with **CM** complexes. In Figures 1.2a and 1.9a of Chapter 1, it is shown, respectively, that at 40°C PNIAA microparticles of microgel **M** complete their transition from swollen/hydrophilic to shrunk/hydrophobic in approximately 3 min, whereas **CM** complexes need five times more time. As soon as this transition period is completed, the increased hydrophobicity of the microparticles and complexes appears to equally affect the decrease in moisture sorption of PET RM 1 and PET RCM 1; as shown in 3.15b, both samples lose approximately the same percent of moisture during the "sorption" isotherm of increasing RH. The fact that PET RM 1, unlike PET RCM 1, loses even more moisture during the receding-RH part of the cycle emphasizes the impact of the PNIAA thermo-responsiveness on moisture desorption. It can be assumed that as RH decreases, PNIAA microparticles "pump out" moisture from the textile substrate through their hydrophilic groups (mostly carboxyl). Since PNIAA is rather hydrophobic at 40°C, it cannot retain this extracted moisture; therefore, it releases it. In the case of PET RCM 1, the presence of CS helps balance this moisture loss. Thus, at the end of the cycle, the moisture loss is not bigger than at the beginning of the cycle.

3.3.5. Moisture regain

The thermo-responsiveness of the functionalized polyesters can be evaluated better through the moisture regain (M_R) results presented in Figure 3.16. Since all polyester samples were first dried at 105°C prior to the analysis, the thermo-responsive PNIAA microparticles – components also of **CM** complexes – were expected to have collapsed structures. Once exposed to humid environment again, they would swell at different extents depending on temperature and RH, resulting in higher M_R values compared with the reference polyester. Furthermore, if particles or complexes were re-hydrated at 20°C, higher moisture absorption would be expected for polyester owing to the swelling of the microparticle or complex structure, compared with re-hydration at 40°C where their structure would remain collapsed.

Indeed, at all studied RH values (Figures 3.16a–3.16d), the average M_R of microgel-functionalized polyesters PET RM 1 and PET RCM 1 were found to be higher than those of PET R 1 at 20°C, and lower than them at 40°C. More specifically, at 20°C, PET RCM 1 exhibited the highest average M_R compared with both PET R 1 and PET RM 1 at all studied RH values, reaching values between 2.5% and 5.5%. As expected, at 20°C, both PET RM 1 and PET RCM 1 exhibited their highest average M_R values at 95% RH (4.4% and 5.5%, respectively), while the average M_R of PET R 1 remained between 1.0% and 2.0% at all RH values.

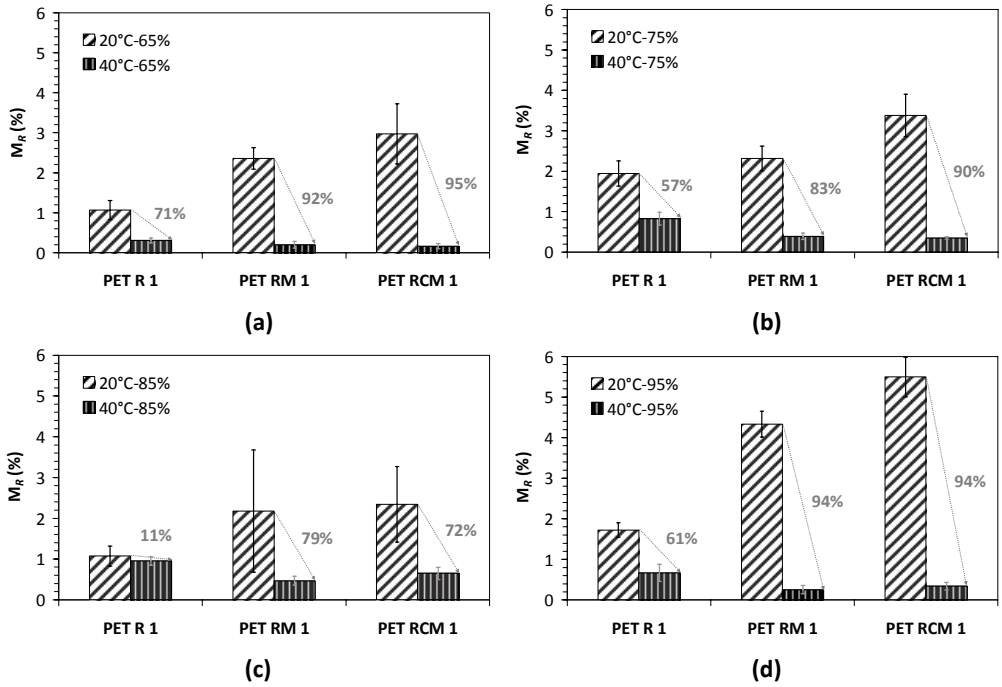

Figure 3.16: Moisture regain (M_R) values of PET R 1, PET RM 1 and PET RCM 1 at 20°C and 40°C, and 65% **(a)**, 75% **(b)**, 85% **(c)** and 95% **(d)** RH.

Surprisingly though, at 85% RH and 20°C, PET RM 1 and PET RCM 1 exhibited minimum average regains and maximum standard errors compared with the rest of their values at the same temperature. This result suggests that there is a critical point of RH at which two phenomena compete; drying due to evaporation, and moisture uptake due to microgel swelling and to absorption from the textile itself. Below that point, i.e. at 65% and 75% RH, moisture absorption prevails even though hindered by simultaneous drying. Above that point, evaporation is limited due to high levels of ambient moisture and, therefore, absorption is predominant. This suggestion is supported by the finding that, at 85% RH, reference PET R 1 exhibits the smallest difference in its M_R values between 20°C and 40°C. Therefore, for this particular type of polyester with the particular porosity, openness factor, weaving structure, and hydrophilicity (or hydrophobicity) due to microgels, 85% RH seems to be a critical parameter. Another result that corroborates this conclusion is that, at 20°C and 85%, the WVTRs of PET R 1 and PET RCM 1 were found to be almost equal to their respective values at 20°C and 95% (Figure 3.12a).

For PET R 1 and PET RCM 1, the largest differences in average M_R values between 20°C and 40°C are observed at lower RH, i.e. 65%. These differences were calculated to be 71% and 95%, respectively (Figure 3.16a). For PET RM 1, the largest difference was found at 95% RH (Figure 3.16d). Indeed, the contribution of the hydrophobic character of PNIAA above its LCST to decreased moisture regains of polyester is more noticeable at high RH, where drying is not as intense as at lower RH. These results combined with the lower WVTRs of PET RM 1 and PET RCM 1 compared with PET R 1 at 40°C-95% RH (Figure

3.10b), and the moisture losses observed at 40°C even with increasing RH (Figure 15b), lead to a clear conclusion; polyester textiles functionalized with PNIAA microparticles (whether alone in suspension or complexed with chitosan) exhibit thermo-responsiveness at a temperature range close to the average human body temperature.

3.4. FURTHER CHALLENGES & RECOMMENDATIONS

In this chapter, the effect of microgel functionalization on water management properties of polyester textiles was investigated, with and without the influence of external stimuli such as pH and temperature changes. The reason for choosing water management properties to explore the impact of microgel functionalization was three-fold. First, they are strongly associated with wear comfort; thus, they are of crucial importance for polyester textiles intended for apparel. Second, stimuli-responsive microgels absorb or expel water regardless if a stimulus is applied to them; the role of the stimulus is to regulate the amount of absorbed or expelled water. And third, even if a stimulus *is* applied, its effect is expressed only in the presence of water. In other words, water is the driving force for microgels to be functional.

Dynamic wetting measurements showed that functionalization with microgel **CM** reduces significantly the total water absorption time of polyester, whereas with microgel **M** it increases it dramatically. However, capillarity was increased in both cases. Changes in pH and the presence of salt did not yield very large differences in total absorption times but they appeared to influence the evolution with time of the contact angle, height and base radius of a water drop on polyester. On the other hand, water vapor transmission, moisture sorption-desorption and moisture regain data pointed to the conclusion that microgels imparted thermo-responsiveness to polyester. In all cases, the special topographic characteristics of the textiles were found to certainly play a role in the overall effect of water management, at times emphasizing the microgel contribution to it and other times masking it. To elucidate more in detail the obtained results, as well as to explore their application to end uses, the following recommendations are proposed for further studies:

- Conduct similar measurements on PET films functionalized with microgels **M** and **CM**. Eliminating parameters such as porosity and roughness, the presence of which is inevitable in the case of textiles, is expected to facilitate the observation of the stimuli-responsiveness of microgels after functionalization.
- Perform dynamic wetting measurements with different wetting agents and apolar media to test the extent of microgel hydrophobicity and intra-molecular hydrogen bond formation.
- Determine capillarity using buffer solutions of different pH values. If possible, thermo-state the capillarity device to study the effect of thermo-responsiveness, as well.
- Perform moisture sorption-desorption cycles and water vapor transmission measurements at RH values lower than 65% and at a wider temperature range with smaller temperature intervals.
- Investigate which water management properties are influenced more and by which microgel properties by e.g. Principal Component Analysis; possibly create a predictive model tailored to predict e.g. the moisture or sweat absorption by microgel-functionalized textiles according to pH or temperature changes of the human skin.

CONCLUSIONS & OUTLOOK

Incorporation of polyelectrolyte microgels into polyester surface layers was proposed in this study as a new path for the functionalization of polyester textiles. Two rather facile and conventional techniques were employed to achieve microgel incorporation: photo-crosslinking through UV irradiation, and thermo-crosslinking following a pad-dry-cure method. Microgels consisting of PNIAA alone or complexed with CS were prepared to have both pH- and thermo-responsive properties, with the aim that these properties would be imparted ultimately to polyester textiles. The concept of polyester functionalization through stimuli-responsive microgels was suggested as an alternative way towards advanced textile-based materials with the ability to adapt to changes in their environment.

Chapter 1

In Chapter 1, microgel preparation and characterization were described and discussed in detail. Based on microgel **M** of pH/thermo-responsive PNIAA microparticles with a zero-charge point at pH 3.4 and an LCST close to 34°C, a novel type of microgel was prepared consisting of polyelectrolyte complexes between PNIAA microparticles and CS (microgel **CM**). According to the results presented, it is concluded that microgel **CM** expresses its pH/thermo-responsiveness within a physiological pH and temperature range of a human body (pH 4.5-7.5, and 20-40°C, respectively). More specifically, **CM** complexes exhibited a zero-charge point at pH 6 (based on potentiometric titration and electrophoretic mobility data) and an LCST at ca. 36°C (based on DSC data). The higher the temperature was, the faster the thermally-induced volume-phase transition occurred, for both microgels **M** and **CM** (based on light transmittance data of UV-Vis spectroscopy). This transition was found to be reversible in both cases, but slower for **CM** complexes compared with PNIAA microparticles alone. Changes in microgel viscosity upon CS addition were not found responsible for this effect. In fact, it was shown that, by using a CS solution of 0.2% (w/v) for the preparation of microgel **CM**, the viscosities of microgels **M** and **CM** showed no significant differences. Furthermore, the critical entanglement concentration of CS was found to be 0.6% (w/v) (based on rheological measurements), i.e. three times higher than the CS concentration used to prepare microgel **CM** in this study. Thus, the formation of a bulk continuous hydrogel system was avoided and no viscosity changes were observed after PNIAA complexation with CS. However, their complexation resulted in a size decrease of complexes **CM** compared with PNIAA microparticles, observed both in hydrated and dry state (based on SEM, cryo-SEM, and DLS data).

The temperature-effect on the size of **CM** complexes was found to be more pronounced in hydrated rather than in dry state. At temperatures above LCST, **CM** complexes were found to be approximately 50% smaller in hydrated state and less than 30% smaller in dry state, compared with their respective sizes below LCST. The pH-effect on the size of **CM** complexes was observed at both 20°C and 40°C; with increasing pH

from 4 to 8, the hydrodynamic size of the complexes decreased and their PDI increased (based on DLS data). However, changes in pH between values 4 and 8 were not found to affect the thermo-response rate of **CM** complexes (based on light transmittance data of UV Vis spectroscopy).

The total charge of **CM** complexes was found to be of positive sign owing to the excess of CS in microgel **CM** (based on polyelectrolyte titration data). This result underlined that **CM** complexes are electrostatically stabilized in the microgel due to mutual repulsion. However, their stability was compromised under certain combinations of pH and temperature. After extensive stability measurements, it was concluded that microgel **CM** can undergo phase-separation with time, especially under the influence of elevated temperature and low pH (based on analytical centrifugation data). Until pH 5, temperature was found to be the main factor affecting (de)stabilization. This effect was attributed to the influence of the PNIAA component of microgel **CM**, as similar trends were found for microgel **M**, as well. Above pH 5, changes in the pH rather than temperature appeared to instigate instability of microgel **CM**. That effect was attributed to the CS component of microgel **CM**, as it was found that CS solutions exhibited increasing precipitation above pH 7 at all studied temperatures.

Finally, the effect of complexation ratio, crosslinking and salts on the physicochemical properties of microgel **CM** was investigated. It was concluded that reversing the complexation ratio of PNIAA and CS (microgel **MC**) resulted in higher LCST but less sharp volume-phase transition, increased microgel hydrophobicity, decreased thermo-response rate and smaller size reduction above LCST. Crosslinking CS with the natural crosslinker genipin (GP) inside microgel **CM** led also to higher microgel hydrophobicity, decreased thermo-response rates and even smaller size reductions above LCST. However, it was found that the resulting microgels **CM** were showing signs of phase-separation only when GP was used at CS/GP ratios between 20/1 and 40/1 (w/w). The addition of low molecular weight electrolytes at concentrations within the range of average values of human sweat revealed that, below LCST, an increase in the hydrodynamic size of **CM** complexes is observed only at higher ionic strength and acidic pH. Above their LCST, neither the increase in salt concentration nor adjustment of pH seems to cause significant size changes.

Chapter 2

In Chapter 2, the microgel functionalization of two types of polyester PET textiles was described, along with its effect on polyester surface, chemical and physical properties. Two techniques were used for microgel incorporation: a) photo-crosslinking via UV irradiation in the presence of the photo-initiator benzophenone; and b) low temperature thermo-crosslinking after polyester amination, using the natural crosslinker genipin. The functionalized textiles were thoroughly characterized using various techniques of surface analysis. It is concluded that microgels **M** and **CM** were durably incorporated into the polyester surface layers (based on SEM, FTIR-ATR and XPS data of functionalized samples rinsed and washed repeatedly even up to 30 times).

The surface morphology of functionalized polyester fibers varied significantly depending on the type of incorporated microgel (based on SEM data). Microgel **M** formed a continuous layer of "pancake-like" microparticle structures on PET fibers (PET RM 1); microgel **CM** appeared as discrete and sparsely, yet uniformly, distributed formations of circular shape (PET RCM 1); microgel **MC** formed lacy layers on and between fibers (PET RMC 1). The functionalization technique used affected also the final surface morphology. Aminated photo-crosslinked polyesters functionalized with microgel **CM** (PET ACM 1) exhibited a much more heterogeneous distribution of **CM** complexes on the fibers, compared with the corresponding non-aminated sample (PET RCM 1). On the other hand, the aminated polyesters thermo-crosslinked with microgel **CM** (PET ACM-T 1) showed a uniform but limited distribution of **CM** complexes on their fibers.

In all cases, functionalization resulted in decreased carboxyl contents and increased total amine contents of polyesters (based on colorimetric measurements); the latter content was found to be higher in the case of microgel **CM**-functionalized polyesters. However, non-aminated microgel **CM**-functionalized polyesters were found to have more than three times higher amine contents than the aminated ones. The effect of microgel functionalization on polyester surface charge was profound (based on streaming potential measurements). The presence of microgel **CM** yielded IEPs at pH values between 5.0 and 6.6, i.e. within the desirable physiological range. The fact that these values did not coincide with the IEP of fully coated substrates with microgel **CM** (pH 7.1) reflects the partial surface coverage of polyester fibers after functionalization.

Microgel functionalization of PET textiles with a more open and porous initial structure (PET 1 type) resulted in further relaxation of this structure, decreased macro-roughness (waviness) and increased or sustained surface macro-porosity (based on topographical analysis). Opposite effects were observed for the denser textiles (PET 2 type). The effect of pH changes on the fiber micro-roughness was more pronounced for the microgel **CM**-functionalized samples of the PET 2 type. These results indicated higher swelling of **CM** complexes above pH 6 (based on average arithmetic roughness (R_a) data). However, amination appeared to alleviate this effect.

Finally, it is concluded that physical properties of polyester textiles such as whiteness, yellowness and resistance to wrinkling are significantly affected by microgel-functionalization, as well as by amination (based on data of reflectance spectroscopy and crease recovery angles). The presence of microgel **CM** on polyesters caused an increased of almost four times in the yellowness index, owing to the innate yellowish color of CS solutions. The effect of microgel **CM** on aminated polyesters was not as intense, because amination itself appeared to cause a significant decrease of approximately 10 units in the polyester whiteness index and an increase in the yellowness index of ca. 3 units. Particularly in the case of aminated thermo-crosslinked polyesters (compared with photo-crosslinked), the effect of microgel **CM** on the yellowness index of polyester was balanced or masked by the slight blue-green coloration developed during the genipin crosslinking reaction.

With respect to the crease recovery angles, denser polyesters (PET 2 type) were proven more susceptible to wrinkling after microgel functionalization, as well as after amination. Nonetheless, despite the observed reduction in crease recovery angles, all

values measured were still within acceptable levels. The denser polyesters of the PET 2 type were also weakened much more after functionalization, compared with the more open and light-weight polyesters of the PET 1 series (based on tensile strength data). In fact, the mechanical strength of the former polyesters was reduced by almost 50% after microgel incorporation. Also in this case, amination appeared to play a predominant role in degradation of polyester properties, as aminated samples exhibited tensile strength values four times lower than those of reference polyester.

Chapter 3

In Chapter 3, the influence of microgel incorporation on the water management properties of the functionalized polyester textiles was investigated. It is concluded that, in the case of PET 1 type of samples, functionalization with microgel **CM** decreases total water absorption times almost three times, whereas microgel **M** increases them by more than four times, compared with reference polyester (based on dynamic wetting measurements with the sessile drop technique). The weaving structure of polyester textiles plays also a role in the absorption process, and it was found that for the denser type (PET 2), functionalization with microgel **CM** causes an even greater decrease of ca. 85% in the total water absorption time, compared with PET 1 samples. Amination increases also the hydrophilicity, and therefore wettability, of polyester but its effect was more pronounced in the case of the dense PET 2 polyester.

Furthermore, it is concluded that the effect of pH is more evident in the case of the microgel **M**-functionalized polyester; its absorption times were found to be 30–50% shorter above pH 6, compared with those at pH 4. For microgel **CM**-functionalized polyesters, it was found that the absorption times of all buffer solutions were shorter than those of plain water. It is suggested that all microgel-functionalized polyesters go through an "incubation" period when they first come in contact with a water drop (based on data from the evolution of the contact angle, height and base radius of water drops with time). During this period, the dried collapsed microgel layers become slowly and gradually wetted. Subsequently, water absorption within the microparticle/complex structure occurs, and absorption in the textile structure either follows or happens simultaneously. It is also concluded that CS promotes water absorption within and by the polyester structure (based on water uptake and capillarity data). More specifically, polyester functionalization with CS-containing microgels leads to faster water uptakes and increased capillarity values, compared with functionalization with microgel **M** only.

At 20°C and 65% RH (standard textile testing conditions), the WVTRs of microgel-functionalized polyesters were higher than the transmission rates of reference polyester. At 40°C, i.e. above the microgel LCST, this difference in WVTR was even greater. A similar effect was observed for aminated thermo-crosslinked polyesters, as well. However, the higher the RH was, the smaller became the differences between the WVTRs of reference and microgel **CM**-functionalized polyesters. It was also concluded that at 40°C and 65% RH, microgel **CM**-functionalized polyesters needed more time to reach equilibrium moisture uptakes, than at 20°C and 65% RH. During cycles of increasing and decreasing RH at 20°C, microgel **CM**-functionalized polyester exhibited a hysteresis in moisture

desorption much more pronounced than in the case of microgel **M**-functionalized polyester. However, by increasing the temperature above the microgel LCST this hysteresis disappeared, and the microgel **M**-functionalized polyester exhibited bigger moisture losses than the microgel **CM**-functionalized polyester (based on moisture sorption-desorption measurements). These findings lead to the conclusion that thermo-responsiveness was indeed imparted from the microgels to the polyester textiles. This conclusion is further supported by the fact that both microgel **M**- and microgel **CM**-functionalized polyesters regained more moisture at 20°C but less at 40°C, compared with reference polyester, even at high RH of 95%.

Combining the above conclusions drawn from each chapter of this thesis, two main remarks can be stated:

a) The initial aim, which was to impart pH- and thermo- responsive properties from microgels to polyester textiles, expressed within a physiological pH/temperature range, was achieved.

b) A single generic pattern cannot be drawn regarding the way that functionalized polyesters adapt to ambient conditions because, as shown, the expression of their responsive properties is the combined result of the microgel type, the polyester type and the functionalization technique. However, this conclusion emphasizes the main advantage of microgel-functionalized polyester textiles; they are dynamic and versatile systems, the properties of which can be tailored according to the requirements of a particular application. In other words, it was shown that materials with different properties (e.g. enhanced or limited water wettability, positive or negative surface charge, increased or decreased surface roughness) can be developed using the same systems in different variations.

Undoubtedly, there are points that need further consideration, such as optimizing the parameters of each functionalization technique to reduce degradation of polyester, the loss of its mechanical strength or the development of unwanted coloration. Moreover, designing an experiment to test the applicability of these materials (microgels only and/or microgel-functionalized polyester textiles) in e.g. controlled adsorption/release systems would give a significant insight into their potential. Relevant considerations and recommendations have been summarized at the end of each chapter to emphasize that there is certainly scope for further development of this research.

BIBLIOGRAPHY

Abd El-Mohdya HL, Safrany A, Radiation Physics and Chemistry **77**, 273 (2008)

Abdel-Halim ES, Abdel-Mohdy FA, Al-Deyab SS, El-Newehy MH, Carbohydrate Polymers **82**, 202 (2010)

Akkaya A, Pazarlioglu NK, Journal of Applied Polymer Science **121**, 690 (2011)

Al Sagheer FA, Al-Sughayer MA, Muslim S, Elsabee MZ, Carbohydrate Polymers **77**, 410 (2009)

Alem H, Duwez A-S, Lussis P, Lipnik P, Jonas AM, Demoustier-Champagne S, Journal of Membrane Science **308**, 75 (2008)

Andrady AL,Torikai A, Kobatake T, Journal of Applied Polymer Science **62**, 1465 (1996)

Ashruf CMA, Sensor Review **22**, 322 (2002)

Bahaj H, Benaddi R, Bakass M, Bayane C, Journal of Applied Polymer Science **115**, 2479 (2010)

Bendak A, El-Marsafi S-M, Journal of Islamic Academy of Sciences **4**, 275 (1991)

Berger S, Zhang H, Pich A, Advanced Functional Materials **19**, 554 (2009)

Bessada R, Silva G, Paiva MC, Machado AV, Applied Surface Science **257**, 7944 (2011)

Bhat VT, James NR, Jayakrishnan A, Polymer International **57**, 124 (2008)

Bide M, Phaneuf M, Brown P, McGonigle G, LoGerfo F, in J. V. Edwards et al. (Eds.), Modified Fibers with Medical and Specialty Applications, Springer, pp. 91–124 (2006)a

Bide M, Phaneuf M, Quist W, Dempsey D, LoGerfo F, *United States Patent* No: US007037527B2 (2006)b

Bilisik K, Demiryurek O, Fibers and Polymers **11**, 805 (2010)

Boyd S, Yamazaki H, Biotechnology Techniques **7**,277 (1993)

Brannon-Peppas L, Harland RS, Superabsorbent Polymer Technology, Elsevier, Amsterdam (1990)

Brugnerotto J, Lizardi J, Goycoolea FM, Arguelles-Monal W, Desbrieres J, Rinaudo M, Polymer **42**, 3569 (2001)

Bulmus V, Patır S, Tuncel SA, Piskin E, Journal of Applied Polymer Science **88**, 2012 (2003)

Buono M, Ball K, Kolkhorst F, Journal of Applied Physiology **103**, 990 (2007)

Burchard W, Ross-Murphy SB, Physical Networks–Polymers and Gels, Elsevier Science, Essex (1990)

Burey B, Bhandari R, Howes T, Gidley MJ, Critical Reviews in Food Science and Nutrition **48**, 361 (2008)

Butler MF, Ng Y-F, Pudney PDA, Journal of Polymer Science. Part A: Polymer Chemistry **41**, 3941 (2003)

Buyle G, Materials Technology **24**, 46 (2009)

Cai W, Gupta RB, Journal of Applied Polymer Science **83**, 169 (2002)

Calvimontes A, Topographic characterization of polymer materials at different length scales and the mechanistic understanding of wetting phenomena, Dissertation, Leibniz-Institut für Polymerforschung Dresden e.V., Dresden (2009)

Calvimontes A, Dutschk V, Stamm M, Textile Research Journal **80**, 1004 (2010)a

Calvimontes A, Hasan MMB, Dutschk V, in P. Dobnik Dubrovski (Ed.), Woven Fabric Engineering, pp. 71–92, Sciyo, Rijeka (2010)b

Cametti C, Chemistry and Physics of Lipids **155**, 63 (2008)

Campolongo MJ, Kahn JS , Cheng WL, Yang DY, Gupton-Campolongo T, Luo D, Journal of Materials Chemistry **21**, 6113 (2011)

Carpi F, De Rossi D, IEEE Transactions on Information Technology in Biomedicine **9**, 295 (2005)

Cassie ABD, Baxter S, Transactions of the Faraday Society **40**, 546 (1944)

Chang M-J, Myerson AS, Kwei TK, Journal of Applied Polymer Science **66**, 279 (1997)

Chang MW, Stride E, Edirisinghe M, Journal of the Royal Society Interface **8**, 451 (2011)

Chen H, Liu Z, Cebe P, Polymer **50**, 872 (2009)

Chen K-S, Tsai J-C, Chou C-W, Yang M-R, Yang J-M, Materials Science and Engineering C **20**, 203 (2002)

Chen S-C, Wu Y-C, Mi F-L, Lin Y-H, Yu L-C, Sung H-W, Journal of Controlled Release **96**, 285 (2004)

Cheng H, Zhu J-L, Sun Y-X, Cheng S-X, Zhang X-Z, Zhuo R-X, Bioconjugate Chemistry **19**, 1368 (2008)

Cherenack K, Zysset C, Kinkeldei T, Münzenrieder N, Tröster G, Advanced Materials **22**, 5178 (2010)

Chhatre SS, Tuteja A, Choi W, Revaux A, Smith D, Mabry JM, McKinley GH, Cohen RE, Langmuir **25**, 13625 (2009)

Cho J, Heuzey MC, Begin A, Carreau PJ, Journal of Food Engineering **74**, 500 (2006)

Chow TS, Journal of Physics: Condensed Matter **10**, 445 (1998)

Christodoulakis KE, Vamvakaki M, Macromolecular Symposia **291–292**, 106 (2010)

Chuang M-C, Windmiller JR, Santhosh P, Valdes Ramirez G, Galik M, Chou T-Y, Wang J, Electroanalysis **22**, 2511 (2010)

Cohen Stuart MA, Huck WTS, Genzer J, Müller M, Ober C, Stamm M, Sukhorukov GB, Szleifer I, Tsukruk VV, Urban M, Winnik F, Zauscher S, Luzinov I, Minko S, Nature Materials **9**, 101 (2010)

Curti PS, de Moura MR, Veiga W, Radovanovic E, Rubira AF, Muniz EC, Applied Surface Science **245**, 223 (2005)

Dakhara SL, Anajwala CC, Systematic Reviews in Pharmacy **1**, 121 (2010)

Daly E, Saunders BR, Physical Chemistry Chemical Physics **2**, 3187 (2000)

Danon A, Stair PC, Weitz E, The Journal of Physical Chemistry C **115**, 11540 (2011)

De Rossi D, Carpi F, Scilingo EP, Advances in Colloid and Interface Science **116**, 165 (2005)

Den Boer W, Active matrix liquid crystal displays [fundamentals and applications], Elsevier (2005)

Denesyuk NA, Hansen J-P, Journal of Chemical Physics **121**, 3613 (2004)

Deng J, Wang L, Liu L, Yang W, Progress in Polymer Science **34**, 156 (2009)

Deo HT, Patel NK, Patel BK, Journal of Engineered Fibers and Fabrics **3**, 23 (2008)

Detloff T, Sobisch T, Lerche D, Powder Technology **174**, 50 (2007)

Djabourov M, Polymer International **25**, 135 (1991)

Donelli I, Taddei P, Smet PF, Poelman D, Nierstrasz VA, Freddi G, Biotechnology and Bioengineering **103**, 845 (2009)

Drobota M, Aflori M, Barboiu V, Digest Journal of Nanomaterials and Biostructures, **5**, 35 (2010)

Ende MTA, Peppas NA, Journal of Applied Polymer Science **59**, 673 (1996)

Engin M, Demirel A, Engin EZ, Fedakar M, Measurement **37**, 173 (2005)

Fayolle B, Richaud E, Colin X, Verdu J, Journal of Materials Science **43**, 6999 (2008)

Fechine GJM, Rabello MS, Souto Maior RM, Catalani LH, Polymer **45**, 2303 (2004)

Ferrero F, Tonin C, Peila R, Pollone Ramella F, Coloration Technology **120**, 30 (2004)

Geever LM, Minguez CM, Devine DM, Nugent MJD, Kennedy JE, Lyons JG, Hanley A, Devery S, Tomkins PT, Higginbotham CL, Journal of Material Science **42**, 4136 (2007)

Geismann C, Ulbricht M, Macromolecular Chemistry and Physics **206**, 268 (2005)

Geismann C, Yaroshchuk A, Ulbricht M, Langmuir **23**, 76 (2007)

Gibson PW, Polymer Testing **19**, 673 (2000)

Glampedaki P, de Klein J, Warmoeskerken MMCG, Jocic D, The 9th World Textile Conference (AUTEX2009), May 26-28, 2009, Izmir–Cesme, Turkey, Proceedings, pp. 480-487 (2009) (ISBN 978-975-483-787-2)

Glampedaki P, Dutschk V, Jocic D, Warmoeskerken MMCG, Biotechnology Journal **6**, 1219 (2011)a

Glampedaki P, Jocic D, Dutschk V, Warmoeskerken MMCG, Surface modification of polyester fabrics by grafting pH/thermo-responsive microgels with UV irradiation, in Surface Modification Technologies XXIV (Proceedings), T.S. Sudarshan, E. Beyer, L.-M. Berger, (Eds.), pp. 131-138, Valardocs (2011)b

Glampedaki P, Jocic D, Warmoeskerken MMCG, Progress in Organic Coatings **72**, 562 (2011)c

Glampedaki P, Tourrette A, Warmoeskerken MMCG, Jocic D, The 8th World Textile Conference (AUTEX2008), June 24-26, 2008, Biella, Italy, Proceedings (CD-ROM), 6 pages (2008)a

Glampedaki P, Tourrette A, Warmoeskerken MMCG, Jocic D, 2nd International Scientific Conference "Textiles of the Future" – Futurotextiel 2008, November 13-15, 2008, Kortrijk, Belgium, Proceedings (CD-ROM), 10 pages (2008)b

Glampedaki P, Zhao J, Campagne C, Jocic D, Warmoeskerken MMCG, The 10th World Textile Conference (AUTEX2010), June 21-23, 2010, Vilnius, Lithuania, Proceedings, 4 pages (2010) (ISBN 978-609-95098-2-2)

Goddard JM, Hotchkiss JH, Progress in Polymer Science **32**, 698 (2007)

Gokarneshan N, Fabric Structure and Design, New Age International (P) Ltd., New Delhi (2004)

Gouveia IC, Antunes LC, Gomes AP, The Journal of The Textile Institute **102**, 203 (2011)

Grafahrend D, Heffels KH, Beer MV, Gasteier P, Moeller M, Boehm G, Dalton PD, Groll J, Nature Materials **10**, 67 (2011)

Griffin WC, Journal of the Society of Cosmetic Chemists **1**, 311 (1949)

Gulyaeva ZG, Aldoshina IV, Zansokhova MF, Rogacheva VB, Zezin AB, Kabanov KA, Polymer Science U.S.S.R. **32**, 714 (1990)

Gupta B, Grover N, Singh H, Journal of Applied Polymer Science **112**, 1199 (2009)

Ha ST, Park OO, Im SH, Macromolecular Research **18**, 321 (2010)

Hamman J, Marine Drugs **8**, 1305 (2010)

Hartig SM, Greene RR, Dikov MM, Prokop A, Davidson JM, Pharmaceutical Research **24**, 2353 (2007)

Hasan MMB, Calvimontes A, Synytska A, Dutschk V, Textile Research Journal **78**, 996 (2008)

Hawkins CL, Davies MJ, Biochimica et Biophysica Acta **1504**, 196 (2001)

He D, Susanto H, Ulbricht M, Progress in Polymer Science **34**, 62 (2009)

Helgeson ME, Chapin SC, Doyle PS, Current Opinion in Colloid & Interface Science **16**, 106 (2011)

Hirokawa Y, Tanaka T, The Journal of Chemical Physics **81**, 6379 (1984)

Hoare T, Pelton R, Current Opinion in Colloid and Interface Science **13**, 413 (2008)

Holly FJ, in Schrader ME, Loeb G (Eds.), Modern Approaches to Wettability: Theory and Applications, pp. 213–248, Plenum Press, New York (1992)

Holly FJ, Refojo MF, Journal of Biomedical Materials Research **9**, 315 (1975)

Holmes SA, Journal of Applied Polymer Science **61**, 255 (1996)

Hornby AS, Oxford Advanced Learner's Dictionary, 4th edition, Cowie AP (Ed.), Oxford University Press (1989)

Hosokawa M, Nogi K, Naito M, Yokoyama T (Eds.), Nanoparticle Technology Handbook, pp. 20-23, Elsevier, Amsterdam (2007)

Hossain MM, Mussig J, Herrmann AS, Hegemann D, Journal of Applied Polymer Science **111**, 2545 (2009)

Hu J, Li Y, Yeung K-W, Wong ASW, Xu W, Textile Research Journal **75**, 57 (2005)

Hu J-L, Liu B-H, Liu W-G, Textile Research Journal **76**, 853 (2006)

Hu S-G, Jou, C-H, Yang M-C, Journal of Applied Polymer Science **86**, 2977 (2002)

Huang J, Chen Y, Textile Research Journal **80**, 422 (2010)

Huang W, Jang J, Fibers and Polymers **10**, 27 (2009)

Hwang J, Shin H, Korea-Australia Rheology Journal **12**, 175 (2000)

Il'ina AV, Varlamov VP, Applied Biochemistry and Microbiology **41**, 5 (2005)

Ishino C, Okumura K, The European Physical Journal E Soft Matter **25**, 415 (2008)

Ito Y, Hasuda H, Sakuragi M, Tsuzuki S, Acta Biomaterialia **3**, 1024 (2007)

IUPAC. Compendium of Chemical Terminology, 2nd ed. (the "Gold Book"), compiled by D. McNaught and A. Wilkinson, Blackwell Scientific Publications, Oxford (1997)

Jacobasch H-J, Progress in Organic Coatings **17**, 115 (1989)

Jacobasch H-J, Simon F, Werner C, Bellmann C, Technisches Messen **63**, 447 (1996)

Janata E, Proceedings of the Indian Academy of Sciences-Chemical Science **114**, 731 (2002)

Jiang SX, Qin WF, Guo RH, Zhang L, Surface & Coatings Technology **204**, 3662 (2010)

Jin X, Xiao CF, An SL, Wang YT, Jia GX, Journal of Applied Polymer Science **102**, 2685 (2006)

Jocic D, Research Journal of Textile and Apparel **12**, 58 (2008)

Jocic D, Tourrette A, Glampedaki P, Warmoeskerken MMCG, Materials Technology: Advanced Performance Materials **24**, 14 (2009)

Jones CD, Lyon LA, Macromolecules **33**, 8301 (2000)

Kabanov VA, Zezin AB, Pure and Applied Chemistry **56**, 343 (1984)

Kabanov VA, Zezin AB, Rogacheva VB, Prevish VA, Makromolekular Chemie **190**, 2211 (1989)

Kaetsu I, Uchida K, Shindo H, Gomi S, Sutani K, Radiation Physics and Chemistry **55**, 193 (1999)

Kamel MM , El Zawahry MM, Helmy H, Eid MA, Journal of the Textile Institute, **102**, 220 (2011)

Kardas I, Lipp-Symonowicz B, Sztajnowski S, Journal of Applied Polymer Science **119**, 3117 (2011)

Karg M, Hellweg T, Current Opinion in Colloid & Interface Science **14**, 438 (2009)

Khurma JR, Rohindra DR, Nand AV, Polymer Bulletin **54**, 195 (2005)

Kim SY, Zille A, Murkovic M, Guebitz G, Cavaco-Paulo A, Enzyme and Microbial Technology **40**, 1782 (2007)

Kiser PF, Wilson G, Needham D, Journal of Controlled Release **68**, 9 (2000)

Kleinen J, Klee A, Richtering W, Langmuir **26**, 11258 (2010)

Kleinen J, Richtering W, The Journal of Physical Chemistry B **115**, 3804 (2011)

Klitzing v. R, Physical Chemistry Chemical Physics **8**, 5012 (2006)

Kong M, Chen XG, Xing K, Park HJ, International Journal of Food Microbiology **144**, 51 (2010)

Krayukhina MA, Samoilova NA, Yamskov IA, Russian Chemical Reviews **77**, 799 (2008)

Kumari K, Kundu PP, Journal of Microencapsulation **26**, 8500513, 54 (2009)

Kumirska J, Czerwicka M, Kaczynski Z, Bychowska A, Brzozowski K, Thoming J, Stepnowski P, Marine Drugs **8**, 1567 (2010)

Lam YL, Kan CW, Yuen CWM, Journal of Applied Polymer Science **121**, 267 (2011)

Lang FR, Pitton Y, Mathieu HJ, Landolt D, Moser EM, Fresenius Journal of Analytical Chemistry **358**, 251 (1997)

Lapeyre V, Ancla C, Catargi B, Ravaine V, Journal of Colloid and Interface Science **327**, 316 (2008)

Leane MM, Nankervis R, Smith A, Illum L, International Journal of Pharmaceutics **271**, 241 (2004)

Lee J, Moroi Y, Langmuir **20**, 4376 (2004)

Lee JW, Kim SY, Kim SS, Lee YM, Lee KH, Kim SJ, Journal of Applied Polymer Science **73**, 113 (1999)

Lee S-W, Lim J-M, Bhoo S-H, Paik Y-S, Hahn T-R, Analytica Chimica Acta **480**, 267 (2003)

Lei MK, Liu Y, Li YP, Applied Surface Science **257**, 7350 (2011)

Leroux F, Perwuelz A, Campagne C, Behary N, Journal of Adhesion Science and Technology **20**, 939 (2006)

Levinton-Shamuilov G, Cohen Y, Azoury M, Chaikovsky A, Almog J, Journal of Forensic Science **50**, 1367 (2005)

Li K, Liu H, Zhang Q-C, Xue C-G, Wu X-P, Chinese Physical Letters **24**, 1502 (2007)

Li Y; Luo ZX, Journal of the Textile Institute **91**, 302 (2000)

Liang CY, Krimm S, Journal of Molecular Spectroscopy **3**, 554 (1959)

Lichter JA, Van Vliet KJ, Rubner MF, Macromolecules **42**, 8573 (2009)

Lim S-H, Hudson SM, Journal of Macromolecular Science. Part C-Polymer Reviews **43**, 223 (2003)

Limam Z, Selmi S, Sadok S, El Abed A, African Journal of Biotechnology **10**, 640 (2011)

Liu B, Hu J, FIBERS & TEXTILES in Eastern Europe **13**, 45 (2005)

Liu B-S, Yao C-H, Fang S-S, Macromolecular Bioscience **8**, 432 (2008)a

Liu Y, Chen X, Xin JH, Bioinspiration & Biomimetics **3**, 046007 (2008)b

Lopergolo LC, Lugao AB, Catalani LH, Polymer **44**, 6217 (2003)

Lopez-Leon T, Ortega-Vinuesa J-L, Bastos-Gonzalez D, Elaissari A, Journal of Physical Chemistry B **110**, 4629 (2006)

Lopez-Santos C, Yubero F, Cotrino J, Gonzalez-Elipe AR, ACS Applied Materials and Interfaces **2**, 980 (2010)

Luxbacher T, Prüfen und Messen (Testing and Measuring) **2010**, 74 (2010)

Lymberis A, Olsson S, Telemedicine Journal and E-health **9**, 379 (2003)

Makino K, Hiyoshi J, Ohshima H, Colloids and Surfaces B: Biointerfaces **19**, 197 (2000)

Manyukova II, Safonov VV, Fibre Chemistry **41**, 169 (2009)

Mazinani S, Ajji A, Dubois C, Journal of Polymer Science: Part B: Polymer Physics **48**, 2052 (2010)

Mazrouei-Sebdani Z, Khoddami A, Mallakpour S, Colloid Polymer Science **289**, 1035 (2011)

McCullough EA, Kwon M, Shim H, Measurement Science and Technology **14,** 1402 (2003)

Meng H, Hu J, Journal of Intelligent Material Systems and Structures **21**, 859 (2010)

Mi F-L, Shyu S-S, Peng C-K, Journal of Polymer Science. Part A: Polymer Chemistry **43**, 1985 (2005)

Mi F-L, Sung H-W, Shyu S-S, Su C-C, Peng C-K, Polymer **44**, 6521 (2003)

Mihai M, Dragan ES, Colloids and Surfaces A: Physicochemical and Engineering Aspects **346**, 39 (2009)

Mihailovic D, Saponjic Z, Radoicic M, Radetic T, Jovancic P, Nedeljkovic J, Radetic M, Carbohydrate Polymers **79**, 526 (2010)

Morrow NR, McCaffery FG, in Padday JF (Ed.), Wetting, Spreading and Adhesion, Academic Press Inc., London (1978)

Mun GA, Khutoryanskiy VV, Nurkeeva ZS, Sergaziyev AD, Fefelova NA, Rosiak JM, Journal of Polymer Science: Part B: Polymer Physics **42**, 1506 (2004)

Nakae H, Yoshida M, Yokota M, Journal of Materials Science **40**, 2287 (2005)

Neoh KG, Teo HW, Kang ET, Tan KL, Langmuir **14**, 2820 (1998)

Nge TT, Yamaguchi M, Hori N, Takemura A, Ono H, Journal of Applied Polymer Science **83**, 1025 (2002)

Nissen KE, Stuart BH, Stevens MG, Baker AT, Journal of Applied Polymer Science **107**, 2394 (2008)

Nji J, Li G, Smart Materials and Structures **19**, 035007 (2010)

Noel S, Liberelle B, Robitaille L, De Crescenzo G, Bioconjugate Chemistry **22**, 1690 (2011)

Ogulata RT, Mavruz S, FIBRES & TEXTILES in Eastern Europe **18**, 71 (2010)

Ohe T, Yoshimura Y, Abe I, Ikeda M, Shibutani Y, Textile Research Journal ***77***, 131 (2007)

Omeroglu S, Karaca E, Becerir B, Textile Research Journal **80**, 1180 (2010)

Onuki Y, Nishikawa M, Morishita M, Takayama K, International Journal of Pharmaceutics **349**, 47 (2008)

Osterby B, McKelvey RD, Hill L, Journal of Chemical Education **68**, 424 (1991)

Ostrowska-Czubenko J, Gierszewska-Druzynska M, Carbohydrate Polymers **77**, 590 (2009)

Park S, Jayaraman S, MRS Bulletin **28**, 585 (2003)

Parvinzadeh M, Ebrahimi I, Radiation Effects and Defects in Solids **166**, 408 (2011)

Patterson M, Galloway S, Nimmo M, Experimental Physiology **85**, 869 (2000)

Pelton R, Advances in Colloid and Interface Science **85**, 1 (2000)

Petzold G, Goltzsche C, Mende M, Schwarz S, Jaeger W, Journal of Applied Polymer Science **114**, 696 (2009)

Philipp B, Dautzenberg H, Linow K-J, Kötz J, Dawydoff W, Progress in Polymer Science **14**, 91 (1989)

Phillips GO, Williams PA, Handbook of Hydrocolloids, Woodhead Publishing, 2000

Ploymalee S, Charuchinda S, Srikulkit K, Journal of Applied Polymer Science **116**, 473 (2010)

Prabaharan M, Mano JF, Macromolecular Bioscience **6**, 991 (2006)

Pradip, Maltesh C, Somasundaran P, Kulkarni RA, Gundiah S, Langmuir **7**, 2108 (1991)

Prochazkova S, Varum KM, Ostgaard K, Carbohydrate Polymers **38**, 115 (1999)

Radhakumary C, Antonty M, Sreenivasan K, Carbohydrate Polymers **83**, 705 (2011)

Ramirez-Fuentes YS, Bucio E, Burillo G, Polymer Bulletin **60**, 79 (2008)

Ranby B, Polymer Engineering and Science **38**, 1229 (1998)

Rinaudo M, Progress in Polymer Science **31**, 603 (2006)

Rinaudo M, Pavlov G, Desbrieres J, International Journal of Polymer Analysis and Characterization **5**, 267 (1999)

Routh AF, Zimmerman WB, Journal of Colloid and Interface Science **261**, 547 (2003)

Rukuiziene Z, Milasius R, FIBRES & TEXTILES in Eastern Europe **14**, 36 (2006)

Sampath MB, Senthilkumar M, Journal of Industrial Textiles **39**, 163 (2009)

Saunders BR, Vincent B, Advances in Colloid and Interface Science **80**, 1 (1999)

Saunders BR, Vincent B, Journal of the Chemical Society, Faraday Transactions **92**, 3385 (1996)

Saville BP, Physical Testing of Textiles, Woodhead, Cambridge, 2000

Sawada K, Sugimoto M, Ueda M, Park CH, Textile Research Journal **73**, 819 (2003)

Schild HG, Progress in Polymer Science **17**, 163 (1992)

Schmidt H, Marcinkowska D, Cieslak M, FIBRES & TEXTILES in Eastern Europe **13**, 66 (2005)

Schmidt S, Zeiser M, Hellweg T, Duschl C, Fery A, Möhwald H, Advanced Functional Materials **20**, 3235 (2010)

Shahinpoor M, Schneider H-J (Eds.), Intelligent Materials, Royal Society of Chemistry, Cambridge (2008)

Shchipunov Y, Postnova I, Composite Interfaces **16**, 251 (2009)

Shim BS, Chen W, Doty C, Xu C, Kotov NA, Nano Letters **8**, 4151 (2008)

Siemer SR, Wood LL, Calton GJ, Application of agricultural polyammonium acrylate or polyacrylamide hydrogels, United States Patent 5185024 (1993)

Silva CL, Pereira JC, Ramalho A, Pais AACC, Sousa JJS, Journal of Membrane Science **320**, 268 (2008)

Simovic L, Skundric P, Pajic-Lijakovic I, Ristic K, Medovic A, Tasic G, Journal of Applied Polymer Science **117**, 1424 (2010)

Singh A, Sharma PK, Garg VK, Garg G, International Journal of Pharmaceutical Sciences Review and Research **4**, Article 016, 97 (2010)

Stawski D, Bellmann C, Colloids and Surfaces A: Physicochemical and Engineering Aspects **345**, 191 (2009)

Stroeks A, Polymer **42**, 9903 (2001)

Tajdini F, Amini MA, Nafissi-Varcheh N, Faramarz MA, International Journal of Biological Macromolecules **47**, 180 (2010)

Tanaka T, Physical Review Letters **40**, 820 (1978)

Thijs HML, Remzi Becer C, Guerrero-Sanchez C, Fournier D, Hoogenboom R, Schubert US, Journal of Materials Chemistry **17**, 4864 (2007)

Thünemann AF, Müller M, Dautzenberg H, Joanny J-F, Löwen H, Advanced Polymer Science **166**, 113 (2004)

Tiwary AK, Sapra B, Jain S, Recent Patents on Drug Delivery & Formulation **1**, 23 (2007)

Tokita M, Tanaka T, The Journal of Chemical Physics **95**, 4613 (1991)

Tran-Cong Q, Nagaki T, Yano O, Soen T, Macromolecules **24**, 1505 (1991)

Tsuchida E, Journal of Macromolecular Science, Part A **31**, 1 (1994)

Turecek F, Syrstad EA, Journal of the American Chemical Society **125**, 3353 (2003)

Ulbricht M, Reactive & Functional Polymers **31**, 165 (1996)

Ulbricht M, Matuschewski H, Oechel A, Hicke H-G, Journal of Membrane Science **115**, 31 (1996)

Urban MW (Ed.), Handbook of stimuli-responsive materials, John Wiley and Sons (2011)

Van Langenhove L, Hertleer C, Catrysse M, Puers R, Van Egmond H, Matthijs D, Smart Textiles, in Wearable eHealth Systems for Personalised Health Management, Lymberis A, de Rossi D (Eds.), IOS Press, pp. 344-352 (2004)

Vladkova T, International Journal of Polymer Science **2010**, Article ID 296094, 22 pages (2010)

Wang Q, Zhao Y, Xu H, Yang X, Yang Y, Journal of Applied Polymer Science **113**, 321 (2009)

Wang WP, Du Y-M, Wang X-Y, World Journal of Microbiology and Biotechnology **24**, 2717 (2008)

Wang X, Qiu X, Wu C, Macromolecules **31**, 2972 (1998)a

Wang ZL, Kang ZC (Eds.), Functional and smart materials. Structural evolution and structure analysis (1st Ed.), Plenum Press, New York (1998)b

Wenzel PN, Industrial and Engineering Chemistry **6**, 988 (1936)

Whitehouse AGR, Proceedings of the Royal Society of London, Series B, Biological Sciences **117**, 139 (1935)

Woo H-G, Li H (Eds.), Advanced functional materials, Springer (2011)

Wu C-S, Polymers Advanced Technologies (2011) DOI: 10.1002/pat.1899

Wu C, Zhou S, Au-yeung SCF, Jiang S, Die Angewandte Makromolekulare Chemie **240**, 123 (1996)

Xing Z-C, Han S-J, Shin Y-S, Kang I-K, Journal of Nanomaterials **2011**, Article ID 929378, 18 pages (2011)

Xinming L, Yingde C, Lloyd AW, Mikhalovsky SW, Sandeman SR, Howel CA, Liewen L, Contact Lens & Anterior Eye **31**, 57 (2008)

Yang B, Yang W, Journal of Membrane Science **218**, 247 (2003)

Yang CQ, Bresee RR, Fateley WG, Applied Spectroscopy **44**, 1035 (1990)

Yang P, Zhang X, Yang B, Zhao H, Chen J, Yang W, Advanced Functional Materials **15**, 1415 (2005)

Yang W, Ranby B, Journal of Applied Polymer Science **62**, 545 (1996)a

Yang WT, Ranby B, Polymer Bulletin **37**, 89 (1996)b

Yoo MK, Sung YK, Lee YM, Cho CS, Polymer **41**, 5713 (2000)

Yoshinari E, Furukawa H, Horie K, Polymer **46**, 7741 (2005)

You Z, Cao H, Gao J, Shin PH, Day BW, Wang Y, Biomaterials **31**, 3129 (2010)

Zhang H, Wu S, Tao Y, Zang L, Su Z, Journal of Nanomaterials **2010**, Article ID 898910, 5 pages (2010)a

Zhang J, Xia W, Liu P, Cheng Q, Tahirou T , Gu W, Li B, Marine Drugs **8**, 1962 (2010)b

Zhang J-T, Keller T-F, Bhat R, Garipcan B, Jandt KD, Acta Biomaterialia **6**, 3890 (2010)c

Zhang X-Z, Chu C-C, Chemical Communications, 350 (2004)

Zhang X-Z, Xu X-D, Cheng S-X, Zhuo R-X, Soft Matter **4**, 385 (2008)

Zhang X-Z, Yang Y-Y, Chung T-S, Ma K-X, Langmuir **17**, 6094 (2001)

Zhou X, Chen XG, Kong M, Liu CS, Cha DS, Kennedy JF, Carbohydrate Polymers **73**, 265 (2008)

Zhu A, Chen T, Colloids and Surfaces B: Biointerfaces **50**, 120 (2006)

SUMMARY

A new approach to polyester functionalization was proposed in this study: incorporation of stimuli-responsive polyelectrolyte microgels into the surface layers of commercial ready-to-use textiles. Two paths were followed to achieve incorporation based on conventional well-known and industrially acceptable techniques of curing by UV irradiation or heating. More specifically, the incorporation procedures in this study involved: a) photo-crosslinking with UV irradiation in the presence of the photo-initiator benzophenone; or b) low temperature thermo-crosslinking, after amination of polyester, through the natural crosslinker genipin. The aim of functionalization was to impart stimuli-responsiveness from the microgels to polyester itself, in order to develop advanced textile materials adaptive to ambient conditions.

The microgels used consisted of pH/thermo-responsive poly(*N*-isopropylacrylamide-*co*-acrylic acid) (PNIAA) microparticles either alone or in the form of polyelectrolyte complexes with oppositely charged macromolecular chains of chitosan (CS). PNIAA has a lower critical solution temperature (LCST) close to the average human body temperature, at which it undergoes a volume-phase transition from swollen/hydrophilic to de-swollen/hydrophobic. Apart from thermo-responsive, PNIAA is also pH-responsive owing to the carboxyl groups of its acrylic acid units which become ionized above ca. pH 4. On the other hand, CS is a natural amine-rich polysaccharide with a pK_a of 6.3. Below pH 6.3, the amine groups of CS become protonated and attract water molecules, whereas above pH 6.3 CS macromolecules lose gradually their positive charges and release water. Mixing CS solutions with a microgel of PNIAA microparticles at particular ratios resulted in formation of CS/PNIAA complexes in suspension (denoted as microgel **CM**). Several techniques were employed to characterize the microgels in terms of morphology, size, charge, response rate, and physicochemical stability, such as SEM, DLS, potentiometric titrations, UV-Vis spectroscopy, and analytical centrifugation, respectively. It was found that **CM** complexes have an LCST at 35.8°C and reach their zero-charge point at pH 6.0. Their thermo-response rate was found to be slower than that of PNIAA microparticles and changes in pH between values 4 and 8 appear not to affect it significantly. However, an increase in pH from acidic to alkaline values causes a decrease in the hydrodynamic sizes of **CM** complexes. Also, a temperature shift from 20°C to 40°C results in approximately 50% reduction of the **CM** complexes size in hydrated state (from ca. 970 nm to ca. 500 nm). This thermo-responsiveness of **CM** complexes, expressed also in light transmittance changes from translucent to opaque, was found to be reversible. Other factors such as the complexation ratio between CS and PNIAA, the crosslinking of CS with genipin, and the presence of NaCl in the microgel were also found to influence the size of **CM** complexes. Furthermore, it was shown that the complexes are colloidally stable in microgel **CM** owing to mutual electrostatic repulsion caused by the excess of positive charges provided by CS. However, their physicochemical stability is challenged when the temperature is raised above their LCST and the pH shifts to acidic.

For the incorporation of the above microgels into polyester surface layers, two types of poly(ethylene terephthalate) (PET) woven textiles were chosen: one light-weight with an openness factor of 0.5%, and a heavier, thicker and denser one with an openness factor of 0%. Both photo-crosslinking and thermo-crosslinking techniques involved first impregnation of the textiles with benzophenone or genipin solution, respectively, and after drying at room temperature, impregnation with microgels followed. In the case of thermo-crosslinking, polyester needed first to be aminated in order to obtain primary amine groups on its surface that would react with genipin. UV irradiation was performed at 254 nm for 30 min, and thermo-crosslinking at 65°C for 1.5 h. The functionalized samples were characterized in terms of surface morphology, chemical composition, charge, topography, resistance to wrinkling, mechanical strength and other physical properties. For that purpose, a number of analytical techniques were employed such as SEM, XPS, FTIR-ATR, colorimetry, electrokinetic analysis through streaming potential measurements, optical scanning, confocal microscopy, crease recovery, tensile testing, and others. Among the main findings was that functionalized polyester textiles had durably incorporated microgels in their surface layers; the microgel presence resulted in a variety of surface morphologies from a continuous layer to discrete and sparsely distributed circular-shaped formations on the fibers. For microgel **CM**-functionalized polyesters, a change in surface charge was observed from positive to negative values within a pH range between 5.0 and 6.6, depending on the polyester type. These pH values approximate the zero-charge point of **CM** complexes, and they are also within the average pH range of human skin. Microgel-functionalization resulted also in an increase of surface macro-porosity and decrease in macro-roughness of the light-weight PET (PET 1) but it had the opposite effects on the heavier and denser PET type (PET 2). The crease recovery angles were not significantly affected. However, the tensile strength and the whiteness index of all polyesters deteriorated due to the functionalization process.

Finally, the adaptivity of the microgel-functionalized polyesters was investigated in terms of water management properties. To this end, dynamic wetting, water uptake, capillarity, water vapor transmission, moisture sorption/desorption and regain measurements were performed. One of the main findings was that functionalization with microgel **CM** decreases significantly the total water absorption times of polyester, whereas microgel **M** increases them by almost 80%. However, in both cases, the capillarity of functionalized polyesters, i.e. the percent of water that they can take up in their capillaries, was much higher than that of reference polyester. The dynamic contact angles and absorption times were found to be pH-dependent. The water vapor transmission rates of functionalized polyesters were higher than those of reference polyesters, at both 20°C and 40°C and 65% RH. Among other data, the moisture regains confirmed the thermo-responsiveness of the microgel-functionalized polyesters, as they were higher at 20°C and lower at 40°C, compared with the corresponding values of reference polyesters. These findings are significant, as they underline that polyesters functionalized with microgels can have regulated water/moisture uptakes in terms of uptake (or loss) rate, as well as water/moisture content.

The adaptivity that the microgel-functionalized polyester textiles exhibited towards changes in their environment was expressed in different ways; for example, by

changing their surface charge and wettability rate according to the applied pH, or their moisture uptake and transfer rate according to temperature and RH changes. Moreover, these changes in polyester properties occurred within a physiological pH/temperature range of human bodies. This conclusion gives new scope for the development of advanced textile-based materials with possible applications in controlled adsorption or slow release systems suitable for protective and technical clothing, sportswear, as well as every-day apparel.

SAMENVATTING

In dit proefschrift is een nieuwe methode beschreven om polyester substraten te functionaliseren door middel van het aanbrengen van stimulatie-responsieve poly-elektrolyt microgels in de oppervlakte laag van textiel. Er zijn twee strategieën gevolgd, gebaseerd op conventionele bekende en industrieel geaccepteerde technieken, te weten het crosslinken met behulp van UV-straling en crosslinking met gebruik van thermische energie. In deze studie is het functionaliseren van het substraat gebaseerd op de toepassing van a) foto-crosslinking door middel van UV-straling in de aanwezigheid van de foto-initiator benzephenone en b) warmte-crosslinking bij lage temperatuur van geamineerde polyester door gebruik te maken van de natuurlijke crosslinker genipin. Het doel van het functionaliseren is het realiseren van stimulie-responsiviteit in geavanceerde polyester substraten om daarmee het aanpassingsvermogen van het substraat aan veranderende omgevingscondities te realiseren.

De gebruikte microgels bestaan uit pH/temperatuur-responsieve poly(*N*-isopropylacrylamide-*co*-acryl zuur) (PNIAA) microdeeltjes, die alleen of in de vorm van poly-electroliet complexen met tegengesteld geladen macromoleculaire ketens van chitosan (CS) aanwezig zijn. PNIAA heeft een lage kritische oplostemperatuur (LCST), die vrijwel overeenkomt met de menselijke lichaamstemperatuur, waarbij het een faseverandering ondergaat van de gezwollen/hydrofiele naar de ongezwollen/hydrofobe fase. Naast temperatuur-responsiviteit is PNIAA ook pH-responsief door de carboxylgroepen van het acrylzuur, die geïoniseerd worden boven ca. pH 4. CS is een natuurlijke polysacharide die veel aminogroepen bevat. De pK_a van CS is 6.3. Onder pH 6.3 worden de amine groepen van CS geprotoneerd, terwijl boven pH 6.3 de CS macromoleculen geleidelijk hun positieve lading verliezen, waarbij water vrijkomt. De combinatie van CS oplossingen en een microgel van PNIAA microdeeltjes in specifieke verhoudingen, resulteerde in de vorming van CS/PNIAA complexen als colloïdale oplossing (hierna microgel **CM** genoemd). Diverse technieken zijn gebruikt om de microgels te karakteriseren op het gebied van morfologie, grootte, lading, responsie snelheid en fysisch-chemische stabiliteit door middel van SEM, DLS, potentiometrische titraties, UV-Vis spectroscopie en analytische centrifugatie. Het is vastgesteld dat **CM** complexen een LCST hebben bij een temperatuur van 35.8°C en ongeladen zijn bij pH 6.0. De temperatuurresponssnelheid bleek lager te zijn dan die van PNIAA microdeeltjes en de pH variatie tussen 4 en 8 had geen significant effect. Echter, verhoging van de pH van zure naar basische waarden verkleint de hydrodynamische grootte van **CM** complexen. Ook een temperatuurverandering van 20°C naar 40°C resulteert in ongeveer 50% reductie van de grootte van **CM** complexen in gehydrateerde staat (van ca. 970 naar 500 nm). Deze temperatuurresponsie van **CM** complexen, ook visueel waarneembaar door lichttransmissie verandering van doorzichtig naar ondoorzichtig, bleek reversibel. Andere factoren zoals de complexvorming ratio tussen CS en PNIAA, crosslinking van CS met genipin, en de aanwezigheid van NaCl in de microgel bleken ook van invloed op de grootte van **CM** complexen. Ook vertoonden de complexen colloïdaal stabiliteit van microgel **CM** door de wederzijdse elektrostatische afstoting, veroorzaakt door de

overmaat aan positieve lading geleverd door CS. Echter, hun fysisch-chemische stabiliteit neemt af wanneer de temperatuur wordt verhoogd tot boven de LCST en de pH-waarde daalt tot in het zure gebied.

Voor de opname van bovengenoemde microgels in polyester oppervlaktelagen zijn twee types poly(ethylene terephtalate) (PET) gekozen: één lichtgewicht met een openheidsfactor van 0.5%, en een zwaardere, dikkere, en dichtere met een openheidsfactor van 0%. Bij de toepassing van foto-crosslinking en warmte-crosslinking technieken is het noodzakelijk om vooraf het substraat te impregeneren met een benzophenone of met een genipin oplossing. Vervolgens wordt het doek gedroogd bij kamertemperatuur. Daarop volgend wordt het doek geïmpregneerd met microgels. Indien warmte-crosslinking wordt toegepast is het noodzakelijk dat het polyester substraat wordt geamineerd om primaire aminen op het oppervlak te genereren die kunnen reageren met genipin. UV bestraling met een golflengte van 254 nm is gedurende 30 minuten uitgevoerd en de warmte-crosslinking heeft plaatsgevonden bij een temperatuur van 65°C gedurende 1.5 uur. De gefunctionaliseerde monsters zijn gekarakteriseerd in termen van oppervlakte morfologie, chemische samenstelling, lading, topografie, weerstand tegen kreuk, mechanische sterkte en andere fysische eigenschappen. Voor het karakteriseren van de monsters zijn analytische technieken toegepast zoals SEM, XPS, FTIR-ATR, kleurmeting, elektronkinetische analyse onder andere door middel van stromingspotentiaal, optische scan, confocal microscopie, kreukherstellendheid en trek- en rekspanning. Belangrijke conclusies zijn dat gefunctionaliseerd polyestersubstraat permanent opgenomen microgels in hun oppervlaktelagen bevat; de aanwezige microgel resulteert in een grote diversiteit van oppervlakte morfologieën variërend van een dekkende laag tot verspreide cirkelvormige formaties op de vezels. Bij **CM**-gefunctionaliseerde polyesters werd een omslagpunt in de oppervlaktelading van positieve naar negatieve waarden waargenomen bij een pH-waarde die varieert tussen pH 5.0 en 6.6. Het omslagpunt bleek afhankelijk te zijn van het type polyester. Deze pH waarden van de gefunctionaliseerde polyesters benaderen het nulladingpunt van **CM** complexen op zich en liggen ook binnen de gemiddelde pH waarde van de menselijke huid. Microgel functionalisatie resulteerde ook in een toename van de oppervlakte macro-porositeit en afname in macro-ruwheid van de lichtgewichte PET (PET 1), maar vertoonde een tegengesteld effect op de zwaardere en dichtere PET (PET 2). De zogenaamde kreukherstelhoeken vertoonden geen significant verschil tussen de verschillende soorten polyester. Opmerkelijk was de afname van de treksterkte en van de witheidsgraad van het doek als gevolg van het functionalisatieproces.

Tenslotte is de adaptiviteit van de microgel gefunctionaliseerde polyesters onderzocht op het gebied van water management eigenschappen. De hiervoor toegepaste technieken omvatten dynamische bevochtiging, wateropnamevermogen, capillariteit, verdampingssnelheid, vochtabsorptie/desorptie en textielreprise metingen. Er is geconcludeerd dat het functionaliseren van polyester met microgel **CM** de totale waterabsorptietijd significant verlaagde, terwijl de waterabsorptietijd bij de toepassing van microgel **M** toenam met bijna 80%. In beide gevallen was de capillariteit, d.w.z. het percentage water dat is opgenomen in de capillairen, significant hoger dan dat van het

referentie polyester. De dynamische contacthoeken en absorptietijden bleken pH-afhankelijk. De verdampingssnelheid van water, bij temperaturen van 20°C en 40°C en een relatieve vochtigheid van 65%, is in geval van gefunctionaliseerde polyesters hoger dan die van de referentie polyesters. De temperatuur-responsie van microgel gefunctionaliseerde polyesters wordt onder meer bevestigd door de waargenomen textielreprise die hoger was bij 20°C en lager bij 40°C, in vergelijking met de waarden van de referentie polyesters. Deze waarnemingen zijn belangrijk omdat ze aantonen dat polyesters, die gefunctionaliseerd zijn met microgels, de water/vochtopname kunnen reguleren voor zowel de opnamesnelheid als het opgenomen percentage water.

Het aanpassingsvermogen dat microgel gefunctionaliseerde polyester substraten laten zien op veranderingen in hun omgeving is op verschillende manieren aangetoond. Bijvoorbeeld door het veranderen van de oppervlaktelading en de vochtopnamesnelheid behorende bij de toegepaste pH of door het veranderen van de vochtopname behorende bij de toegepaste temperatuur en relatieve vochtigheid. Bovendien vonden deze veranderingen plaats binnen de fysiologische pH en temperatuur niveaus van het menselijk lichaam. Deze bevindingen openen een nieuw toepassingsgebied voor de ontwikkeling van geavanceerde textielmaterialen met gecontroleerde adsorptie of langzame afgifte van bepaalde stoffen. Dergelijke toepassingen zijn denkbaar in zowel beschermende als sport- en dagelijkse kleding.

LIST OF ABBREVIATIONS & ACRONYMS

CS: Chitosan
CM: Microgel of chitosan/poly(*N*-isopropylacrylamide-*co*-acrylic acid) polyelectrolyte complexes
DLS: Dynamic light scattering
DSC: Differential scanning calorimetry
FTIR-ATR: Fourier transform infra-red-Attenuated total reflectance
GP: Genipin
IEP: Isoelectric point
LCST: Lower critical solution temperature
M: Microgel of poly(*N*-isopropylacrylamide-*co*-acrylic acid) microparticles
MC: Microgel of poly(*N*-isopropylacrylamide-*co*-acrylic acid)/chitosan polyelectrolyte complexes (reverse ratio of **CM**)
NIPAAm: *N*-isopropylacrylamide
PDADMAC: Poly(diallyldimethylammonium chloride)
PDI: Polydispersity index
PET: Poly(ethylene terephthalate)
PET A: Poly(ethylene terephthalate) aminated
PET ACM: Poly(ethylene terephthalate) aminated functionalized with microgel **CM** through UV irradiation
PET ACM-T: Poly(ethylene terephthalate) aminated functionalized with microgel **CM** through thermo-crosslinking with genipin
PET R: Poly(ethylene terephthalate) reference
PET RCM: Poly(ethylene terephthalate) functionalized with microgel **CM**
PET RM: Poly(ethylene terephthalate) functionalized with microgel **M**
PET RMC: Poly(ethylene terephthalate) functionalized with microgel **MC**
PNIAA: Poly(*N*-isopropylacrylamide-*co*-acrylic acid)
PNIPAAm: Poly(*N*-isopropylacrylamide)
PSS: Sodium poly(ethylene sulfonate)
RH: Relative humidity
SEM: Scanning electron microscopy
UV: Ultra violet
Vis: Visible
WI: Whiteness index
WVTR: Water vapor transmission rate
XPS: X-ray photoelectron spectroscopy
YI: Yellowness index

APPENDIX I:

Analytical centrifugation graphs

- **CS - 20°C**

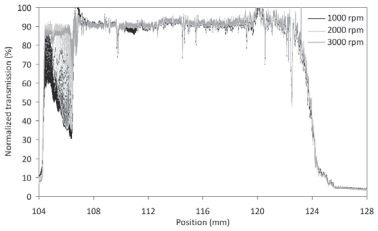

pH 4

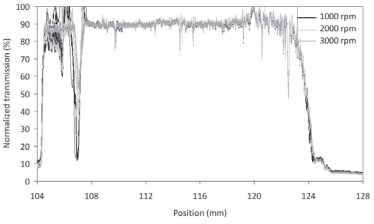

pH 6

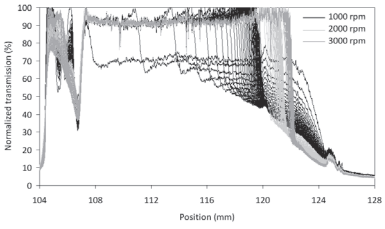

pH 8

- **CS - 40°C**

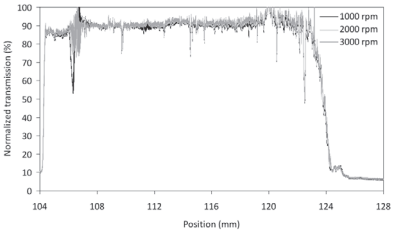

pH 4

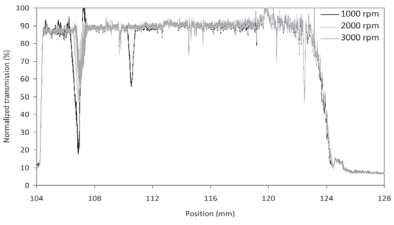

pH 6

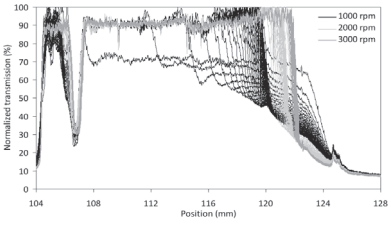

pH 8

- **M - 20°C**

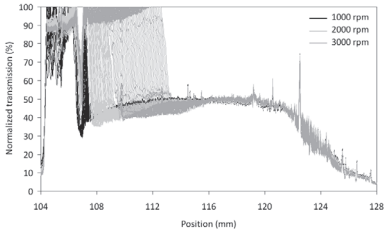

pH 4

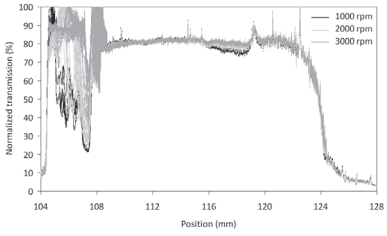

pH 6

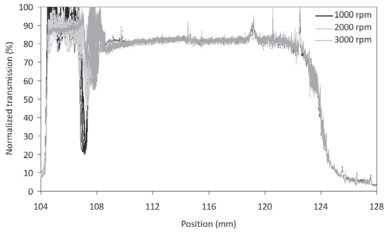

pH 8

- **M - 40°C**

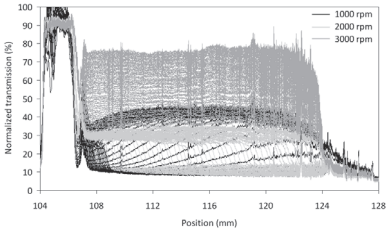

pH 4

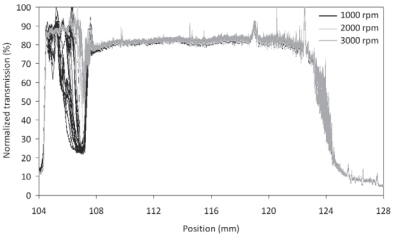

pH 6

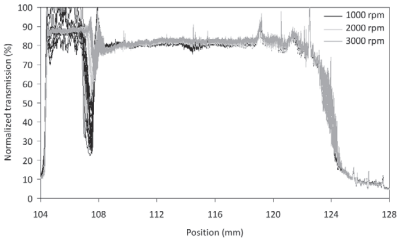

pH 8

- **CM - 20°C**

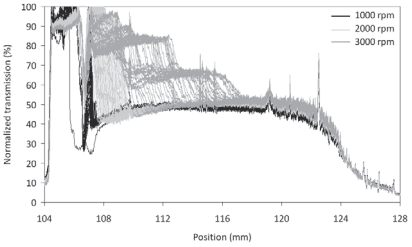

pH 4

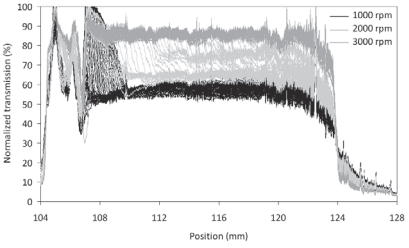

pH 6

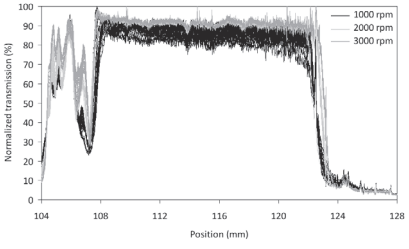

pH 8

- **CM - 40°C**

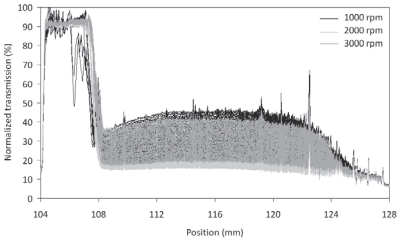

pH 4

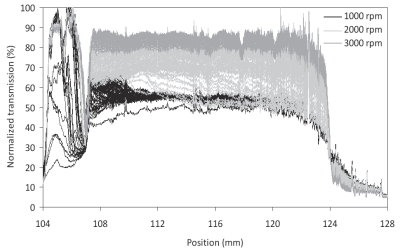

pH 6

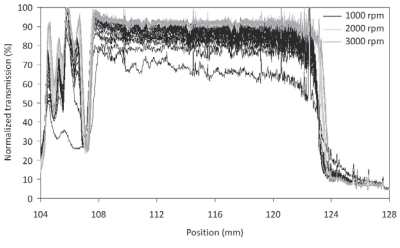

pH 8

- **M - 36°C**

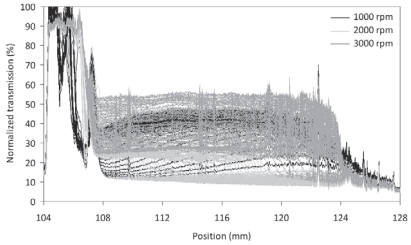

pH 4

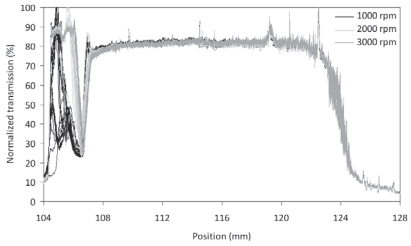

pH 6

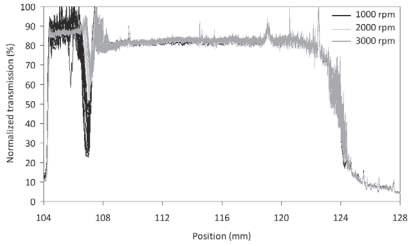

pH 8

- **CM - 36°C**

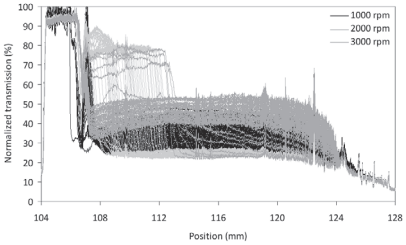

pH 4

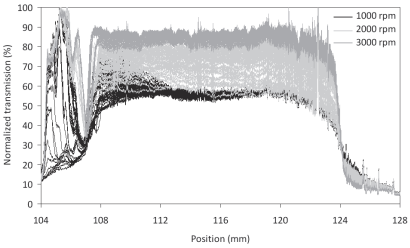

pH 6

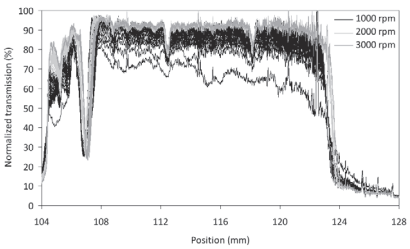

pH 8

- **GP - 20°C**

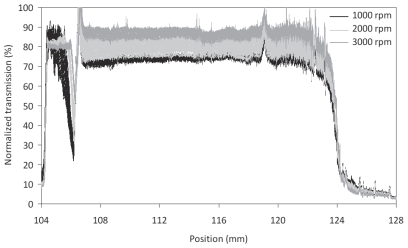

CM with CS/GP 2/1

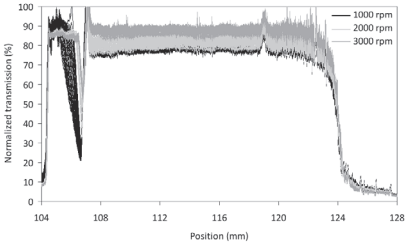

CM with CS/GP 4/1

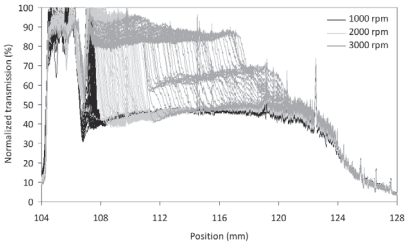

CM with CS/GP 20/1

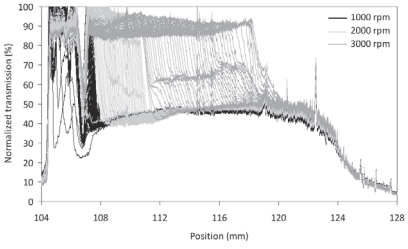

CM with CS/GP 40/1

- **GP - 40°C**

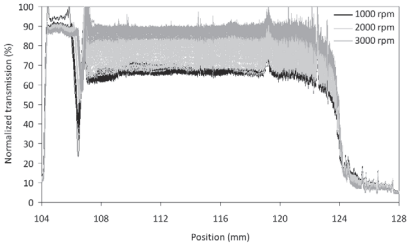

CM with CS/GP 2/1

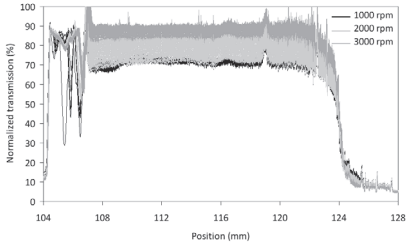

CM with CS/GP 4/1

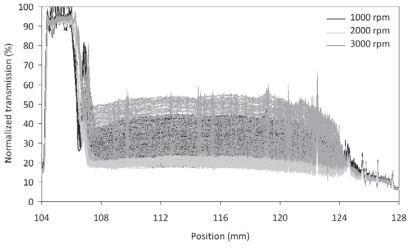

CM with CS/GP 20/1

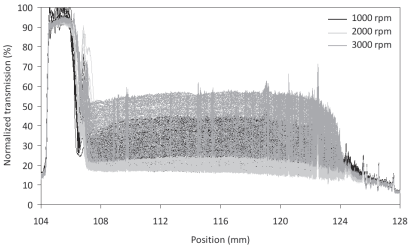

CM with CS/GP 40/1

- **CS/GP 20/1**

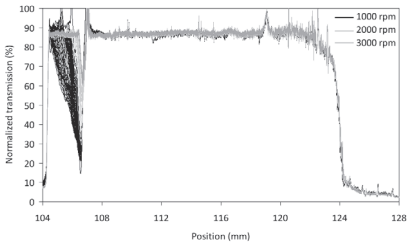

20°C

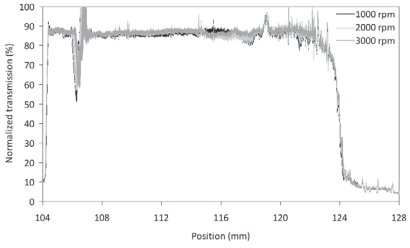

40°C

- **CS/GP 40/1**

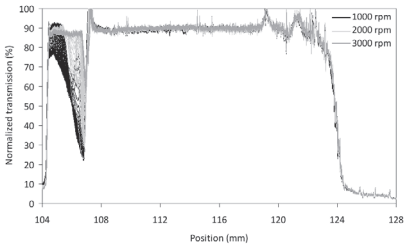

20°C

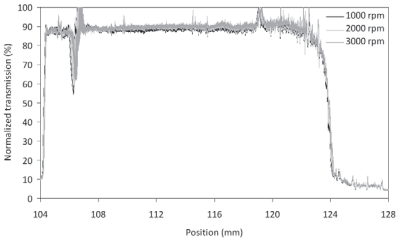

40°C

APPENDIX II:

Topographic images

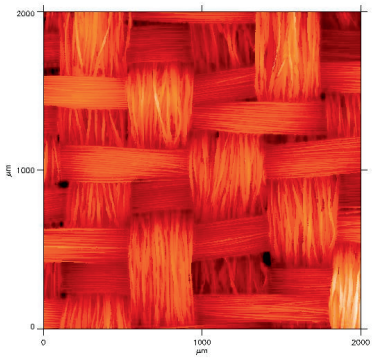

PET R 1 – 2D scanned

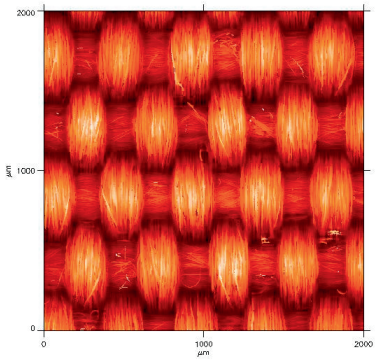

PET R 2 – 2D scanned

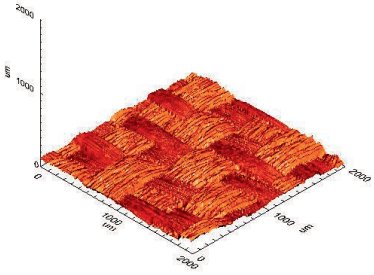

PET R 1 – 3D reconstruction

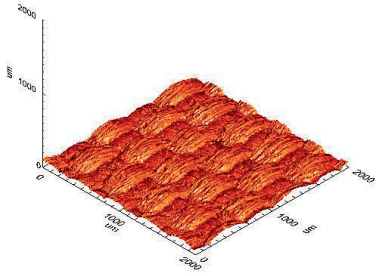

PET R 2 – 3D reconstruction

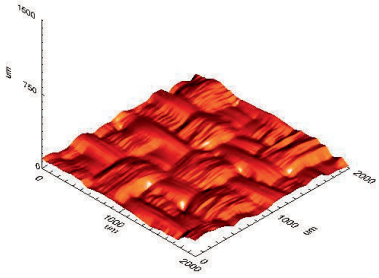

PET R 1 – 3D filtrate

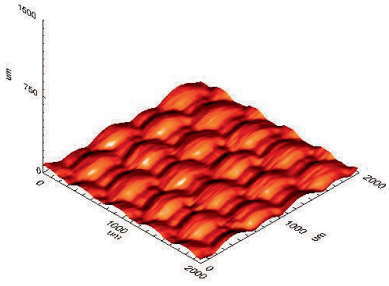

PET R 2 – 3D filtrate

(Macro-roughness (waviness) determination)

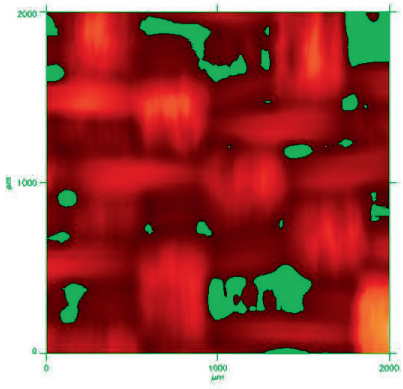

PET R 1

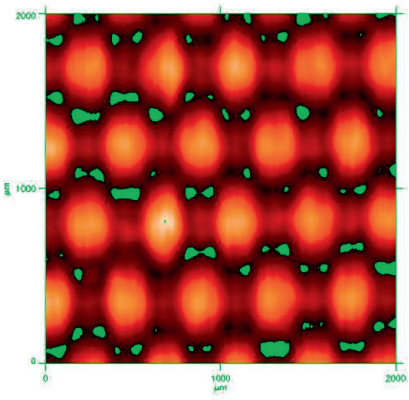

PET R 2

(Surface macro-porosity determination based on chromatic aberration)

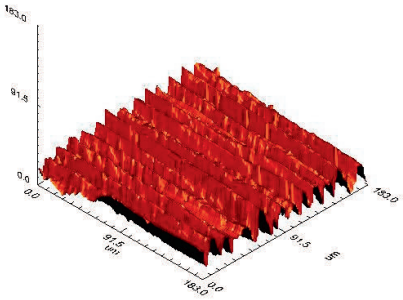

PET R 1 – 3D warp

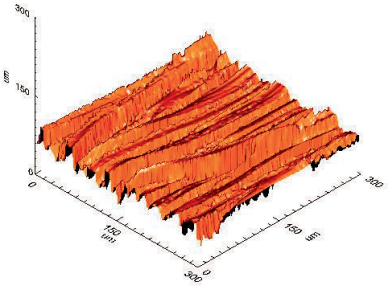

PET R 1 – 3D weft

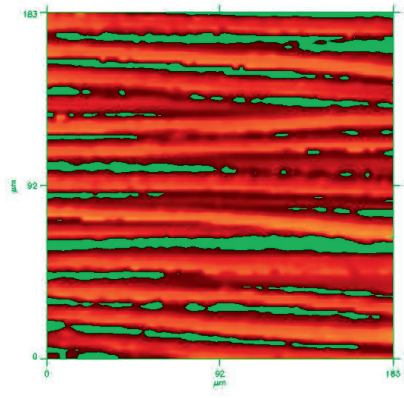

PET R 1–2D projection warp

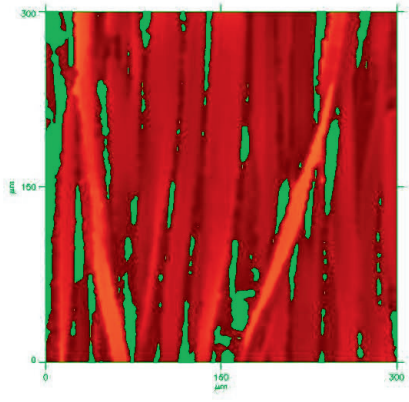

PET R 1–2D projection weft

(Surface micro-porosity determination based on chromatic aberration)

ACKNOWLEDGEMENTS

Apparently, it was not just *my* world that turned upside down since I first moved to the Netherlands 4.5 years ago to embark on my doctorate. Economical, political, and geological phenomena have shaken our cosmos (the "Greek and Euro- crisis", the "Arab spring", the Fukushima triple disaster, and so on), even athletic wonders, as FC Twente won the Dutch championship in 2010☺! It has been undoubtedly a challenging and demanding, yet enriching journey for me and it is my ultimate duty and a pleasure to acknowledge all those who accompanied me through it.

«Στους γονείς μου οφείλω το ζην, στους δε δασκάλους μου το ευ ζην»
Μέγας Αλέξανδρος (356–323 π.Χ.)
"I am indebted to my parents for my being and to my teachers for my well-being"
Alexander the Great (356–323 BC)

I am deeply grateful to my supervisor and promoter, Prof. Dr. Ir. Marijn Warmoeskerken, who has been more than a professor, indeed a true pedagogue, encouraging me during the toughest of times. I always appreciated how he never treated me as a subordinate but valued my opinion, seeking always the silver lining in discussions.

I would also like to extend my gratitude to all members of my graduation committee for their participation, and especially to Prof. Dr. Vincent Nierstrasz and Dr. habil. Reinhard Miller for their trouble to travel to the Netherlands from abroad for this purpose. My special thanks also to Assoc. Prof. Dr. Victoria Dutschk, my fairy God-mother as I call her, for her constant and multi-fold support. Her guidance was like light in a dark room for me. I hope we will continue to collaborate for many years to come.

My genuine gratitude and appreciation goes to Dr. Dragan Jocic, leader of the Advanbiotex project, for offering me initially the position of "early-stage researcher" in his project, enabling me to pursue my PhD studies in the Netherlands. My sincere thanks go also to all past members of the Advanbiotex project, as they truly helped me in their own way to become a stronger person.

There is a long line of teachers, professors, mentors and former bosses in Greece, Spain and Germany, who all contributed to the course of my educational and professional life throughout the years. I never forget my starting point so I will always be indebted to all of them for setting an example for me.

However, I would have never made it this far if it were not for the unconditional love and infinite support of my parents, Eleni and Demetrios Glampedakis, who founded my life on strong pillars of ethos and humility. Along with my beloved brother, Eftychios, they are the most noble and honorable people I have ever met, and I am truly blessed to have them in my life.

Σα βγεις στον πηγαιμό για την Ιθάκη,
να εύχεσαι νάναι μακρύς ο δρόμος,
γεμάτος περιπέτειες, γεμάτος γνώσεις.
...
Πάντα στον νου σου νάχεις την Ιθάκη.
Το φθάσιμον εκεί είν' ο προορισμός σου.
Αλλά μη βιάζεις το ταξείδι διόλου.
Καλλίτερα χρόνια πολλά να διαρκέσει·
και γέρος πια ν' αράξεις στο νησί,
πλούσιος με όσα κέρδισες στον δρόμο,
μη προσδοκώντας πλούτη να σε δώσει η Ιθάκη.
...
Κι αν πτωχική την βρεις, η Ιθάκη δεν σε γέλασε.
Έτσι σοφός που έγινες, με τόση πείρα,
ήδη θα το κατάλαβες η Ιθάκες τι σημαίνουν.

Ιθάκη, Κ. Π. Καβάφης (1863–1933 μ.Χ.)

As you set out on your journey to Ithaca,
hope that the road is long,
full of adventure, full of knowledge.
...
Always keep Ithaca in your mind;
to reach her is your destiny.
But do not rush your journey in the least.
Better that it last for many years;
that you drop anchor at the island an old man,
rich with all you've gained on the way,
not expecting Ithaca to make you rich.
...
And if you find her poor, Ithaca did not deceive you.
As wise as you'll have become, with so much experience,
you'll have understood, by then, what these Ithacas mean.

Ithaca by C. P. Cavafy (1863–1933 AD)

And what a journey indeed… One that gave me the opportunity to meet with so many people from various countries and backgrounds, and to travel to places throughout Europe, even to Africa and Japan.

Our group has welcomed so many collaborators over the last few years. I would like to thank all of them, past and present EFSM members, industrial partners, postdocs, students, and guest scientists, for the stimulating meetings, the AUTEX trips, and the good memories. Particularly I would like to thank Pramod, my very first *kamergenoot* (office-mate) and a talking-and-walking encyclopedia of Dutch life (☺!), who also helped me find my house on the university campus; a house which soon became more than a home to me (…and office and lab, my true headquarters!). Special thanks also to Gerrit for being a good listener, always willing to help whether in "poster rescues" or Dutch translations (hartstikke bedankt!), and to Jiayan who was an eager student with whom we started the first experiments on polyester.

But apart from very dynamic, we were also a quite…mobile group! In fact, just when I finally learned to pronounce "Hogekamp" we moved to "Buitenhorst" ("BH" (beha ☺) in short…!). After six movings (office 2, lab 2, house 2) in and out of campus, there are many people to whom I am grateful for all the technical and friendly support: Yvonne, for all the Dutch communications and warm talks, Veronique for perfectly handling all my travel declarations and for helping me in every way she could, Leo for guarding my packages from Greece till they were safely delivered to me (my parents are also thankful for that!), the ICTS team of Arjen, Cor, Ralph and Rob for managing multiple computer-related matters and for gifting us a weathered yet functional dartboard (☺), to "Benno…the builder" or else the ultimate lab technician always willing to help out with set-ups and with a mischievous warm smile on his face, to Bert and Laura for making my life easier whenever I needed to perform measurements in their lab, to Marc for helping me find my way through Horst during my first year at UT, and last but not least to Herman and all the ladies of the BTC reception and cantine for their warm and friendly chats that got me through many excruciatingly long days in the lab.

There were also several external collaborators who helped me with my doctoral research all these years and I am grateful to all of them. I would like to thank especially Dr. Stephane Giraud and Dr. Christine Campagne from ENSAIT-France for introducing Jiayan to me and for offering their facilities for my first measurements on polyester textiles, Dr. Reinhard Miller from MPI Golm-Germany who hosted my one-month stay in his group, along with his co-workers Dr. Jürgen Krägel, Dr. Rainer Wüstneck and all other group members who immediately made me feel welcome, and finally Dr. Alfredo Calvimontes, Dr. Petr Formanek, Mrs. Gudrun Petzold and Sabine Genest from IPFDD-Germany for hosting and facilitating my two-month stay in their laboratories, during which I obtained a great deal of the results presented in this thesis. Last but not least, I would like to thank Mr. Robert Kuipers from Verosol for providing my precious working material, the polyester textiles, and for always being available for discussion.

I am sincerely indebted to all of you.

«...χάρις ὑμῖν καὶ εἰρήνη ἀπὸ Θεοῦ πατρὸς ἡμῶν καὶ Κυρίου Ἰησοῦ Χριστοῦ.
Εὐχαριστῶ τῷ Θεῷ μου ἐπὶ πάσῃ τῇ μνείᾳ ὑμῶν,
πάντοτε ἐν πάσῃ δεήσει μου ὑπὲρ πάντων ὑμῶν μετὰ χαρᾶς τὴν δέησιν ποιούμενος
ἐπὶ τῇ κοινωνίᾳ ὑμῶν εἰς τὸ εὐαγγέλιον ἀπὸ πρώτης ἡμέρας ἄχρι τοῦ νῦν...»
Αποστόλου Παύλου, Προς Φιλιππησίους, Επιστολή 1η , στίχοι 2:5

"…grace be unto you, and peace, from God our Father, and from the Lord Jesus Christ.
I thank my God upon every remembrance of you,
always in every prayer of mine for you all, making request with joy
for your fellowship in the gospel, from the first day until now…"
Apostle Paul, To the Philippians, Epistle 1, verses 2:5

My final thanks I extend to all my friends who supported me through the years and continued to include me in their lives despite the physical distance between us, as well as to all the new friends I made during my PhD studies. I start with my fantastic paranymphs, Ashok and Jie, whom I like to tease reminding them that in Greek a paranymph is a little girl in a white fluffy dress that stands beside a bride at her wedding (☺!). Ashok is a great philanthropist of high intellect and a trully proactive friend who, regardless of any work load or multiple obligations, will always drop a line, make a call, or pay a visit no matter how far he might be. So thank you, dear friend, for doing me the honor of being my paranymph. Jie has been my very last *kamergenoot* of my PhD "career". Strangely enough though, we have hardly coincided at the office since we both had to spend extended periods of time on trips. Nonetheless, people's chemistry worked its miracles and since we share the same sense of humour, I have had some good and stress-relieving laughs with both him and Elly! He is a loyal and genuinely caring friend who proves his willingness to help in practice. I wish you, Jie, all the best for your own PhD. I am sure you will be successful.

I would also like to thank all past and present friends that occasionally formed the unofficial "Greek society at UT" (☺!) for all the fun times, the *glentia*, and the …group

therapy sessions as “educational immigrants” that we all were away from our country and our families. My special thanks go to my favourite Dutch-Greek blondie Pavlina for all the good times we spent in the last four years doing our PhDs in parallel, and for introducing me to the TCCB borrel community (☺!). Many thanks also to Panos and Demetris S. (in a looong line of Demetrises!) for keeping me sane, especially during the madness of the writing period. For this, I also need to thank Nick (the Greek??), as well as Sami who always supported me when I needed his help. Oya, Roel, Mark 1, Mark 2, Bertie, Jacob, and Alberto, thank you all for the psychological boost and the heartfelt words whenever our paths crossed.

Last but surely not least, special thanks to Panagioti M., my dearest old-time friend who always tries to cheer me up on the first frustrating days of my trips and supports me at every step, to Kosta K. for all the travelling adventures, to Kyriako, Juanito, Ioanna and Maria for always welcoming me in the warmest manner whenever I return to Greece, and especially to Michali and Alexandro for never forgetting about me despite our busy lives and the distance.

You are always in my thoughts and I wish only the best for you all.

AUTHOR BIOGRAPHY

Pelagia Glampedaki was born and educated in Greece. After graduating with honors from the American College Anatolia in Thessaloniki, she studied Chemistry at the Aristotle University of Thessaloniki with specialization in Chemical Technology and Industrial Chemistry. As a graduate chemist, she worked in Spain at the Instituto de Investigaciones Químicas y Ambientales de Barcelona (IIQAB) – Consejo Superior de Investigaciones Científicas (CSIC) with a scholarship of the European program "Leonardo da Vinci" under the supervision of Dr. Maria Rosa Infantes. After returning to Greece, she was admitted to a program for postgraduate studies in the Department of Chemistry of the Aristotle University of Thessaloniki, while working at the same time in the research department of an enological company. In 2006 she obtained a Master's degree in Polymer Chemistry and Technology, completing her thesis (cum laude) under the supervision of Assoc. Prof. Dr. Sofia Pegiadou-Koemtzopoulou. Despite being accepted in two programs for PhD studies in Thessaloniki and for a Product manager position in Athens, she decided to move to the Netherlands in 2007, after being selected to do her doctoral research as a Marie Curie fellow at the University of Twente. Until the end of 2010 she worked on the Advanbiotex project (Excellence Grant, FP6 EU program, project leader: Dr. D. Jocic) in the group of Engineering of Fibrous Smart Materials. During this period, she also realized a three-month stay in Germany divided between the Max-Planck-Institut für Kolloid- und Grenzflächenforschung, under the supervision of Dr. habil. Reinhard Miller, and the Leibniz-Institut für Polymerforschung Dresden e. V. (IPFDD), under the supervision of Dr. Alfredo Calvimontes and Mrs. Gudrun Petzold. After several collaborations inside and outside the Netherlands, she completed her PhD thesis presented in this book, under the supervision of Prof. Dr. Ir. Marijn M.C.G. Warmoeskerken, and with the support of Assoc. Prof. Dr. habil. Victoria Dutschk.

In 2009 Pelagia Glampedaki was considered among the finalists for the Ten Cate award for best PhD presentation at the AUTEX2009 Conference, and in 2011 her article "Functional finishing of aminated polyester using biopolymer-based polyelectrolyte microgels" was included in the highlights of the special issue "Polymer and Textile Biotech" of the *Biotechnology Journal*, presented on-line as "article of the week" (October 17-23, 2011). The overall scientific ouput of her research work is listed below.

SCIENTIFIC OUTPUT

Peer-reviewed publications

1) **P. Glampedaki**, G. Petzold, V. Dutschk, R. Miller, M.M.C.G. Warmoeskerken, Physicochemical properties of biopolymer-based pH/thermo-responsive polyelectrolyte complexes. (*submitted*)
2) **P. Glampedaki**, J. Krägel, G. Petzold, V. Dutschk, R. Miller, M.M.C.G. Warmoeskerken, Polyester textile functionalization through incorporation of pH/thermo-responsive microgels. Part I: Microgel preparation and characterization. (*submitted*)
3) **P. Glampedaki**, A. Calvimontes, V. Dutschk, M.M.C.G. Warmoeskerken, Polyester textile functionalization through incorporation of pH/thermo-responsive microgels. Part II: Polyester functionalization and characterization, *Journal of Materials Science* (2011) (DOI: 10.1007/s10853-011-6006-6). (*in press*)
4) **P. Glampedaki**, V. Dutschk, D. Jocic, M.M.C.G. Warmoeskerken, Functional finishing of aminated polyester using biopolymer-based polyelectrolyte microgels, *Biotechnology Journal* **6**(10), 1219-1229 (2011).
5) **P. Glampedaki**, D. Jocic, M.M.C.G. Warmoeskerken, Moisture absorption capacity of polyamide 6,6 fabrics surface functionalised by chitosan-based hydrogel finishes, *Progress in Organic Coatings* **72**(3), 562-571 (2011).
6) **P. Glampedaki**, D. Jocic, V. Dutschk, M.M.C.G. Warmoeskerken, Surface modification of polyester fabrics by grafting pH/thermo-responsive microgels with UV irradiation, in: T.S. Sudarshan, E. Beyer, L.-M. Berger (Eds.), *Surface Modification Technologies XXIV*, pp. 131-138, Valardocs (2011) (ISBN 978-81-910571-2-6).
7) **P. Glampedaki**, E. Hatzidimitriou, A. Paraskevopoulou, S. Pegiadou-Koemtzopoulou, Surface tension of still wines in relation to some of their constituents: A simple determination of ethanol content, *Journal of Food Composition and Analysis* **23**, 373-381 (2010).
8) **P. Glampedaki**, V. Dutschk, S. Pegiadou-Koemtzopoulou, Study of the emulsifying ability of still wines and grapeseed oil. (*to be submitted*)
9) D. Jocic, A. Tourrette, **P. Glampedaki**, M.M.C.G. Warmoeskerken, Application of temperature and pH responsive microhydrogels for functional finishing of cotton fabric, *Materials Technology: Advanced Performance Materials* **24**, 14-23 (2009).

Conference contributions

1) **P. Glampedaki,** A. Calvimontes, V. Dutschk, M.M.C.G. Warmoeskerken, Characterization of microgel-functionalized stimuli-responsive textiles by means of surface analysis, *IUPAC International Congress on Analytical Sciences 2011 (ICAS2011)*, *May 22-26, 2011, Kyoto, Japan*, Book of Abstracts, 23pC2-07 (2011). *(oral presentation)*
2) **P. Glampedaki,** V. Dutschk, D. Jocic, M.M.C.G. Warmoeskerken, Functional finishing of aminated polyester using biopolymer-based polyelectrolyte microgels, *7th International Conference on Polymer and Textile Biotechnology (IPTB2011) & Final Workshop of COST ACTION 868 on Biotechnical Functionalization of Renewable Polymeric Materials, March 2-4, 2011, Milan, Italy*, Proceedings (CD-ROM), F104 (2011) (ISBN 978-889-667-901-2). *(oral presentation)*
3) **P. Glampedaki**, Tunable wettability of polyester fabrics functionalized by chitosan/poly(N-isopropylacrylamide-co-acrylic acid) microgels, in: D. Jocic (Ed.), *Surface modification systems for creating stimuli responsiveness of textiles*, *Advanbiotex workshop proceedings, November*

25, 2010, University of Twente, Enschede, The Netherlands, pp. 61-76 (2010) (ISBN 978-90-365-3122-1). *(oral presentation)*

4) **P. Glampedaki**, D. Jocic, V. Dutschk, M.M.C.G. Warmoeskerken, Surface modification of polyester fabrics by grafting pH/thermo-responsive microgels with UV irradiation, *24th International Conference on Surface Modification Technologies (SMT24), September 7-9, 2010, Dresden, Germany*, Book of Abstracts, p. 32 (2010). *(oral presentation)*
5) **P. Glampedaki**, J. Zhao, C. Campagne, D. Jocic, M.M.C.G. Warmoeskerken, Polyester functionalization using thermoresponsive microparticles, *The 10th World Textile Conference (AUTEX2010), June 21-23, 2010, Vilnius, Lithuania*, Proceedings (CD-ROM) (4 pages) (2010) (ISBN 978-609-95098-2-2). *(oral presentation)*
6) **P. Glampedaki**, J. de Klein, M.M.C.G. Warmoeskerken, D. Jocic, Surface modification of polyamide via grafted chitosan-based responsive hydrogels, *The 9th World Textile Conference (AUTEX2009), May 26-28, 2009, Izmir-Cesme, Turkey*, Proceedings (CD-ROM), pp. 480-487 (2009) (ISBN 978-975-483-787-2). *(oral presentation)*
7) **P. Glampedaki**, A. Tourrette, M.M.C.G. Warmoeskerken, D. Jocic, Application of bulk and micro-hydrogels for obtaining cotton with responsiveness towards temperature and pH, *2nd International Scientific Conference "Textiles of the Future" – Futurotextiel 2008, November 13-15, 2008, Kortrijk, Belgium*, Proceedings (CD-ROM) (10 pages) (2008). *(oral presentation)*
8) **P. Glampedaki**, Research dissemination facilitates innovation, *Marie Curie Conference – Euroscience Open Forum 2008 (ESOF2008), July 17-22, 2008, Barcelona, Spain*, Book of abstracts, P-74, p. 33 (2008). *(poster)*
9) **P. Glampedaki**, A. Tourrette, M.M.C.G. Warmoeskerken and D. Jocic, Preparation and properties of stimuli-responsive surface modifying systems applicable to textiles, *The 8th World Textile Conference (AUTEX2008), June 24-26, 2008, Biella, Italy*, Proceedings (CD-ROM) (6 pages) (Poster 124) (2008). *(poster)*
10) D. Jocic, **P. Glampedaki**, A. Navarro, M.M.C.G. Warmoeskerken, Developing "smart" cotton fabric by coating with biopolymer-based hydrogel, *International Conference: Intelligent Textiles and Mass Customization (ITMC2007), November 15-17, 2007, Casablanca, Morocco*, Proceedings, pp. 538-547 (2007). *(poster)*
11) **P. Glampedaki**, A. Tourrette, M.M.C.G. Warmoeskerken, D. Jocic, Advanced biopolymer-functionalized textile materials – ADVANBIOTEX project, *Innovation Festival "Powered by Twente", Session: Materials & High-Tech Systems, October 25-26, 2007, Business & Science Park, Enschede, The Netherlands* (2007). *(poster)*
12) **P. Glampedaki**, A. Paraskevopoulou, E. Hatzidimitriou, Stability of cosmetic emulsions from red wine, grape seed oil and mastic resin, *9th Chemistry Conference of Greece and Cyprus, April 2007, Larnaca, Cyprus*, Proceedings (CD-ROM) (2007). *(oral presentation)*
13) **P. Glampedaki**, E. Hatzidimitriou, A. Paraskevopoulou, S. Pegiadou-Koemtzopoulou, Study and applications of the surface tension of still wines, *5th International Congress on Food Technology, March 2007, Thessaloniki, Greece*, Proceedings Vol. **2**, p. 123-130 (2007). *(poster)*

Other

1) **P. Glampedaki**, Biopolymer-based polyelectrolyte hydrogels for surface functionalization of synthetic textiles, Periodic colloquium of the Institute of Physical Chemistry and Polymer Physics of the Leibniz Institute for Polymer Research Dresden (IPFDD), September 13, 2010, Dresden, Germany. *(invited talk)*

2) **P. Glampedaki**, Functionalization of polyamide and polyester fabrics using chitosan-based hydrogels, EFSM Working Party meeting, January 21, 2010, Ten Cate Advanced Textiles, Nijverdal, The Netherlands. *(invited talk)*
3) **P. Glampedaki**, Chitosan-based hydrogels for the modification of cotton, polyamide and polyester fabric, EFSM 3rd Annual Meeting, December 10, 2009, Holten, The Netherlands. *(invited talk)*
4) **P. Glampedaki**, part III of a joint presentation on "Advanced Functionality of Textiles by Biopolymer Surface Modification - ADVANBIOTEX project", July 1, 2008, TNO Science & Industry, Department of Innovative Materials, Eindhoven, The Netherlands. *(invited talk)*
5) **P. Glampedaki**, part III (regarding chitosan bulk hydrogels) of a joint presentation on "Advanced Functionality of Textiles by Biopolymer Surface Modification", EFSM Working Party meeting, April 3, 2008, Business and Technology Center - Twente, Enschede, The Netherlands. *(invited talk)*
6) **P. Glampedaki**, part III (regarding bulk hydrogels) of a joint presentation on the Advanbiotex project, March 17, 2008, l'Ecole Nationale Supérieure des Arts et Industries Textiles (ENSAIT), Roubaix, France. *(invited talk)*

7) **P. Glampedaki**, D. Jocic, M.M.C.G. Warmoeskerken, Fast-responding microgels from Chitosan/NIPAAm/Acrylic acid, *OnderzoekSchool ProcesTechnologie (OSPT)*, Booklet of mini-posters (2009).
8) **P. Glampedaki**, D. Jocic, M.M.C.G. Warmoeskerken, Dually sensitive (T, pH) bulk hydrogels based on natural and synthetic polymers, *OnderzoekSchool ProcesTechnologie (OSPT)*, Booklet of mini-posters (2008).
9) **P. Glampedaki**, D. Jocic, M.M.C.G. Warmoeskerken, Textile functionalization via biopolymer surface-modifying systems for medical, safety and protection applications, *OnderzoekSchool ProcesTechnologie (OSPT)*, Booklet of mini-posters (2007).

10) V. Dutschk, J. Zhao, **P. Glampedaki**, M.M.C.G Warmoeskerken, Engineering of Fibrous Smart Materials (abstract, 1 page), *Materials Engineering 2011 – Minisymposium*, *May 25-26, 2011, Eindhoven, The Netherlands*.
11) D. Jocic, A. Tourrette, **P. Glampedaki**, M.M.C.G. Warmoeskerken, Functional finishing of cotton with dual-stimuli-responsive chitosan/poly(N-isopropylacrylamide) micro-hydrogels, *The 86th Textile Institute World Conference, November 18-21, 2008*, *Hong Kong,* Proceedings (CD-ROM), pp. 251-265 (2008) (ISBN 978-962-367-628-1). *(oral presentation)*
12) A. Tourrette, **P. Glampedaki**, M.M.C.G. Warmoeskerken and D. Jocic**,** Surface modification of textile material with biopolymer-based micro- and nano-hydrogels, *The 8th World Textile Conference (AUTEX2008), June 24-26, 2008, Biella, Italy*, Proceedings (CD-ROM) (2008). *(oral presentation)*
13) M.M.C.G. Warmoeskerken, D. Jocic, A. Tourrette, **P. Glampedaki**, Chitosan, een bron van nieuwe mogelijkheden (Chitosan, source for new possibilities), *Congres Innovatie in textiel; topprestaties in functionele kleding, November 2007, Nederlands Textielinstituut (NTI), TNO Industrie en Techniek, Eindhoven*, Presentaties (CD-ROM) (2007). *(oral presentation)*
14) L. Pérez, A. Pinazo, M.T. García, C. Morán, **P. Glampedaki**, MR. Infante, Surfactants of the type mono- and diacyl- glycerides with/without arginine: Structure – Reactivity, *V Reunión del Grupo Especializado de Coloides e Interfases (GECI), July 2003, Vigo, Spain*. *(poster)*